EVALUATION OF DYNAMIC COMPACTION

IN TULSA, OKLAHOMA

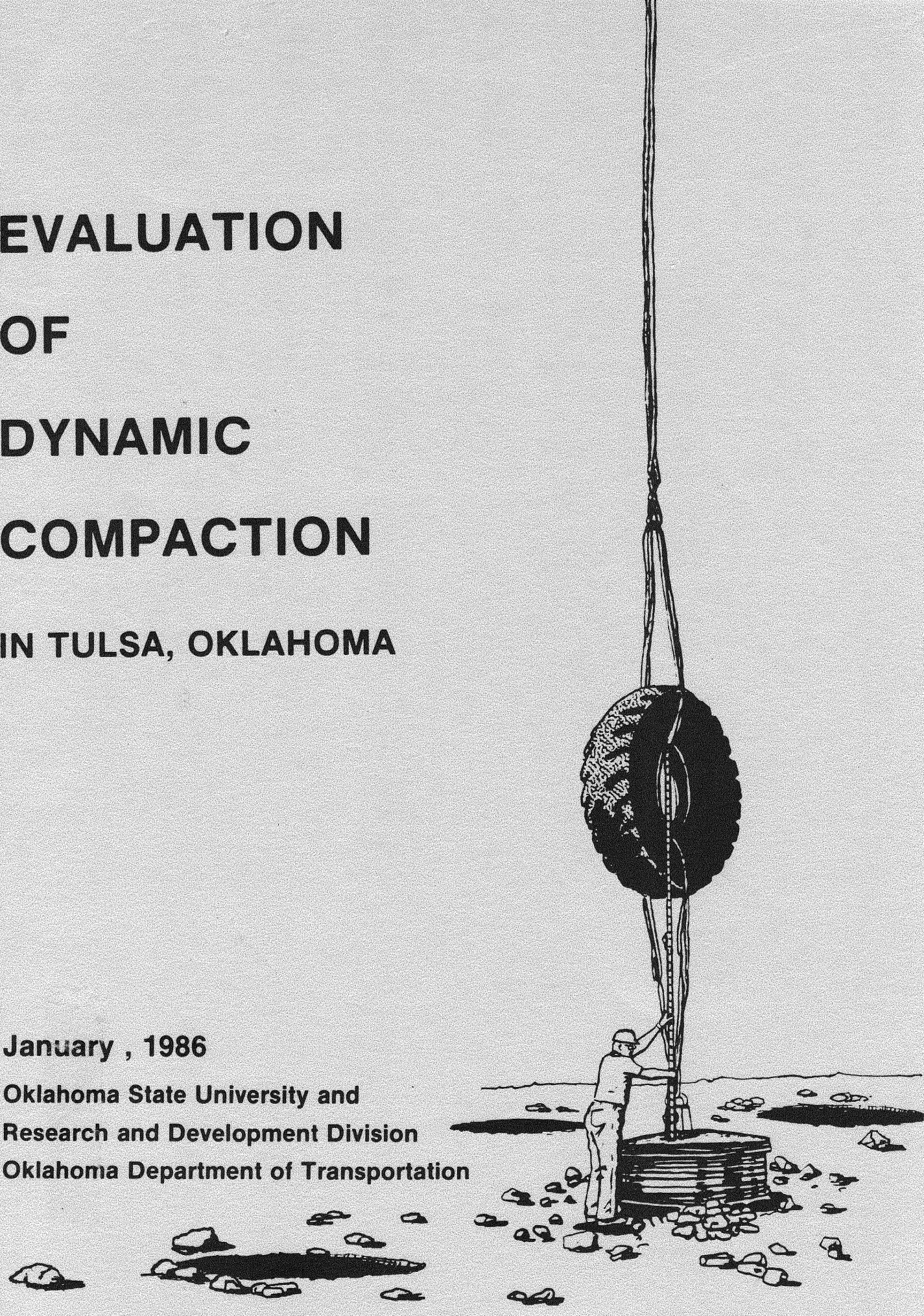

January , 1986

Oklahoma State University and
Research and Development Division
Oklahoma Department of Transportation

TECHNICAL REPORT STANDARD TITLE PAGE

1. REPORT NO.	2. GOVERNMENT ACCESSION NO.	3. RECIPIENT'S CATALOG NO.
FHWA/OK 86(3)		TA710.S635 1986x

4. TITLE AND SUBTITLE	5. REPORT DATE
Evaluation of Dynamic Compaction in Tulsa, Oklahoma	January, 1986
	6. PERFORMING ORGANIZATION CODE

7. AUTHOR(S)	8. PERFORMING ORGANIZATION REPORT
Donald R. Snethen, Michael H. Homan	

9. PERFORMING ORGANIZATION NAME AND ADDRESS	10. WORK UNIT NO.
School of Civil Engineering Oklahoma State University Stillwater, Oklahoma 74078-0327	11. CONTRACT OR GRANT NO. 84-15-3, Item 2141

12. SPONSORING AGENCY NAME AND ADDRESS	13. TYPE OF REPORT AND PERIOD COVERED
Oklahoma Department of Transportation Research and Development Division 200 N.E. 21st Oklahoma City, Oklahoma 73105	Final Report
	14. SPONSORING AGENCY CODE

15. SUPPLEMENTARY NOTES

Done in cooperation with FHWA

16. ABSTRACT

This report describes the installation and monitoring of three test sections to evaluate dynamic compaction as it was applied as a foundation treatment for the approach fills of an interchange on the Gilcrease Expressway (SH 11) in north central Tulsa. The test sections were monitored to assess the performance of dynamic compaction and to provide the data base for recommending changes to the construction process as foundation conditions varied.

Evaluation of the results obtained from the three test sections monitored during the dynamic compaction process indicated that the process improves the strength characteristics of strip mining spoil containing clay with shale fragments and trash. The most consistent improvement occurred in areas where the thickness of the trash was less than a few feet. The presence of a groundwater table did not appear to adversely affect the results. In areas of thicker trash layers, stone columns were successfully constructed using dynamic compaction. With the exception of the inclinometers, all instrumentation performed well and provided very good data to evaluate the dynamic compaction procedure.

17. KEY WORDS	18. DISTRIBUTION STATEMENT
soil mechanics, foundation stabilization, deep compaction, dynamic compaction, dynamic consolidation, heavy tamping	

19. SECURITY CLASSIF. (OF THIS REPORT)	20. SECURITY CLASSIF. (OF THIS PAGE)	21. NO. OF PAGES	22. PRICE
None	None	174	

EVALUATION OF DYNAMIC COMPACTION IN TULSA, OKLAHOMA

By

DONALD R. SNETHEN, Ph.D., P.E.

and

MICHAEL H. HOMAN

School of Civil Engineering
Oklahoma State University
Stillwater, Oklahoma
January, 1986

Submitted to
Research Division
Oklahoma Department of Transportation
Oklahoma City, Oklahoma

This publication was printed and issued by the Oklahoma Department of Transportation as authorized by V. O. Bradley, Director. 135 copies have been prepared and distributed at a cost of $360.25.

METRIC CONVERSION FACTORS

Approximate Conversions to Metric Measures

Symbol	When You Know	Multiply by	To Find	Symbol
	LENGTH			
in	inches	*2.5	centimeters	cm
ft	feet	30	centimeters	cm
yd	yards	0.9	meters	m
mi	miles	1.6	kilometers	km
	AREA			
in^2	square inches	6.5	square centimeters	cm^2
ft^2	square feet	0.09	square meters	m^2
yd^2	square yards	0.8	square meters	m^2
mi^2	square miles	2.6	square kilometers	km^2
	acres	0.4	hectares	ha
	MASS (weight)			
oz	ounces	28	grams	g
lb	pounds	0.45	kilograms	kg
	short tons (2000 lb)	0.9	tonnes	t
	VOLUME			
tsp	teaspoons	5	milliliters	ml
Tbsp	tablespoons	15	milliliters	ml
fl oz	fluid ounces	30	milliliters	ml
c	cups	0.24	liters	l
pt	pints	0.47	liters	l
qt	quarts	0.95	liters	l
gal	gallons	3.8	liters	l
ft^3	cubic feet	0.03	cubic meters	m^3
yd^3	cubic yards	0.76	cubic meters	m^3
	TEMPERATURE (exact)			
°F	Fahrenheit temperature	5/9 (after subtracting 32)	Celsius temperature	°C

*1 in = 2.54 (exactly). For other exact conversions and more detailed tables, see NBS Misc. Publ. 286, Units of Weights and Measures, Price $2.25, SD Catalog No. C13.10:286.

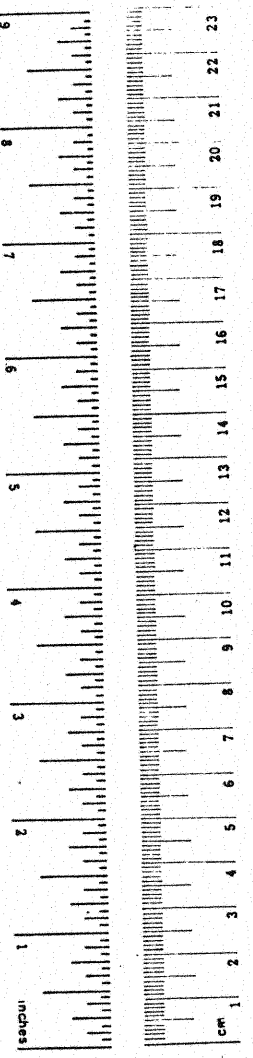

Approximate Conversions from Metric Measures

Symbol	When You Know	Multiply by	To Find	Symbol
	LENGTH			
mm	millimeters	0.04	inches	in
cm	centimeters	0.4	inches	in
m	meters	3.3	feet	ft
m	meters	1.1	yards	yd
km	kilometers	0.6	miles	mi
	AREA			
cm^2	square centimeters	0.16	square inches	in^2
m^2	square meters	1.2	square yards	yd^2
km^2	square kilometers	0.4	square miles	mi^2
ha	hectares (10,000 m^2)	2.6	acres	
	MASS (weight)			
g	grams	0.035	ounces	oz
kg	kilograms	2.2	pounds	lb
t	tonnes (1000 kg)	1.1	short tons	
	VOLUME			
ml	milliliters	0.03	fluid ounces	fl oz
l	liters	2.1	pints	pt
l	liters	1.06	quarts	qt
l	liters	0.26	gallons	gal
m^3	cubic meters	35	cubic feet	ft^3
m^3	cubic meters	1.3	cubic yards	yd^3
	TEMPERATURE (exact)			
°C	Celsius temperature	9/5 (then add 32)	Fahrenheit temperature	°F

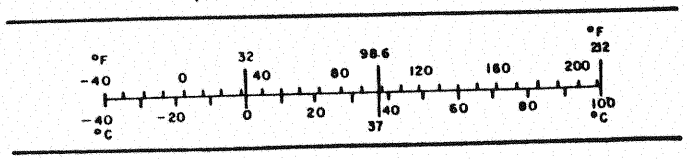

EXECUTIVE SUMMARY

This report describes the installation of instrumentation and monitoring of three field test sections to evaluate dynamic compaction as a deep foundation treatment process in areas underlain by old landfills. The test sections were conducted in conjunction with the foundation treatment for the approach fills and ramps for the interchange at SH 11 (Gilcrease Expressway) and north Yale Avenue in north central Tulsa, Oklahoma. Foundation conditions at the site varied from mining spoil consisting of clay and shale fragments to trash varying in thickness from a few feet to as much as 16 ft. Groundwater tables were encountered at a depth of approximately 18 ft at the east end of the project and at a depth of approximately 5 ft at the west end of the project. The test sections consisted of a pattern of impacts based on the recommended construction sequence instrumented with piezometers and inclinometers. In addition, crater depth with impact and surface elevation between selected passes were monitored. Standard Penetration Test borings were run prior to and following the dynamic compaction.

The results of the instrumentation and observation data obtained from the test sections indicated that dynamic compaction improves the strength characteristics of mining spoil containing clay with shale fragments and trash. The most consistent improvement occurred in areas where the thickness of the trash was less than a few feet. The presence of a groundwater table did not appear to adversely affect the results. In areas of thicker trash layers, the dynamic compaction was supplemented by the use of stone columns constructed by "pounding" the rockfill into the trash layer. The results of the test sections were used to modify the construction sequence during the compaction process as foundation conditions varied.

All instrumentation performed well; however, the inclinometer data were less reliable because the compaction process tended to destroy the inclinometer casings by pushing trash laterally into the casings and pinching them off.

TABLE OF CONTENTS

Chapter Page

LIST OF TABLES

LIST OF FIGURES

Figure Page

Figure

Page

Figure Page

Figure Page

Figure Page

CHAPTER I

INTRODUCTION

Background

Dynamic compaction (dynamic consolidation, heavy tamping, impact densification) is a technique that is used to compact and strengthen loose or soft soils to support roadways, buildings or other heavy construction. This method involves the dropping of a heavy weight from a predetermined height in a grid pattern designed to obtain the maximum amount of input energy with the least amount of effort expended. In certain subsurface conditions, dynamic compaction has proven to be an effective and economical alternative to undercutting and replacing, preloading, deep foundations, and deep vibratory compaction. This method is especially effective for facilities covering large surface areas.

Initially, dynamic compaction was used with great success on naturally deposited loose sands, hydraulically placed sands, and granular rubble fills. Some degree of success has also been reported for clay fills, natural silts and clays, and organic peaty soils. In recent years, the use of dynamic compaction to improve subsurface conditions at old sanitary landfills has drawn much attention in the larger metropolitan areas.

In most sanitary landfills, the input energy from dynamic compaction is great enough to crush any buried containers, and thus, to reduce the thickness of the compressible material. The dynamically compacted sanitary fill material will probably continue to settle because of the decomposition of the organic constituents. However, because the consolidation process was aided by dynamic

compaction, the rate of decomposition will be relatively slow; thus, any future settlements will be gradual with time and should have minimal effect on the performance of the structure constructed upon the improved site.

Most construction sites on which dynamic compaction has been used have only had to deal with one particular subsurface condition. However, as more and more confidence is being placed on the use of this technique with various soil conditions, more engineers are willing to consider dynamic compaction on projects which involve varying subsurface conditions. Also, as the use of dynamic compaction becomes more popular, more contractors are willing to submit bids on such projects. Thus, the possibility of having an inexperienced contractor on a large project involving varying subsurface conditions becomes more prevalent.

Purpose of Study

This study involves a section of the proposed Gilcrease Expressway in Tulsa, Oklahoma, which will pass over an old strip mining area that has subsequently been used as a public sanitary landfill. The clay and shale spoil resulting from the removal of overburden during the mining operations now exists largely in the form of giant windrows. Some of the interceding valleys have since been filled with a mixture of trash and mining spoil and covered with a layer of the latter. An investigation by the Oklahoma Department of Transportation (ODOT) showed that the character of the materials overlying the bedrock (which occurs at depths of 25 to 45 feet) varies erratically, both parallel and perpendicular to the roadway alignment. Basically, three different typical subsurface profiles were identified over the site. The most common typical profile found was shale spoil fill existing to bedrock. The second typical subsurface profile involved trash fill to a depth of 20 feet overlying three feet of lean clay and bedrock with the ground water table at a depth of approximately 15 feet. The third typical subsurface profile involved

shale spoil fill mixed with trash with a high water table. Approximately one-half mile of the expressway, including a major interchange at Yale Avenue, was affected by the described subsurface conditions.

The various fill materials were known to be very loose and compressible. It is felt that even those areas where the shale spoil was predominant would settle excessively and nonuniformly under the weight of the roadway embankment, which will have a maximum height of about 30 feet above the existing grade. Similar subsurface materials have been successfully compacted by dynamic compaction; thus, the ODOT felt that this technique was appropriate in this instance. This is believed to be among the first such projects in which a general contractor with no previous experience in dynamic compaction was awarded the construction contract.

The surface area over which dynamic compaction is to be performed comprises approximately 22 acres. The consulting engineer for the project (W. R. Holway & Associates) prepared the plans and specifications for the work. Because of uncertain results expected from the specified equipment and techniques, the contract required the compaction of three instrumented test sections before proceeding with the production work. Procedures for executing the production work were contingent on an analysis of the results obtained at the test sections.

Test section instrumentation was specified for provision and installation by the contractor, subject to ODOT approval, with the responsibility for data collection, analysis, and recommendations undertaken by the School of Civil Engineering at Oklahoma State University.

Scope of the Investigation

This report describes the instrumentation, data collection and the results of the three dynamic compaction test sections. Continuous monitoring and data

collection activities were provided during the test sections. Following that, the data were analyzed and tentative procedures established to guide the contractor during the production work. As work progressed, frequent site visits were required to evaluate the effectiveness of the established procedures and, where necessary, to recommend modifications of those procedures.

Involvement of the School of Civil Engineering research staff was as follows:

1. Attended the pre-work conference to provide input on the instrumentation to be used during the dynamic compaction of the three test sections.
2. Monitored the installation of all instrumentation.
3. Continuously monitored and collected data during compaction of the test sections.
4. Analyzed data obtained from test sections; provided written recommendations for compaction procedures and criteria based upon analysis of the data and field observations.
5. Intermittently monitored pore pressure devices beyond the test period, as required; provided consultation related to control of the project, including attendance at meetings, as requested by the ODOT.
6. Frequently observed the dynamic compaction operations during progress of the work, to evaluate procedures and, if necessary, to recommend changes.
7. Prepared final report for the three test sections to include a presentation of data collected on each test area along with an analysis of said data, and recommendations for establishing criteria for future projects involving similar foundation materials.

CHAPTER II

STATUS OF DYNAMIC COMPACTION

Introduction

The use of land that just a few years ago would have been deemed undesirable as a foundation material is becoming more and more prevalent in today's construction industry. This is being brought about in the larger metropolitan areas because of the accelerated effort of the cities to grow outward. Land that was once used as a city's sanitary landfill is now being considered as a foundation material for a high-rise office tower, warehouse, or maybe a highway.

Once the decision has been made to use the less desirable land as a foundation for a structure, some sort of action must be taken to improve the engineering characteristics of the soil to the point that it will not only support the structure in mind, but also provide as little differential settlement as possible. One method being used more and more to improve the soil's engineering properties is dynamic compaction (also referred to as dynamic consolidation, heavy tamping, and impact densification).

The densification of loose soil by dropping weights onto the material dates back to antiquity. The first known published reference on the subject involved a site in Germany in 1933 that was recorded by Loos (5). However, not until 1969 was the technique finally promoted by the late French engineer, Louis Menard, as a method that could be used routinely for site improvement. During the past decade, dynamic compaction has come to be an accepted method of improving

poor soils with one of the most beneficial effects being to collapse voids or to densify very loose layers.

Basically, dynamic compaction consists of dropping a heavy weight onto the ground surface to compact the underlying soil. The ultimate goals of this process are improved bearing capacity and decreased differential settlement.

Appropriate Uses

Mayne et al. (8) note that heavy tamping has been used to densify a wide variety of material including sand, sand fill or hydraulically placed sand, silt, clay or silty clay fills, rubble fills, miscellaneous refuse fills and sanitary landfills, mine spoil, rockfills, sinkholes, peat, and collapsible soils. Dynamic compaction can also be used to strengthen potentially liquefiable soil deposits, to collapse abandoned coal mines, and to densify soils under water.

In choosing dynamic compaction as a means of improving poor soil conditions on a project, the technique's potential for improving the given soil type must be assessed. Dumas and Beaton (2) suggest the following general guidelines:

1. All natural soils with greater than 50% passing the No. 200 sieve should be deemed difficult to improve.
2. All natural soils in which the clay fraction is 20% or more should be considered as offering little chance for measurable improvement.
3. All soils with reasonable drainage characteristics can be improved. This includes virtually anything from non-cohesive silts to rockfills containing very large fragments.
4. All types of fills (including clay) can be improved.

The above guidelines concerning fine-grained natural soils assume saturated conditions and are based on the use of dynamic compaction only. The following allowable bearing pressures as presented by Dumas and Beaton (2) may be

considered as reasonable post-treatment design values:

Type of Soils	Allowable Bearing Pressure, kPa
Peat, landfill	50 - 100
Fine grained alluvials silty fills	100 - 150
Heterogeneous fills	100 - 300
Fine silty sand, hydraulic fills	Up to 200
Rockfills	200 - 300
Well graded mixture coarse sand and gravel, no fines	300 - 500

Methodology of Compaction

The weights used in dynamic compaction are usually either concrete blocks, steel plates, or thick steel shells filled with concrete or sand, typically weighing between 5 - 20 ton. However, a 200 ton weight was employed at Nice Airport in the French Riviera (3). The weights are allowed to drop freely from heights ranging up to 40 meters. The weights are usually square or circular in plan with dimensions varying according to the weight needed, material used, and the dynamic bearing capacity of the ground surface being treated. For underwater use, more streamlined designs are used.

From numerous sites investigated by Mayne et al. (8), the total cumulative applied energy levels typically ranged from 30 - 150 ft-ton/sq. ft. However, Mayne et al. (8) also make reference to numerous sites that have been subjected to energy levels in excess of 200 ft-ton/sq ft. This amount of compactive energy allows the improvement of compressible soils up to depths of 50 ft. With special

equipment (3) it is possible to drop heavier weights from greater heights and thus affect soils to depths of 40 meters.

To achieve adequate compaction, proper consideration must be given to the spacing of the applied energy and the time frame between applications of this energy. The spacing of grid points may be estimated as (7):

$$S = (WHN_B/U)^{0.5}$$

where:

S = spacing of grid points

W = weight in tons

H = drop in meters

N_B = number of blows per pass

U = applied energy per unit area = (WH/A_ω)/blow

A_ω = area of the weight

According to Mitchell (10) a typical treatment will result in an average of 2 to 3 blows/m^2. Typically, two or three coverages of an area will be required, separated by time intervals dependent on the rate of dissipation of the excess pore water pressure and strength regain.

During the first phase (or pass) of the project, impact spacing is determined by the depth of the compressible layer, the depth to groundwater, and grain size distribution (8). The initial grid spacing is generally equal to the thickness of the compressible layer. This first phase of treatment is used to compact the deeper layers of soil. Improper spacing and levels of applied energy at this point could result in a layer of dense material at some intermediate level that would make it all but impossible to compact the soil beneath it. After the first phase is completed, the imprints are usually backfilled with the surrounding material and

the site levelled. This causes the working platform to be lowered an amount which is proportional to the densificiation achieved during the pass. The time interval between coverages may vary from days for freely draining coarse sands to weeks for the finer grained soils.

Two or three of the initial "high energy" passes may be required depending upon the results desired as compared with those obtained. The initial passes are followed at the end by low energy passes called "ironing" passes, which are used to densify the surficial layers in the top five feet. During the ironing pass, small impacts by the weight are made over the entire surface.

Mitchell (10) notes that surface settlements may be from two to five percent of the thickness of the zone being densified per coverage.

Theoretical Aspects

Because a theoretical analysis of dynamic compaction was not developed until the late 1970's, early jobs were designed on an empirical basis. This same evolution can be traced to vertical sand drains, grouting, etc.

Gambin (3) makes reference to some of the analyses of the various phenomena which occur during the dynamic compaction process:

1. A comparison with Terzaghi's theory of static consolidation which helped to show the role played by micro-bubbles of gas.
2. The influence of the Love and Rayleigh waves propagation to shake the soil skeleton and rearrange the grains.
3. The influence of the shear deformations as opposed to the volume change deformations, with the former, alone, inducing nonreversible strains even at a low level of stress.
4. The influence of the adiabatic compression of the gas bubbles which creates pressure shock within the liquid phase and helps in the creation

or widening of channels in the soil. These channels act as preferential drainage paths.

5. The influence of liquefaction under cyclic loading which helps to demonstrate the interest of the method to decrease the liquefaction potential of soils in regions prone to earthquakes.

Initially, heavy tamping, as introduced by Techniques Louis Menard, covered principally ballast fills or natural sandy gravel soils. However, it was later found that this field of application could be extended to saturated clays or alluvial soils. Menard and Broise (9) were instrumental in developing the theory behind dynamic consolidation. At one time thinking it impossible to carry out heavy tamping on a saturated clay soil, experience showed them that these soils do actually settle instantly several tens of centimeters and contain micro-bubbles of gas that render them compressible under the effect of dynamic forces.

According to Terzaghi's theory of consolidation, the evacuation of water is a necessary and sufficient condition to allow settlement to occur in a soil mass due to volume variations. However, early observations by Menard and Broise (9) showed that whatever the nature of the soil treated, a tamping operation always resulted in an immediate considerable settlement. This result could not be explained by traditional theories for saturated impermeable soils. Subsequent research showed that most quaternary soils actually contained gas in the form of micro-bubbles, the content varying between 1% for the most unfavorable cases and 4% in the more favorable. Apparently, shocks or mechanical vibrations modify the conditions of equilibrium of these micro-bubbles in a more or less irreversible manner.

As energy is applied to the soil in the form of repeated impacts, the gas in the soil gradually becomes compressed. Menard and Broise (9) noted that as the percentage of gas by volume approaches zero, the soil starts to react as an

incompressible material and at this stage, liquefaction of the soil begins to take place.

One feature that was observed on dynamic consolidation projects was the very rapid dissipation of pore-water pressure which could not be explained by the coefficient of permeability measured before tamping. Menard and Broise (9) explain this behavior in three ways:

1. A very slight local increase in pore-water pressure is sufficient to start a "tearing of the solid tissues" by splitting, and quite naturally the flow of liquid concentrates in these newly created fissures. These preferential drainage paths are generally perpendicular to the direction of lowest stress.
2. It has been observed in the laboratory that the coefficient of permeability increases when the intergranular stresses decrease and that it reaches a maximum value when the soil becomes a liquid, at which instant the pore-water pressure is equal to the total pressure, h. This is partly why, during the dynamic consolidation process which generally results in liquefaction occurring in local conditions, high permeabilities can be observed.
3. Finally, it would appear that the shock waves transform the adsorbed water into free water, thus encouraging an increase in the sectional area of the capillary channels.

Also, during a tamping operation, a large decrease in shear strength is initially noted, with the lowest value being observed when the soil is liquefied or at least approaching liquefaction. At that time the soil matrix is completely destroyed and the adsorbed water is partially transformed into free water. As the pore-water dissipates, a large increase in the shear strength and deformation modulus is noted. This increase may be explained by the closer contact between the soil particles as well as the gradual fixation of new layers of adsorbed water.

Menard and Broise (9) explain the above fundamental aspects on the mechanism of dynamic consolidation for fine grained saturated soils by using a modified presentation of the well known hydraulic system of a cylinder filled with an incompressible fluid and supported by a spring (Figure 1).

The various stages of dynamic consolidation are summarized by Menard and Broise (9) by a series of graphs. Figure 2 relates to the changes in the soil after a single pass. Curve 1 shows the energy applied to the soil by a series of impacts on the same spot, curve 2 the corresponding volume variation of the soil, curve 3 the corresponding evolution of pore-water pressure in relation to the liquefaction pressure, and curve 4 the evolution of the bearing capacity as a function of time. Figure 3 relates to the same parameters as Figure 2 but for a series of passes.

Ground Response

Induced Subsidence

Heavy tamping causes an areal subsidence to occur within the area being treated. For materials situated above the water table this occurs relatively quickly, whereas in soils founded below the water table, the subsidence occurs more slowly as the cyclic pore pressures dissipate with time.

Perhaps the most obvious occurrence of this subsidence are the craters that are formed when the weight is dropped onto the ground. Mayne et al. (8) show a summary of crater depths as a function of the number of blows in Figure 4 for several sites. For these particular sites there was virtually no reported heave outside the point of impact.

Mayne et al. (8) also normalized the crater measurements with respect to the square root of energy per blow (Figure 5), and as can be seen, the data fall within a rather narrow band. Leonards et al. (4) showed that crater measurements might be used for selecting the optimal number of blows per pass. Crater

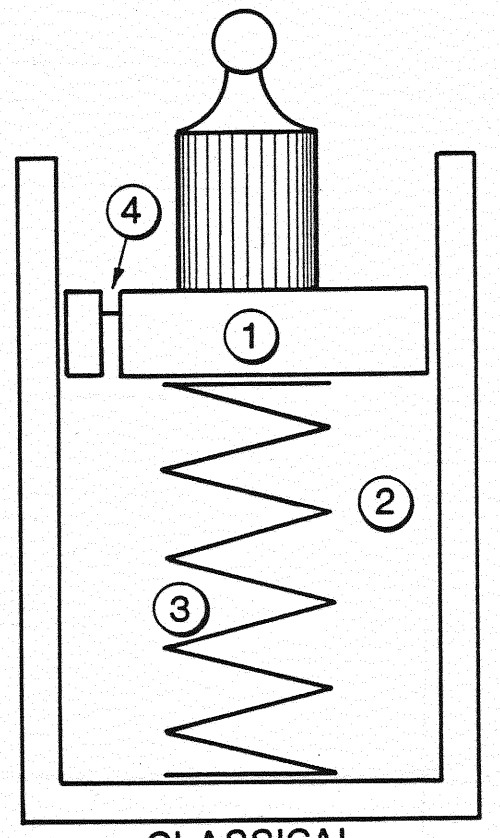

CLASSICAL
CONSOLIDATION THEORY

① FRICTIONLESS PISTON
② INCOMPRESSIBLE LIQUID
③ CONSTANT RATE SPRING
④ FIXED DIAMETER PERFORATION PERMITTING THE ESCAPE OF FLUID UNDER PRESSURE

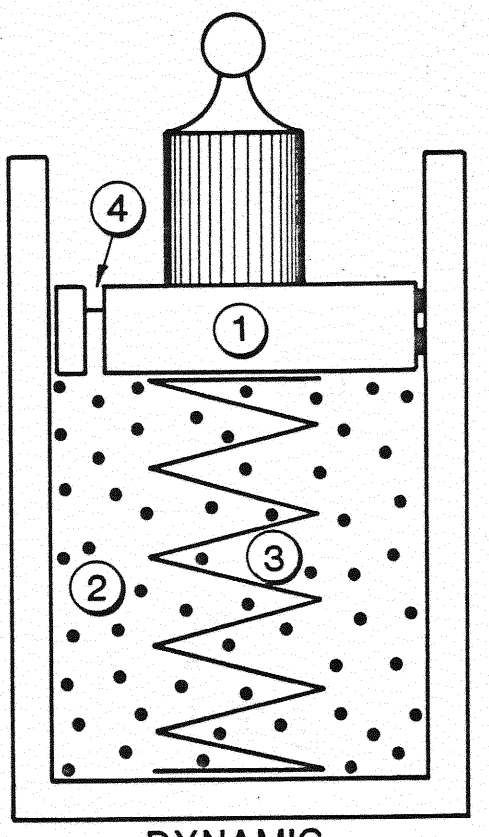

DYNAMIC
CONSOLIDATION THEORY

① FRICTIONAL PISTON
② COMPRESSIBLE FLUID WITH BUBBLES CONTAINING A SMALL PERCENTAGE BY VOLUME OF GAS
③ NON-CONSTANT RATE SPRING (THIXOTROPY WITH FRICTION)
④ VARIABLE DIAMETER PERFORATIONS

Figure 1. Comparison of Traditional and New Theories of Consolidation (9)

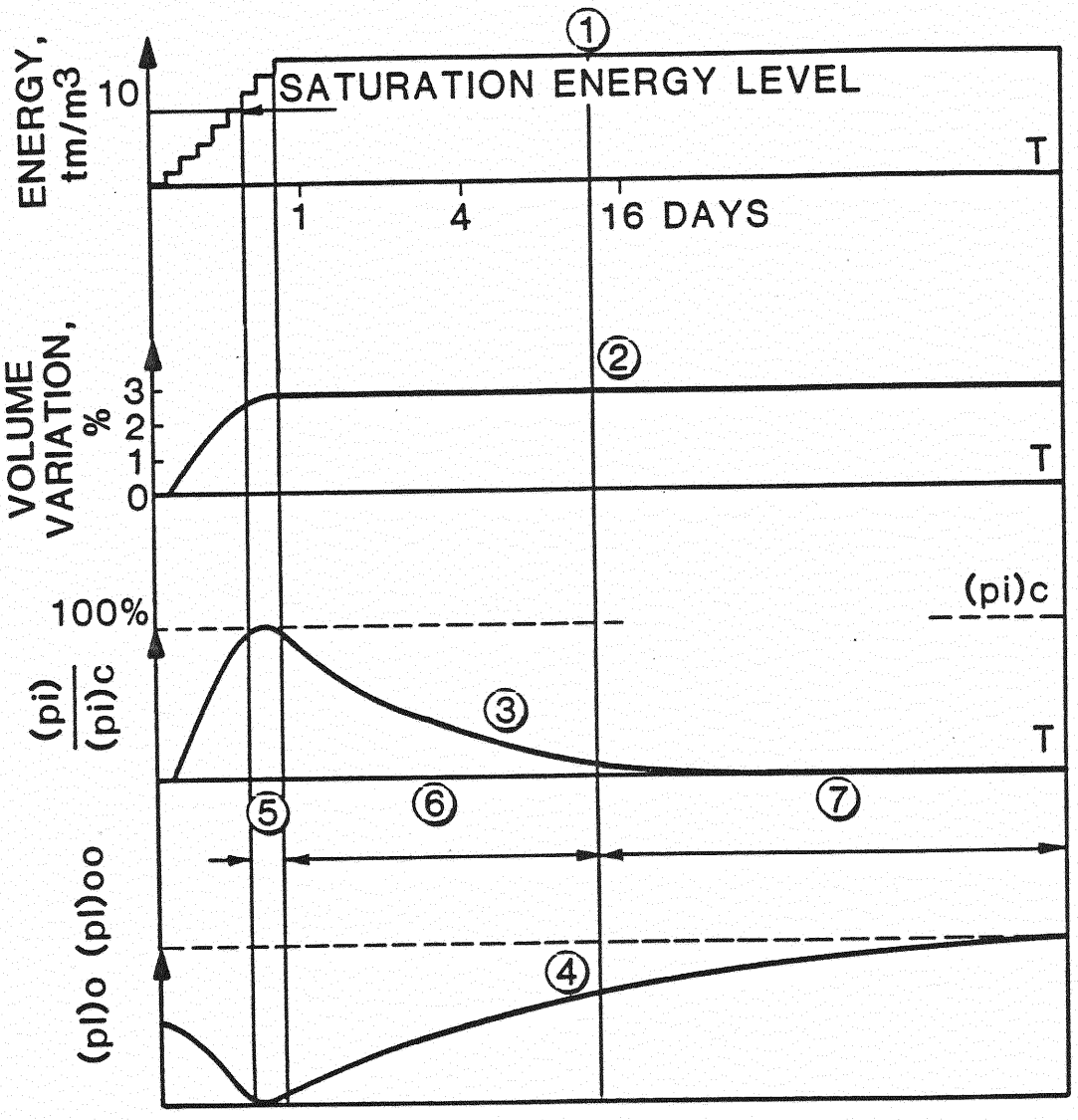

① APPLIED ENERGY, tm/m3

② VOLUME VARIATION WITH TIME T(log scale)

③ RATIO OF PORE-PRESSURE PI TO LIQUEFACTION PRESSURE (pi)c AGAINST TIME T

④ VARIATION OF BEARING CAPACITY OF GROUND WITH TIME T

⑤ LIQUEFACTION PHASE

⑥ PORE-WATER PRESSURE DISSIPATION PHASE

⑦ THIXOTROPIC PHASE

Figure 2. Change in the Soil After Consolidation Phase (9)

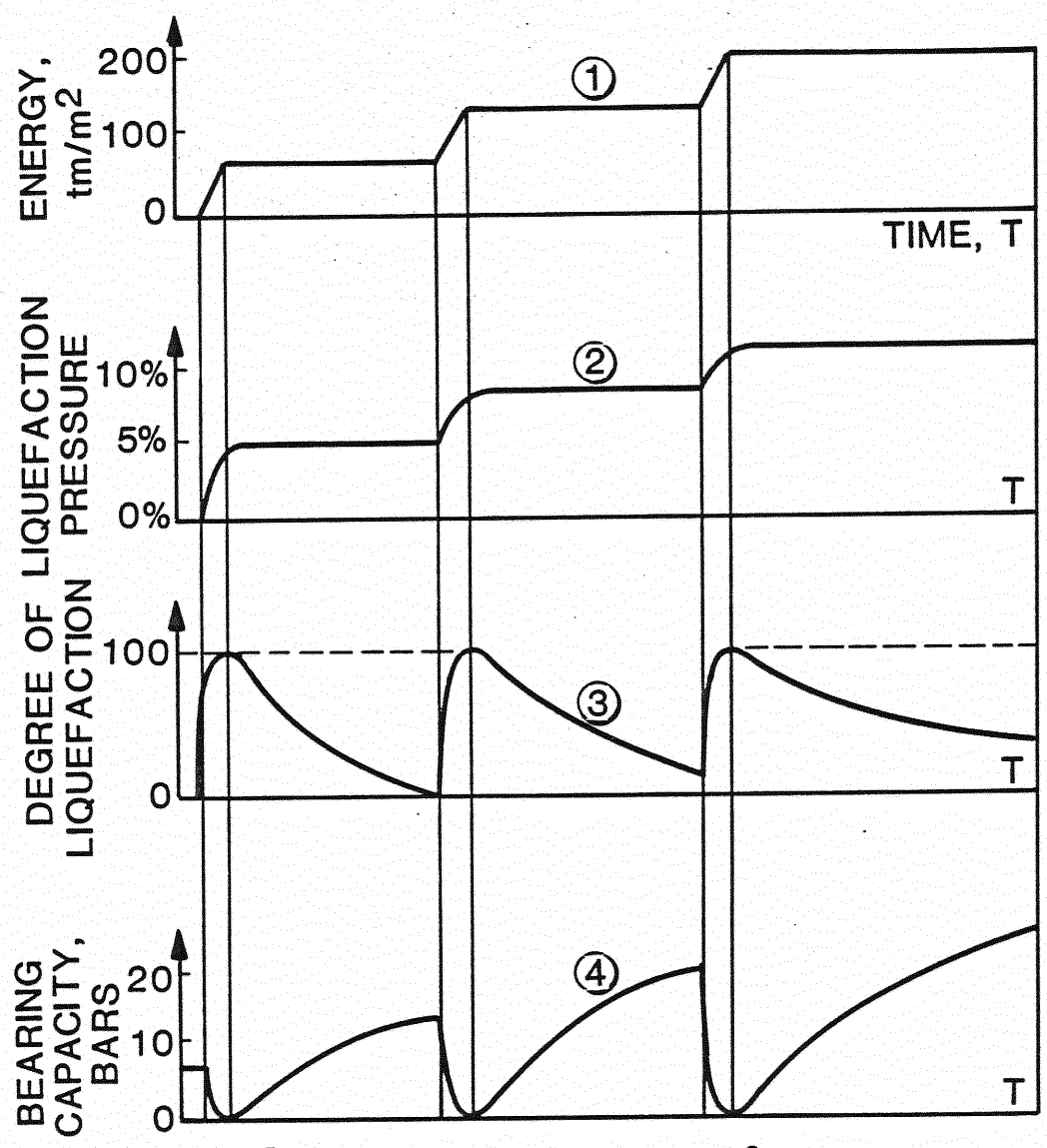

① APPLIED ENERGY IN tm/m^2

② VOLUME VARIATION AGAINST TIME (NORMAL SCALE)

③ RATIO OF PORE-PRESSURE pl TO LIQUEFACTION PRESSURE pi(c)

④ VARIATION OF BEARING CAPACITY

TIME BETWEEN PASSES VARIES FROM ONE TO FOUR WEEKS ACCORDING TO THE SOIL TYPE

Figure 3. Variation of a Soil Subjected to Series of Dynamic Consolidation Phases (9)

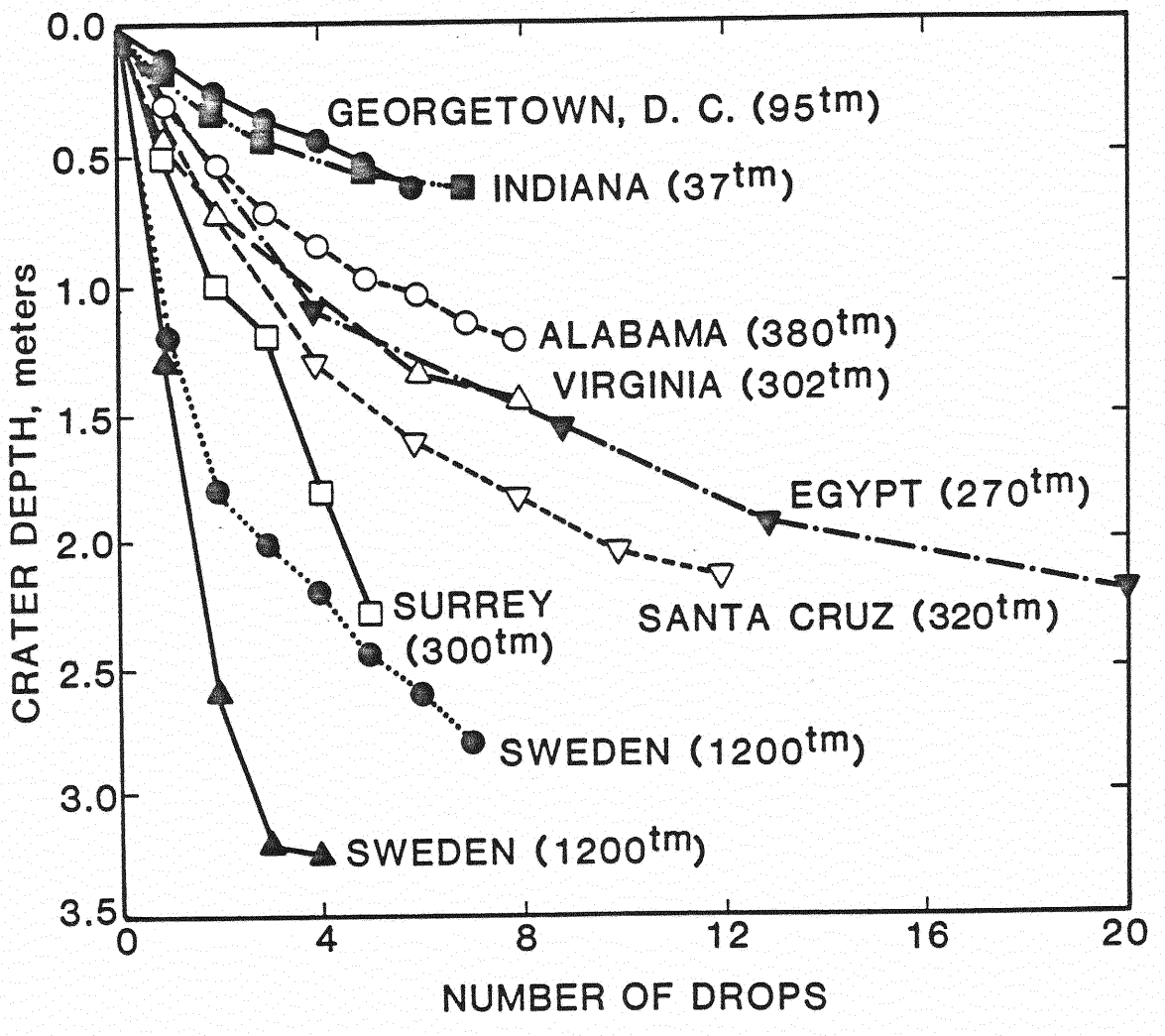

Figure 4. Crater Depths as Function of Number of Blows for Several Different Sites (8)

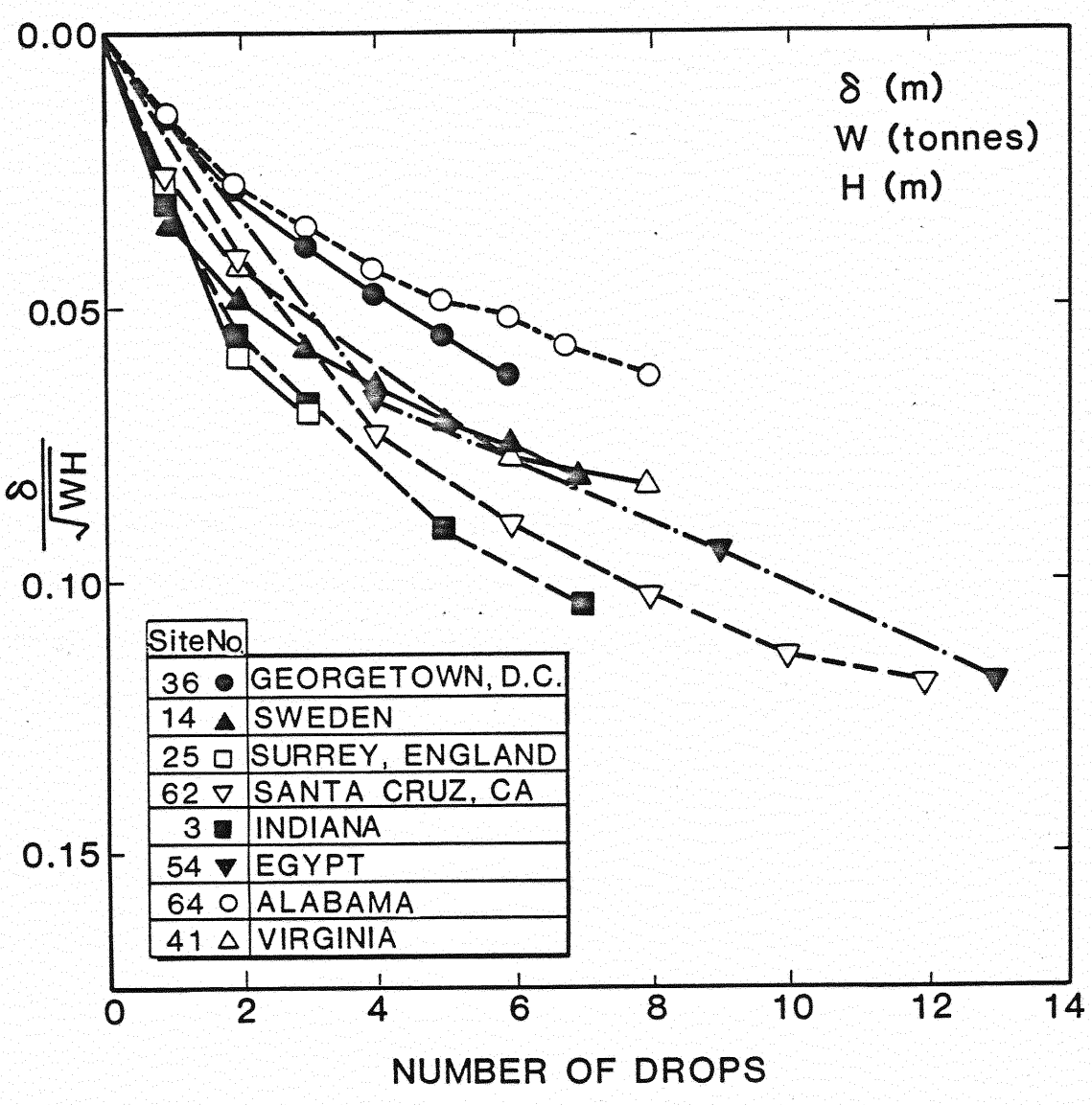

Figure 5. Normalized Crater Measurements (8)

measurements can also be used in estimating the average areal subsidence caused by the dynamic consolidation process.

Normally, after each pass of the dynamic consolidation process, the surface of the site is releveled by bulldozing the surface material into the craters. Mayne et al. (8) noted that several sites have subsided as much as 6 ft. or more after a pass. Gambin (3) shows in Figure 6 that the magnitude of ground surface subsidence is dependent upon the applied energy per unit area. Figure 7 is a review of data collected by Mayne et al. (8) showing a comparison of induced ground settlements for different soil types.

Ground Vibrations

The impact of a falling weight will cause ground surface vibrations. When a dynamic consolidation site is located in an urban environment, the level of ground vibrations becomes a major concern. Peak particle velocities (PPV) are generally used in defining damage criteria for buildings and annoyance levels to human beings. Wiss (13) gives the relationship between PPV and energy as

$$V = C(E)^{\alpha}$$

in which V = peak particle velocity, in inches per second; C = intercept, in inches per second (value of vibration amplitude at E = 1 ft-lb); E = impact energy, in foot-pounds; and α = slope, rate of increase. The value of C has been found generally to be one half. As Mayne et al. (8) show in Figure 8, the attenuation of PPV is site dependent, and is related to the scaled distance (horizontal distance, d, divided by the square root of the energy). From these data Mayne et al. (8) deduced that for preliminary estimates of ground vibration levels, a conservative upper limit appears to be

$$PPV(cm/s) \leq 7\left(\frac{\sqrt{WH}}{d}\right)^{1.4}$$

where d and H are in meters and W in tonnes.

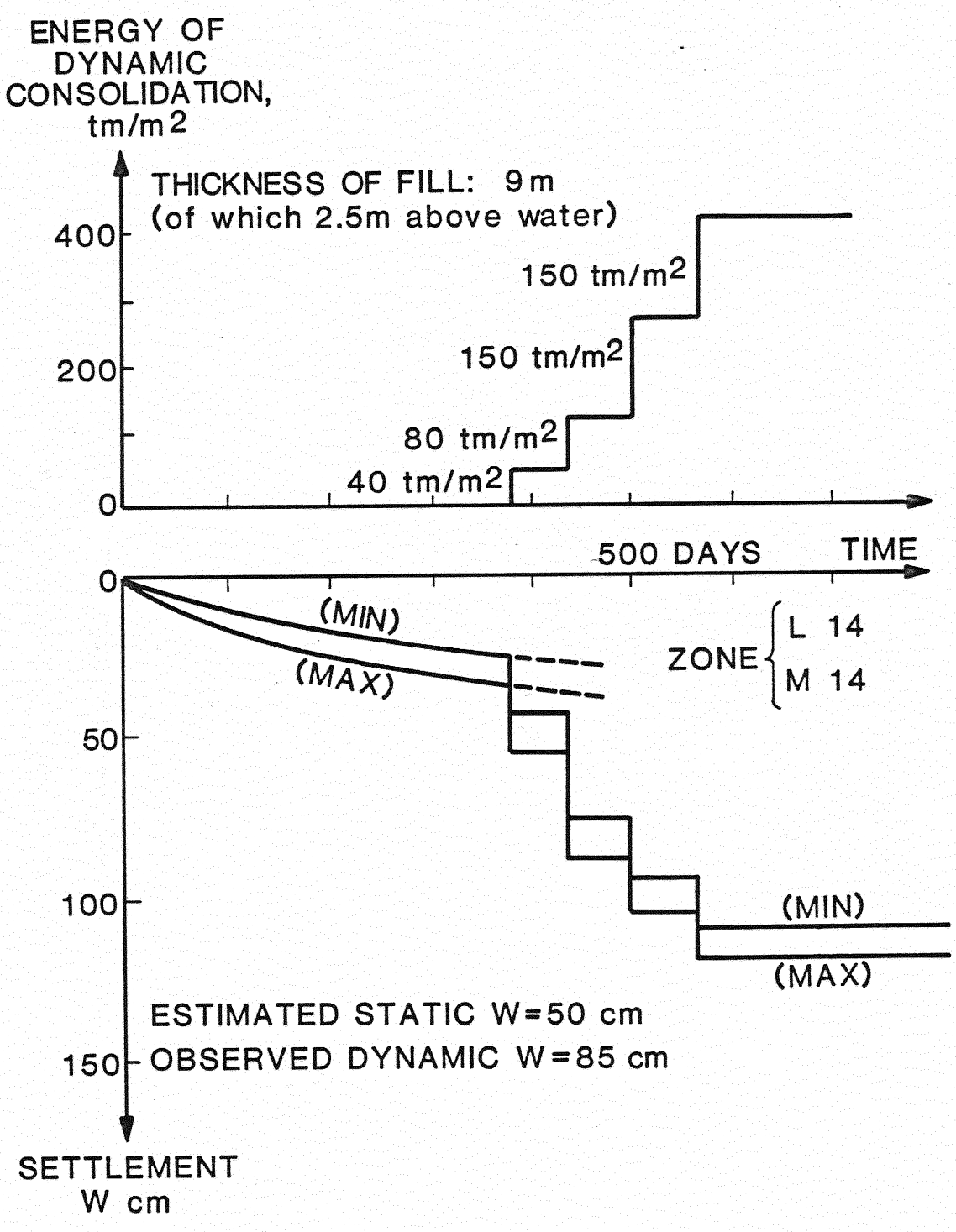

Figure 6. Settlement During Treatment (3)

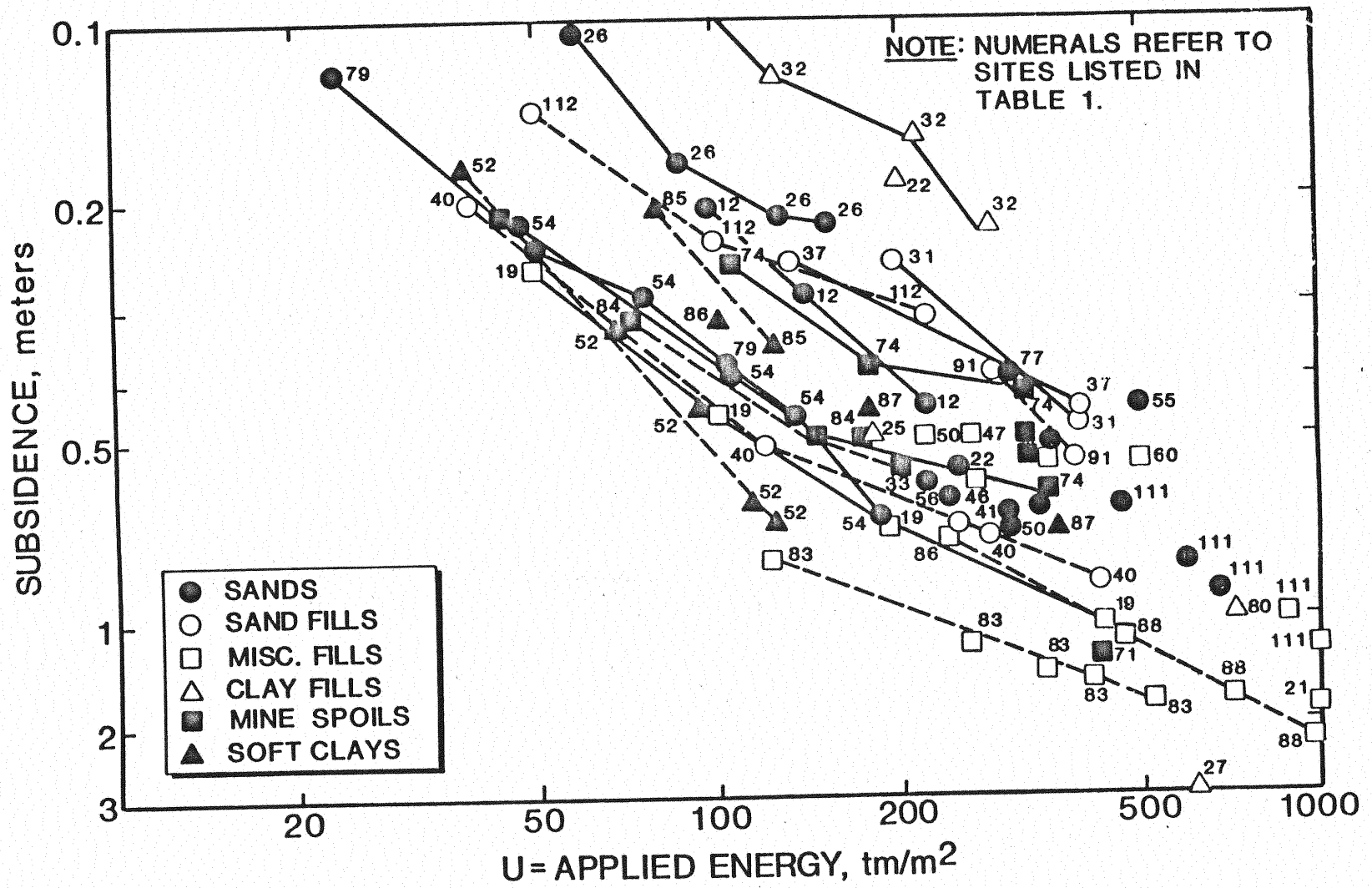

Figure 7. Observed Magnitude of Ground Subsidence With Level of Applied Energy Per Unit Area (8)

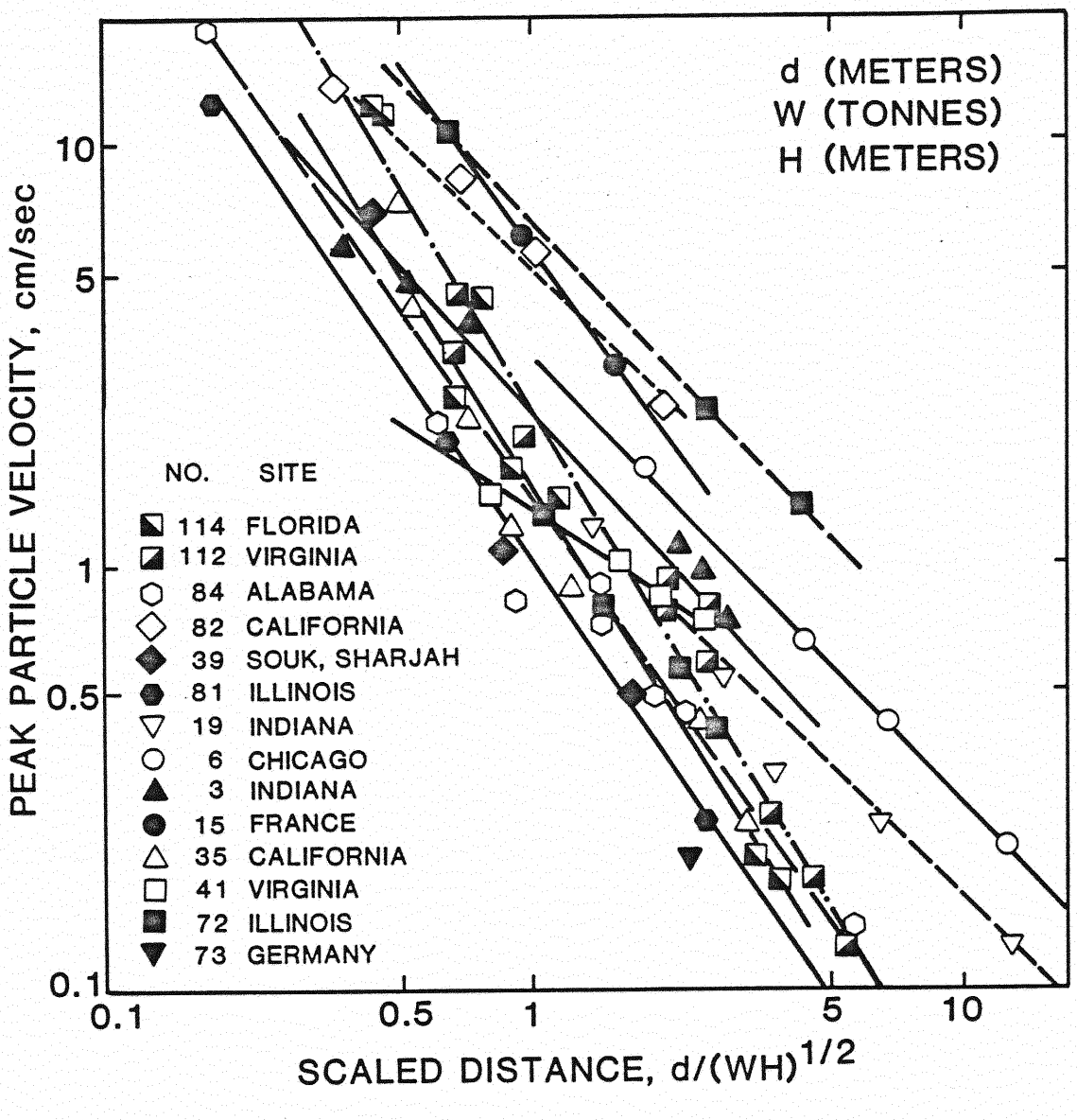

Figure 8. Attenuation of Ground Vibrations Measured on Different Dynamic Compaction Projects (8)

Dumas (1) has acquired considerable experience on the problem of vibrations at dynamic consolidation projects by recording PPV as well as the amplitude and frequency of vibrations at various distances from points of impact. In a study of over 5,000 recordings Dumas concludes that:

1. The frequencies of the vibrations vary between 2 and 12 Hertz; with the most usual values falling between 5 and 8 Hertz.
2. The wave train is weakly damped and comprises 3 to 6 waves of almost constant amplitude.
3. At a distance of 20 m from the point of impact, the vertical and horizontal PPV's remain below the value of 50 mm/sec; admissible as an acceptable limit for a dwelling construction.

Lukas (6) suggests that measurements be taken on heavy tamping projects with a portable seismograph at various distances from the point of impact during the compaction process. These data can then be plotted and used to develop the relationship between particle velocity and scaled energy. These data can be extrapolated to determine the distances that the points of impact should be kept from nearby structures to prevent damage.

Dumas et al. (2) suggests observance of the following formula to insure a safe operation:

$$\frac{\sqrt{H \times M}}{D} = 0.8$$

where:

H = height of fall in meters

M = mass of weight in tonnes

D = distance from impact in meters

Depth of Influence

Of particular interest in any dynamic consolidation project is the depth to

which the falling weight will influence the soil mass. Menard and Broise (9) suggest that the depth of influence, D, is as great as the square root of the product of weight, W, times drop height, H. Leonards (4) analyzed seven cases and reached the conclusion that

$$D = 1/2\sqrt{WH}$$

was more appropriate. However, Lukas (6) concluded that

$$D = (0.65 \text{ to } 0.80)\sqrt{WH}$$

was best suited to the eight cases that he studied. Mayne et al. (8) summarized a number of field experiences in Figure 9 and reached the conclusion that

$$D = 1/2\sqrt{WH}$$

would provide a conservative estimate of the effective depth of dynamic consolidation achieved, in most cases.

Naturally, the depth of influence is dependent upon factors in addition to the impact energy at the ground surface. Soil type will most assuredly play a very important role in determining the depth of influence. Soft layers in the soil mass will dampen the effect of the dynamic forces. Drag forces that inevitably develop as a weight is dropped using a crane make this method much less efficient than a free-fall drop. As Mayne et al. (8) show in Figure 10 (taken from a site analyzed from Massey Coal Terminal, Newport News, Virginia), the amount of ground improvement decreases with depth within a homogeneous soil layer.

It should be evident that the amount of soil improvement to be expected on any one particular site is dependent on the soil type, water conditions, and the amount of input energy per unit area. Mitchell (10) states that in his review of available cases, there appears to be a definable maximum level of improvement.

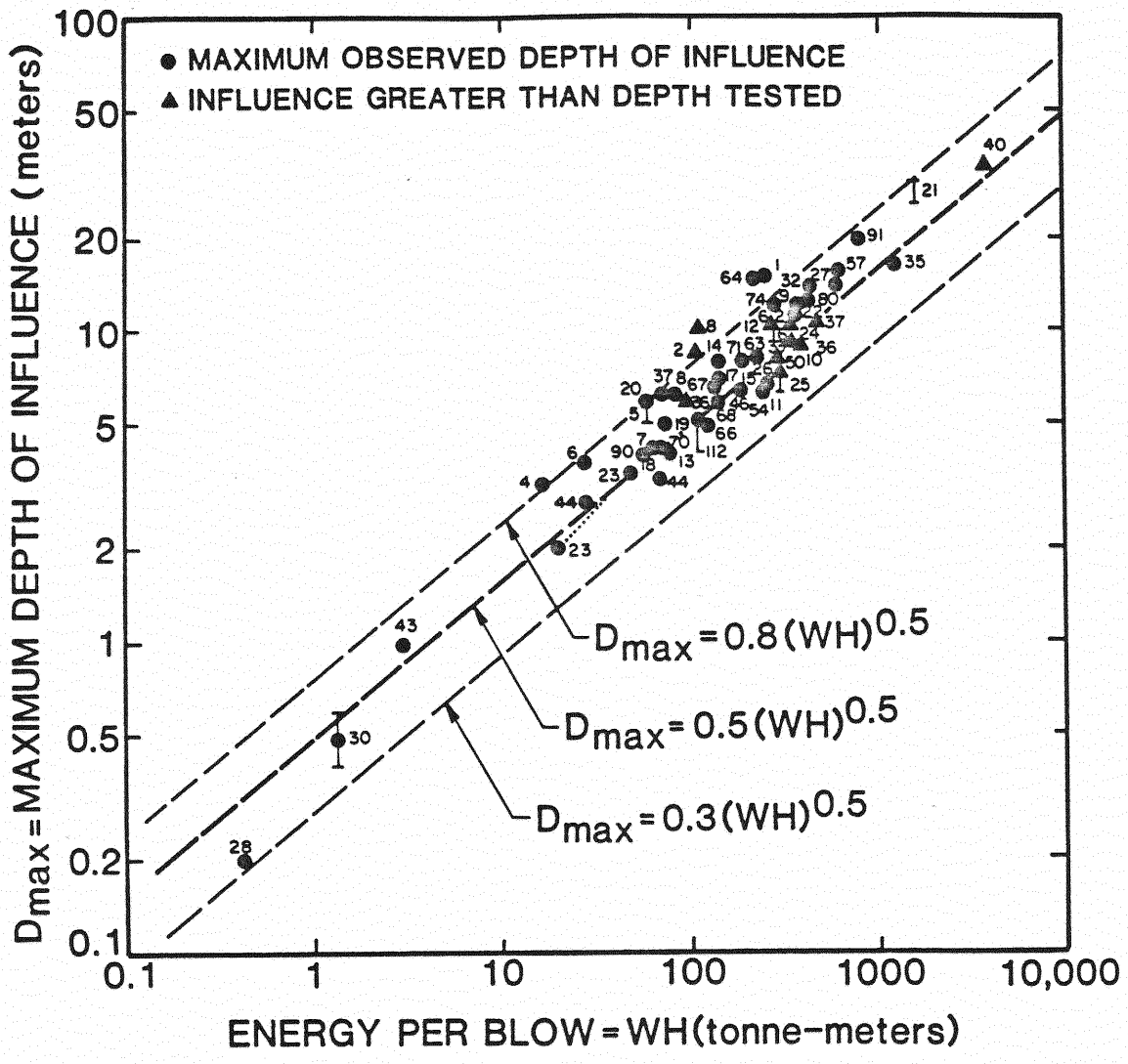

Figure 9. Trend Between Apparent Maximum Depth of Influence and Energy Per Blow (8)

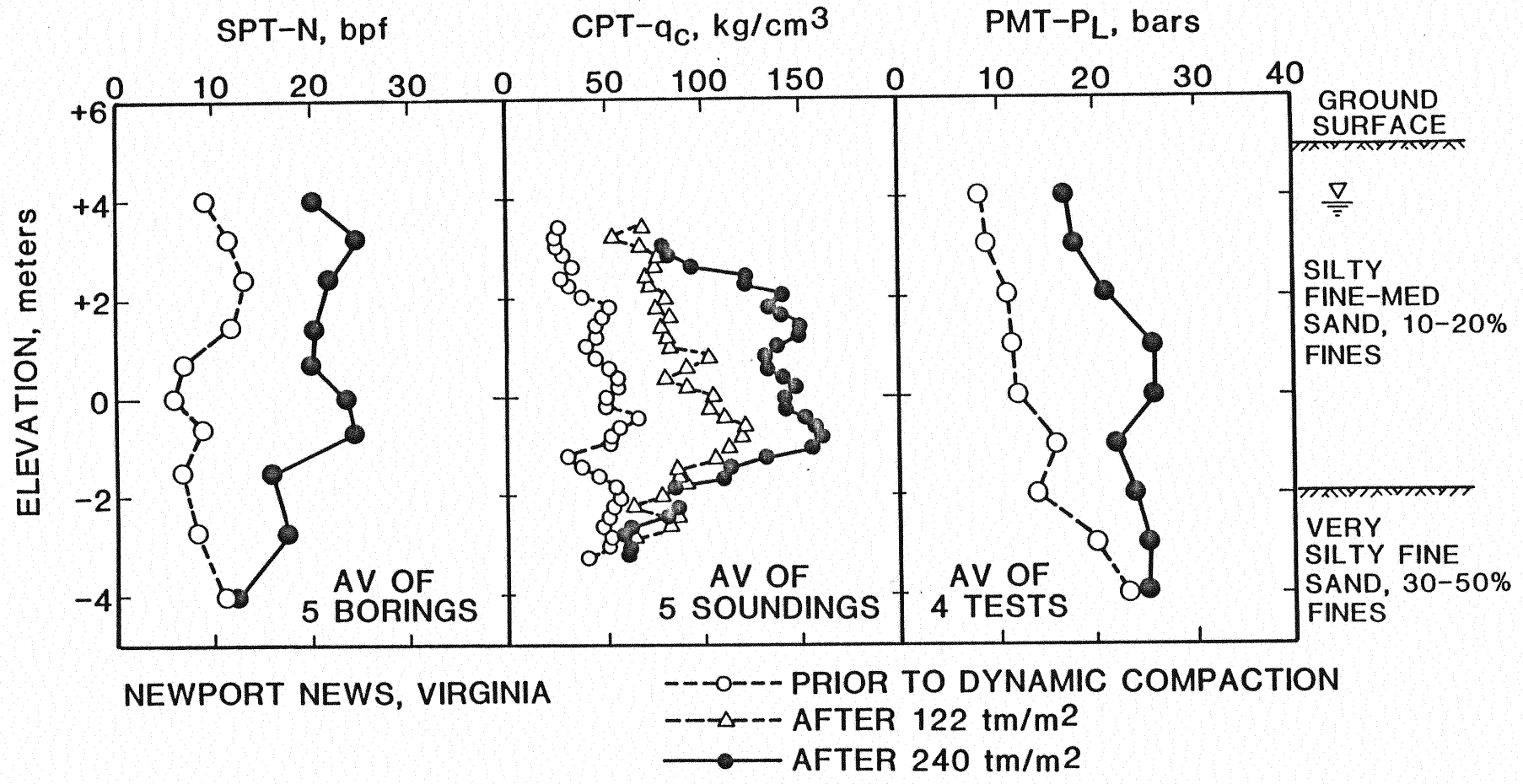

Figure 10. Degree of Improvement From Dynamic Compaction at Massey Coal Terminal, Newport News, Virginia (8)

A study of data collected by Mitchell (10) shows maximum values of cone penetration resistance of 180 kg/cm^2, standard penetration test (SPT) resistance of 45 blows/0.3 m, pressuremeter limit pressure of 3 MPa, and pressuremeter modulus of 25 MPa for clean sands. Mitchell (10) states that finer-grained more compressible soils may have maximum values that are less than half of those shown for the clean sand.

Dumas (2) reports that strength, in terms of bearing capacity, is typically improved by a factor of 2 to 4, and that compressibility, in terms of settlement, can be reduced by a factor of 2 to 10.

Lukas (6) notes from his experience that the number of coverages applied to an area does not appear to affect the depth of improvement.

Experience has shown that, when using an 18 tonne weight, once the rate of penetration is less than 0.15 meters per 2 blows with no surface heave, there is no significant ground improvement from additional blows (12). Thus, once this reduced rate of penetration has been achieved, any further impacts would be considered inefficient.

Site Reconnaissance

Menard et al. (9) note that before any site is to be considered for dynamic compaction, a soil investigation program should be set up which should include:

1. In situ testing such as pressuremeter, vane and penetrometer tests.
2. Sufficient samples to be able to determine moisture content, Atterberg limits and particle size distribution determinations.
3. Sufficient undisturbed samples for visual examination by splitting, and testing in the cyclic and dynamic oedometers.
4. Sufficient boreholes to provide a stratigraphic description representative of the site.

Another important factor to be considered at a dynamic compaction site is the location of the ground water table. High pore pressures that will be generated in fine grained soils can significantly influence the compaction program. Dumas et al. (1) noted that increased pore pressures will generally cause a rise of the ground water level, limit the amount of compactive energy that can be applied in any one pass of the compaction equipment, and cause equipment downtime where pore pressure dissipation requires delays that exceed the time of coverage. In Figure 11, Dumas et al. (1) show a typical time-pore pressure plot for a dynamically compacted sandy silt.

Besides the constraints imposed upon the compaction program, Dumas et al. (1) reported that there is no clear evidence that the water table will affect the soil's potential for improvement. Figure 12 is a typical example that shows little or no change in dynamic cone or SPT values above and below the water table for a clay fill.

Some modifications may have to be made to the compaction program if the water table is less than about two meters below the ground surface. Typically, remedial measures will include either the raising of the platform by importing materials, or installing a dewatering system to lower the ground water level.

When a dynamic compaction site is to be located in an urban environment, special attention must be given to the location and identification of all neighboring structures that could be affected by the ground vibrations. Local by-laws relating to noise and vibrations should be reviewed to insure that no legal obstacles will hamper the project.

A full scale dynamic compaction test is, of course, the most effective means of verifying the applicability of the process to a particular site. However, such tests are costly and time consuming and thus, can rarely be justified for the ordinary construction process.

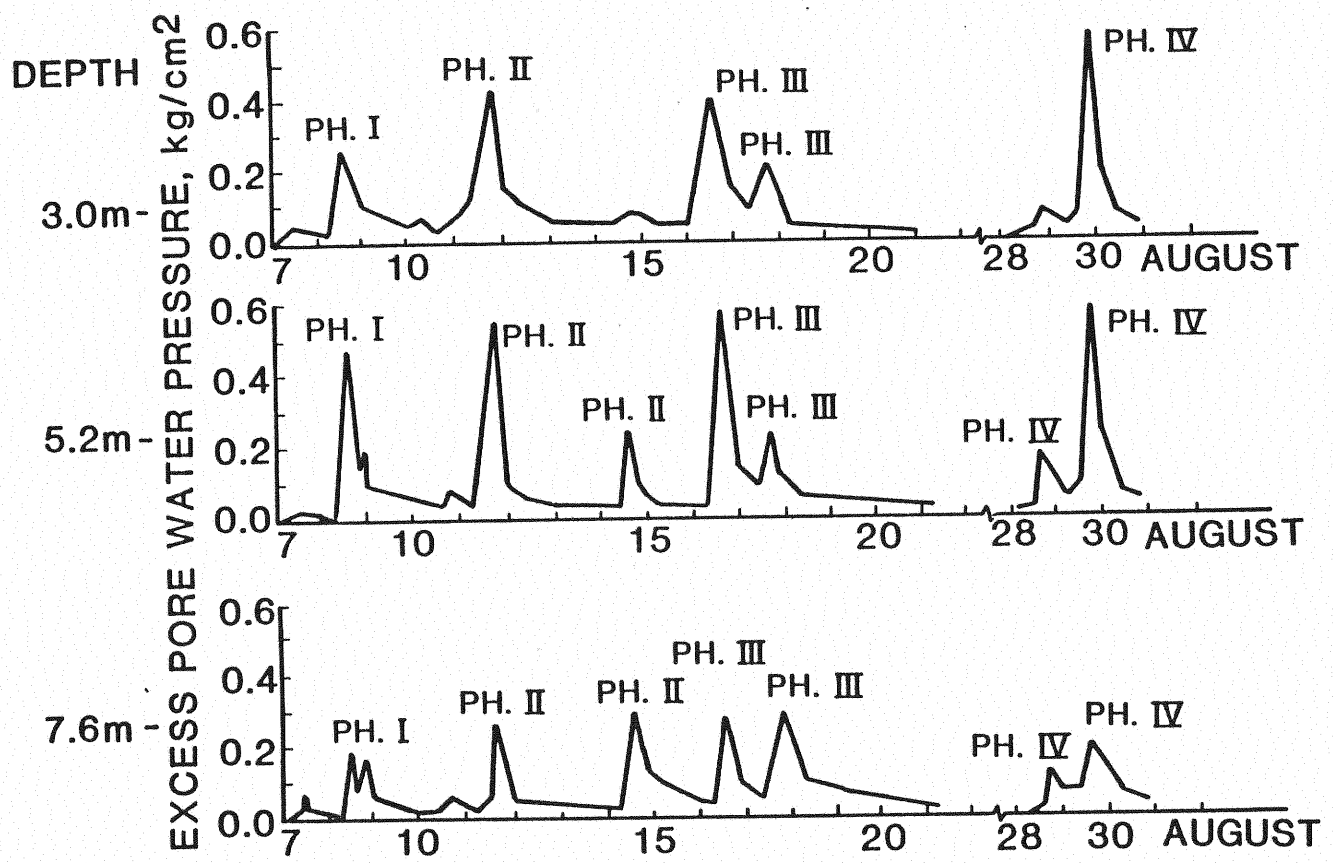

Figure 11. Typical Pore Pressures Behavior in a Sandy Silt at Chandler, Quebec (1)

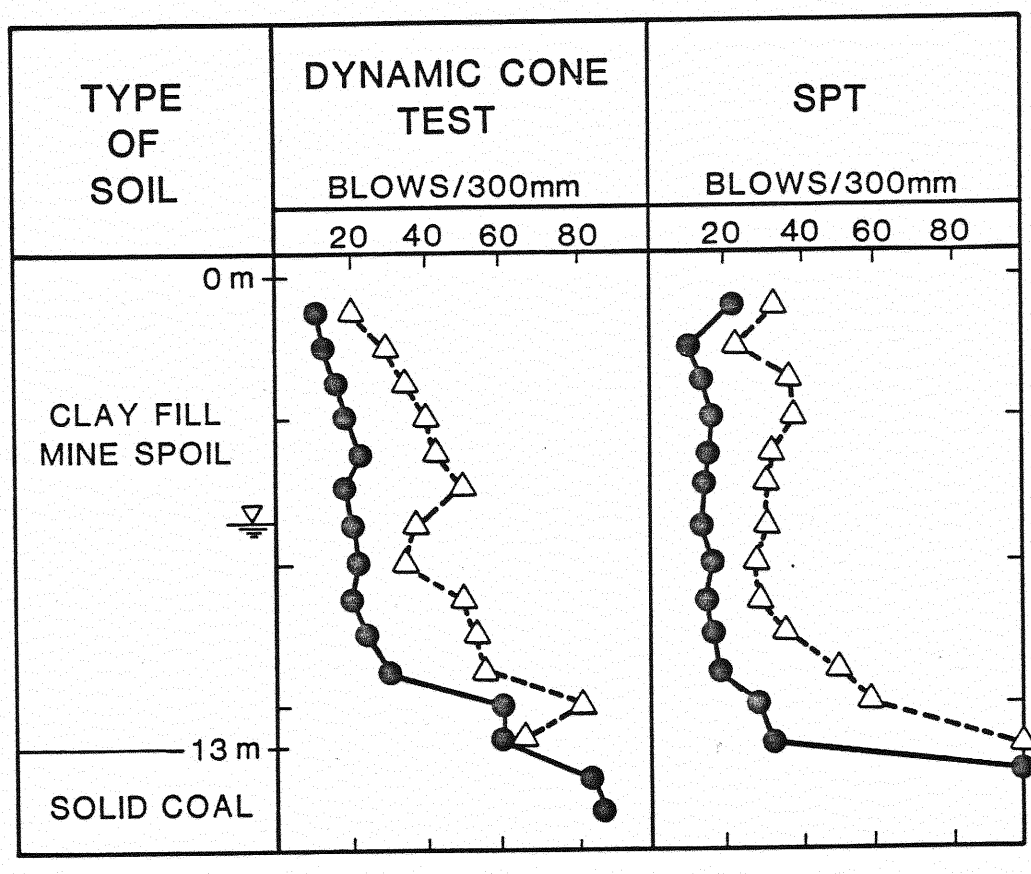

Figure 12. Average SPT and DCPT Test Results in a Clay Fill Near Edmonton, Canada. Note the Non-Influence of the Groundwater (1)

Although it may be difficult in the laboratory to simulate the behavior of the soil in the field to the dynamic compaction process, Menard et al. (9) noted that the dynamic oedometer test results have permitted a fairly accurate determination of the soil's response to the influence of tamping. The dynamic oedometer is a composite form of a triaxial apparatus and an oedometer, which permits the successive static consolidation of the sample while simultaneously transmitting static and dynamic loads to the sample. The apparatus measures, as a function of time, pore-water pressure, horizontal pressure and the corresponding settlements. Thus, the test permits the determination of the number of passes necessary to obtain the required densification, the time required for dissipation of pore-water pressure and therefore the delay between passes, the settlement to be expected under the influence of the tamping operation, and the variation in shear strength by means of a laboratory vane introduced into the sample through the upper piston.

Site Monitoring Techniques

Everyone involved with the dynamic compaction method agrees that suitable and sufficient instrumentation before the commencement of compaction, and the careful monitoring of the degree of improvement during compaction, plays a vital role in achieving the desired results. Control methods are necessary to both verify the soil characteristics of the site and to answer other needs such as research that helps those involved in the process to understand the phenomena that an impacted soil undergoes and to help define the limitations of the process in various types of material.

Dumas (1) defines two types of controls associated with the execution of dynamic compaction:

1. Geotechnical controls: these include the measurement of induced settlement, the monitoring of pore pressure variations, and the use of

in-situ tests to verify that the required soil engineering characteristics have been attained.

2. Protecting controls: this includes mainly the monitoring of the seismic response of nearby structures. However, it may also involve the measurement of total earth pressure, of the lateral displacement of the soil, and of the rotation and translation of structures which are within ten meters from the limits of compaction.

The test methods most generally used in the geotechnical control are the Standard Penetration Test (SPT), the Pressuremeter Test (PMT), the Static Cone Penetration Test (CPT), and the Dynamic Cone Penetration Test (DCPT).

Because Menard et al. (9) developed dynamic compaction into a marketable method of deep soil improvement, and because Menard also introduced PMT equipment to the geotechnical society, a large amount of data exists in terms of pressuremeter modulus and limit pressure. The PMT modulus is a measure of the soil's compressibility and the limit pressure is an indicator of the soil's shear strength.

Dumas et al. (2) suggest the consideration of the following points when determining which test method to use in analyzing compaction test results:

1. The PMT and CPT allows the most accurate determination of a soil's bearing capacity.
2. When the goal is to decrease the soil's liquefaction potential, the SPT is the favored test as it allows the determination of changes in relative density.
3. Coarse grained soils which contain heavy concentration of cobbles and boulders or heterogeneous fills containing hard construction debris and rubble cannot be reliably tested by any of the penetration test methods. With the help of some special methods to introduce the probe, the PMT might be used but the results should be considered as suspect.

Alternatively, plate load testing may be considered for critical applications.

4. With saturated silts and clays, tests that involve the rapid penetration of the probe (such as SPT and DCPT) should be avoided as they promote very high local pore pressures at the tip and thus, yield very conservative results. Tests should be performed only after excess pore pressures created by the compaction have dissipated. Pressuremeter testing should also be considered as sufficiently rapid to be affected by pore pressures, although to a lesser degree it seems than the penetration tests. The PMT will consistently show a greater improvement in fine grained soils than will the SPT or DCPT.
5. In the case of fine grained soils, at least 21 days should be allowed before proceeding with final testing. However, even this long a delay may not be sufficient as there are numerous documented cases that show the continuation of soil improvement for months following treatment.

In the case of old sanitary landfills, conventional tests such as those listed above, may not prove to be appropriate due to the highly variable range of materials and objects that may be encountered at such a site. Thus, Welsh (12) suggests that the use of a large-scale static load test to determine the compressibility before and after treatment would reflect most accurately the results of treatment.

In Figures 13 and 14, Mayne et al. (8) show that the limit pressure above the critical depth tends to increase with the level of applied energy per unit area.

Standard penetration tests and cone penetration tests are generally easier, quicker, and more economical to perform than pressuremeter tests; thus, more data are becoming available for consideration. In Figure 15, Mayne et al. (8) show the relationship between static cone resistance and the applied energy level for

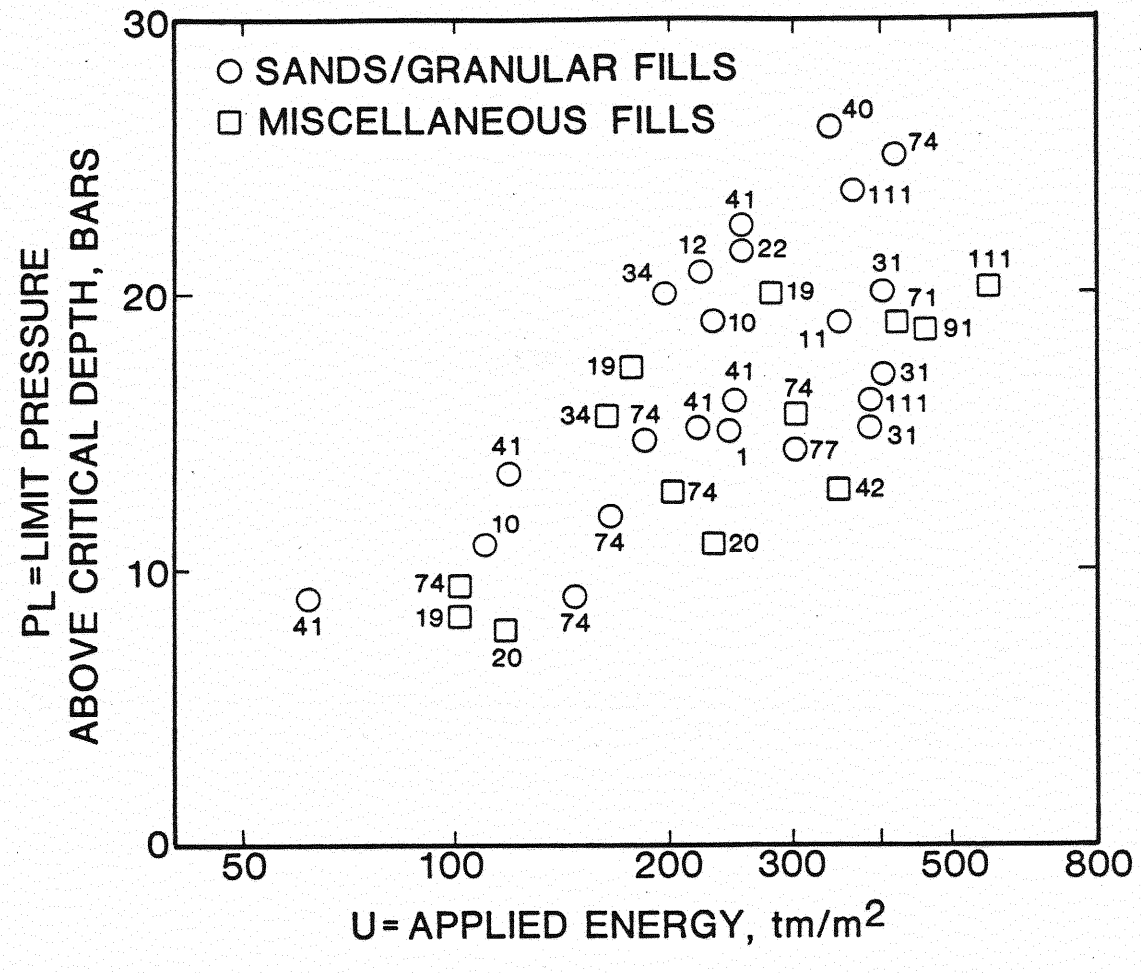

Figure 13. Observed Trend Between Limit Pressure and Applied Energy Level for Granular Soils (8)

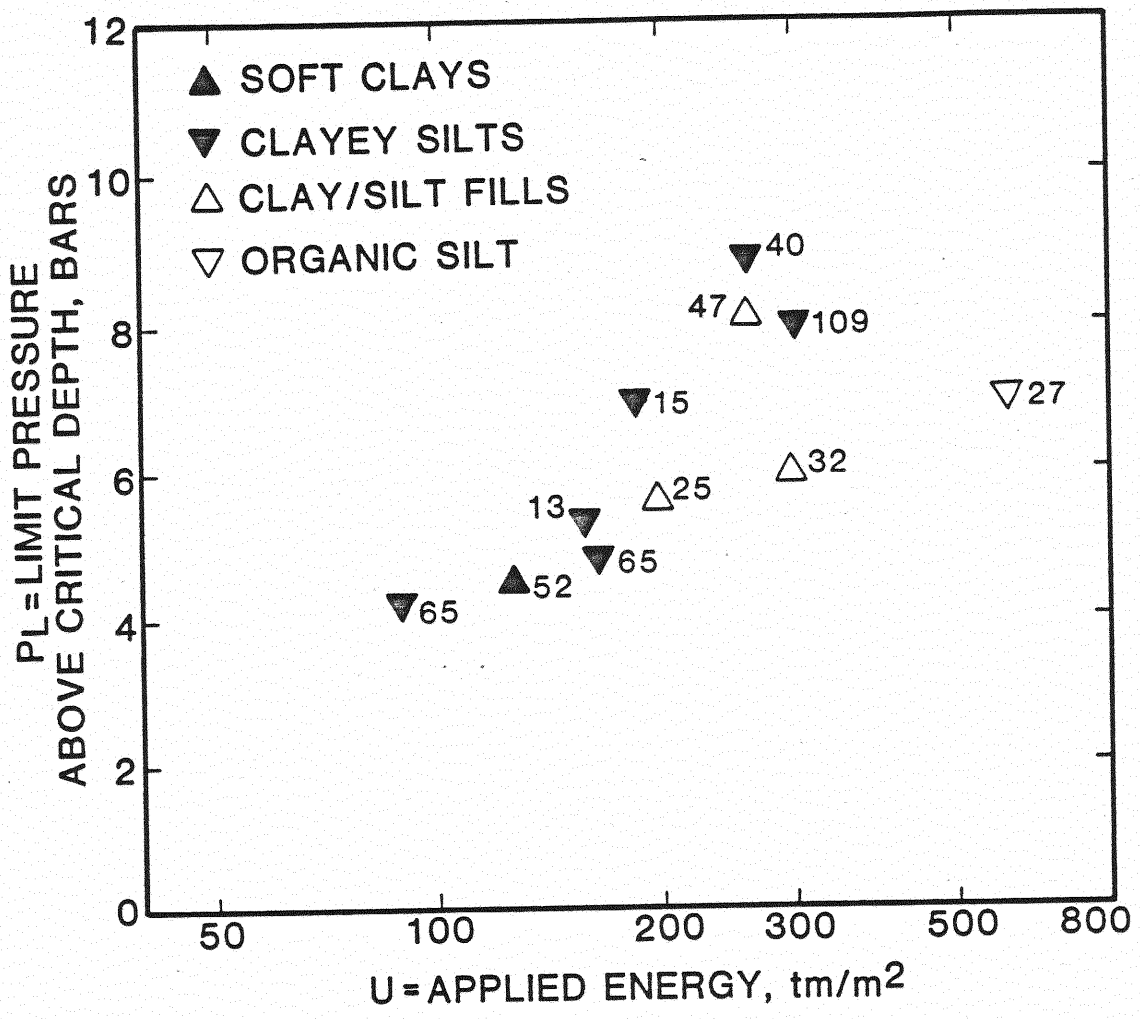

Figure 14. Observed Trend Between Limit Pressure and Applied Energy Level for Cohesive Soils (3)

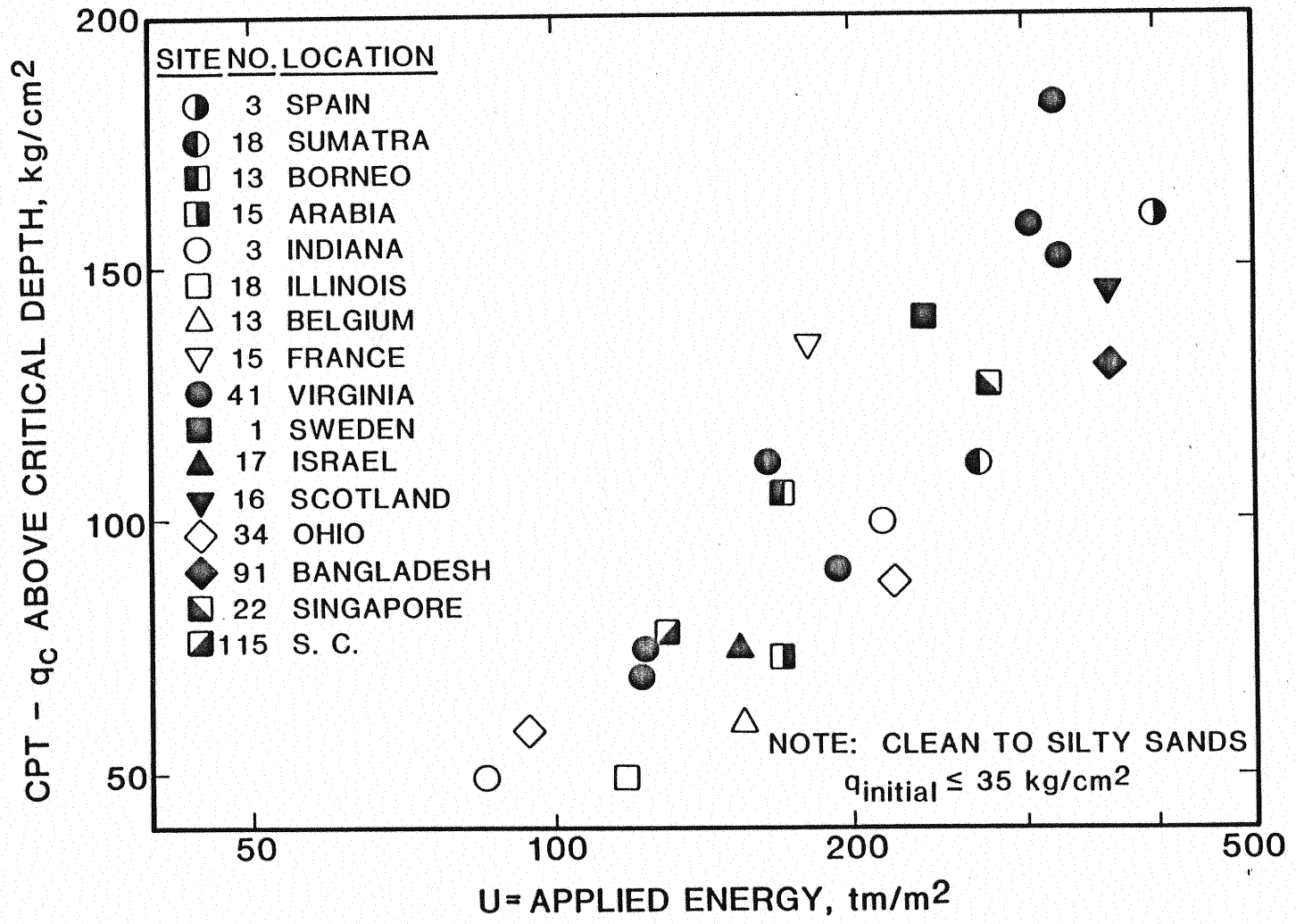

Figure 15. Relationship Between Static Cone Resistance and Applied Energy Level for Granular Soils (8)

granular soils. Figure 16 (8) shows the relationship between the SPT-N value and the applied energy per unit area for various sites.

For the measurement of pore-water pressure, piezometers are generally installed in the ground at different levels in the immediate proximity of the areas to be compacted. Thus, it becomes possible to check when the pore-water pressure rises to the level where the soil becomes liquefied. Furthermore, by means of the measurements made, it is possible to observe how rapidly the excess pore-water pressure dissipates. In fine-grained soils it is most important to allow sufficient time for excess pore water dissipation. At a site with subsurfce conditions consisting of peaty clay, three to four weeks were allowed for the dissipation of pore water pressure between passes (11).

Some means of measuring the total vertical settlement resulting from the heavy tamping will be necessary at each site. Generally, surveying equipment is sufficient to determine the total amount of settlement. Readings should be taken after each pass has been completed and the site releveled with a bulldozer. In some instances, settlement gauges are installed at various places over the site. These become practical when there arises a need to measure the long-term settlement of the project. Long-term settlement may be of interest when compacting old sanitary landfills.

Summary

Dynamic compaction is a powerful deep soil improvement technique that involves the dropping of a heavy weight a predetermined distance to impact the soil. The degree of compaction achieved depends on the energy per drop as well as the sequence of drop points and number of drops per point. Other factors to be considered are the soil type and location of the ground water table, environment, the method of control, and the equipment used to perform the tamping. The ultimate goals of dynamic compaction are the improvement of bearing capacity

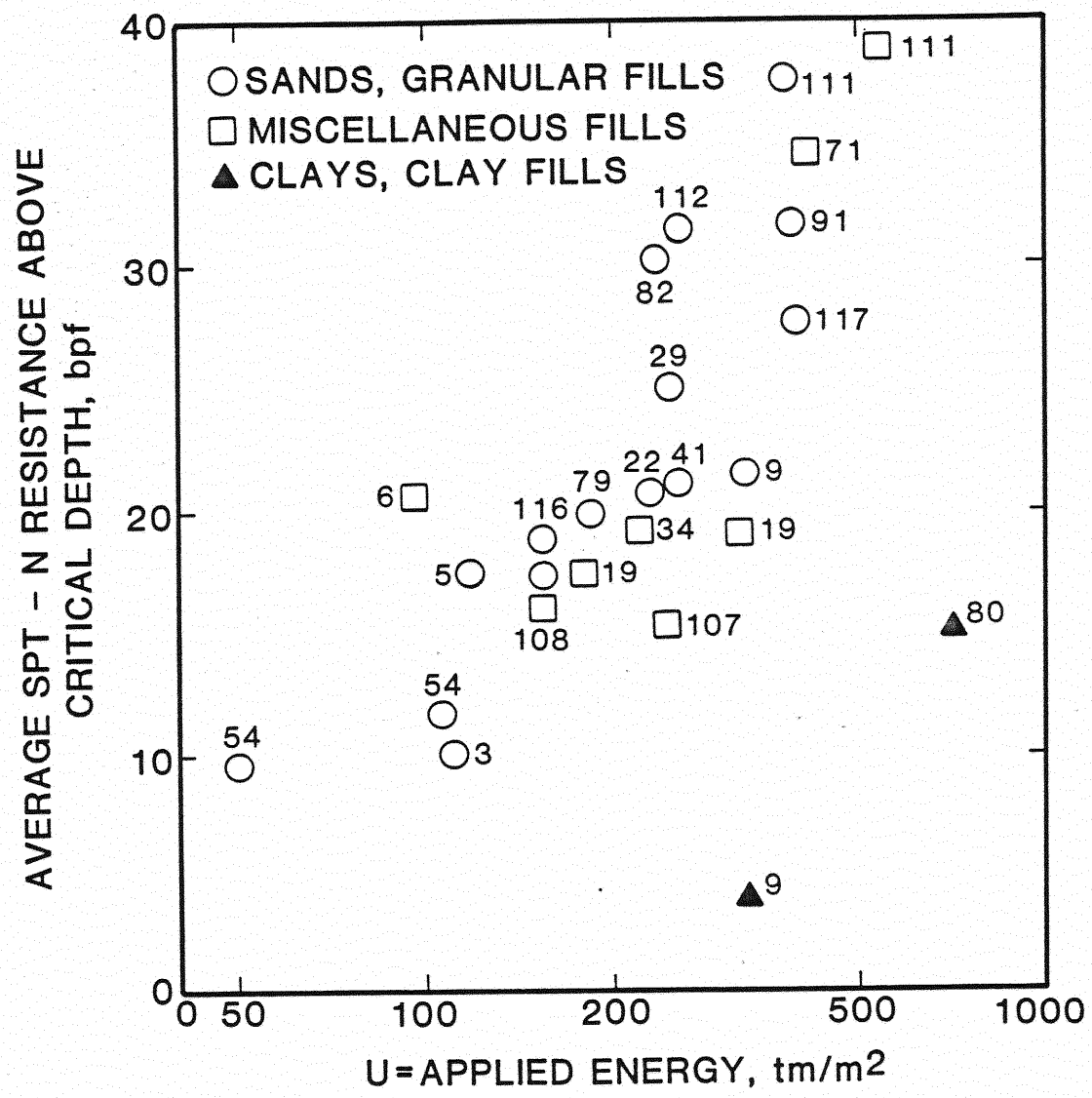

Figure 16. Observed Trend Between SPT-N Value and Applied Energy Per Unit Area (8)

and a decrease in differential settlement. As the technology continues to move forward, it is being found that dynamic compaction is applicable to more and more different soil conditions.

CHAPTER III

TEST SECTIONS: CONSTRUCTION, INSTRUMENTATION, MONITORING

Project Parameters

The proposed Gilcrease Expressway in Tulsa, Oklahoma, is an extension of the existing State Highway 11 and begins approximately three-tenths of a mile west of Sheridan Road on Apache Street, proceeds northwest to Yale Avenue, and continues west to the proposed Keystone Expressway extension (Figure 17).

The roadway alignment crosses an abandoned coal strip mine at Yale Avenue between stations 164+00 and 190+50. No documented evidence on the mining operation was obtained but the Oklahoma Department of Transportation (ODOT) accounts for activity during the 1930's and 1940's. Subsequent to strip mining, the area was used as an uncontrolled sanitary landfill. The mine spoil extends to depths of up to 45 feet below the existing grade. The existing ground surface varies from approximately 670 feet mean sea level (MSL) on the east-quarter to 629 feet MSL on the west end of the project. The project area is essentially all a fill zone with the maximum height of embankment being approximately 30 feet above the existing grade.

The roadway will be a standard four-lane divided highway with an interchange at Yale Avenue. The interchange will consist of exit and entrance ramps to and from Yale Avenue along with a bridge over Yale Avenue.

Surficial Features

The existing terrain in the project area consists of a series of ridges and valleys formed by the strip mining operation. East of Yale Avenue the ridges and

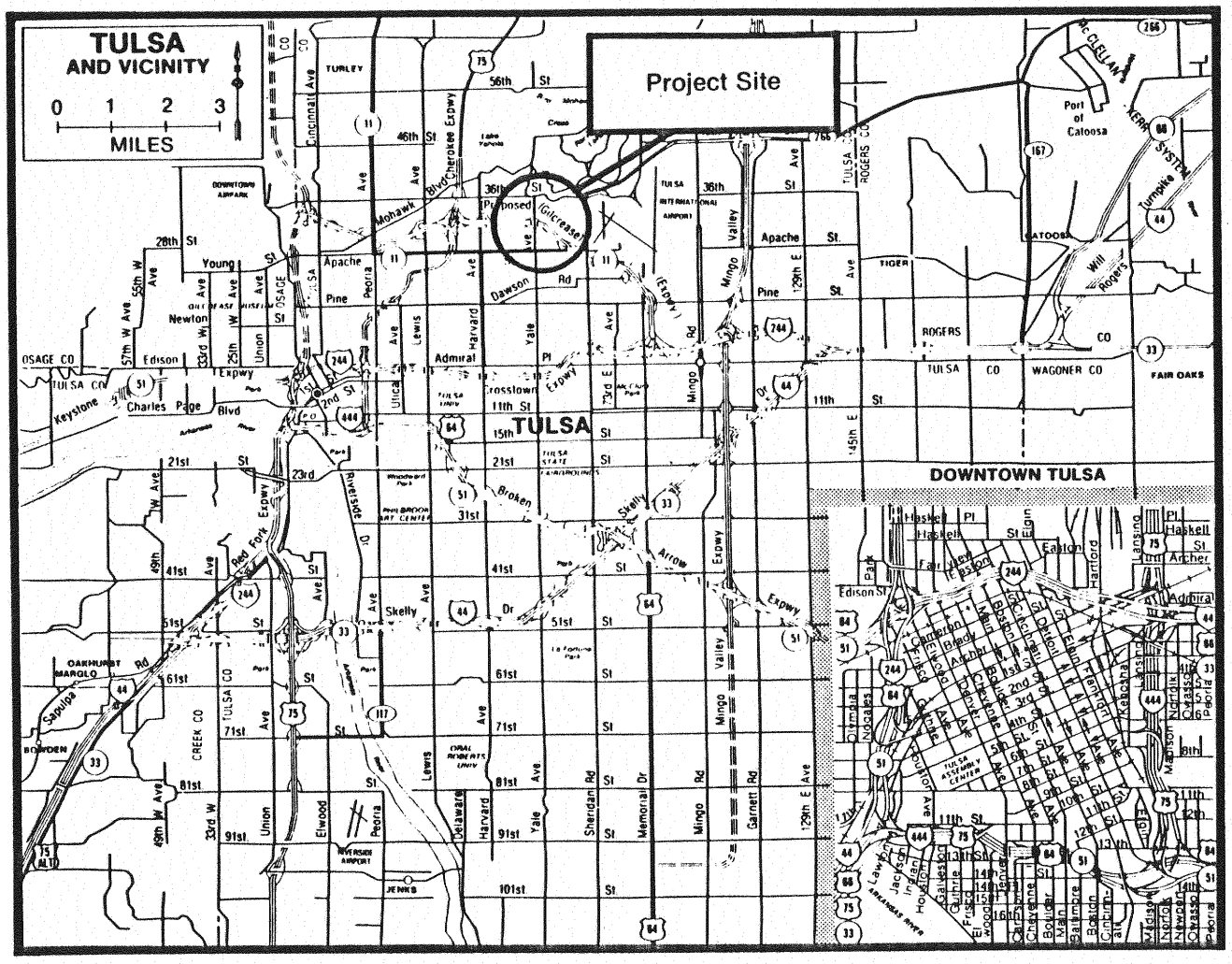

Figure 17. Proposed Gilcrease Expressway

valleys were oriented in an approximately north-south direction, while west of Yale they were oriented in an east-west direction with a less pronounced shape. Randomly deposited trash was found throughout the site primarily in the valleys and along trails. Large vegetation, such as trees and bushes, were found west of Yale which indicates a more undisturbed state. Also on the west side of Yale, there appears to have been some site grading which may have resulted from the burying of trash. Yet another interesting feature west of Yale was the high ground water table between Stations 164+00 and 169+00. In some instances this ground water table was only two or three feet below the surface of the ground.

Geologic Setting

The project lies within the Claremore Cuesta Plains physiographic province and is underlain by the Seminole geologic unit of Pennsylvanian age. The formation dips from east to west at approximately 20 ft/mile and drains to the west and southwest. The sub-unit of the Seminole formation from which the thin coal seam was mined is an unnamed shale member of the Lower Seminole unit. The unconsolidated mine spoil was comprised primarily of residual clay and shale overburden of the above sub-unit that was removed during the mining operation.

Subsurface Exploration

A geotechnical investigation of the site was performed by the ODOT. The investigation included 67 test holes, two cuts along the centerline into the spoil bank ridges with a bulldozer, and numerous field and laboratory tests.

In general, the boring logs indicated the existence of the strip mine spoil and underlying geology. Some of the borings revealed that, through the mining process, the lower Seminole sandstone was exposed. At other locations, the strip mine spoil was underlain by the remaining portion of the unnamed shale in the

lower Seminole unit. Difficulty in the drilling process was encountered between Stations 182+50 and 190+50 because of the heterogeneity and moisture content of the mixed lean clay and trash. There were other random locations throughout the site where small voids could be detected through the observation and feel of the drilling rig as the boring was advanced.

To help characterize the consistency of the spoil material ten SPT borings were made across the site. Based on the data collected, the ODOT estimated an 'N' value of less than 38 for the spoil matrix consisting of clays and highly weathered shales. Generally, test data from the boring logs revealed that the spoil was classified as a lean clay with low plasticity characteristics and moisture contents in many instances near the plastic limit.

Compaction Equipment Parameters

ODOT special provisions for this project required that the crane used in compaction have a minimum capacity of 100 tons, must be capable of lifting a 20 ton weight with a single line to a height of 80 feet, and have a free spooling drum to allow a free-fall of the weight. The boom was to be of sufficient length to allow the weight to drop far enough from the crane to prevent undue disturbance of the crane. A smaller crane was allowed for the ironing pass. Figure 18 is a photograph of the actual crane used on this project.

A bulldozer was required throughout the dynamic compaction operation to fill the impact craters and maintain grade.

A circular weight weighing approximately 18 tons was used for compaction. The weight had a minimum contact pressure of 1,000 pounds per square foot. Figure 19 shows a schematic of the weight with the required dimensions. A square weight, with a seven foot square base, weighing eight tons and having a contact pressure of 200 to 300 pounds per square foot was used for the final ironing pass (Figure 19).

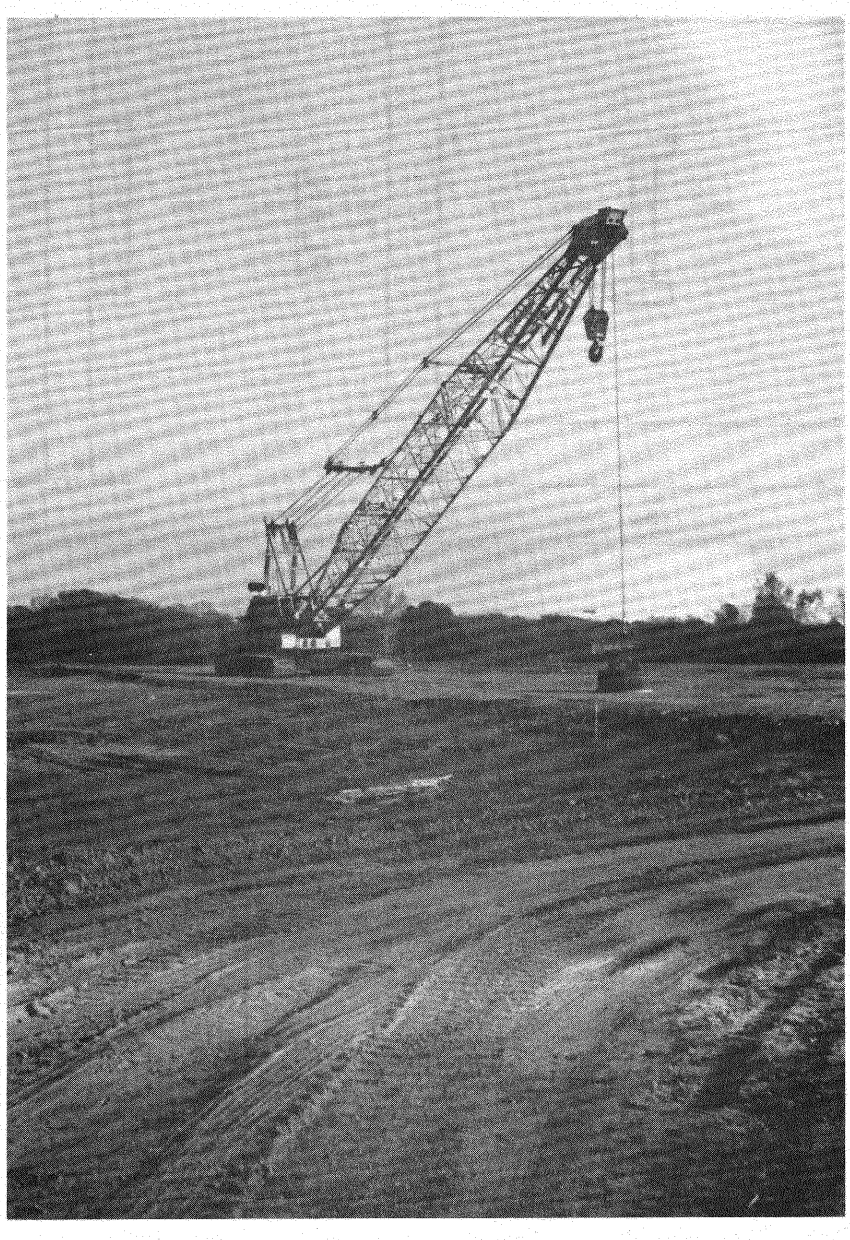

Figure 18. Photograph of Crane Used on Project

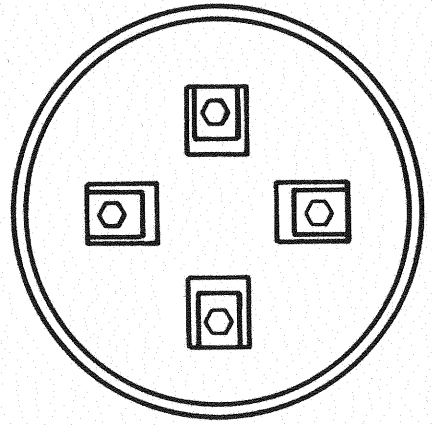

PLAN

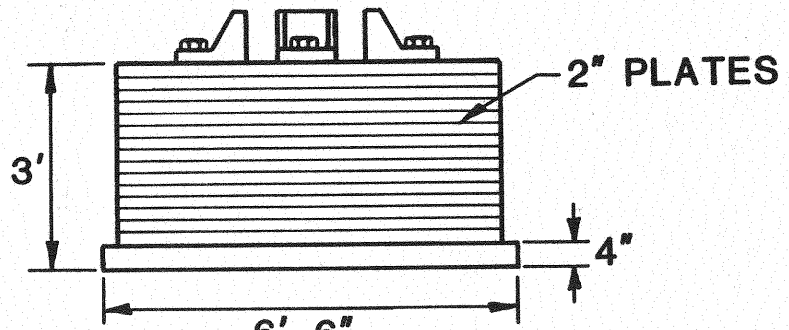

ELEVATION

DYNAMIC CONSOLIDATION WEIGHT
18 TON

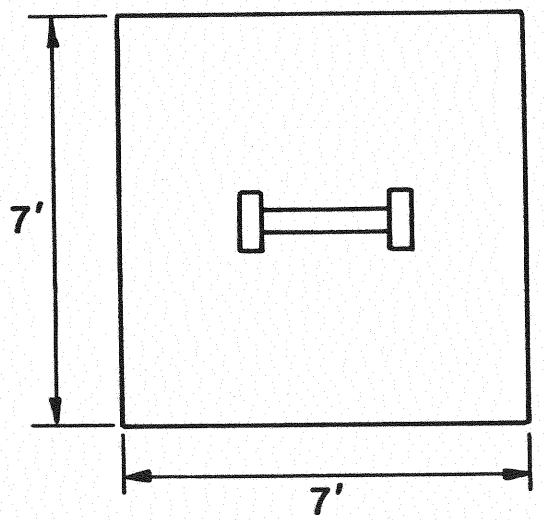

PLAN

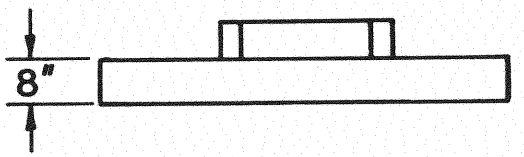

ELEVATION

IRONING CONSOLIDATION WEIGHT
8 TON

Figure 19. Weights Used for Compaction

Construction Methods

The following operational procedures were intended as guides only and were adjusted according to the results obtained from the three test sections. Grid spacing of impact points during a pass was 30 feet plus or minus five feet. The number of drops at each impact point varied from six to eight. After each pass the impact point craters were backfilled with the surrounding material and the area leveled by the bulldozer. Eight consolidation passes were made across the site.

Preliminary findings indicated that Passes No. 1 through 4 would require the dropping of an 18 ton weight from a height of 75 feet, eight times in the same impact point. This provided an equivalent energy equal to 48 ton feet per square foot. Passes No. 5 through 8 each required six drops per impact point from a height of 75 feet for an added energy of 36 ton feet per square foot. The ironing pass was performed with an eight ton weight dropped 20 feet with a 2/3 overlap of each impact point, providing an energy input of 9.8 ton feet per square foot. This provided a total energy input of 93.8 ton feet per square foot.

Impact Pass No. 1 was to begin at the west edge of test section No. 1 on the CRL and proceed to the south on a line at 30 feet intervals, to the outer limits of the area to be compacted. The crane was then to return to the first impact point and proceed to the north in a like manner, to the outer limit of the area to be compacted. This would complete one line of pass No. 1. This procedure was then repeated at the next line (30 feet west) and the process continued to the west until all lines of pass No. 1 were completed to the east edge of Yale Avenue. The remaining passes were to be performed in a like manner as described for pass No. 1.

Compaction on Yale Avenue and east of Yale Avenue was to be completed before compaction work was to begin to the west of Yale Avenue.

Before the ironing pass was begun, test drops for acceptance were to be performed in locations to be determined by the Engineer. The test drops consisted of four drops of the 18 ton weight from a height of 40 feet. Elevations were to be taken atop the weight before the first drop and averaged to determine a reference elevation. The amount of penetration on the last three drops was to be established. Subject to test procedure modification, penetration not exceeding a cumulative total of four inches for the three drops would indicate sufficient compaction to proceed with the ironing pass. If more than four inches of penetration occurred from the three drops, additional dynamic compaction would be required.

Test Section No. 1

Test Section Parameters

Test Section No. 1 was located at Station 179+00 and from the plans provided by the Project Engineer, it can be seen that this test section was on the edge of a ridge of natural material. This test section was located beneath the deepest section of an embankment to be built on a future contract and represents the conditions that exist between Stations 172+00 and 181+00. Borings provided by the ODOT indicated the presence of mine spoil, consisting of a silty clay with shale fragments, from the surface to bedrock in this area. A hard weathered shale with small limestone seams was located at depths ranging from approximately 24 feet to 43 feet in this test area. A two to three foot thick layer of crusher-run limestone rock with a maximum size of 10 inches was placed over the test area prior to compaction.

Instrumentation

Prior to compaction and subsequent to the placement of the rock platform, a

subcontractor drilled three test holes for the purpose of performing Standard Penetration Tests (SPT) at various depths. The first boring was located at Station 179+00 on the centerline (CRL). The second boring was located 30 feet to the south of the CRL at Station 179+00 while the third boring was located 30 feet to the north of the CRL at the same station. Due to an error in the location of these test holes, they were located 15 feet further from the centerline than originally planned.

While at the site, the subcontractor was also responsible for installing the inclinometers and piezometers. Three inclinometers were placed along the CRL at Stations 178+97.5, 179+02.5, and 179+12.5. All three inclinometers were founded in the bedrock. Inclinometer No. 1 (Station 178+97.5) was installed to a depth of 44 feet, while the other two inclinometers reached a depth of 46 feet. The inclinometer equipment used for this project was manufactured by the Slope Indicator Company (SINCO). The Digitilt Recorder-Processor-Printer (RPP) Inclinometer System consists of a movable Digitilt Sensor, a portable RPP Indicator (Model 50368), an interconnecting electrical cable, and a Slope Indicator inclinometer guide casing that was permanently installed in the ground. A schematic of the Inclinometer set-up is shown in Figure 20.

The two piezometers were set immediately above the undisturbed shale. Due to an error in location, the piezometers were set 15 feet further from the CRL than originally planned. One piezometer was set 30 feet to the north of the CRL at Station 179+15 while the second piezometer was set 30 feet to the south of the CRL at Station 178+85. The piezometers used in this project were also produced by the SINCO. The Electrical Piezometer System consisted of the digital indicator (Model 56449), the transducer, and the interconnecting electrical cable. Figure 21 is a schematic of the piezometer set-up.

Other instrumentation used at the site consisted of a level and level rod used to check the crater depth versus impact at each drop point. On predetermined

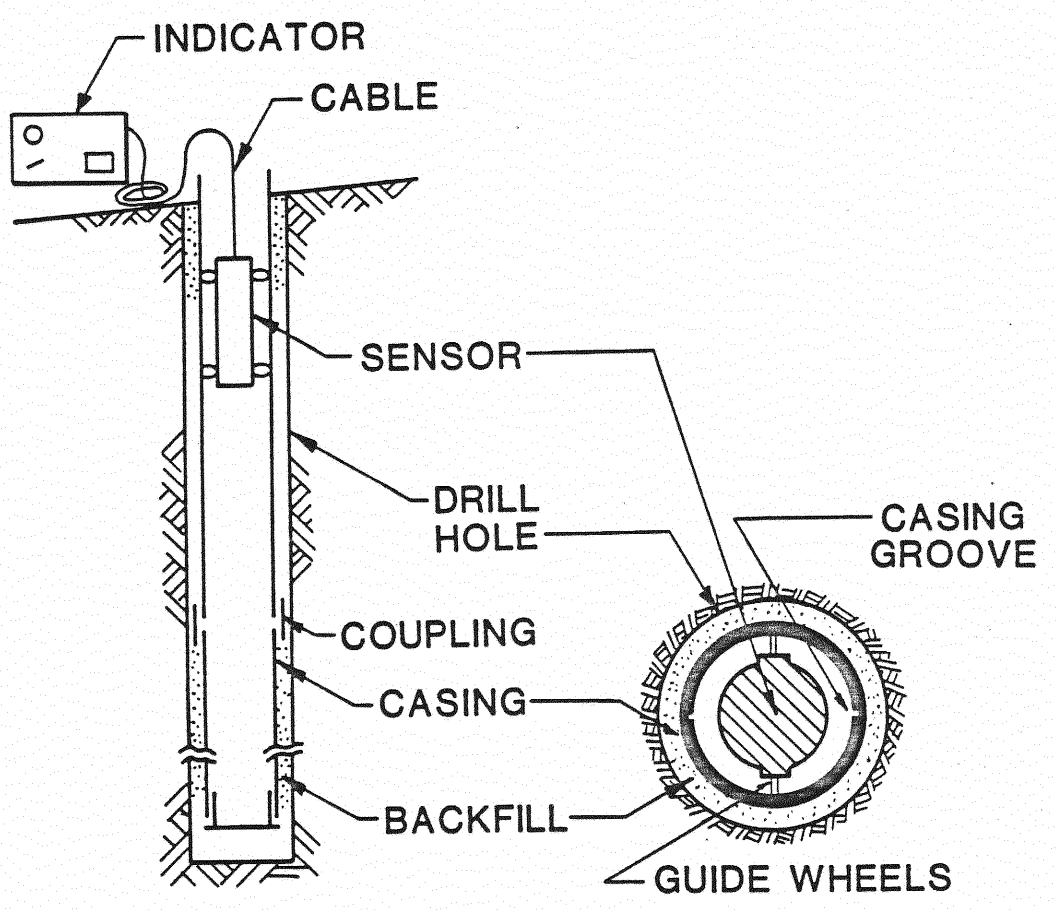

Figure 20. Inclinometer Set-Up

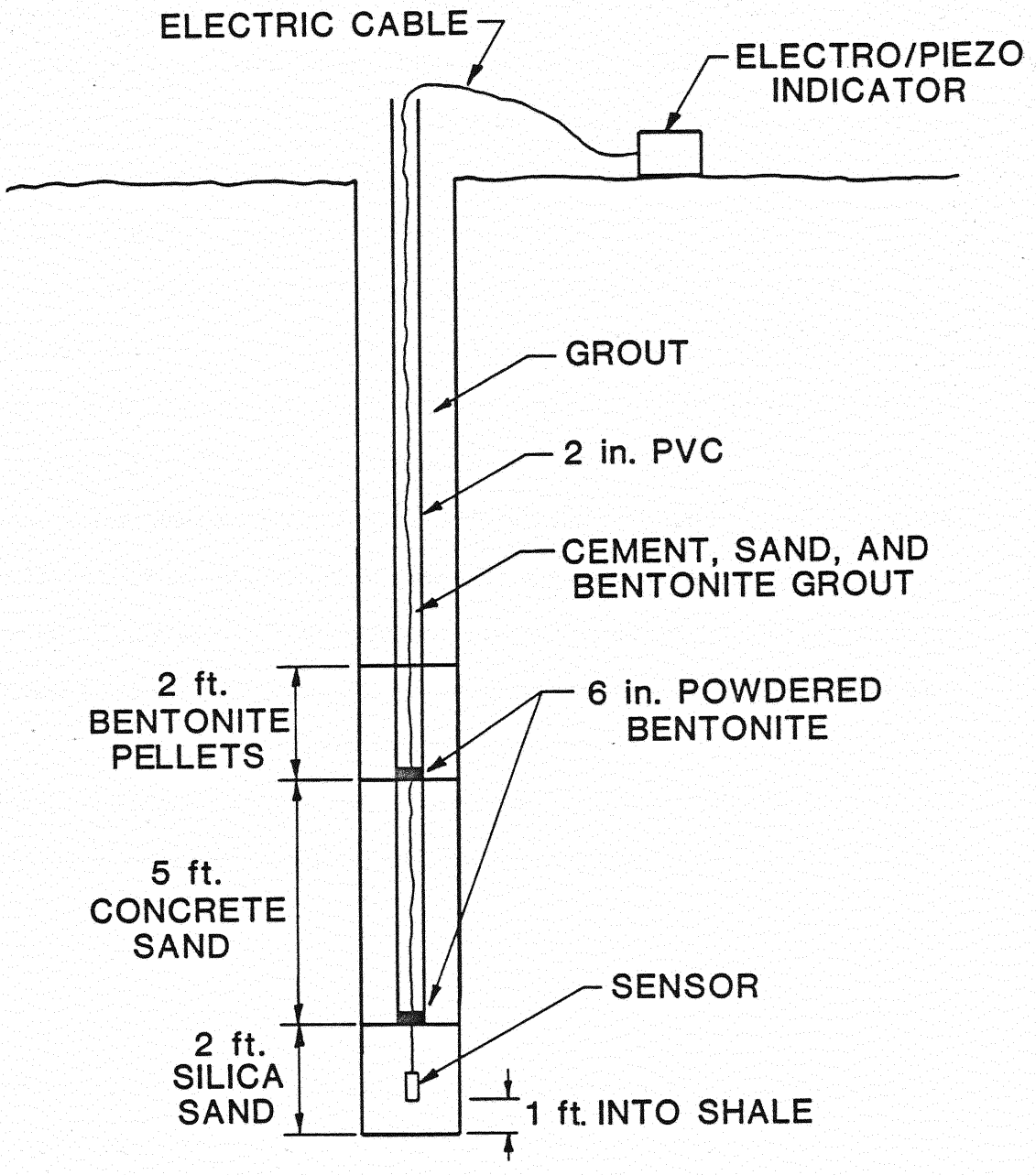

Figure 21. Piezometer Set-Up

impact points, the depth of the crater was determined after each drop of the weight. To eliminate, as much as possible, the effect of spalling of the crater sides, readings were taken before the weight was removed from the crater. Care was taken as to where the level rod was placed on the weight as sometimes the weight would hit the side of the crater when being dropped and come to rest in a tilted position at the bottom of the crater. To eliminate as much of this error as possible, readings were always taken at the middle of the weight. However, a slight problem also arose in being able to actually place the level rod onto the weight. As the number of impacts at a drop point increased, a layer of rock and mine spoil would build up on top of the weight. An attempt was always made to remove this layer of build-up but the attempt was not always successful.

The level and level rod were also used to determine the amount of surface heave across the test section after all compaction was completed. Initial readings were taken parallel and perpendicular to the CRL before compaction was started and then again after the completion of the compaction.

A layout of the test section with the appropriate instrumentation is shown in Figure 22. Figure 23 is a photograph showing the instrumentation as set up in the field.

Testing Procedure

Because of a misinterpretation of the impact sequence by OSU personnel, this test section did not exactly follow the impact sequence suggested by the Design Engineer. The actual impact sequence followed in this test section was as shown in Figure 24a with the impact sequence as suggested by the Design Engineer as shown in Figure 24b. However, it should be noted that the set spacing of approximately 30 feet between centers of the impact points for a particular pass was observed.

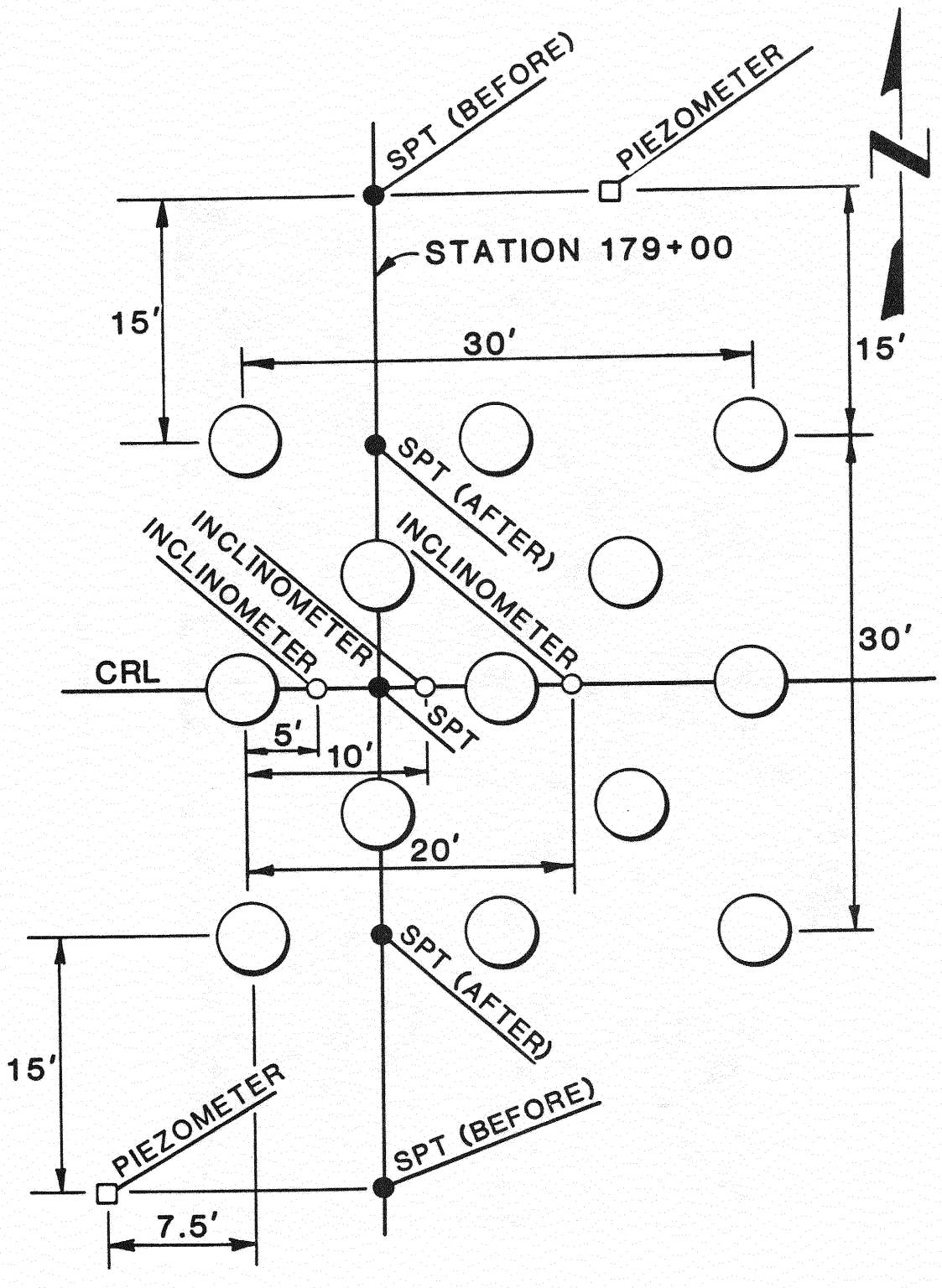

Figure 22. Test Section No. 1 Instrumentation Layout

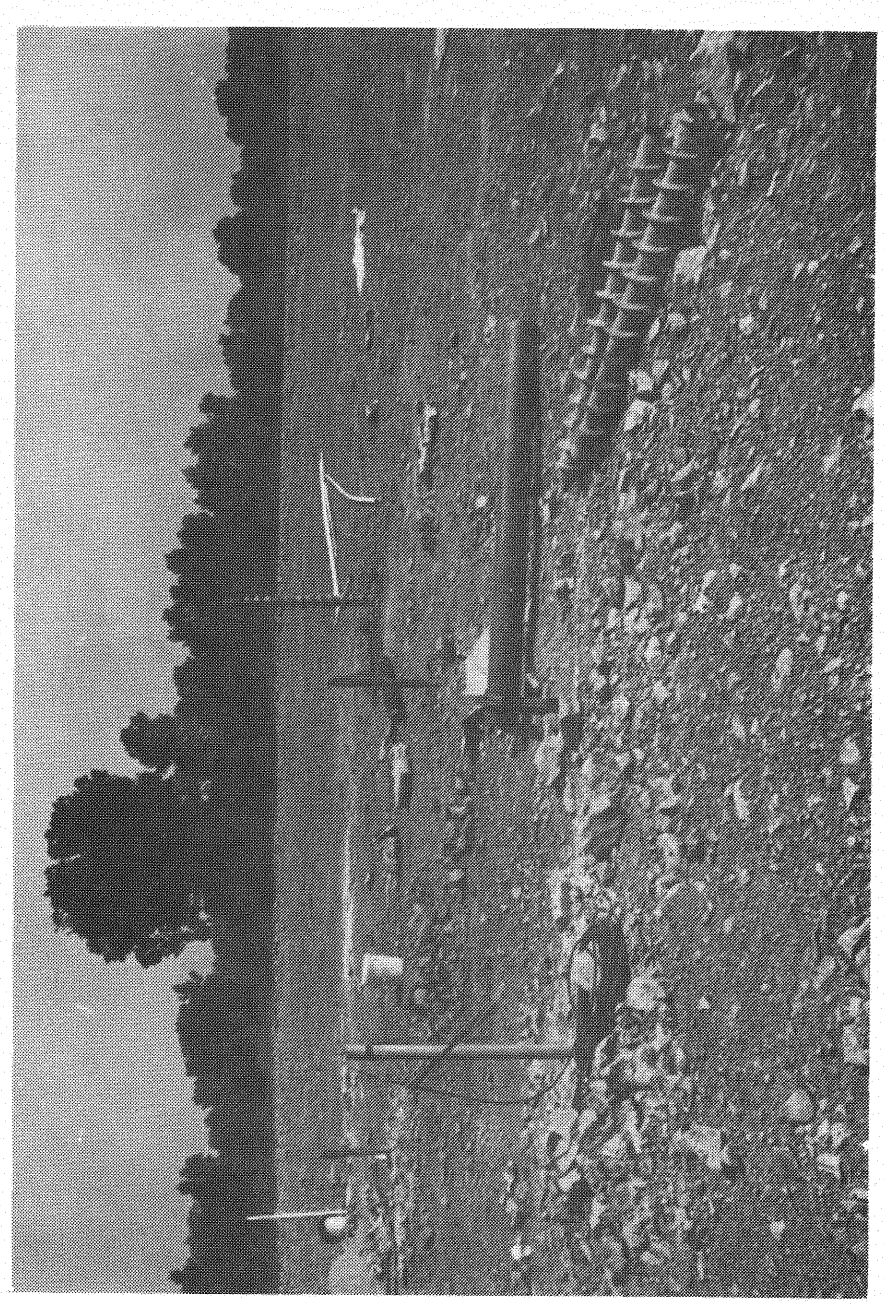

Figure 23. Photograph of Instrumentation at Test Section No. 1

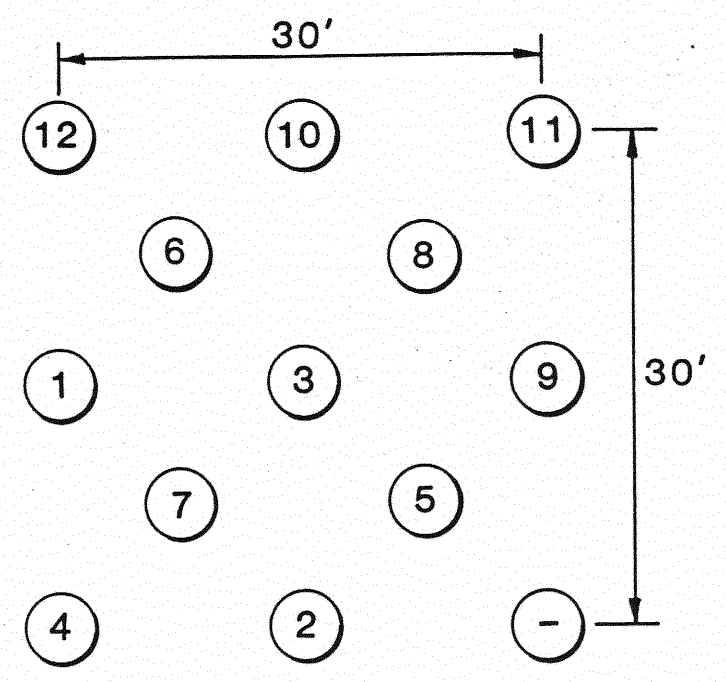

Figure 24a. Actual Impact Sequence, Test Section No. 1

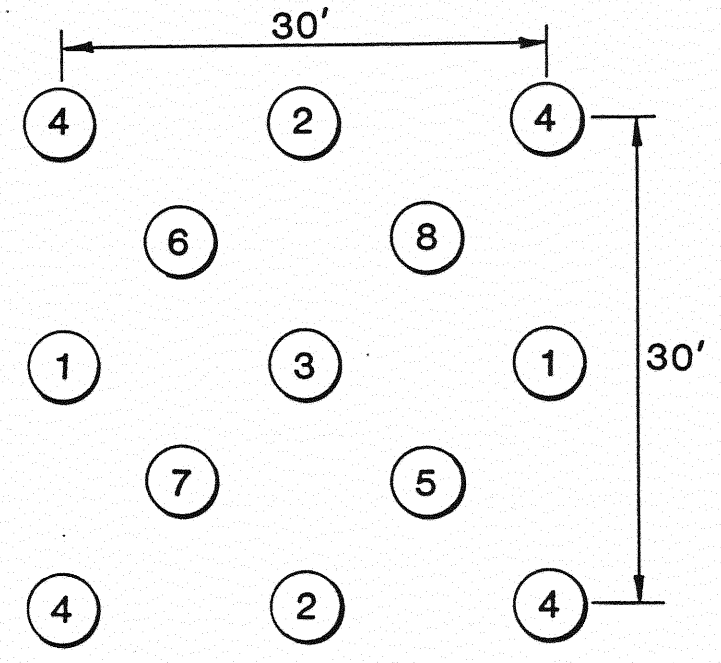

Figure 24b. Design Impact Sequence, Test Section No. 1

Prior to compaction, original inclinometer profile data were obtained. This was accomplished by placing the Digitilt Sensor at the bottom of the hole and then taking readings every two feet as the sensor was moved up the inclinometer casing. The Digitilt sensor provides an electrical signal proportional to the angle of inclination from its vertical axis. Because the sensor contains two servo-accelerometers mounted with the sensitive axes 90 degrees apart, the sensor must be reversed 180 degrees after the first set of data is recorded and the readings repeated. The difference between the two readings at each depth was used to compute the deflection from vertical (profile of the casing), or more importantly, was compared to subsequent surveys to determine displacements (changes in inclination).

A broken crane cable made possible a second set of inclinometer readings after the fifth impact at the first impact point. An attempt was made to obtain another set of readings at the completion of the test section, but all three casings were squeezed off at a depth of approximately six feet below ground surface.

Both piezometers were monitored during the test section. However, because the piezometers were dry prior to and during the compaction no results were obtained.

As noted earlier, crater depths were monitored after each blow at predetermined impact points. The results obtained were consistent with previously reported data. Crater depths were monitored at Impact Point Numbers 1, 3, 4, 7, 8, 9, 11, and 12. A summary of the total crater depths along with the number of impacts at that point can be found in Table I of Appendix A.

As stated previously, a subcontractor was responsible for obtaining SPT data before compaction of the test section. Upon completion of the test section, the subcontractor returned to collect SPT data to be compared with that taken prior to compaction. The SPT data collected subsequent to compaction on the CRL was within one foot of the test hole used prior to compaction. However, the test holes

located north and south of the CRL were drilled approximately 15 feet closer to the CRL than those drilled prior to compaction. Thus, any comparison made between the before and after results on these two holes should take this into account.

It should be noted here that no releveling work was performed during this test section. This facilitated the observance of the total heave of the test area subsequent to compaction.

Test Section No. 2

Test Section Parameters

Test Section No. 2 was located at Station 189+00. The top two or three feet at this test section consisted of clay and shale fragment mine spoil. Debris consisting of paper, wood, metal, rubber, etc., was found to a depth of about 20 feet. Beneath the debris there was a two or three foot layer of the mine spoil fill overlying the hard weathered shale. This test section represents the conditions that exist between Stations 182+00 and 192+00. A two to three foot thick layer of crusher-run limestone rock with a maximum size of 10 inches was placed over the test area prior to compaction.

Instrumentation

As with Test Section No. 1, prior to compaction and subsequent to the placement of the rock platform, a subcontractor drilled three test holes for the purpose of performing Standard Penetration Tests at various depths. The first boring was located on the CRL at Station 189+00. The other borings were located 15 feet north and 15 feet south of the CRL at Station 189+00.

The subcontractor was also responsible for installing the inclinometers and piezometers. Although results obtained from the inclinometer data collected at

Test Section No. 1 were inconclusive, it was determined from the data collection experience that the use of two inclinometers placed at strategic points could produce the desired results at Test Section No. 2. Thus, one inclinometer casing was installed in the SPT hole located on the CRL while the second inclinometer casing was installed on the CRL between impact points for passes one and three (i.e., 15 feet east of the first casing). Inclinometer No. 1 (set in the SPT hole) was set at a depth of 26 feet while Inclinometer No. 2 was set at a depth of 28 feet.

The two piezometers were set in the mine spoil fill immediately below the base of the trash. Piezometer No. 1 (northwest corner of test section) was set at a depth of 20 feet while Piezometer No. 2 (southeast corner of test section) was set at a depth of 19 feet.

Again, the level and level rod were used to monitor crater depths after each impact and subsidence of the test area after releveling.

A layout of the test section with the appropriate instrumentation is shown in Figure 25. Figure 26 is a photograph showing the instrumentation as set up in the field.

Testing Procedure

Prior to compaction, original inclinometer profile data and piezometer readings were taken and ground surface elevations were determined along the CRL and perpendicular to the CRL at Station 189+00. Level readings were taken 50 feet in all four directions from Station 189+00.

Impact pass No. 1 consisted of two impact points. The west impact point received eight blows while the east impact point received six blows. The number of blows on the east impact point was reduced because of the time and energy required to remove the weight after the sixth blow. As the number of blows increased, the weight became burdened with trash spalling from the sides of the crater. This added weight along with some apparent suction forming between the

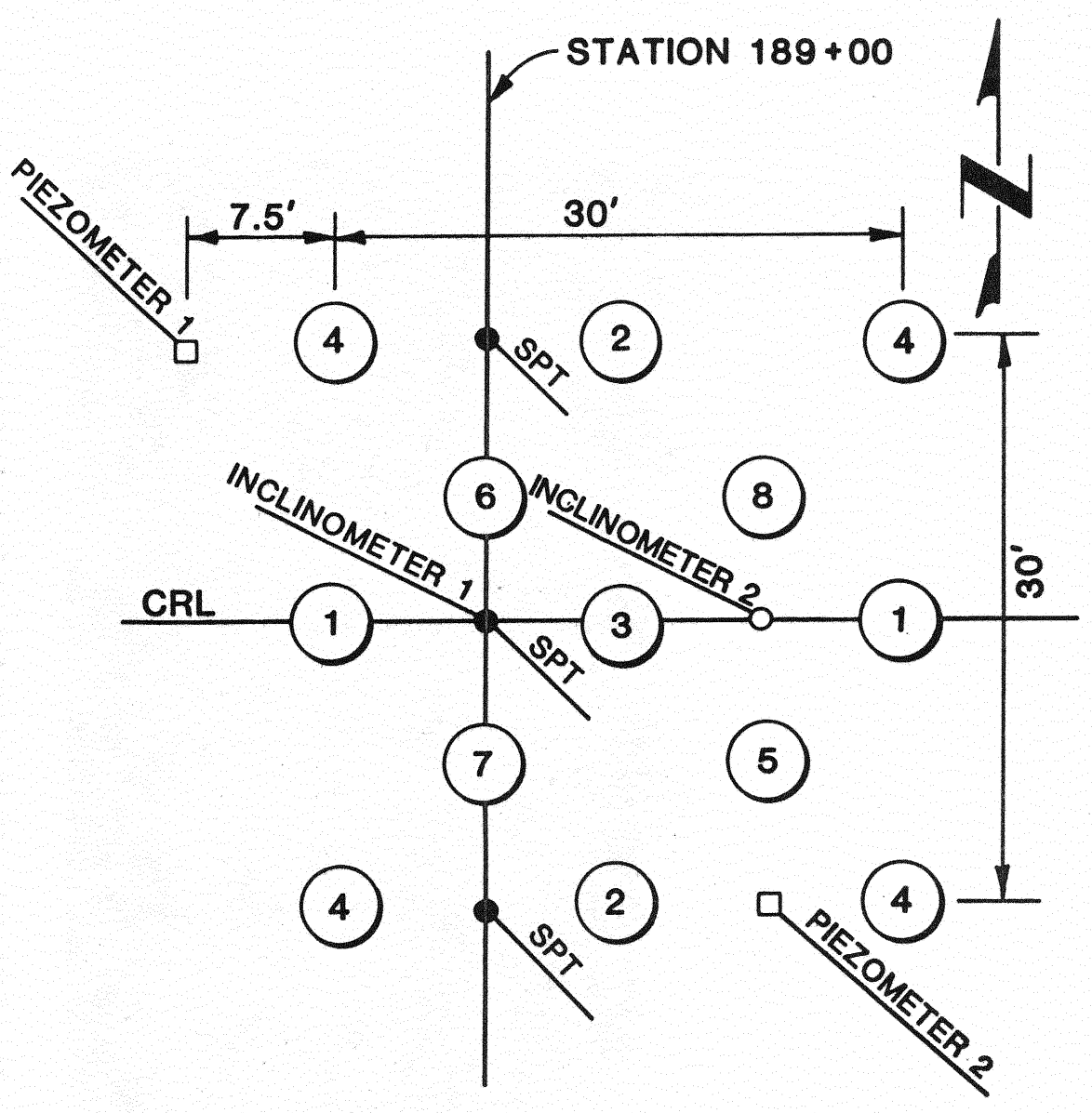

Figure 25. Test Section No. 2 Instrumentation Layout

Figure 26. Photograph of Instrumentation at Test Section No. 2

bottom of the weight and the bottom of the crater, made it most difficult to remove the weight after the sixth blow. It was felt that any further blows could cause the weight to become permanently lodged in the crater. Crater depths were monitored after each blow at both impact points. Piezometer readings were also recorded during the compaction process. Piezometer No. 1 was monitored for the west impact point while piezometer No. 2 was monitored for the east impact point. Upon completion of the two impact points, readings were attempted in both inclinometers. However, Inclinometer No. 2 was pinched off at 11 feet below the ground surface. Because it appeared that the weight was actually punching through the trash and compacting only that trash immediately beneath the weight, it was surmised that a piece of debris was pushed out laterally into the inclinometer casing causing it to be displaced enough so that the inclinometer sensor could not travel down the casing. It was possible to take readings in Inclinometer No. 1.

Impact pass No. 2 also consisted of two impact points. Both the north and south impact points received six blows. The number of blows on the impact points of this pass was reduced for the same reason as in pass No. 1. Once again, crater depths were monitored after each blow at both impact points. Piezometer readings were also recorded during the impact sequence. Piezometer No. 1 was monitored for the north impact point and piezometer No. 2 was monitored for the south impact point. Upon completion of the pass, Inclinometer No. 1 was once again read.

After all instrumentation were read, the test area was releveled by using a bulldozer to fill in the craters resulting from the first two passes with surrounding material. The bulldozer operator was instructed to use material from as far out as level readings were determined prior to compaction. After the releveling was completed ground surface elevations were determined as close to the original reading locations as possible.

Impact pass No. 3 consisted of one impact point which received seven blows. Crater depths were checked after each impact and piezometer readings from piezometer No. 1 were recorded throughout the compaction procedure. Inclinometer No. 1 was again read after this pass.

Impact pass No. 4 consisted of four impact points. The northwest impact point received six blows, the northeast impact point received six blows, the southwest impact point received three blows, and the southeast impact point received six blows. Crater depths were checked after each blow for the southwest and northeast impact points. Total crater depths were recorded for the southeast and northwest impact points. Piezometer No. 1 was monitored for the northwest and northeast impact points, while piezometer No. 2 was monitored for the southeast impact point. Neither piezometer was monitored during compaction at the southwest impact point. Inclinometer No. 1 was again read after the completion of this pass. After all instrumentation had been read, the test section was releveled and ground surface elevations recorded as close to the initial readings as possible.

Impact pass Nos. 5 and 6 consisted of one impact point each. Impact pass No. 5 received four blows while impact pass No. 6 received three blows. Total crater depths only, were recorded after each pass. Piezometer No. 2 was monitored for impact pass No. 5 and piezometer No. 1 was monitored for impact pass No. 6. No inclinometer data were collected after either of these passes.

Impact pass Nos. 7 and 8 also consisted of one impact point each. Both impact passes received four blows. Crater depths were checked after each blow for both passes. Piezometer No. 1 was monitored for both impact passes. Inclinometer No. 1 was read after impact pass No. 8. After all instruments were read the test section was again releveled and ground surface elevations obtained.

Seven days after the completion of the test site, the subcontractor returned to conduct the post-test section borings. All three borings were located within

one foot of their respective original borings. The Standard Penetration Tests were performed at the same depths as before so a comparison could be made between the two results.

Test Section No. 3

Test Section Parameters

Test Section No. 3 was located at Station 165+00. The top five or six feet at this test section consisted of clay and shale fragment mine spoils. This was underlain by approximately 12 feet of silty clay and shale fragments mixed with some trash. Beneath this material was two or three feet of stiff silty clay and shale fragments which rested on the hard weathered shale. The ground water table at the time of exploration was approximately four feet below the ground surface. This test section represents the conditions between Stations 164+00 and 171+00. A four to five foot thick layer of crusher-run limestone with a maximum size of 10 inches was placed over the test area prior to compaction.

Instrumentation

As with Test Sections 1 and 2, prior to compaction and subsequent to the placement of the rock platform, a subcontractor drilled three test holes for the purpose of performing Standard Penetration Tests at various depths. The first boring was located on the CRL at Station 165+00. The other borings were located 15 feet north and 15 feet south of the CRL at Station 165+00.

The subcontractor was also responsible for installing the inclinometers and piezometers. As with Test Section No. 2, two inclinometers were used. One inclinometer casing was installed on the CRL in the first SPT boring (i.e., between impact points for passes one and three) and the other was set 15 ft east of the first casing. Inclinometer No. 1 was set at a depth of 26 feet while Inclinometer No. 2 was set at a depth of 36 feet.

Four piezometers were installed at Test Section No. 3: Piezometer No. 1 (northwest corner of test section) was set at a depth of 21 feet; Piezometer No. 2 (northeast corner of test section) was set at a depth of 28 feet; Piezometer No. 3 (southeast corner of test section) was set at a depth of 22 feet; Piezometer No. 4 (southwest corner of test section) was set at a depth of 31 feet.

Again, the level and level rod were used to monitor crater depth after each impact and subsidence of the test area after releveling.

A layout of the test section with appropriate instrumentation is shown in Figure 27. Figure 28 is a photograph showing the instrumentation as set up in the field.

Testing Procedure

Prior to compaction, original inclinometer profile data and piezometer readings were taken and ground surface elevations were determined along and perpendicular to the CRL at Station 165+00. Level readings were taken 50 feet in all four directions from Station 165+00.

Impact pass No. 1 consisted of two impact points. The west impact point received seven blows while the east impact point received eight blows. The number of blows on the west impact point was reduced because of the time and energy required to remove the weight after the seventh blow as previously explained (i.e., Test Section No. 2). Crater depths were monitored after each blow at both impact points. Piezometer readings were monitored at the two closest piezometers to the impact point during the compaction process. Piezometer Nos. 1 and 3 were monitored during the compaction at the west impact point. Piezometer No. 1 was monitored after impacts 1, 2, 3, 4 and 7 while Piezometer No. 3 was monitored after impacts 5 and 6. Piezometer Nos. 2 (impacts 7, 8) and 3 (impacts 1, 2, 3, 4, 5, 6) were monitored during compaction at

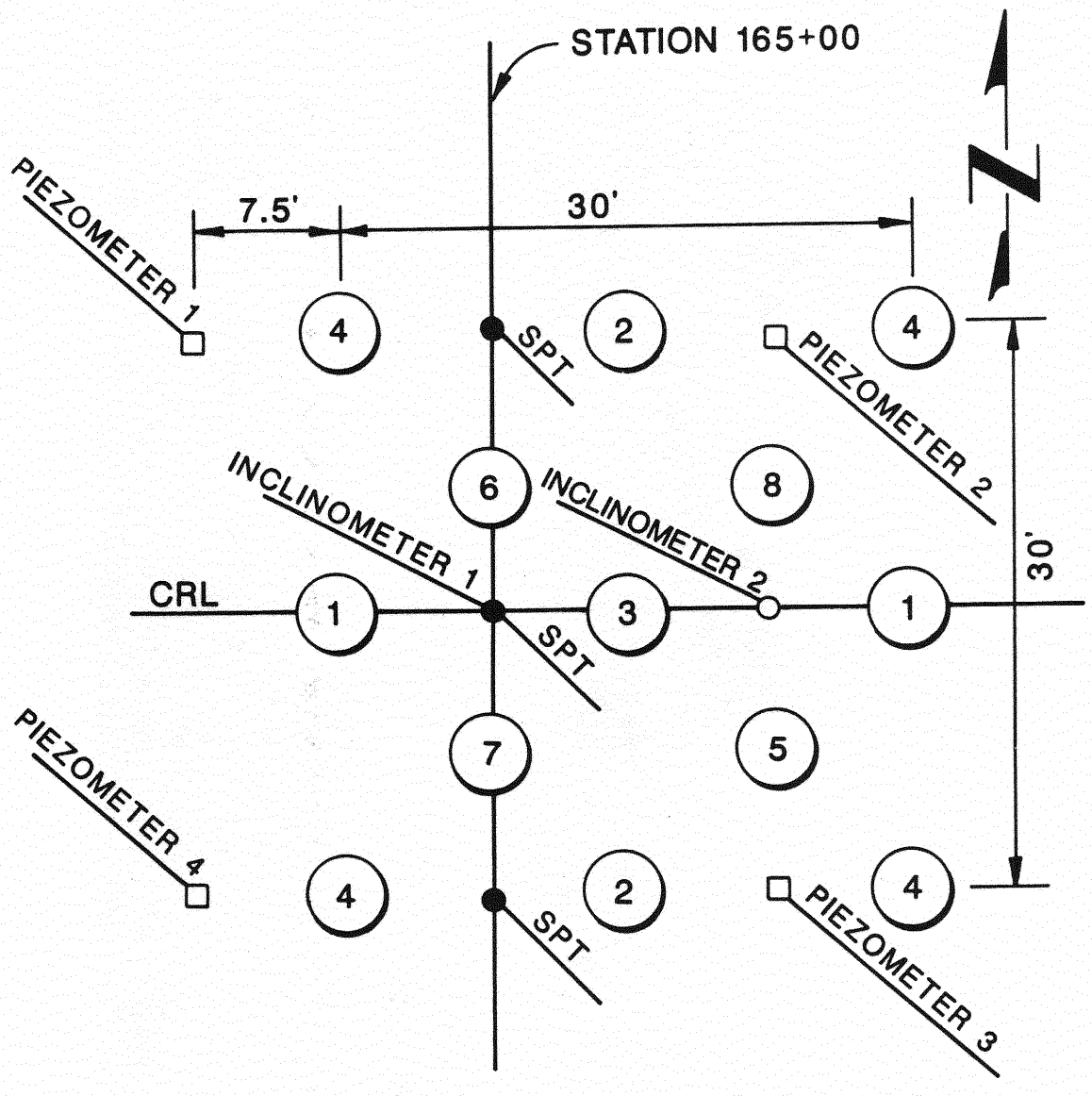

Figure 27. Test Section No. 3 Instrumentation Layout

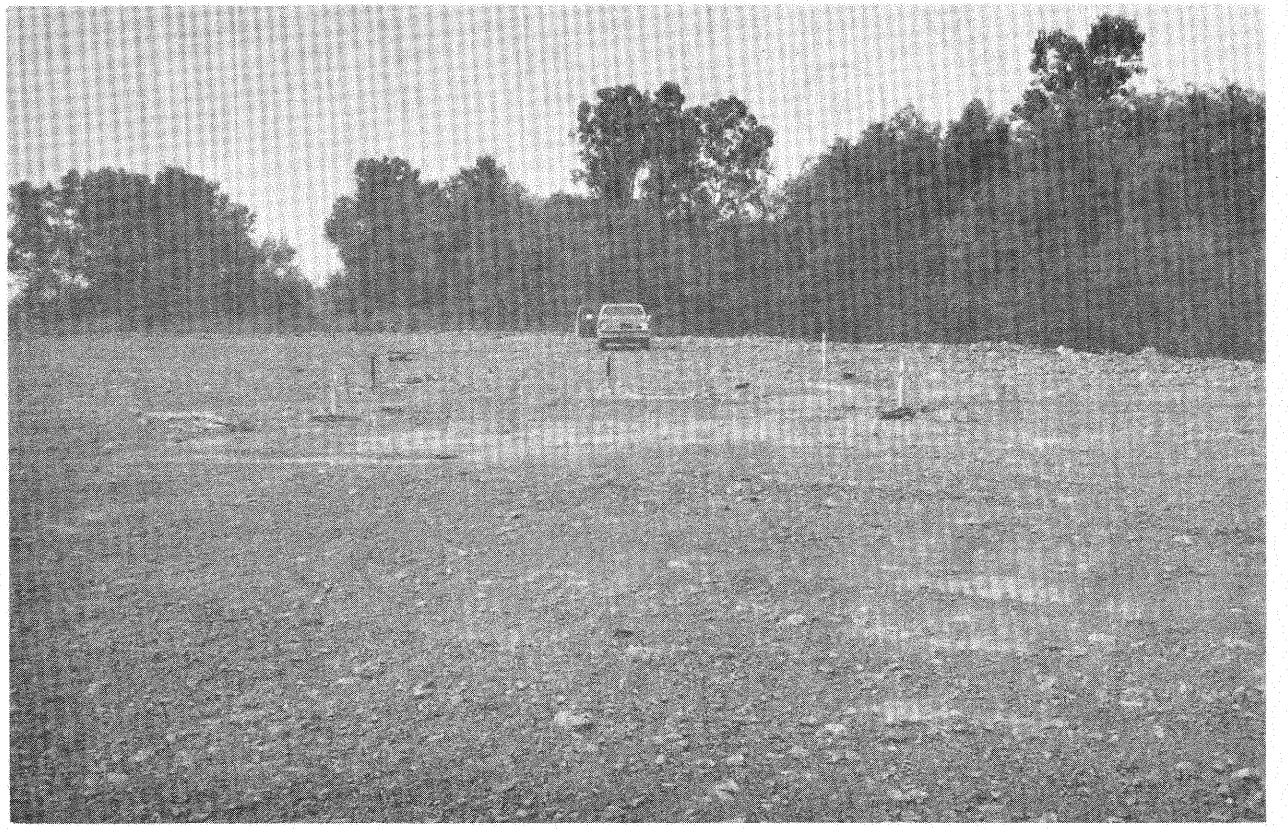

Figure 28. Photograph of Instrumentation at Test Section No. 3

the east impact point. Upon completion of the two impact points, inclinometer readings were taken in both casings.

Impact pass No. 2 consisted of two impact points, both of which received eight blows. Crater depths were monitored after each blow at both impact points. Piezometer Nos. 3 (impacts 1, 2, 3, 4, 5) and 4 (impacts 6, 7, 8) were monitored during compaction at the south impact point. Piezometer Nos. 1 (impacts 4, 5, 6, 7, 8) and 2 (impacts 1, 2, 3) were monitored during compaction at the north impact point. Upon completion of the two impact points, inclinometer readings were taken in both casings.

Impact pass No. 3 consisted of one impact point which received eight blows. Crater depths were checked after each impact. Piezometer Nos. 2 (impacts 1, 2, 3, 8) and 3 (impacts 4, 5, 6, 7) were monitored during the compaction. Attempts were made to take inclinometer readings after the pass but both inclinometers were pinched-off at a depth of approximately 6 to 7 feet. No further inclinometer readings were attempted.

Impact pass No. 4 consisted of four impact points, all of which received eight blows. Crater depths were checked after each blow for the southwest and northeast impact points. Total crater depths were recorded for the southeast and northwest impact points. Piezometer Nos. 4 (impacts 1, 2, 3, 4, 5, 6) and 1 (impacts 7, 8) were monitored during compaction at the southwest impact point. Piezometer Nos. 2 (impacts 1, 2, 3, 8) and 1 (impacts 4, 5, 6, 7) were monitored during compaction at the northeast impact point. Piezometer Nos. 3 (impacts 1, 2, 3, 4, 5, 6) and 2 (impacts 7, 8) were monitored during compaction at the southeast impact point. Piezometer Nos. 1 (impacts 1, 2, 3, 4) and 4 (impacts 5, 6, 7, 8) were monitored during the compaction at the northwest impact point.

After all the instrumentations were read, the test area was releveled using a bulldozer to fill in the craters from the first four passes with surrounding

material. After the releveling was completed ground surface elvations were determined as close to the original reading locations as possible.

Impact pass Nos. 5 and 6 consisted of one impact point each, both of which received six blows. Total crater depths were recorded for both impact points. Piezometer No. 3 was monitored during compaction of pass No. 5 and Piezometer No. 1 was monitored during compaction of pass No. 6.

Impact pass Nos. 7 and 8 consisted of one impact point each, both of which received six blows. Crater depths were checked after each blow for both impact points. Piezometer No. 4 was monitored during compaction of pass No. 7 and Piezometer No. 2 was monitored during compaction of pass No. 8.

After all the instruments were read the test area was again releveled and ground surface elevations obtained.

Ten days after completion of the test site, the subcontractor returned to conduct the post-test section borings. All three borings were located within one foot of their respective original borings. Standard Penetration Tests were performed at the same depths as before so a comparison could be made between the two results.

CHAPTER IV

RESULTS AND DISCUSSION

Because of the uncertain results that were anticipated by the specified equipment and techniques, the contract for this project required the compaction of test sections that were representative of the various conditions found at the site. Procedures for executing the remainder of the work were then contingent on an analysis of the results obtained at the test sections. This chapter discusses those results obtained from the test sections and the recommendations for any changes in procedure for the remainder of the work.

Test Section No. 1

As stated earlier, Test Section No. 1 was located at Station 179+00. This test section represents mine spoil consisting of a lean clay and shale fragments full depth to bedrock (approximately 40 feet). In this test section, it was recommended by the Design Engineer that the first four passes receive eight blows at each impact point while passes five through eight receive six blows at each impact point. Reference is made to Figures 24a and 24b for the actual impact sequence used as compared with the design impact sequence. The actual impact sequence varied somewhat from the design impact sequence, and thus, the impact sequence used in the remainder of the work. However, it was felt by those involved with the project that because of the relatively small size of the test section, and because there was no evidence of any ground water table, the results from the test section as compacted would probably be very similar to the results if compacted according to the design.

Due to the inexperience of the crane operator in this type of work, a broken cable resulted from the swivel weight cutting the cable as it slammed into the weight upon impact. This occurred on the fifth blow at the first impact point. The operator became much more efficient in using his brake to stop the cable as the day progressed.

Inclinometer Data

The results from the inclinometers proved to be inconclusive; however, the trends were consistent with the results obtained by STS Consultants who were performing similar tests on a separate test section approximately 100 feet to the west along the CRL. The inclinometer casing above the ground surface leaned toward impact point No. 1 and an inflection point occurred between six and nine feet below ground surface. After completion of the test section, all three casings were pinched off at a depth of approximately six feet below the ground surface.

Piezometer Data

No results were obtained from the two piezometers, as both were dry throughout the compaction of the test section.

Crater Depths

The results of the crater depth measurements were consistent with previously reported data. However, the total depths were somewhat greater than expected. The average total crater depth of the seven impact points receiving eight blows was 7.4 feet. The average total crater depth of the four impact points receiving less than eight blows was also 7.4 feet. The total crater depth at the impact point that received 14 blows was 9.7 feet. A summary of crater depths with the number of blows at each impact point is found in Table I of Appendix A.

Plots of the total depth versus impacts (Figures 29 through 36, Appendix A) show that the material properties were improving, as the slope of the curve becomes relatively constant after three or four impacts. This was further substantiated by the plots of incremental depth versus number of impacts (Figures 29 through 36, Appendix A). This material never really "tightened up" as some soils do; however, the degree of improvement was significant. One interesting point to note, is the leveling off of the incremental depth plots after three or four impacts at all of the points monitored. This shows that the amount of deformation became essentially constant after this minimal number of impacts. In other words, impacting does not cause significant material improvement after three or four blows. This same fact was realized by Welsh (12) when he noted that significant soil improvement does not occur when the incremental crater depth is less than about 0.5 feet after two impacts. The practical implication of this is that the possibility exists for reducing the number of impacts per pass. However, it would seem impractical to reduce the number of passes if the depth of influence criteria was not being met. These criteria do appear to be met. For example, using the equation

$$D = 1/2\sqrt{WH}$$

the depth of influence (D) is approximately 18 feet. SPT results taken after the completion of compaction indicate that the depth of influence at the CRL is 12 feet and approximately 25 feet at the offset locations.

Figure 37 in Appendix A shows a plot of crater depths normalized with respect to the square root of energy per blow versus impact. This is a convenient method used to compare results from various dynamic compaction projects (8). In Figure 37, the upper plot is from a project with similar subsurface conditions in

Jefferson County, Alabama (8). As can be seen from the graph, all results from this project plot in a relatively close band and they all fall below the results obtained from Alabama.

SPT Data

It should be noted that the two borings north and south of the CRL made before compaction were 15 feet further from the CRL than the borings made after compaction. The "N" values reported before and after compaction of the test section all show typical results (see Figures 38 through 40, Appendix A). Specifically, the upper five or six feet exhibits a reduction in strength after compaction. This is caused by the undisturbed material used to backfill the craters. Below the five foot depth the improvement in "N" values is significant. From the before "N" values north of the CRL it is apparent that the material was quite soft. This explains the significant improvement in strength after compaction. The area south of the CRL was not initially quite as soft; thus, although the degree of improvement was significant, it was not quite as much as that achieved in the area to the north. The after compaction boring located on the CRL actually showed a decrease in strength below about 12 feet. Although unusual, these phenomena might be explained by the high before compaction "N" values. Since the compaction process was started near the CRL boring, the proximity of low strength materials would result in minimal confinement from the surrounding soils.

Heaving

Visual inspection of the craters during the compaction process indicated a punching shear failure. However, a small amount of heaving occurred which suggests a local shear failure. While a local shear failure might have occurred as

a result of the first one or two impacts, the heaving may also be caused by the build-up of excess pore pressures in the top few feet of material which had a high moisture content. Without any confinement above the material, excess pore pressure build-ups would result in a heaving of the material. No releveling was performed during the compaction process of this test section.

Recommendations

Based on the results obtained from test Section No. 1, the following recommendations were made for the remainder of work between Stations 172+00 and 181+00.

1. The number of impacts for passes one through four were reduced from eight to six. This reduced the input energy from 48 ton feet/square foot to 36 ton feet/square foot. It was felt that this reduction would not have a significant effect on the final results of the compaction process.
2. The last two sets of impact passes were combined, which in effect reduced the total number of passes from eight to six. It was recommended that pass No. 5 be combined with pass No. 7 and pass No. 6 be combined with pass No. 8. This helped to significantly reduce production time for the remainder of the work while still providing the desired results.

Test Section No. 2

Test Section No. 2 was located at Station 189+00. This test section represents mixed strip mine spoil and trash to various depths underlain by strip mine spoil consisting of lean clay and shale fragments which is underlain by the undisturbed sandstone or shale (at approximately 27 feet). A groundwater table exists in the lower portion of the trash layer at a depth of approximately 15 feet.

The Design Engineer recommended the same pass sequence for this test section as was recommended for Test Section No. 1. Once again, the first four passes were to receive eight blows per impact point with the remaining four passes to receive six blows per impact point. However, only one of the 13 impact points in the test section (Pass No. 1, west point) received the full number of blows. The remaining points did not receive the full number of impacts because of problems with the weight "sticking" in the crater. This problem was attributed to a combination of two things: (1) the amount of trash and soil collecting on the weight as it spalled from the sides of the crater made the weight much heavier and (2) increased suction between the weight and the material at the bottom of the crater.

Inclinometer Data

More inclinometer data were collected on this test section because inclinometer No. 1 was kept in service longer. Inclinometer No. 2 could not be used after the first pass. The data that were collected showed a somewhat erratic pattern in the direction of the CRL. For example, in the direction parallel to the CRL there was no movement of the inclinometer casing in the upper eight feet after the first two passes. After the third pass some movement was recorded in the upper four feet away from the point of impact. After the fourth pass an inflection point was developed at approximately six feet. An attempt to secure more data was made after pass No. 8; however, the inclinometer casing was pinched off at approximately six feet below the ground surface.

All inclinometer data collected from this test section are consistent with the data from Test Section No. 1 and that reported by STS Consultants. The somewhat erratic pattern can more than likely be traced to the compaction of the trash. Most probably, a board or some similar object was pushed laterally into the inclinometer casing to give such results.

Piezometer Data

Both piezometers appeared to have responded properly during the compaction process. During the compaction process the piezometer closest to the specific impact point was monitored. The results show that "peak" points occurred in the pore pressure at piezometer No. 1 within a second or two after each impact (Figures 41,43,45,46,48,50,51,52, Appendix B). No such "peaks" occurred in the data from piezometer No. 2 (Figures 42,44,47,49, Appendix B). This may be due to the manner in which the piezometer was installed or it may be a result of the sensor being located in a much less permeable material than piezometer No. 1.

The heights of the "peaks" from piezometer No. 1 were, as expected, much greater when the point of impact was closer to the piezometer. The pore pressure essentially dissipated within a few seconds after each blow with some residual pore pressure remaining in both piezometers after each impact point was completed. By the end of the day the residual pore pressure in piezometer No. 1 had accumulated to 4.4 psi as compared with the original value of 2.2 psi, while the residual pore pressure in piezometer No. 2 had accumulated to 5.3 psi as compared with the original value of 1.3 psi. As can be seen in Figure 53 of Appendix B, the pore pressures dissipated essentially to the original values in approximately one week.

Crater Depths

Total crater depths for this test section were much greater than those obtained at Test Section No. 1. Table II in Appendix B shows that all craters were at least eight feet deep with more than half of the craters being greater than eleven feet deep. Figures 54 through 62 in Appendix B show the total crater depth and incremental crater depth versus number of impacts. As can be seen, the

incremental crater depth never really "leveled-off" for most of the impact points. For most of the impact points the magnitude of the incremental crater depth for the last blow was at least 1.5 feet. The normalized crater depths are presented in Figure 63, Appendix B, for comparison purposes. As expected, the plots from Test Section No. 2 are much steeper than those from Test Section No. 1. This can be attributed to the greater crater depths experienced at Test Section No. 2. As in the first test section, the data from this test section plotted in a rather narrow band.

The problems with the weight "sticking" in the crater and the extreme depth of the craters are most important from a construction point of view. Both problems result in drastic increases in time and energy to the contractor. The obvious response would be to reduce the number of drops per pass. However, crater depths of at least eight feet were experienced with as few as three or four drops with absolutely no "leveling-off" of the incremental crater depths being observed.

SPT Data

The "N" values from borings before and after compaction of the test section show erratic results (Figures 64 through 66, Appendix B). Due to the nature of the test procedure and the material encountered, such results were expected. It was hoped that enough of the mine spoil had been mixed with the trash to form a more uniform and, thus, stronger material. However, it does not appear that this was the case. The large peaks on the curves are most likely "harder" pieces of trash (i.e., fiber glass, metal, tires, etc.). More borings were performed seven days after the completion of the test section which was adequate time for most of the excess pore pressures to dissipate.

Subsidence

Subsidence data were collected after passes two, four, and eight (Figures 67 and 68, Appendix B). Most of the subsidence appears to have occurred after the first two passes. The reduced amount of subsidence that occurred subsequent to pass No. 2 might be a result of the difficulty in releveling such a small area by using material only from the boundaries of the test section. It was observed during the releveling operation that the bulldozer operator continuously moved further from the boundaries of the test section to obtain material to fill the craters. From the elevations plotted in Figures 67 and 68 of Appendix B the average amount of subsidence over the area is approximately one foot. It can be seen from the figures that had the releveling operation been confined to the area directly affected by the compaction procedure, a greater average amount of subsidence would have been realized.

Recommendations

Based on the quantity and quality of results obtained from this test section, it was recommended that the same instrumentation plan and data collection sequence be used in Test Section No. 3.

The SPT data and the crater depth data indicated that the dynamic consolidation process was not as effective in this area that is underlain by a significant thickness of trash. Because of this, the following recommendations were presented to the ODOT:

Consider the use of stone columns constructed using the dynamic compaction process. This would only be necessary from Stations 185 to 190+50. Stations 181 to 185 contain only thin layers (approximately five feet) of trash and it was felt that this can be effectively treated with the dynamic consolidation method. At the time of this report those involved with the project felt that the

use of stone columns in lieu of the static load test was desirable. The specifics of the stone columns were to be agreed upon later. However, the columns would probably be placed under the main lanes between Stations 185 and 190+50 during pass No. 2. Three "test" columns were constructed to determine the feasibility of their use. The results of the test columns are presented in Appendix D. It was recommended that the stone columns be constructed by impacting the location four times (but not to exceed the number of impacts to cause a crater depth of eight feet), the crater depth checked, and the craters backfilled with the rock fill to the original surface. The location then received two additional cycles of four impacts each with the crater depths being monitored. When the incremental crater depth dropped below six inches per impact, the process would be discontinued. All other impact passes will be treated as "normal" dynamic consolidation passes with the number of blows to be set by the site Engineer.

Test Section No. 3

Test Section No. 3 was located at Station 165+00. This test section represents mix strip mine spoil and trash to various depths underlain by strip mine spoil consisting of lean clay and shale fragments which is underlain by undisturbed shale (at approximately 19.5 ft). A groundwater table exists in the mixed spoil and trash at a depth of approximately 5 ft.

The Design Engineer recommended the same pass sequence for this test section as was recommended for Test Section No. 1. With the exception of Pass No. 1 (west point) all of the impact points received the full number of blows. Pass No. 1 (west point) received seven of the specified eight blows.

Inclinometer Data

Inclinometer data were again difficult to obtain because of loss of service of

the casings. Initial profiles were taken for both casings. Additional profiles were taken after passes 1 and 2 for both casings. Both inclinometer casings were "pinched-off" at a depth of approximately six to seven feet. The data were consistent with the previous test sections; that is the casings were deflected away from the impact point and an inflection point occurred between six and nine feet below the ground surface.

Piezometer Data

With the exception of Piezometer No. 2 all of the piezometers appeared to have responded properly during the compaction process. The two closest piezometers to the specific impact point were monitored during impacting of the point. Generally the closest piezometer was monitored during the first four or five impacts with the next closest piezometer monitored during the balance of the impacts. The data from the piezometer monitored during the compaction process are presented in Appendix C (Figures 69 through 90). Piezometer No. 2 did not show any peak responses during the entire compaction process; however, it did display some build-up in pore pressure as the compaction process proceeded. The remaining piezometers showed peaks in the pore pressure within a second or so following the impact. Most of the pore pressure increase dissipated as rapidly as it occurred. Generally, the higher peaks occurred when the piezometer in question was closer to the impact point, as would be expected. By the end of the test section compaction, the increases in pore pressures were approximately 5 psi, 6.5 psi, 5 psi, and 1 psi for Piezometer Nos. 1, 2, 3, and 4, respectively. The pore pressure increases were dissipated to essentially the pre-compaction values in about one week (Figures 91 and 92, Appendix C).

Crater Depths

Total crater depths for this test section were somewhat greater than those obtained at Test Section No. 1 but considerably less than those obtained at Test Section No. 2. Table III, Appendix C, shows that all craters were at least eight feet deep with the majority between nine and eleven feet deep. Figures 93 through 101 in Appendix B show the total crater depth and incremental crater depth versus number of impacts. For most of the impact points monitored, the incremental crater depths leveled off between three and five impacts which is comparable to the responses at Test Section No. 1. The magnitude of the incremental crater depth at the last impact was between 0.5 and 1 foot which combined with the "leveling-off" trend indicates that the effectiveness of the compaction process is not significantly increased beyond four or five impacts. The normalized crater depths are presented in Figure 102, Appendix C, for comparison purposes. The plots are not as steep as those obtained for Test Section No. 2 because the crater depths are not as great.

SPT Data

The "N" values from borings before and after compaction of the test show a consistent pattern of improvement between approximate depths of five and fifteen feet. Below this depth the pattern becomes erratic especially in Boring 3, south of the CRL. This erratic pattern is probably due to presence of larger shale fragments, although the subcontractors boring information did not indicate significant differences in the amount or size of fragments.

Subsidence

Subsidence data were collected after passes 4 and 8 when the test section was re-leveled. Figures 106 and 107, Appendix C, show that most of the

subsidence occurred during the first four passes which is consistent with the incremental crater depth data. The average subsidence over Test Section No. 3 was between 1 and $1\frac{1}{2}$ feet. The problem with the bulldozer moving outside the assumed boundaries of influence experienced at Test Section No. 2 were essentially eliminated by better coordination with the operator.

Recommendations

Based on the results of the test section, the compaction sequence west of Yale Avenue was modified to that recommended following Test Section No. 1 (i.e., six impacts for each of the eight passes and combine passes five through eight into two passes). If excessive crater depths result on pass one (i.e., eight feet or more after four impacts) and/or problems with sticking in the crater become excessive, the effort is reduced to four impacts per point and the area of greater crater depths delineated for additional compaction or the use of compacted stone columns. If stone columns are not used in areas exhibiting excessive crater depths after all eight passes, an additional pass (or two passes) should be included along with some additional rock cover to attain the energy required for the modified compaction sequence. This procedure was utilized for some "soft" spots identified during the compaction process and worked well.

CHAPTER V

CONCLUSIONS

An evaluation of the results obtained from the three test sections monitored during the dynamic compaction process at the Gilcrease Expressway in Tulsa, Oklahoma, produced the following conclusions:

1. Dynamic compaction improves the strength characteristics of strip mining spoil containing a lean clay with shale fragments. The presence of a ground water table did not appear to adversely affect the results.

2. The most consistent improvement in the mine spoil material was realized in those areas with less trash.

3. Compaction beyond the first three to five impacts did not cause a significant incremental change in crater depth in the mine spoil material.

4. Based on the SPT data and the implications of the crater depths, dynamic consolidation does not appear to effectively improve the strength characteristics of trash fill that is more than a few feet thick. Where the trash fill is more than a few feet thick, consideration should be given to additional treatment such as stone columns.

5. Inclinometers do not appear to be a reliable method for monitoring lateral subsurface movement in mine spoil and trash.

6. The electrical piezometers performed very well during the compaction process and provided excellent data where they were properly installed.

REFERENCES

1. Dumas, Jean C., "Dynamic Consolidation: Its Development in Canada," a paper presented at the Conference on Construction in Difficult Soils under the auspices of the Canadian Society for Civil Engineering, Thunder Bay, Ontario, February 5, 1982.

2. Dumas, Jean C., and Nelson F. Beaton, "Limitations and Risks of Dynamic Compaction," a paper presented at Geotec III Conference held in Atlanta, Georgia, 1984.

3. Gambin, M. P., "The Menard Dynamic Consolidation at Nice Airport," Proceedings, 8th European Conference on Soil Mechanics and Foundation Engineering, Helsinki, May, 1983, pp. 231-234.

4. Leonards, Gerald A., William A. Cutter, and Robert D. Holtz, "Dynamic Compaction of Granular Soils," Journal of the Geotechnical Engineering Division, ASCE, Vol. 106, No. GT1, January, 1980, pp. 35-44.

5. Loos, W., "Comparative Studies for Compacting Cohesionless Soils," Proceedings, 1st International Conference on Soil Mechanics and Foundation Engineering, Vol. III, Harvard Univ., Cambridge, Mass., June, 1936, pp. 174-178.

6. Lukas, R. G., "Densification of Loose Deposits by Pounding," Journal of the Geotechnical Engineering Division, ASCE, Vol. 106, GT4, April, 1980, pp. 435-446.

7. Mayne, Paul W., Luther H. Bondra, and John S. Jones, Jr., "I-65 Impact Densification Study-Jefferson County, Alabama," Law Engineering Report No. B-3241, February, 1983.

8. Mayne, Paul W., John S. Jones, Jr., and Jean C. Dumas, "Ground Response to Dynamic Compaction," Journal of Geotechnical Engineering, ASCE, Vol. 110, No. 6, June, 1984, pp. 757-774.

9. Menard, L., and Y. Broise, "Theoretical and Practical Aspects of Dynamic Consolidation," Geotechnique 25, No. 1, March, 1975, pp. 3-17.

10. Mitchell, J. K., "Soil Improvement, State-of-the-Art Report," Proceedings, 10th International Conference on Soil Mechanics, Vol. 4, Session 12, Stockholm, 1981, pp. 509-565.

11. Ramaswamy, S. D., Mohamed A. Aziz, Raja V. Subrahamanyam, M. H. Abdul Khader, and Seng-Lip Lee, "Treatment of Peaty Clay by High Energy Impact," Journal of the Geotechnical Engineering Division, ASCE, Vol. 105, No. GT8, August, 1979, pp. 957-967.

12. Welsh, J. P., "Dynamic Deep Compaction of Sanitary Landfill to Support Superhighway," Proceedings, 8th European Conference on Soil Mechanics and Foundation Engineering, Helsinki, 1983, pp. 319-321.

13. Wiss, J. F., "Construction Vibrations: State-of-the-Art," Journal of the Geotechnical Engineering Division, Vol. 107, GT2, February, 1981, pp. 167-182.

APPENDIX A

RESULTS FROM TEST SECTION NO. 1

TABLE I

SUMMARY OF CRATER DEPTHS, TEST SECTION NO. 1

Impact Point	Number of Impacts	Crater Depth (Ft)
1	8	6.5
2	8	8.0
3	8	8.3
4	8	5.3
5	8	7.5
6	6	7.0
7	6	6.5
8	5	7.9
9	8	8.2
10	3	8.0
11	8	8.3
12	14	9.7

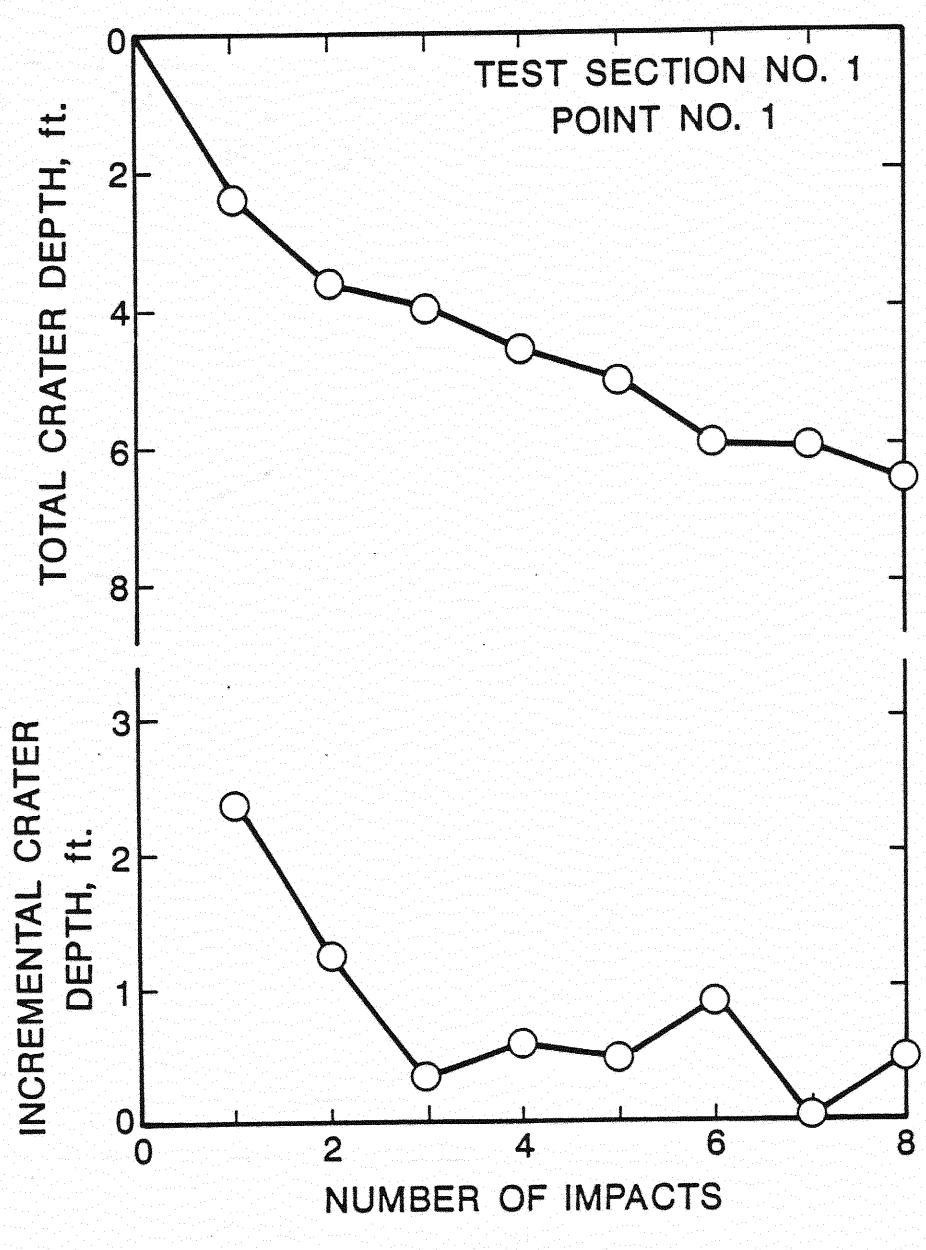

Figure 29. Crater Depth Versus Number of Impacts: Point No. 1, Test Section No. 1

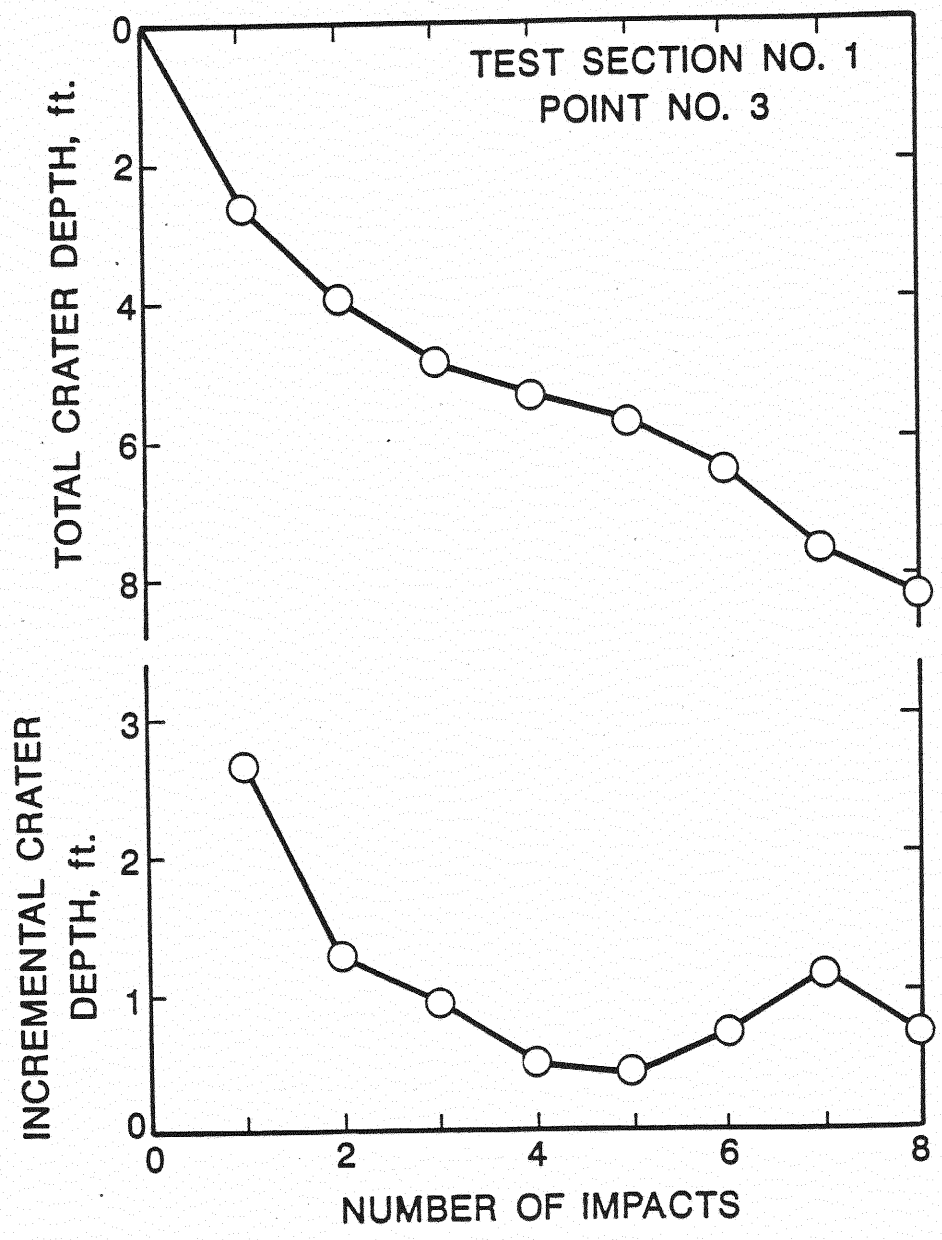

Figure 30. Crater Depth Versus Number of Impacts: Point No. 3, Test Section No. 1

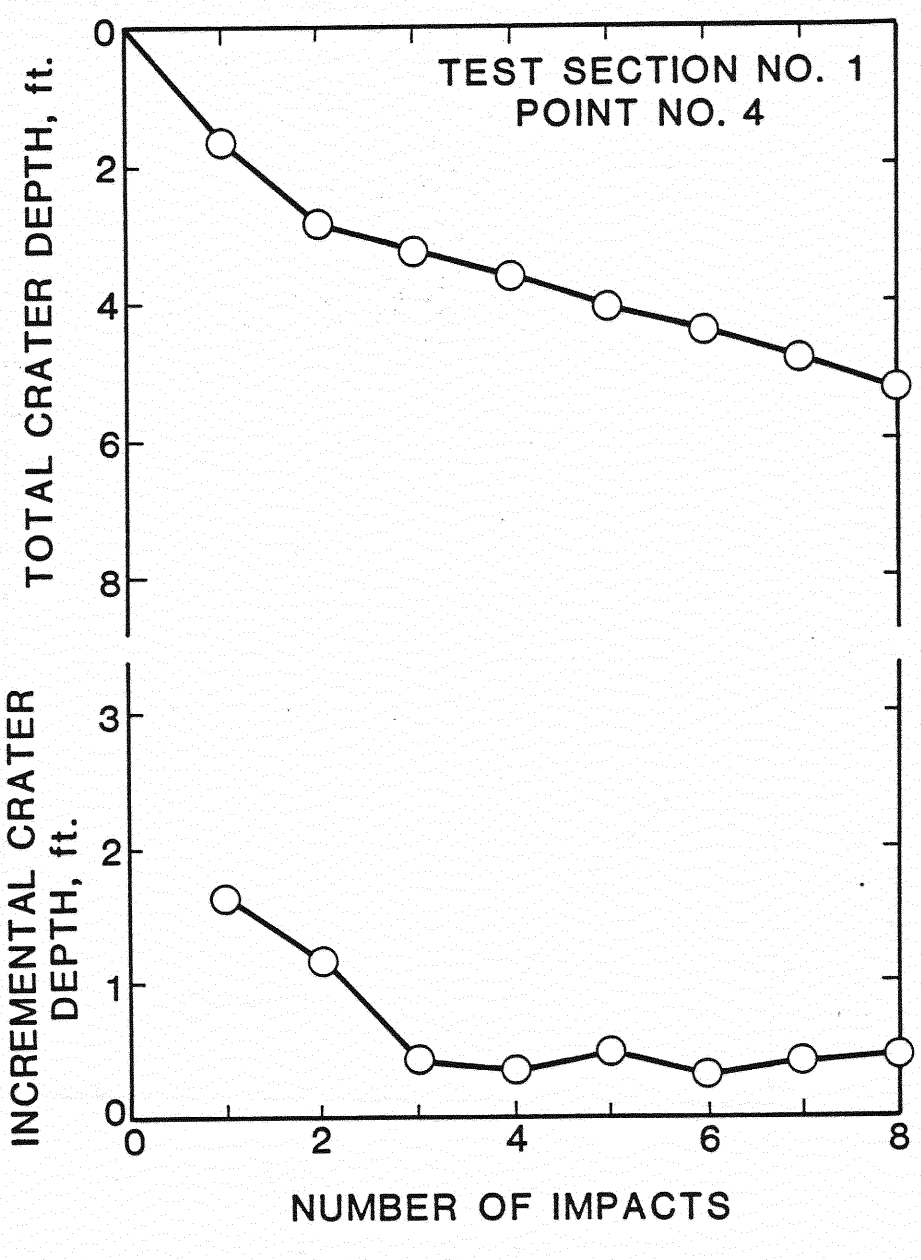

Figure 31. Crater Depth Versus Number of Impacts: Point No. 4, Test Section No. 1

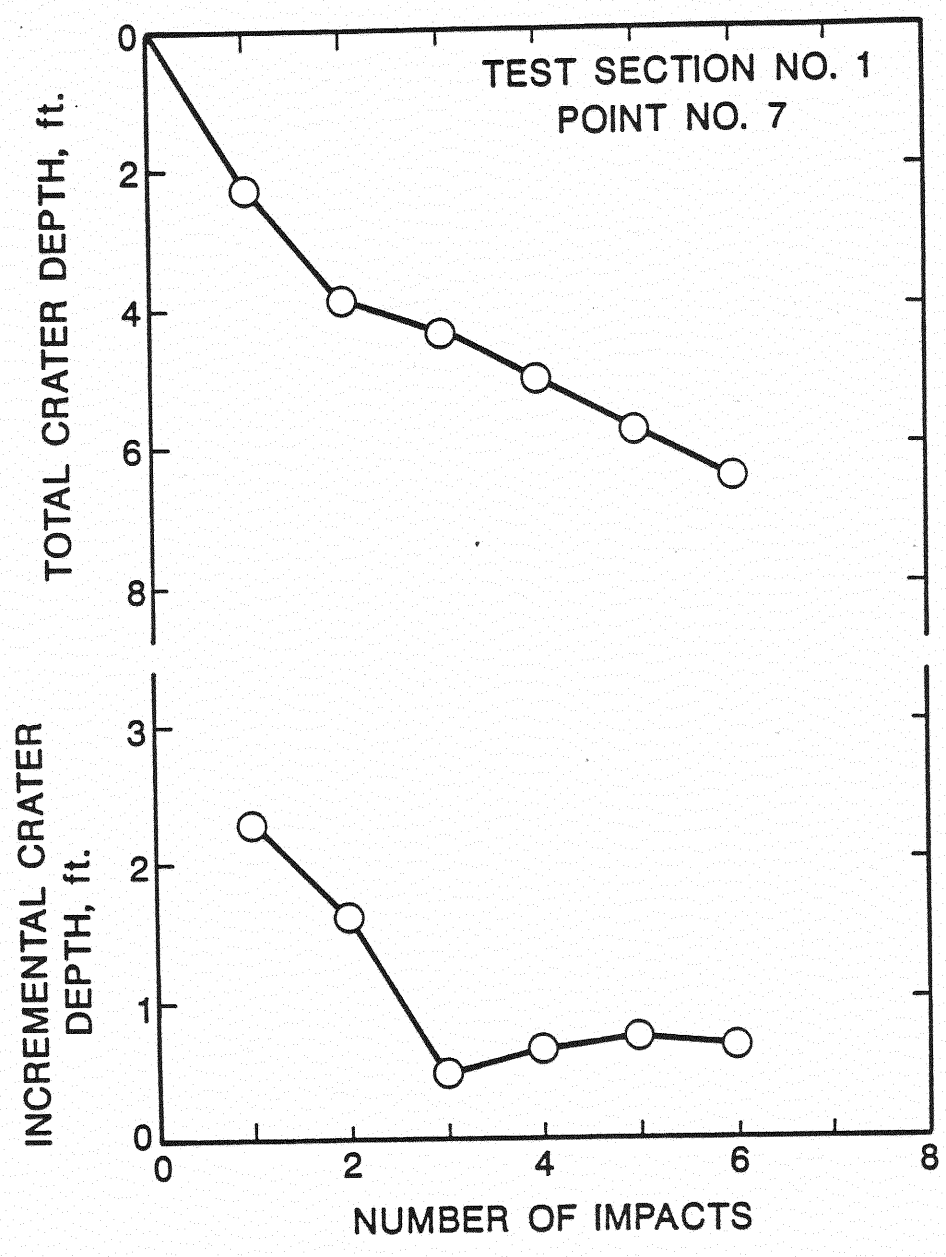

Figure 32. Crater Depth Versus Number of Impacts: Point No. 7, Test Section No. 1

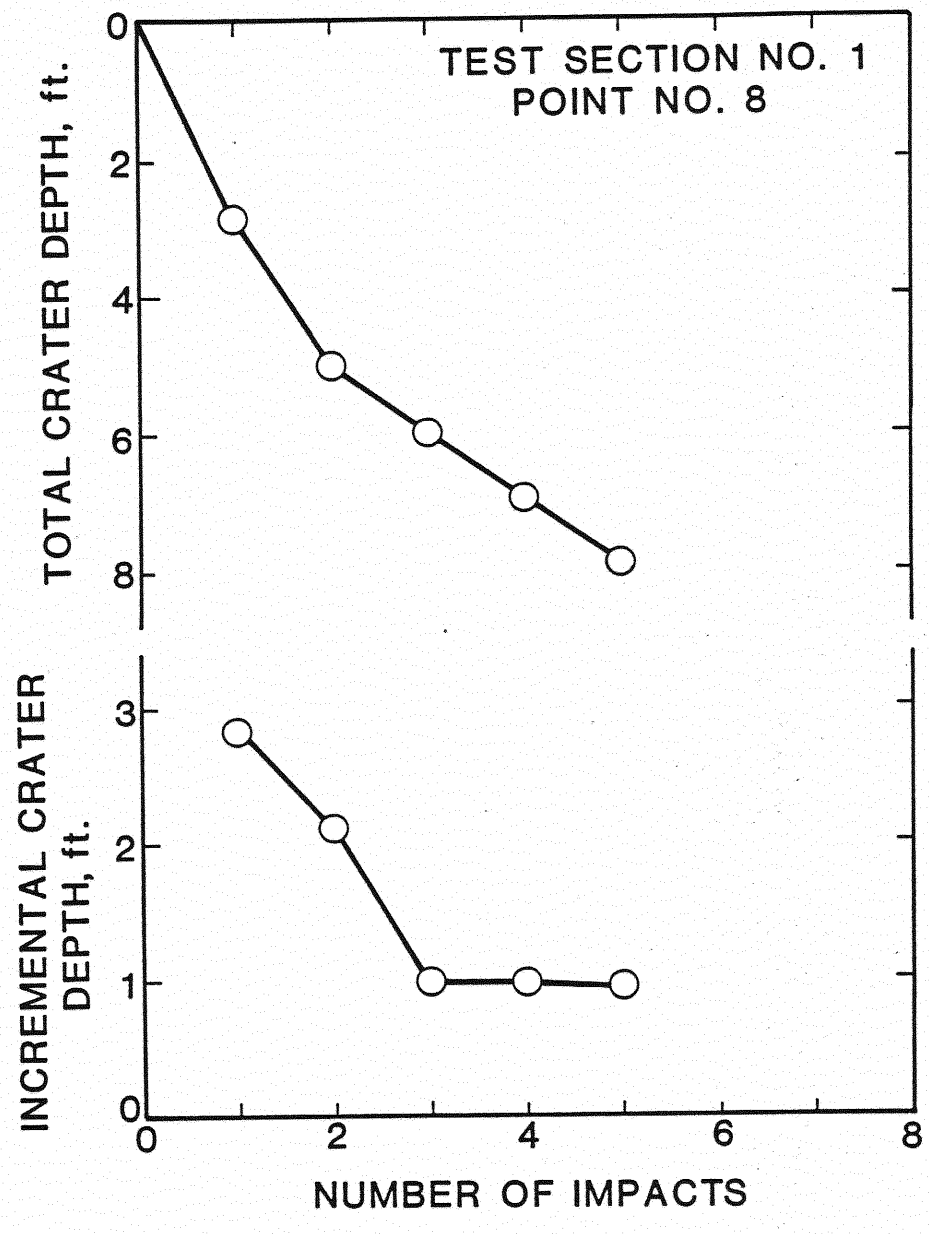

Figure 33. Crater Depth Versus Number of Impacts: Point No. 8, Test Section No. 1

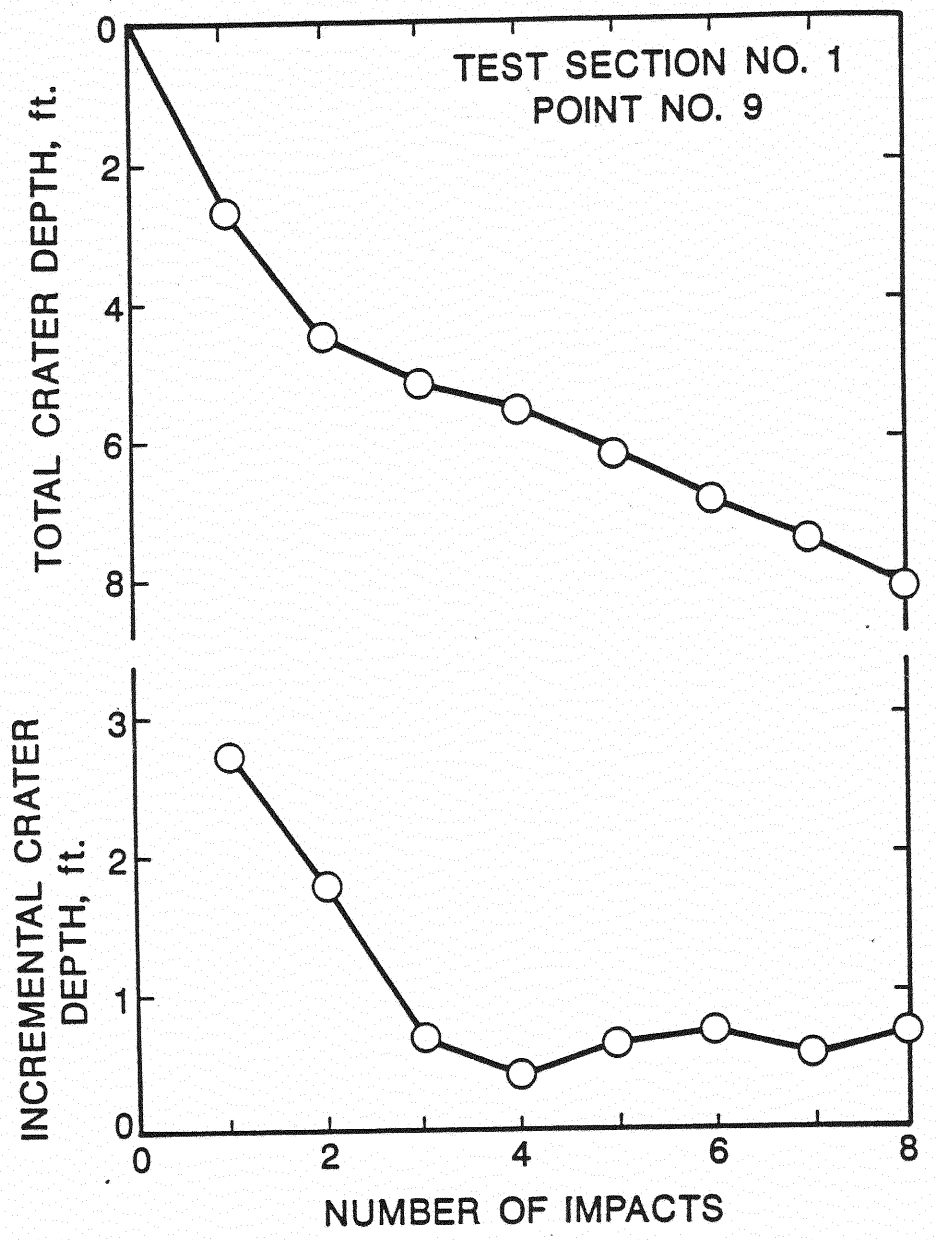

Figure 34. Crater Depth Versus Number of Impacts: Point No. 9, Test Section No. 1

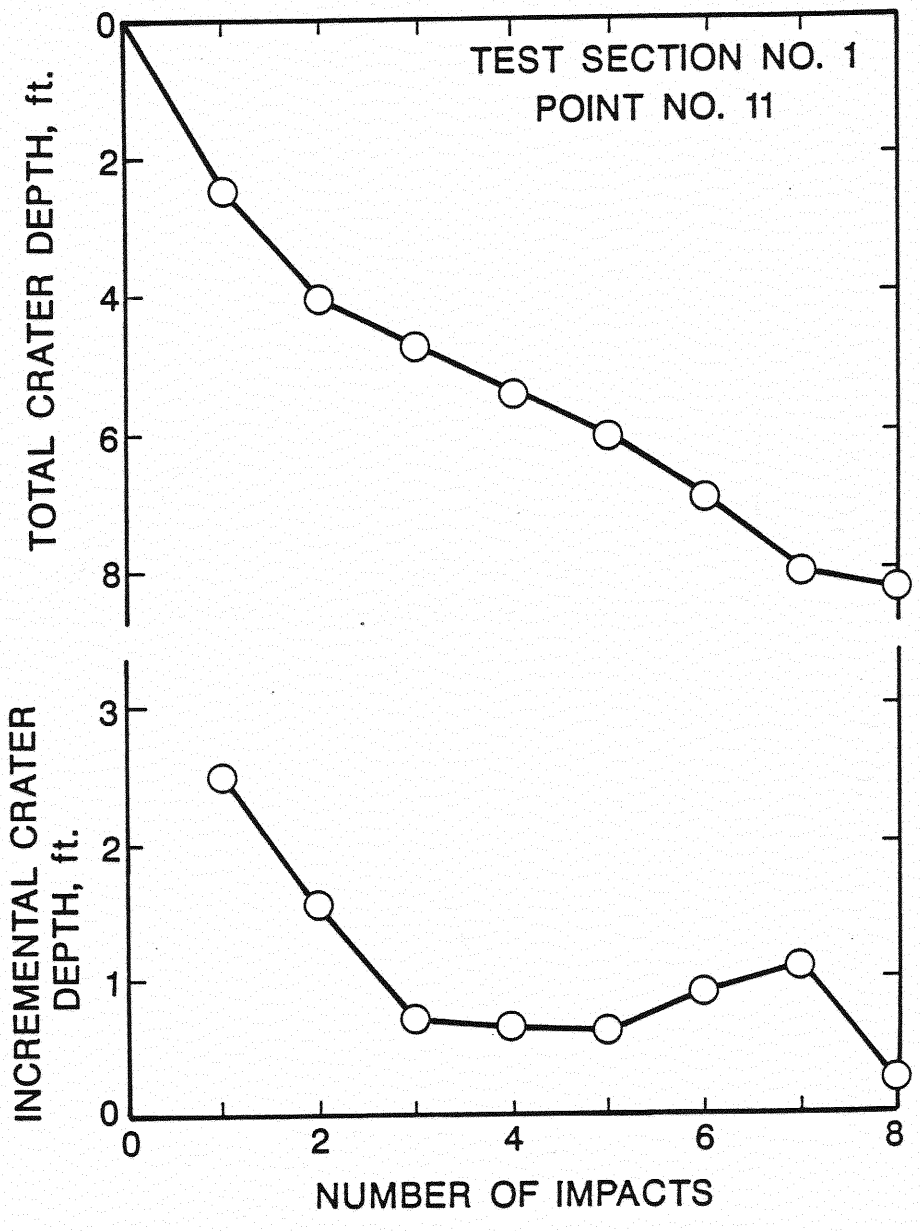

Figure 35. Crater Depth Versus Number of Impacts: Point No. 11, Test Section No. 1

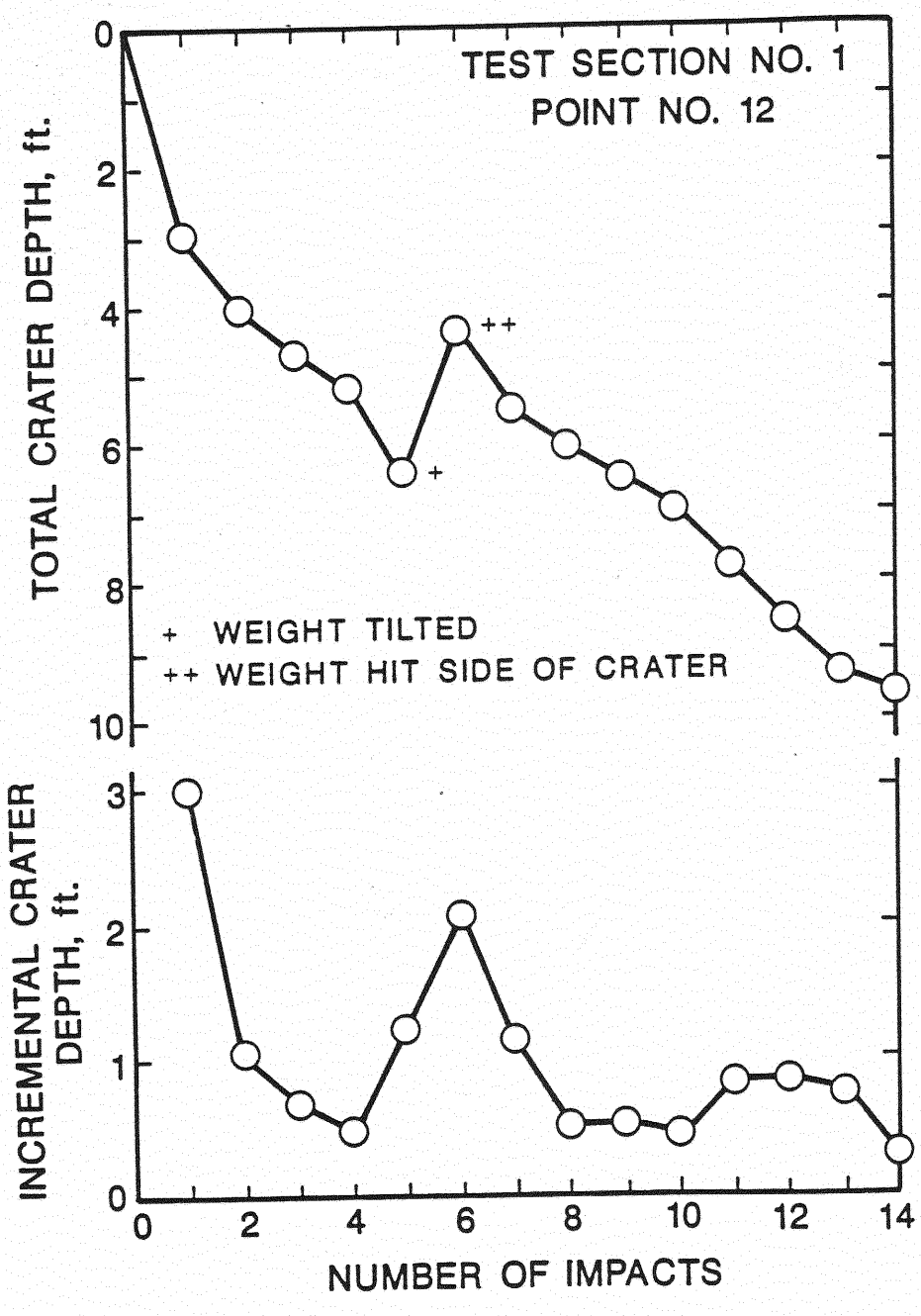

Figure 36. Crater Depth Versus Number of Impacts: Point No. 12, Test Section No. 1

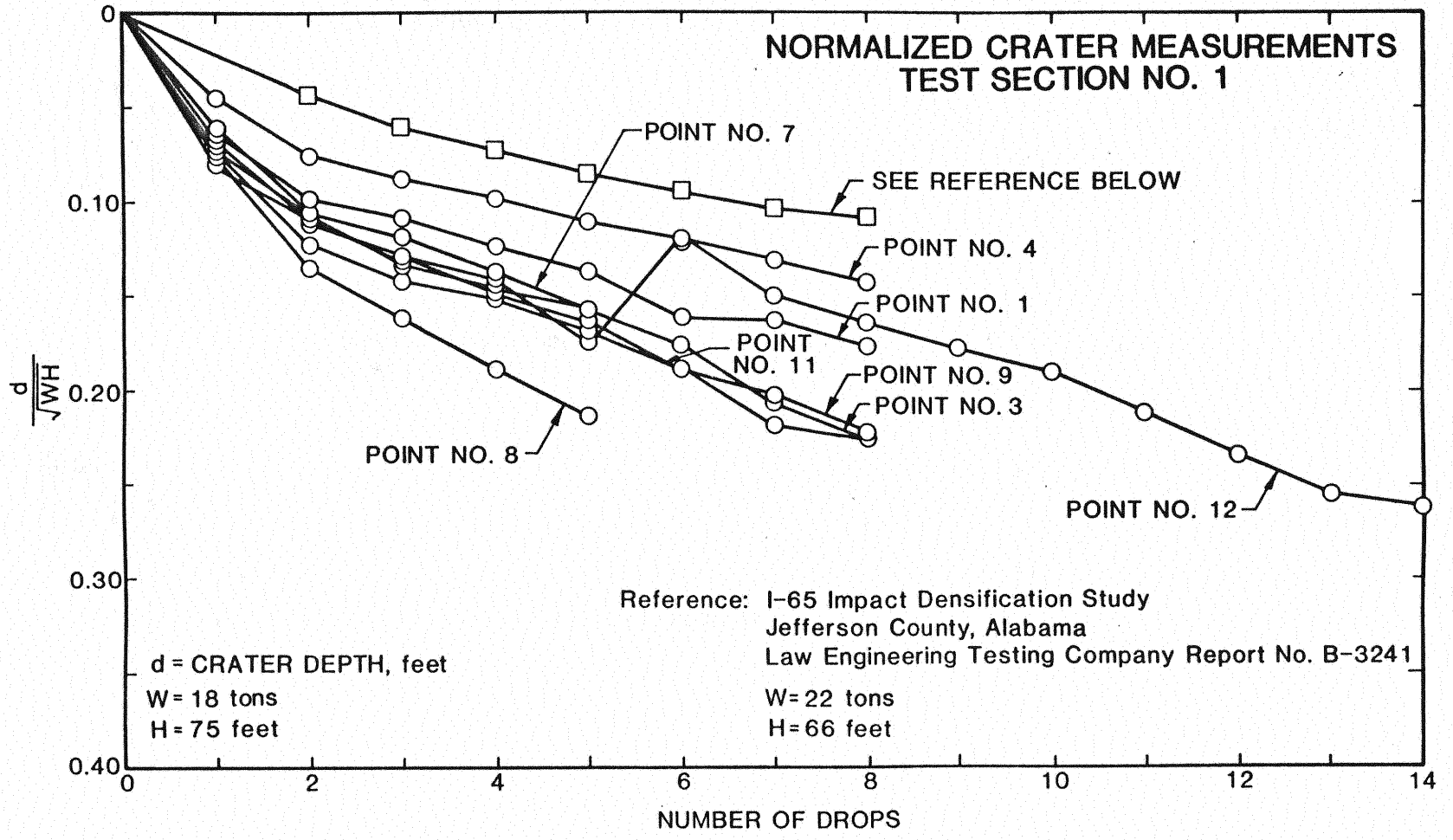

Figure 37. Normalized Crater Measurements, Test Section No. 1

TEST SECTION NO. 1 - BORING NO. 1
(CRL)

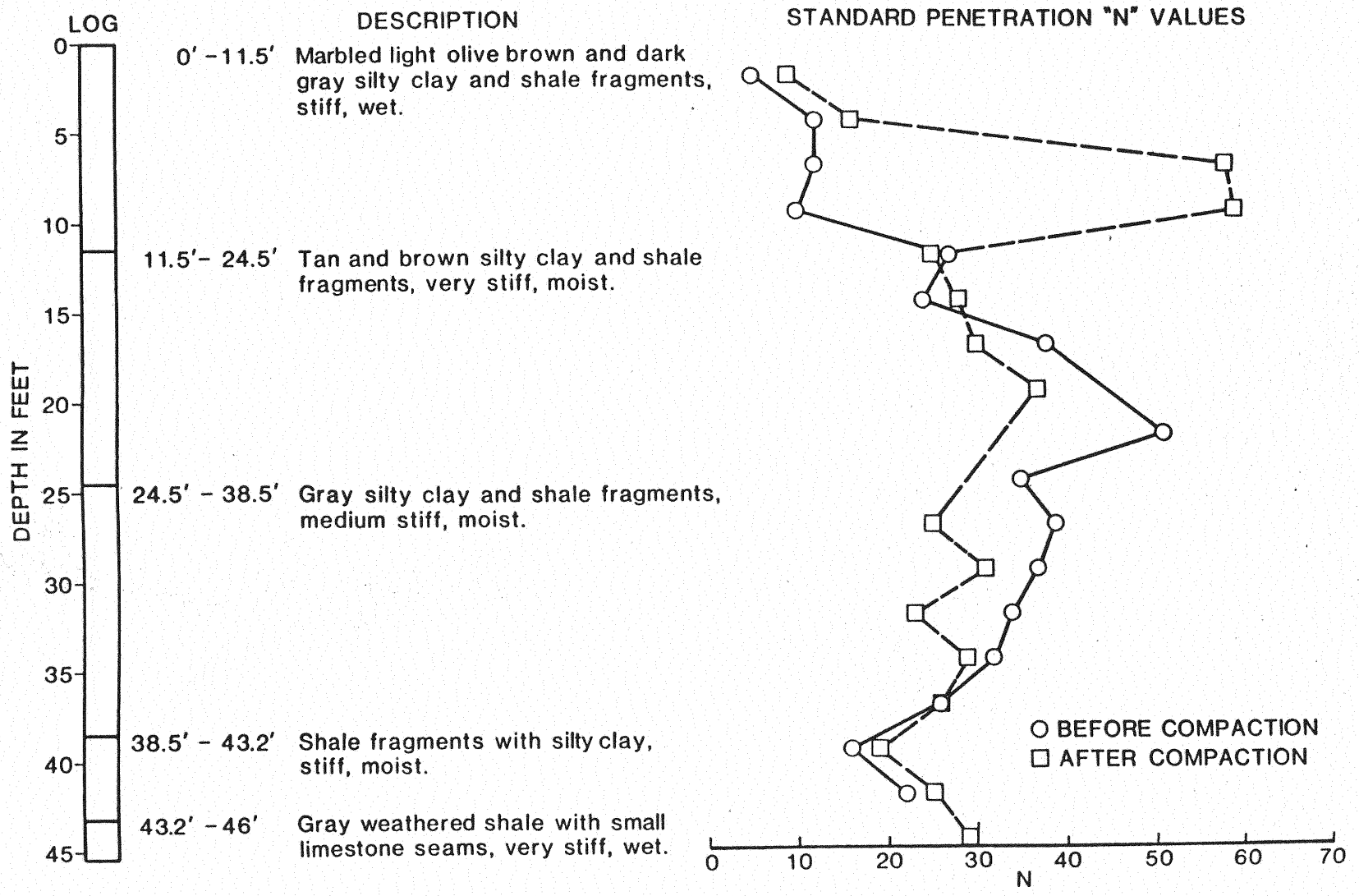

Figure 38. Standard Penetration Test Results, Along CRL, Test Section No. 1

TEST SECTION NO. 1 - BORING NO. 2
(SOUTH OF CRL)

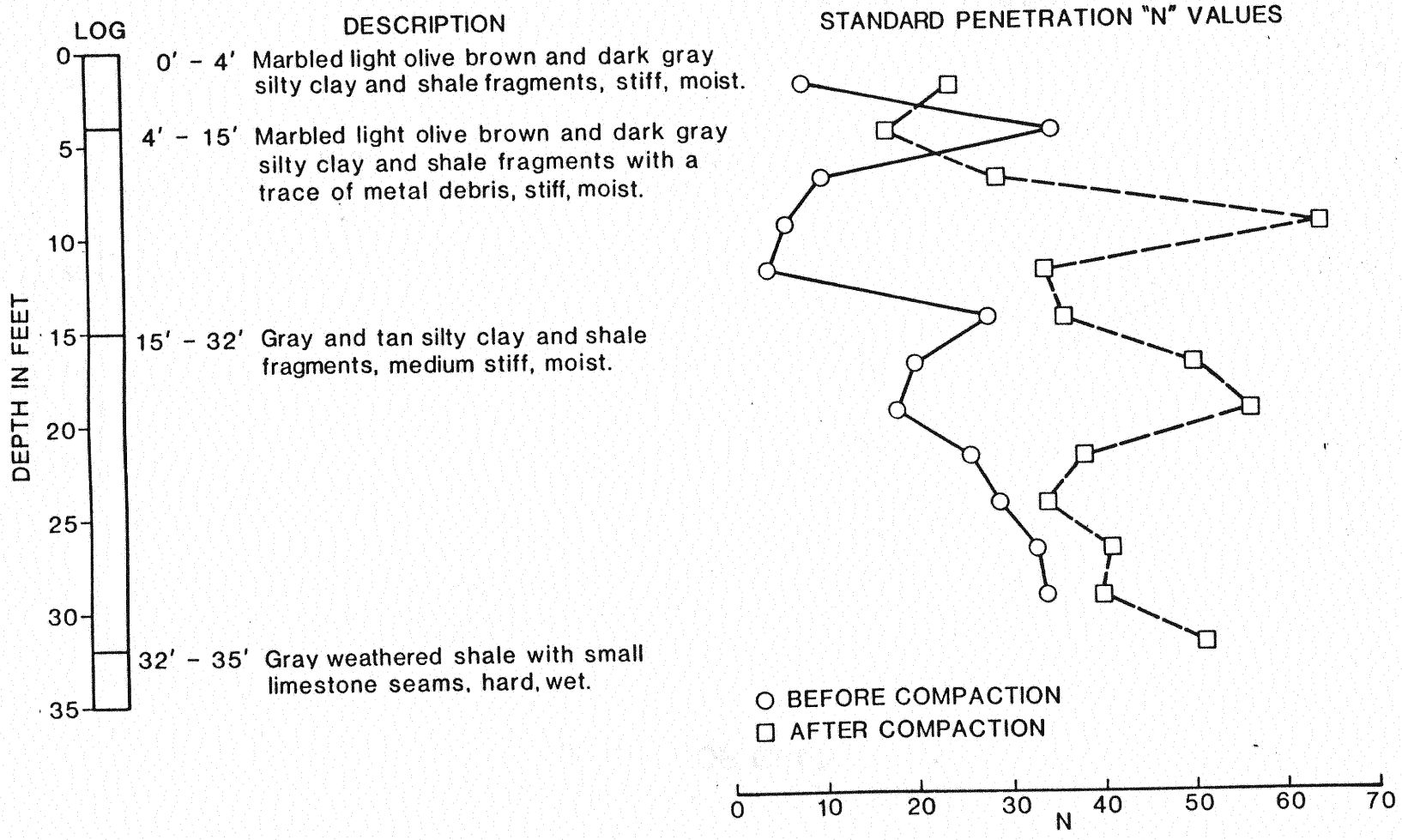

Figure 39. Standard Penetration Test Results, South of CRL, Test Section No. 1

TEST SECTION NO. 1 – BORING NO. 3
(NORTH OF CRL)

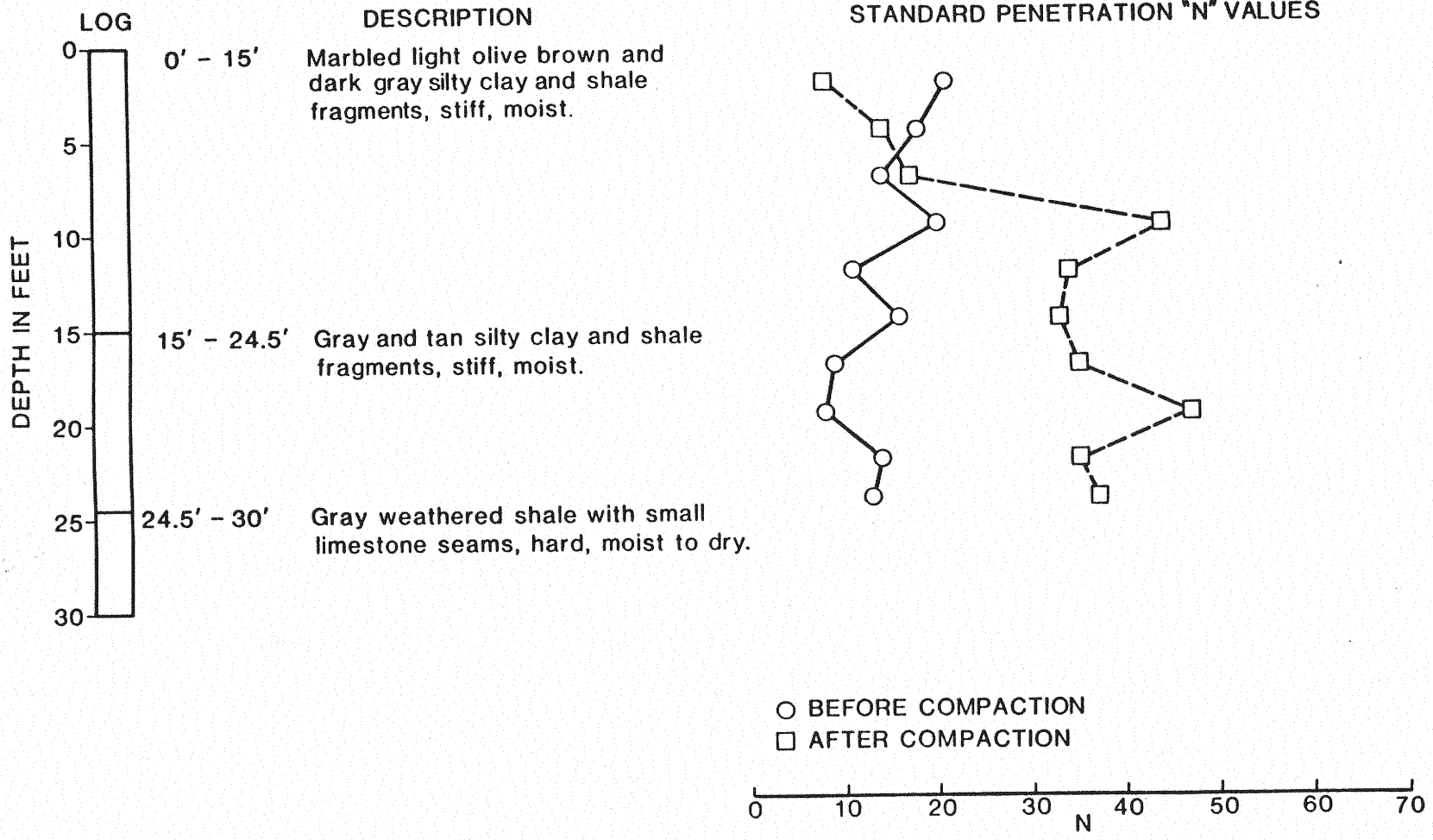

Figure 40. Standard Penetration Test Results, North of CRL, Test Section No. 1

APPENDIX B

RESULTS FROM TEST SECTION NO. 2

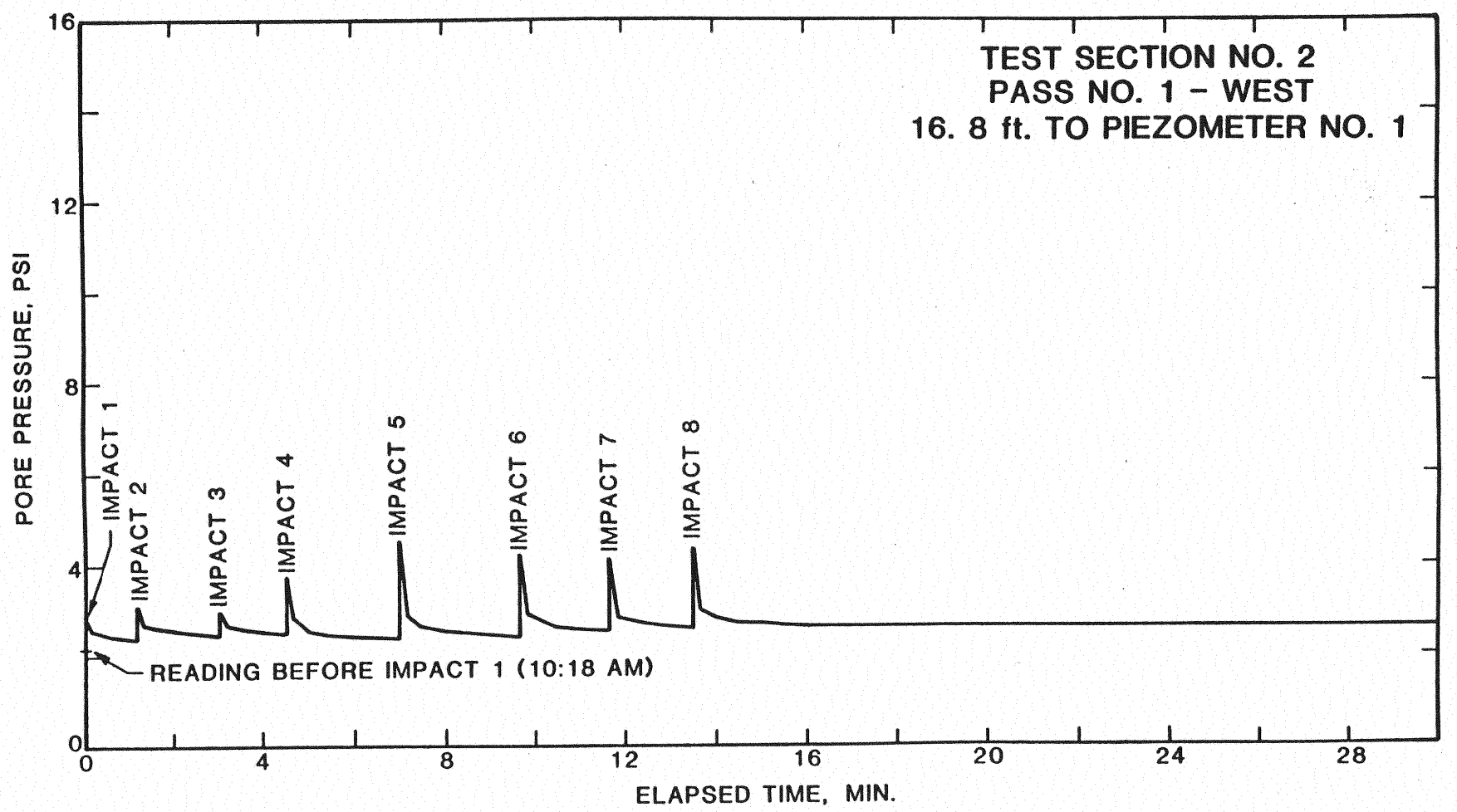

Figure 41. Piezometer Data, Pass No. 1 - West, Test Section No. 2

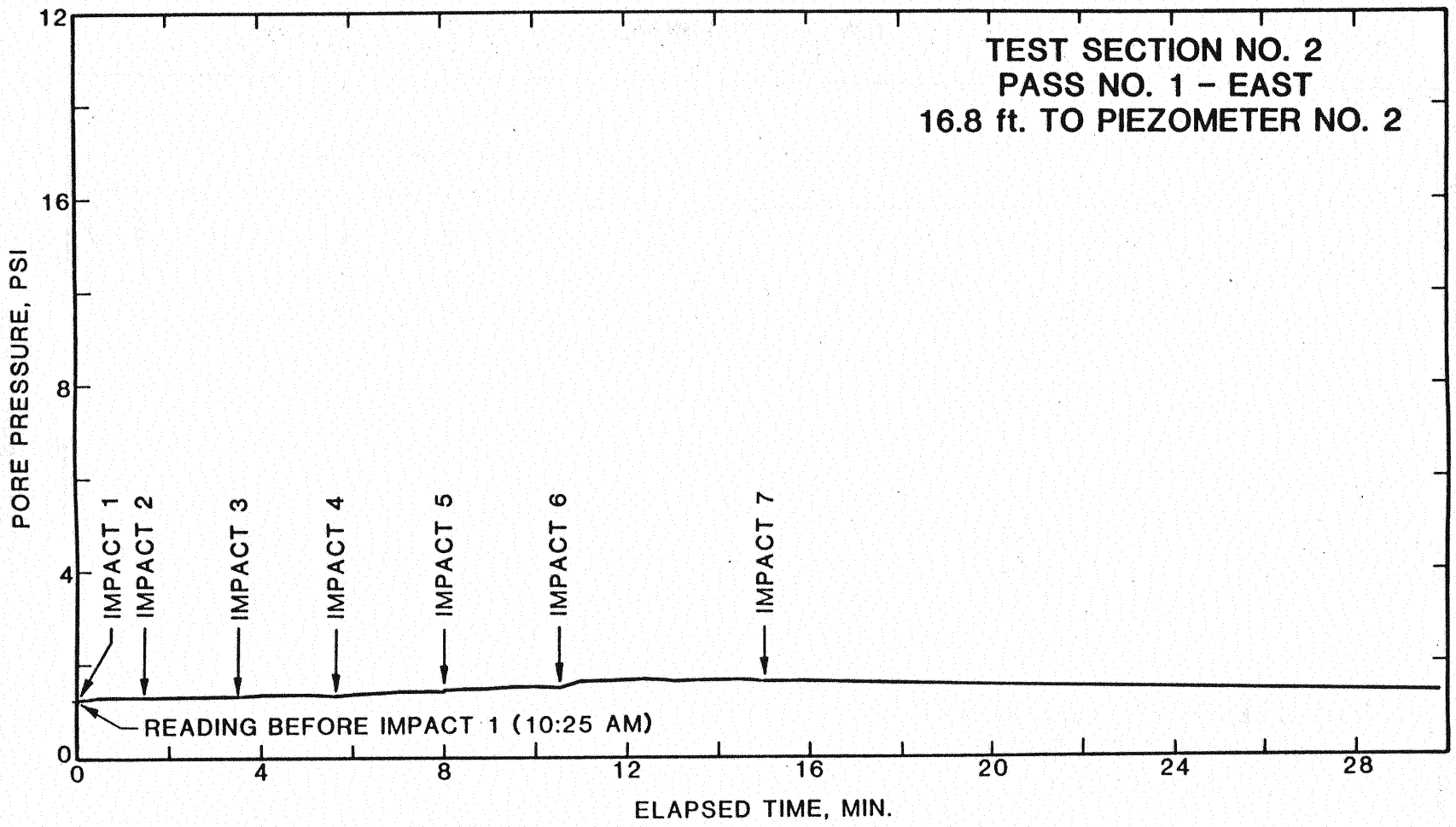

Figure 42. Piezometer Data, Pass No. 1 - East, Test Section No. 2

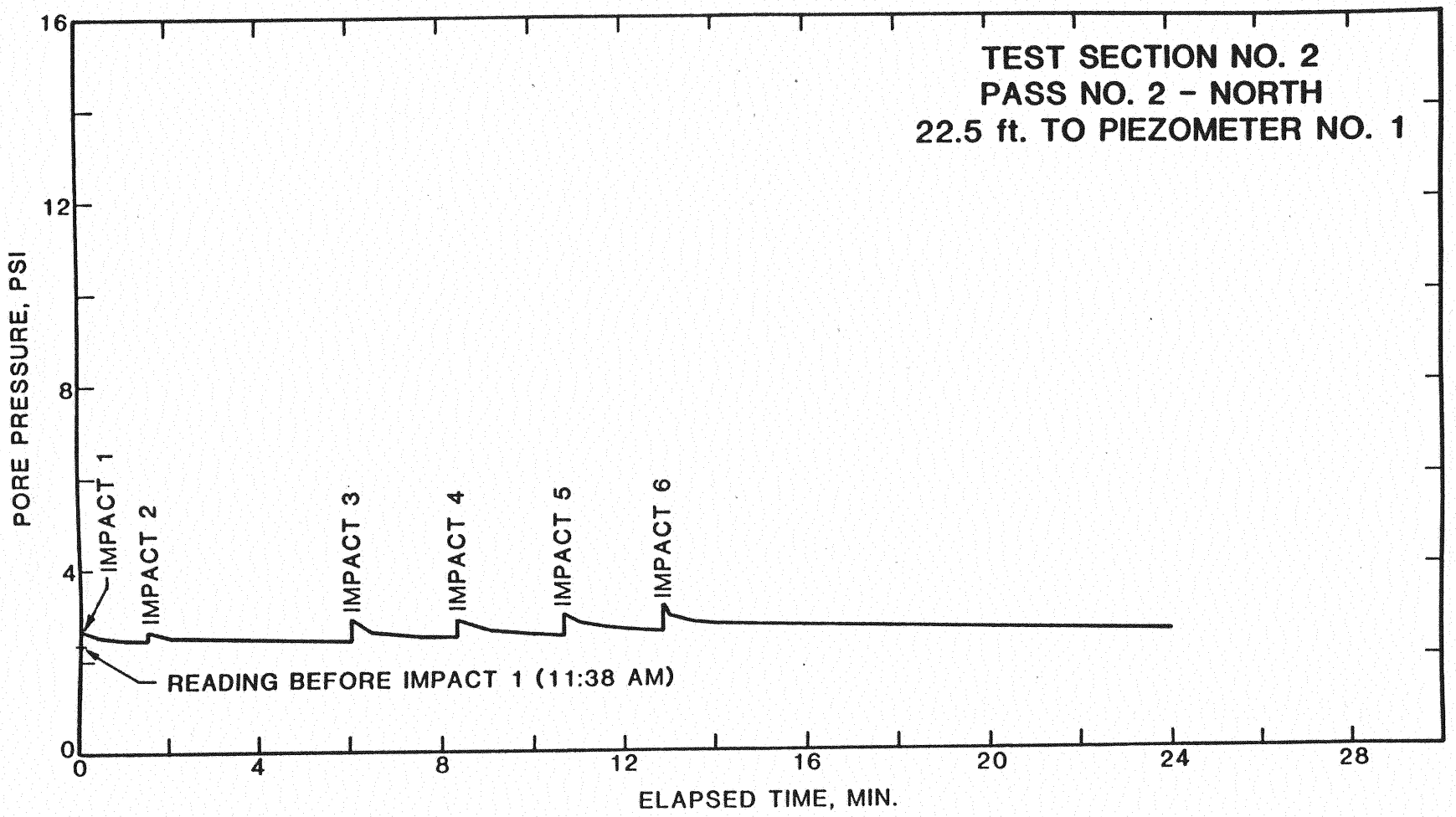

Figure 43. Piezometer Data, Pass No. 2 - North, Test Section No. 2

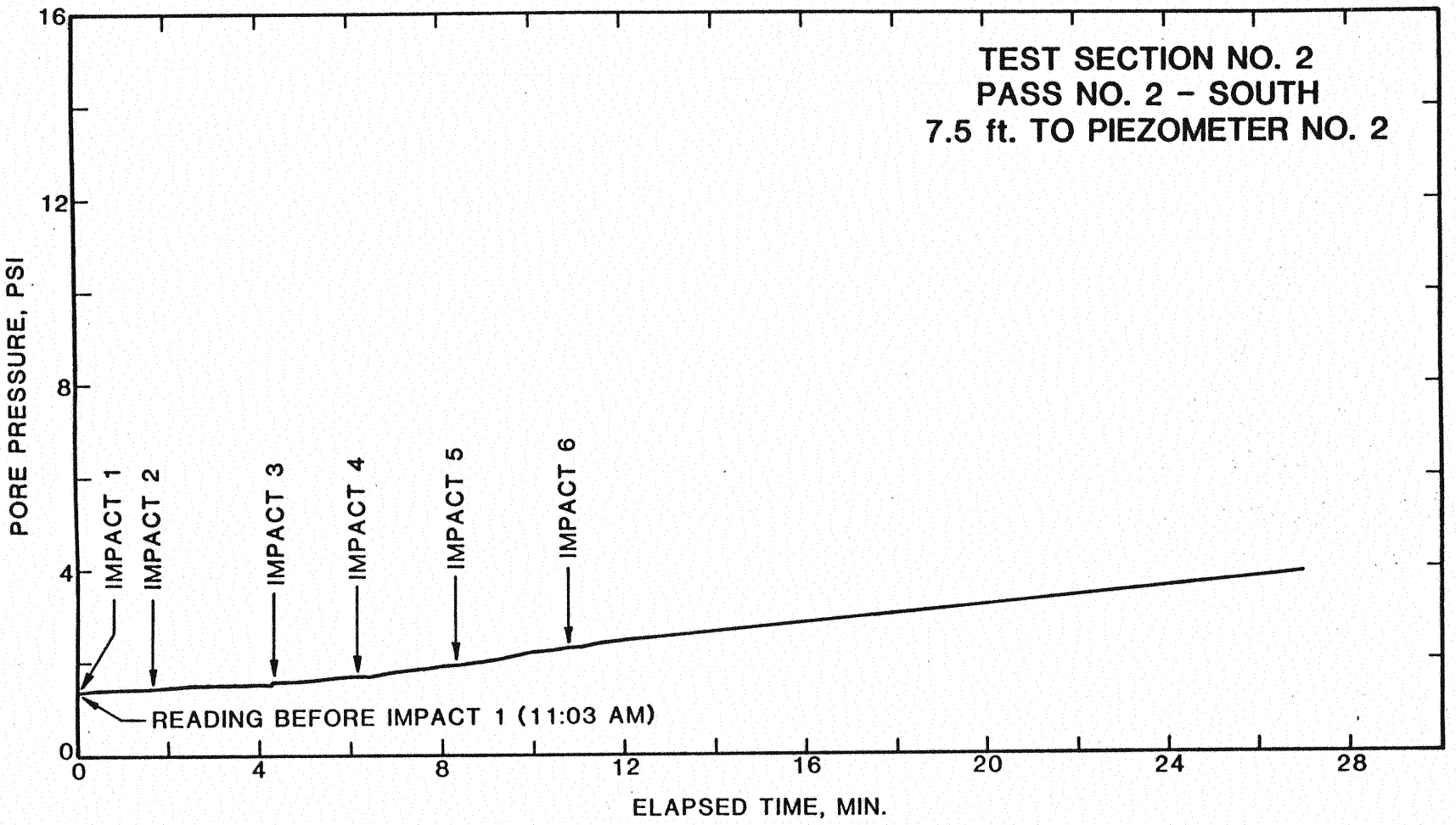

Figure 44. Piezometer Data, Pass No. 2 - South, Test Section No. 2

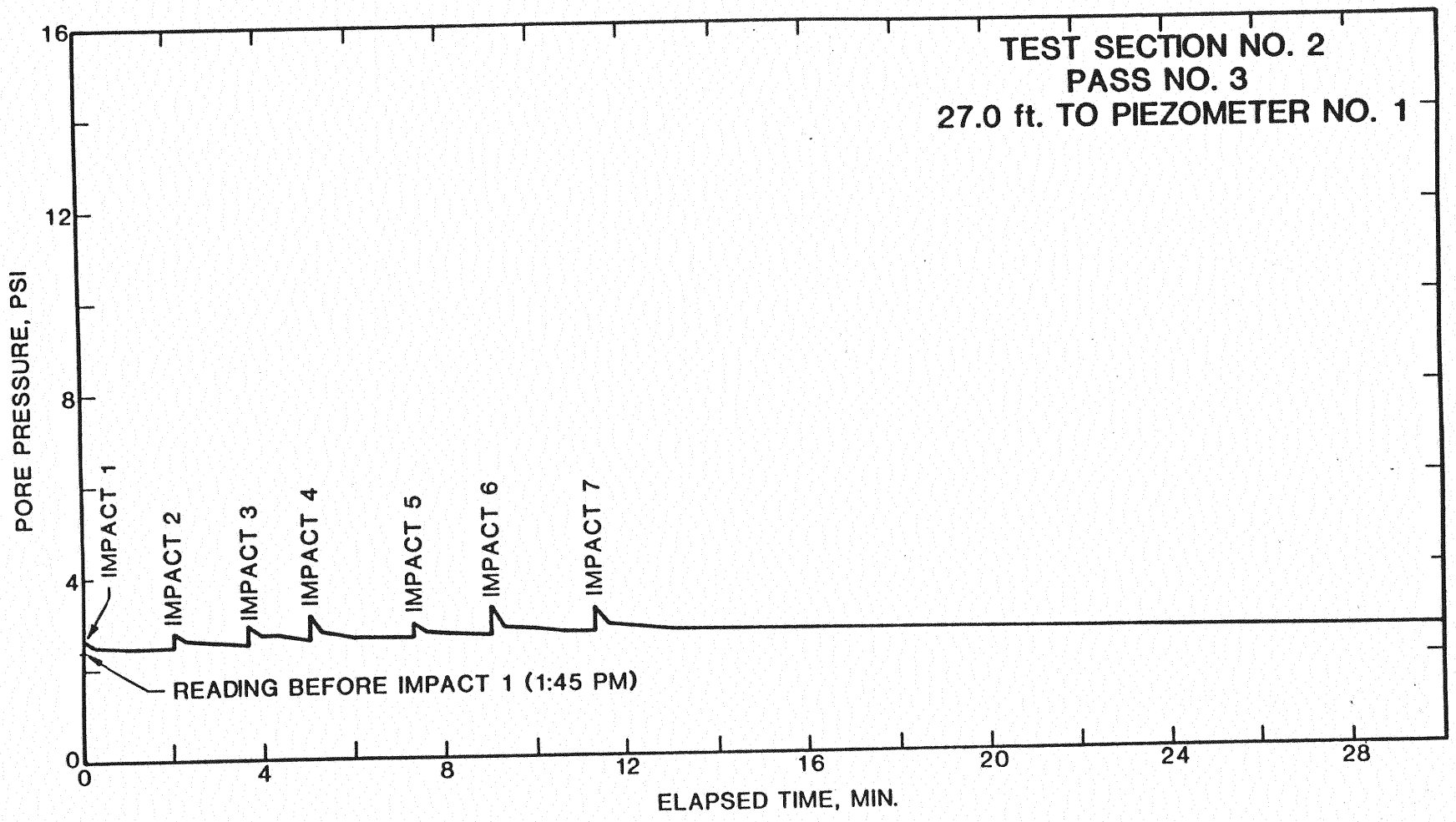

Figure 45. Piezometer Data, Pass No. 3, Test Section No. 2

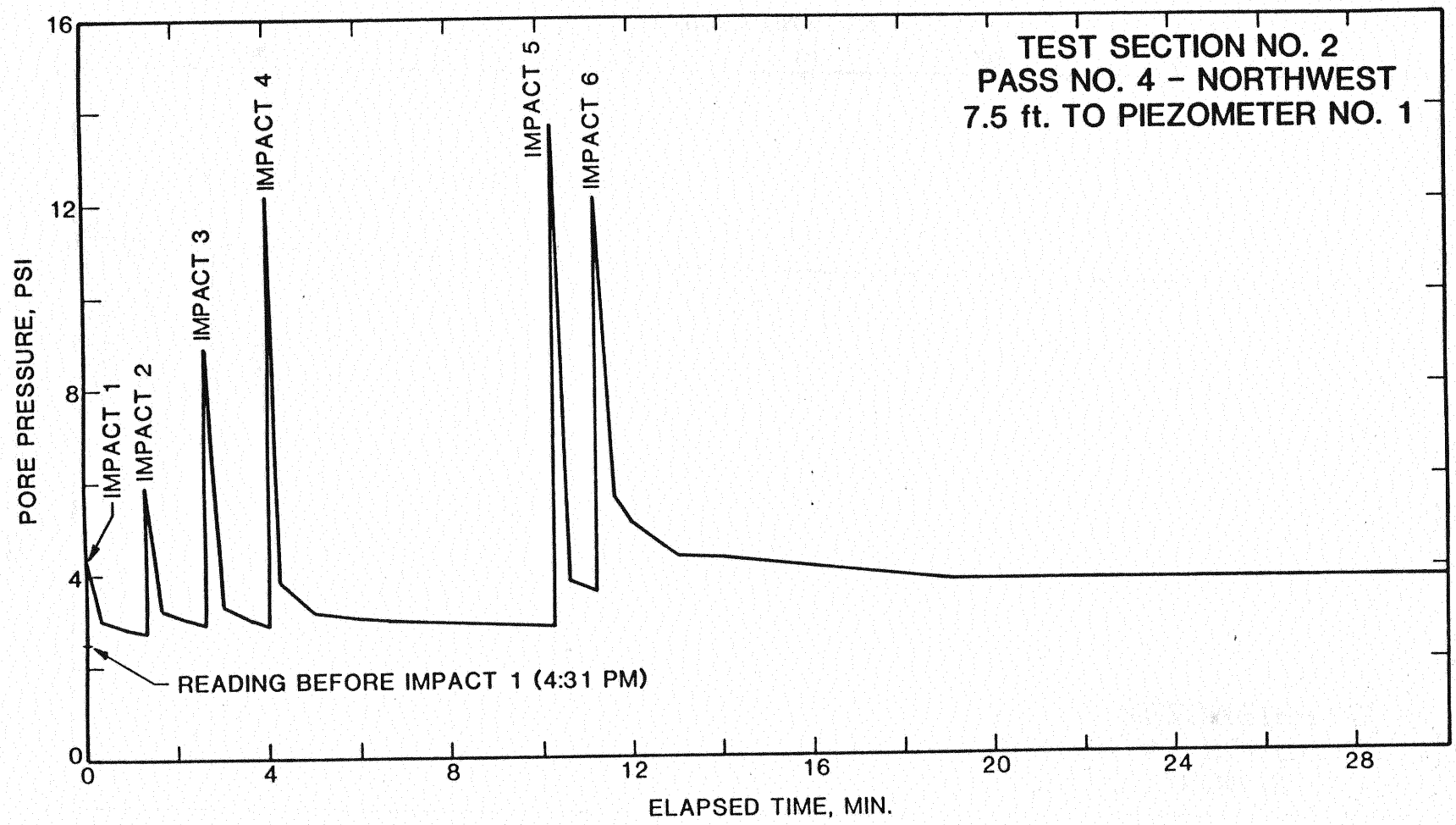

Figure 46. Piezometer Data, Pass No. 4 - Northwest, Test Section No. 2

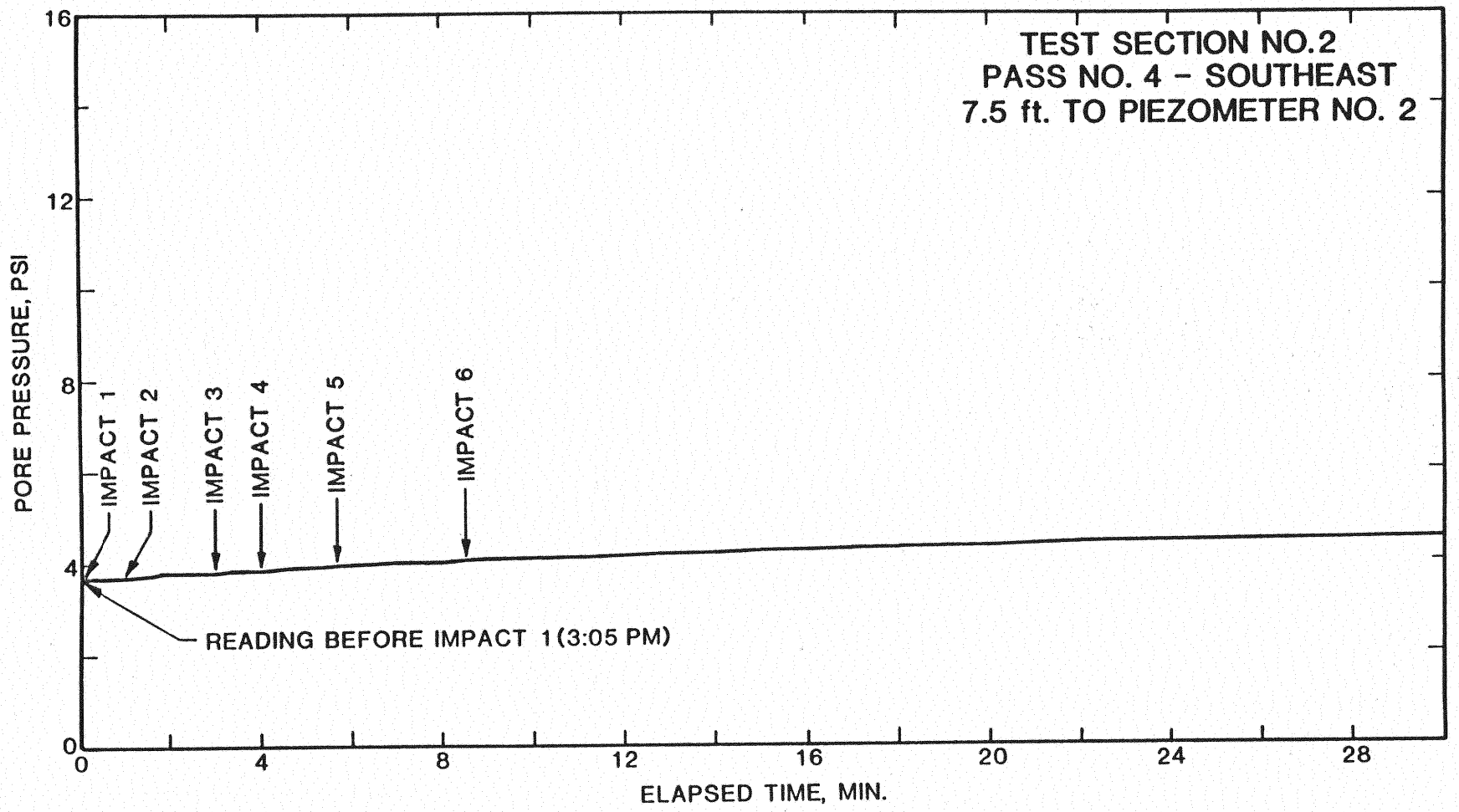

Figure 47. Piezometer Data, Pass No. 4 - Southeast, Test Section No. 2

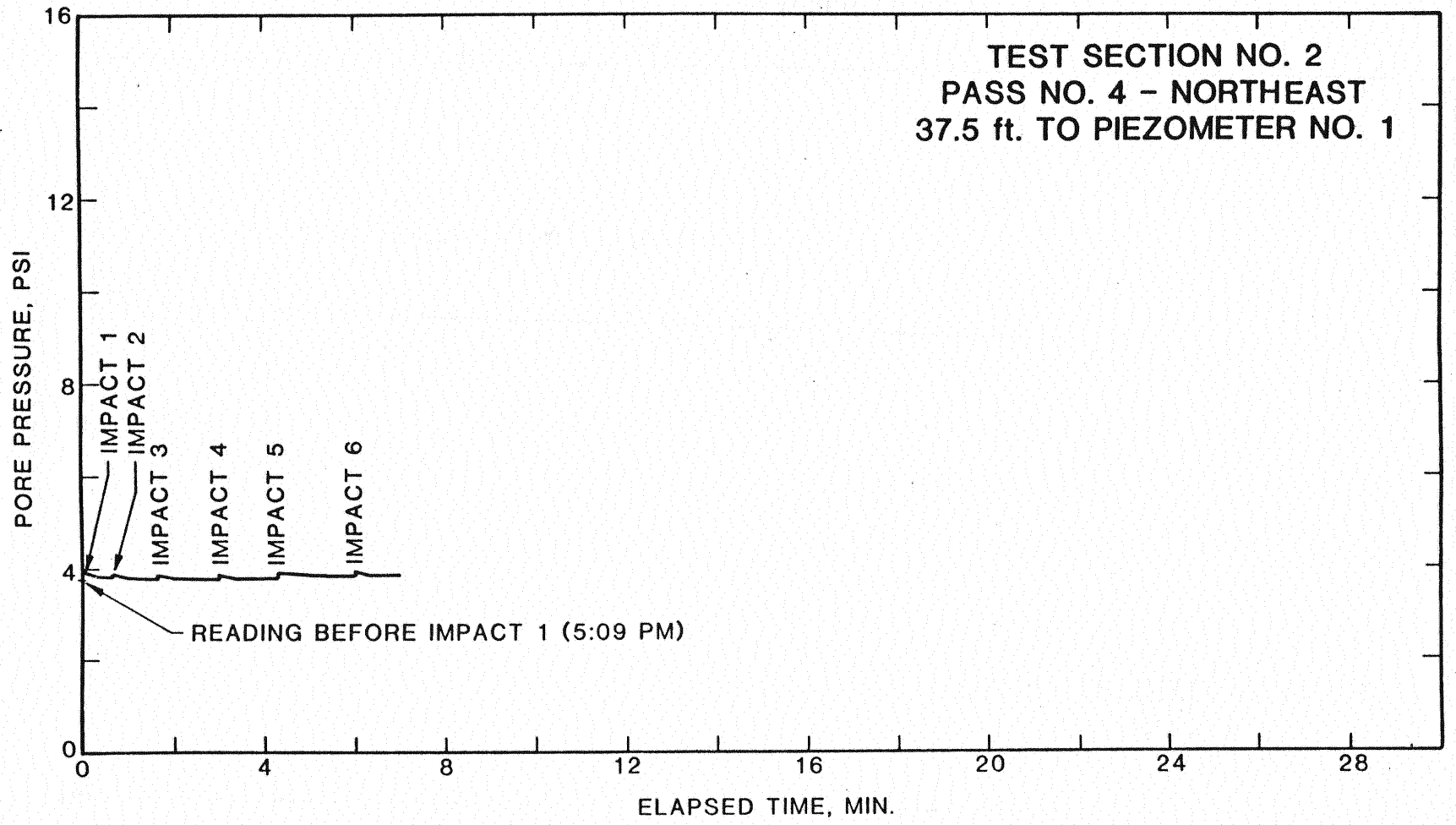

Figure 48. Piezometer Data, Pass No. 4 - Northeast, Test Section No. 2

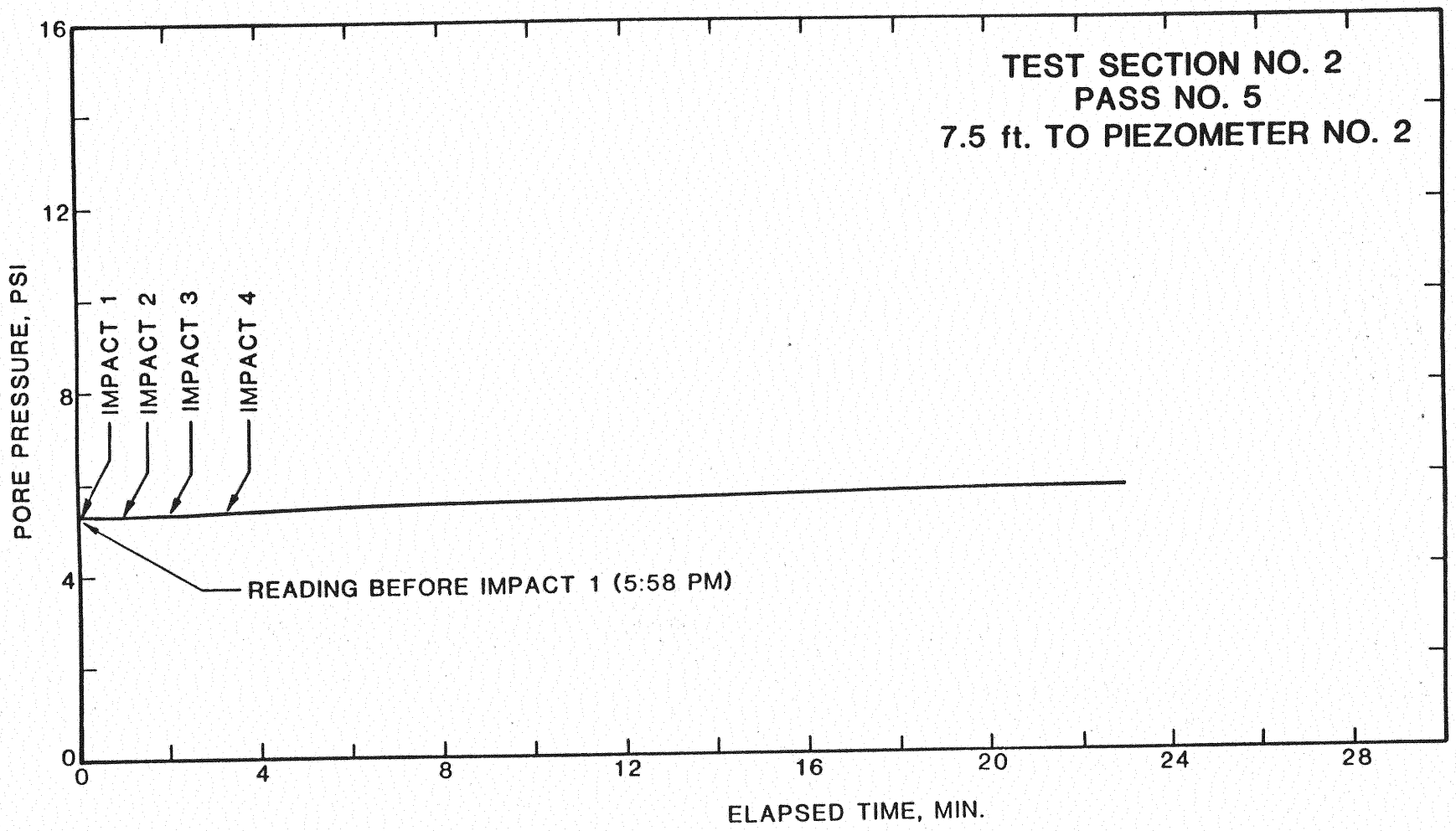

Figure 49. Piezometer Data, Pass No. 5, Test Section No. 2

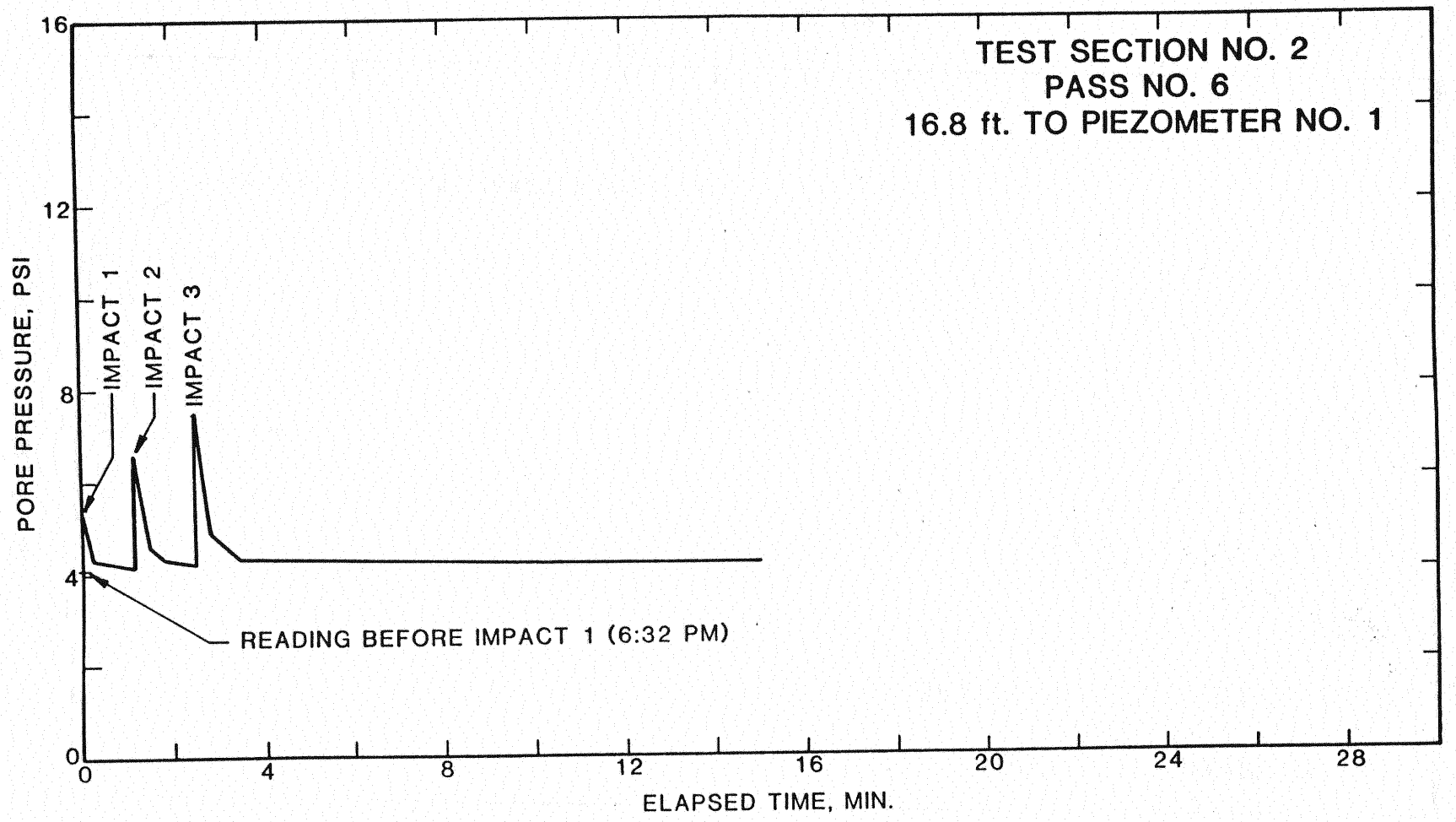

Figure 50. Piezometer Data, Pass No. 6, Test Section No. 2

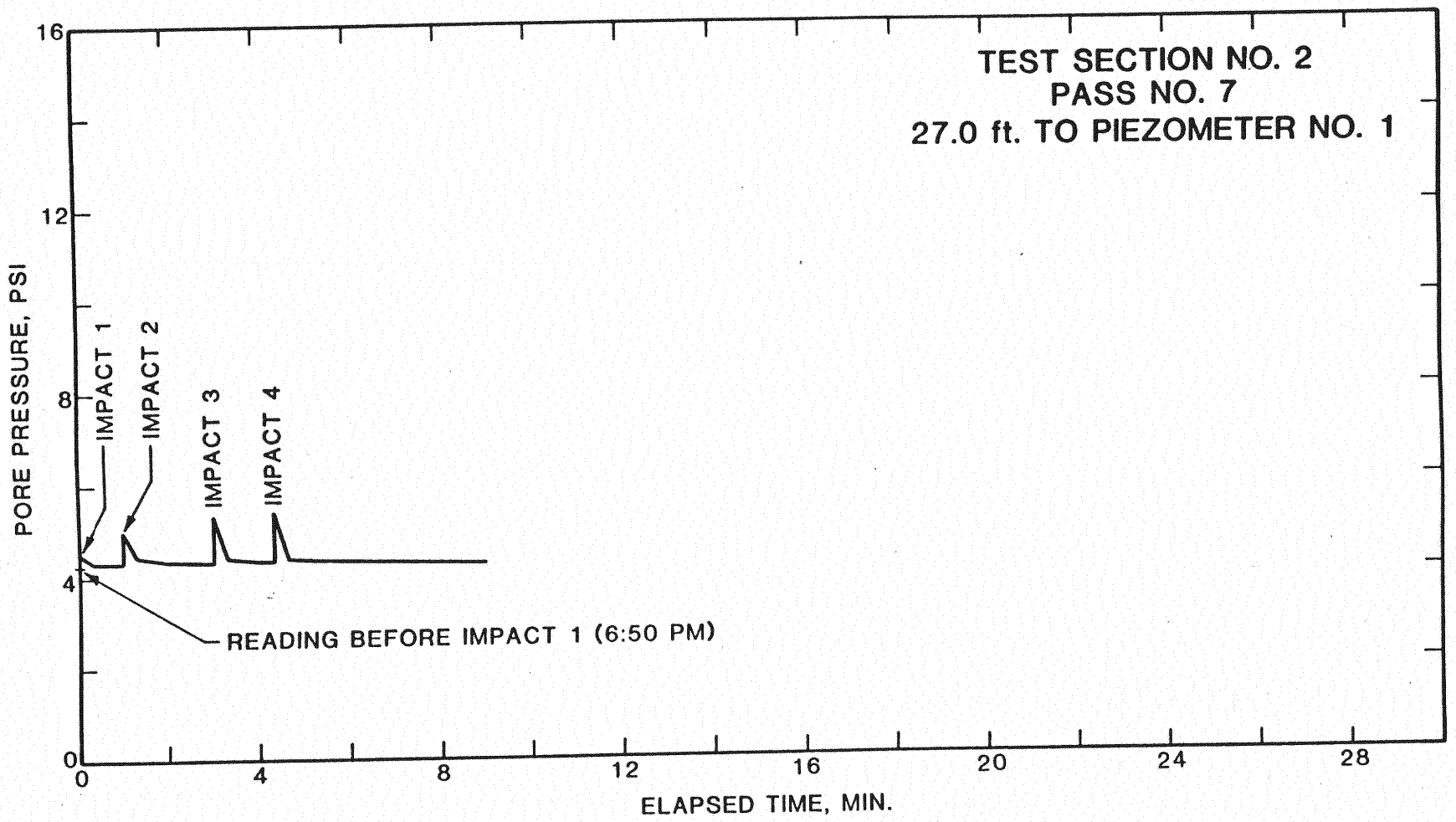

Figure 51. Piezometer Data, Pass No. 7, Test Section No. 2

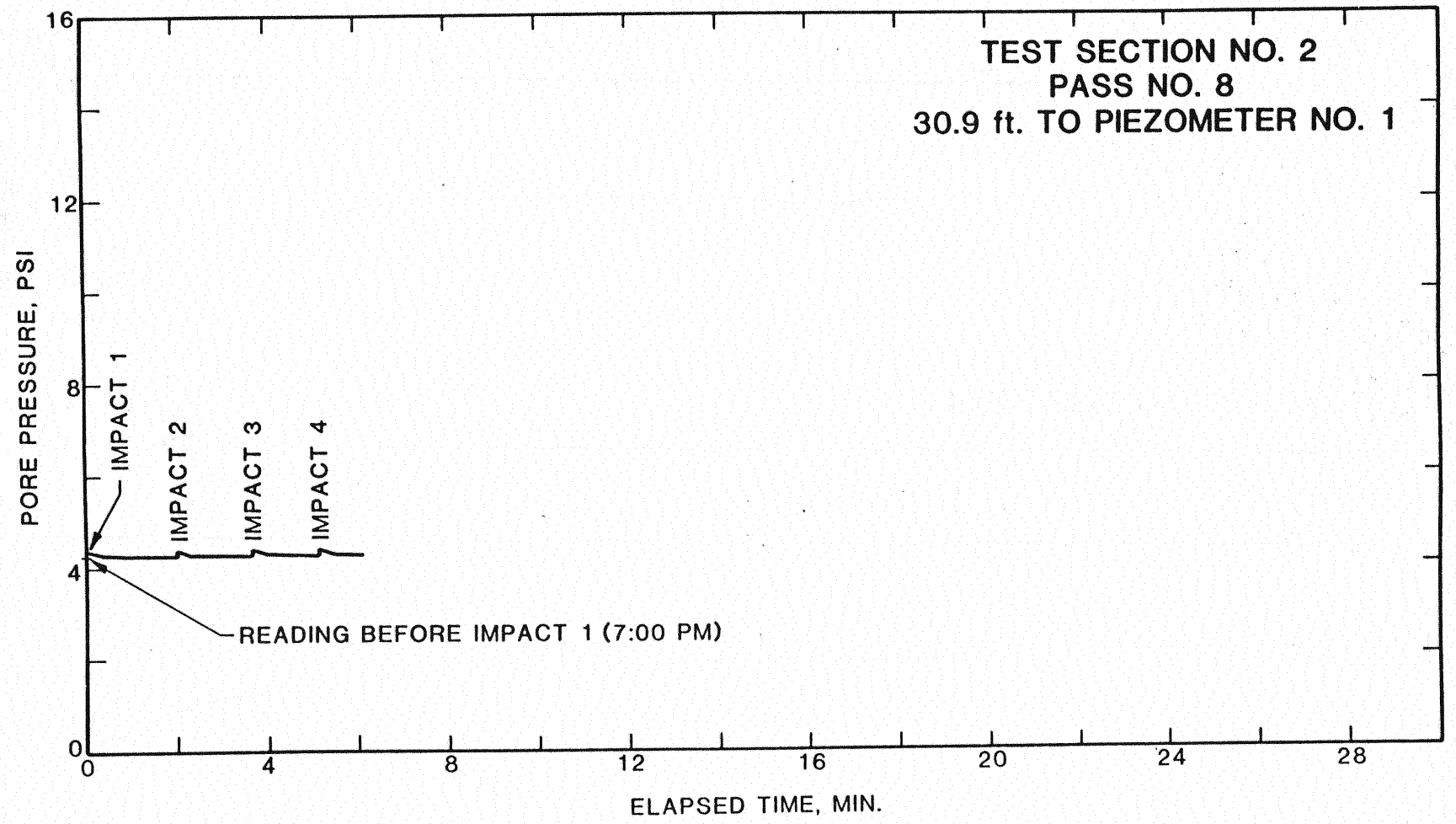

Figure 52. Piezometer Data, Pass No. 8, Test Section No. 2

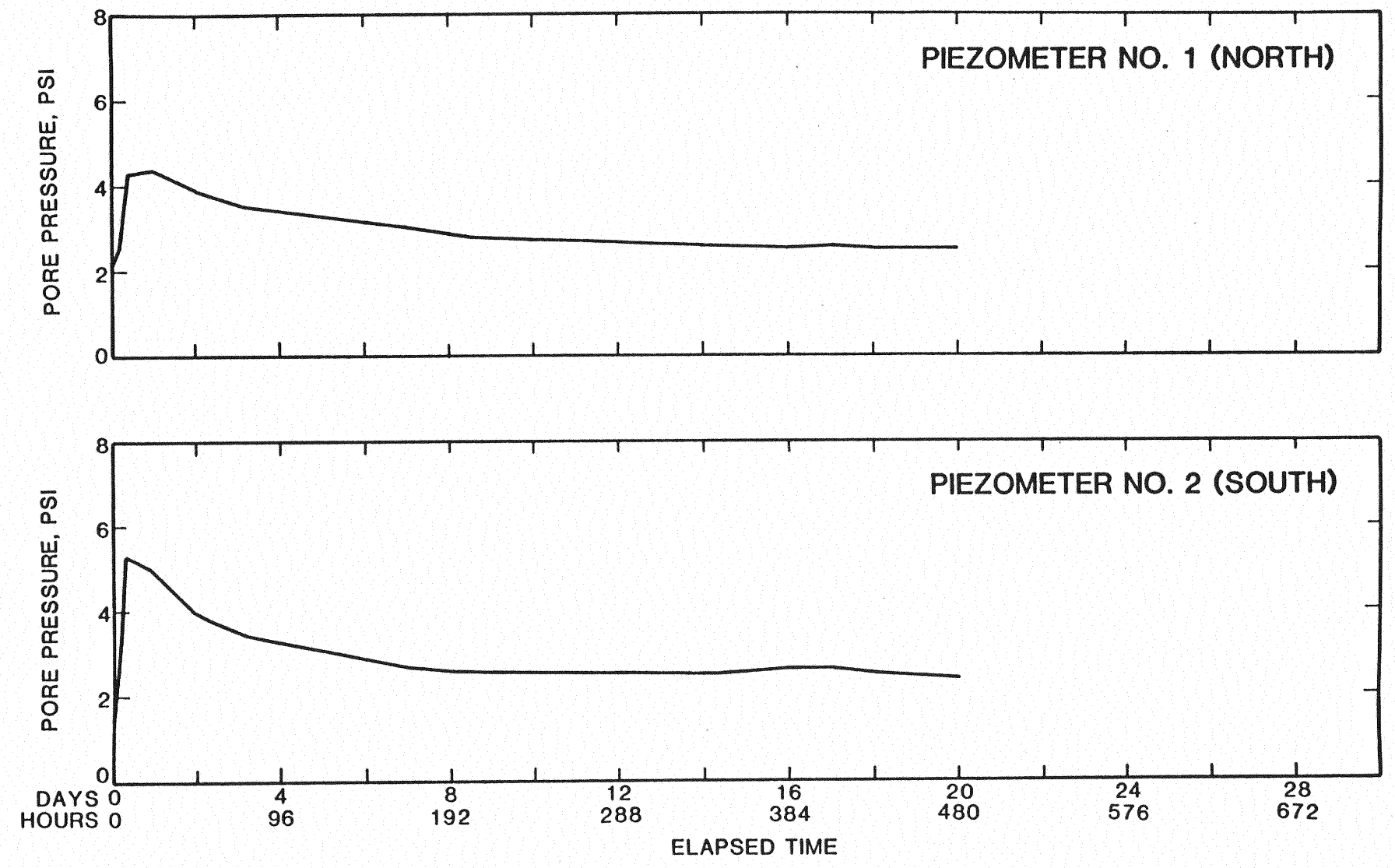

Figure 53. Long-Term Pore Pressure Dissipation, Test Section No. 2

TABLE II

SUMMARY OF CRATER DEPTHS, TEST SECTION NO. 2

Pass No.	Location	Number of Impacts	Crater Depth (Ft)
1	West	8	12.5
1	East	6	13.1
2	South	6	13.6
2	North	6	13.6
3	---	7	11.5
4	Southwest	3	8.5
4	Northeast	6	11.9
4	Southeast	6	11.0*
4	Northwest	6	12.0*
5	---	4	10.0*
6	---	3	8.0*
7	---	4	7.9
8	---	4	9.4

*Depth measured after weight removed from crater.

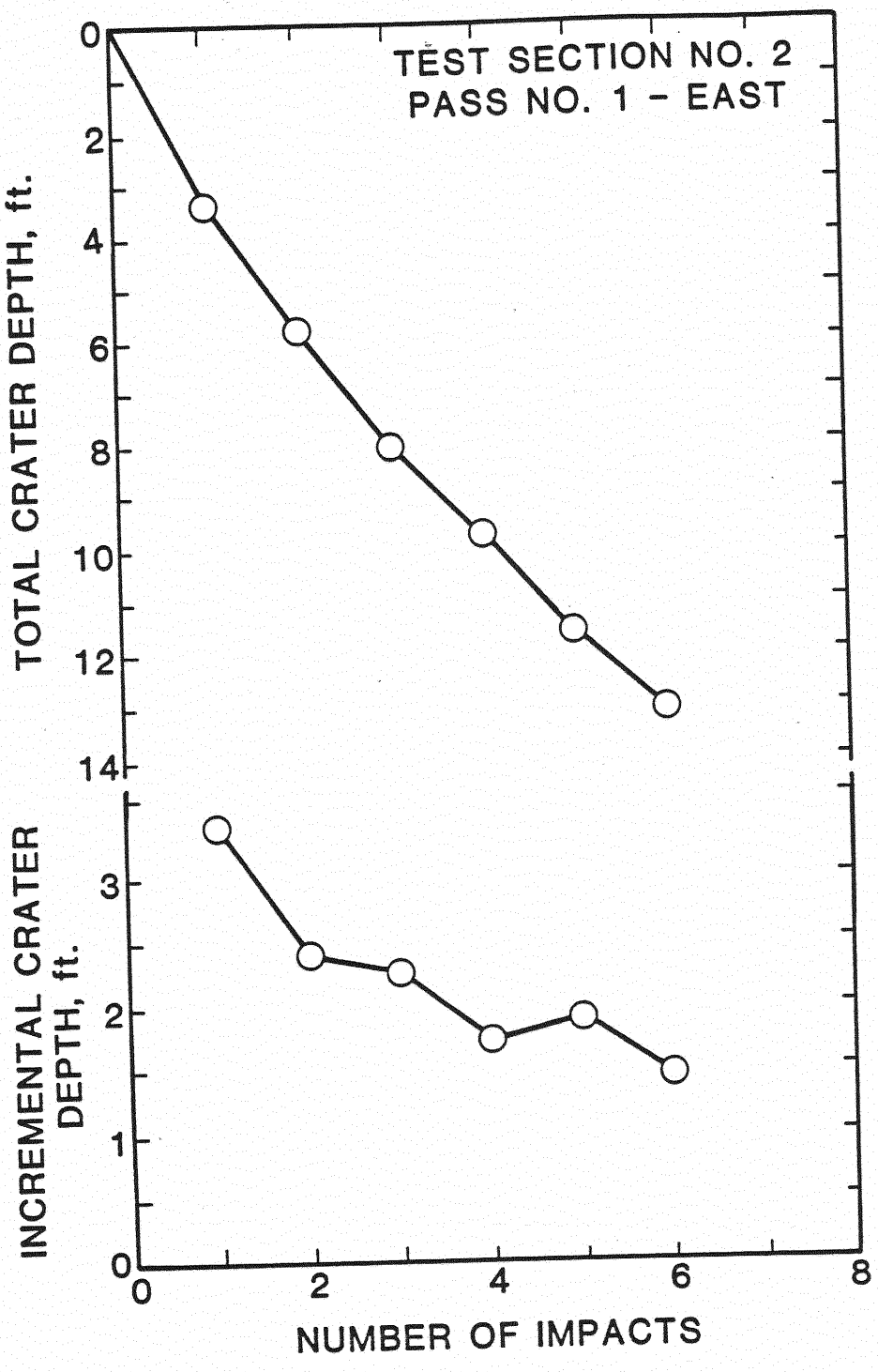

Figure 54. Crater Depth Versus Number of Impacts: Pass No. 1 - East, Test Section No. 2

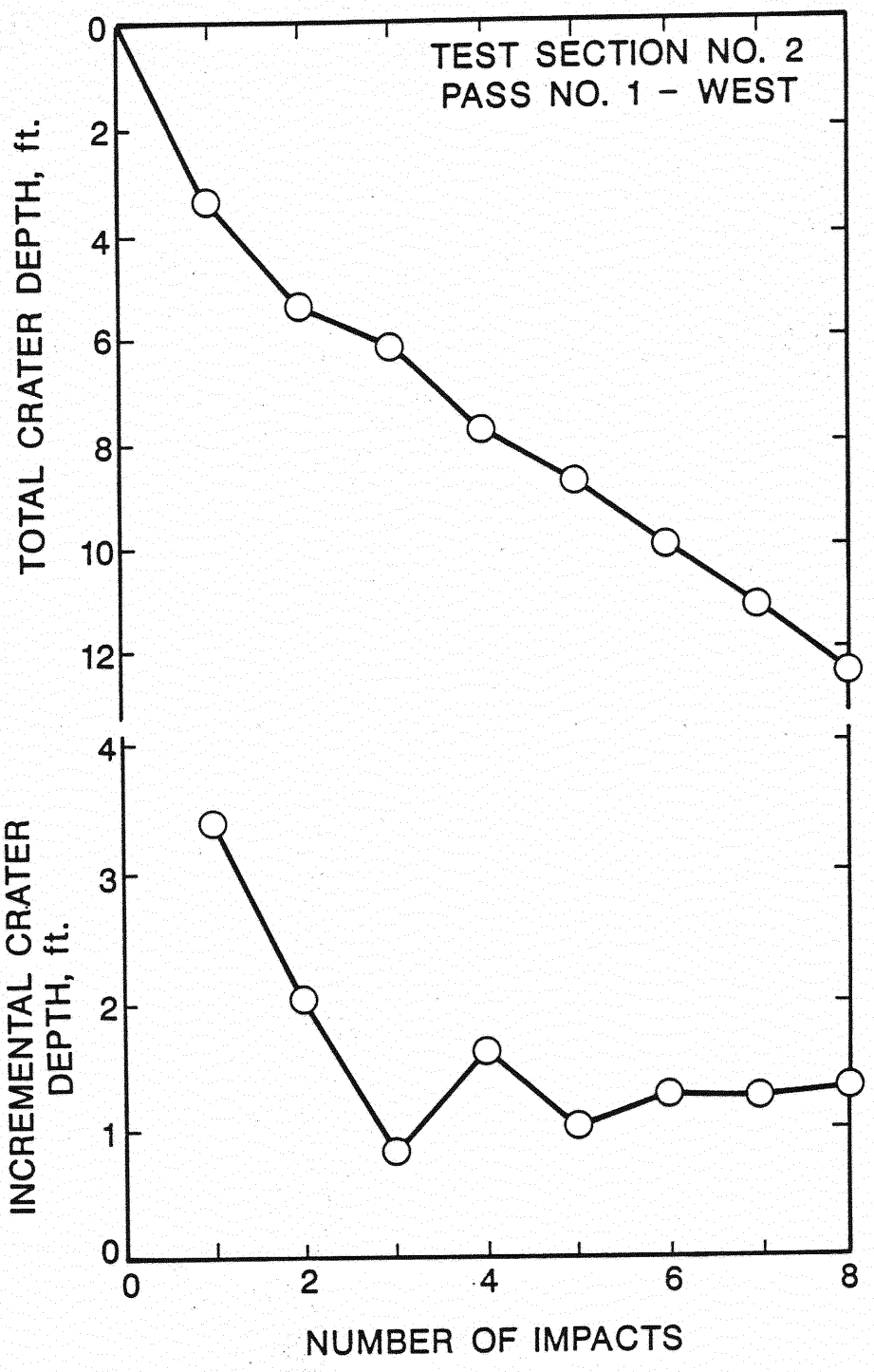

Figure 55. Crater Depth Versus Number of Impacts: Pass No. 1 - West, Test Section No. 2

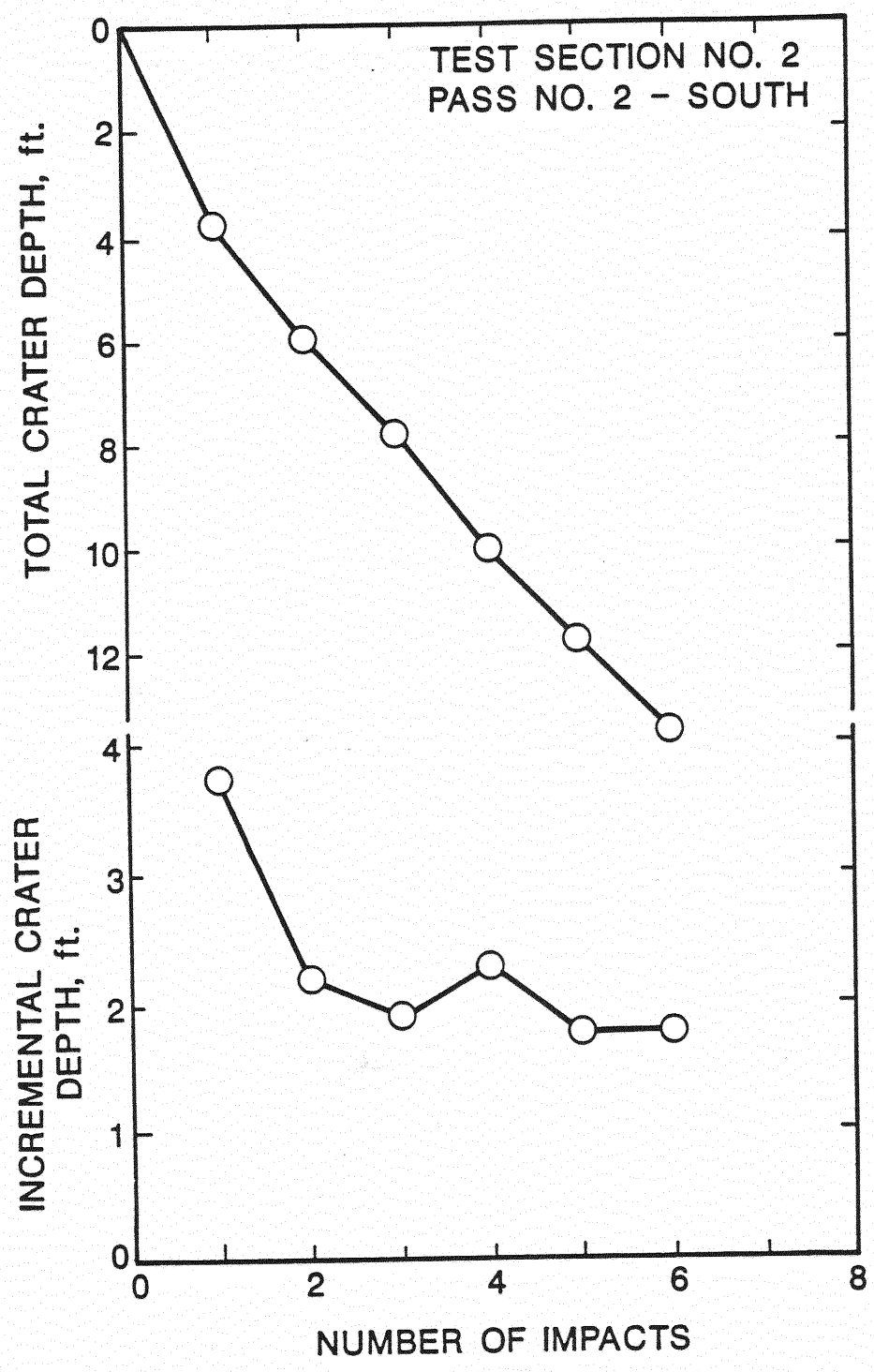

Figure 56. Crater Depth Versus Number of Impacts: Pass No. 2 - South, Test Section No. 2

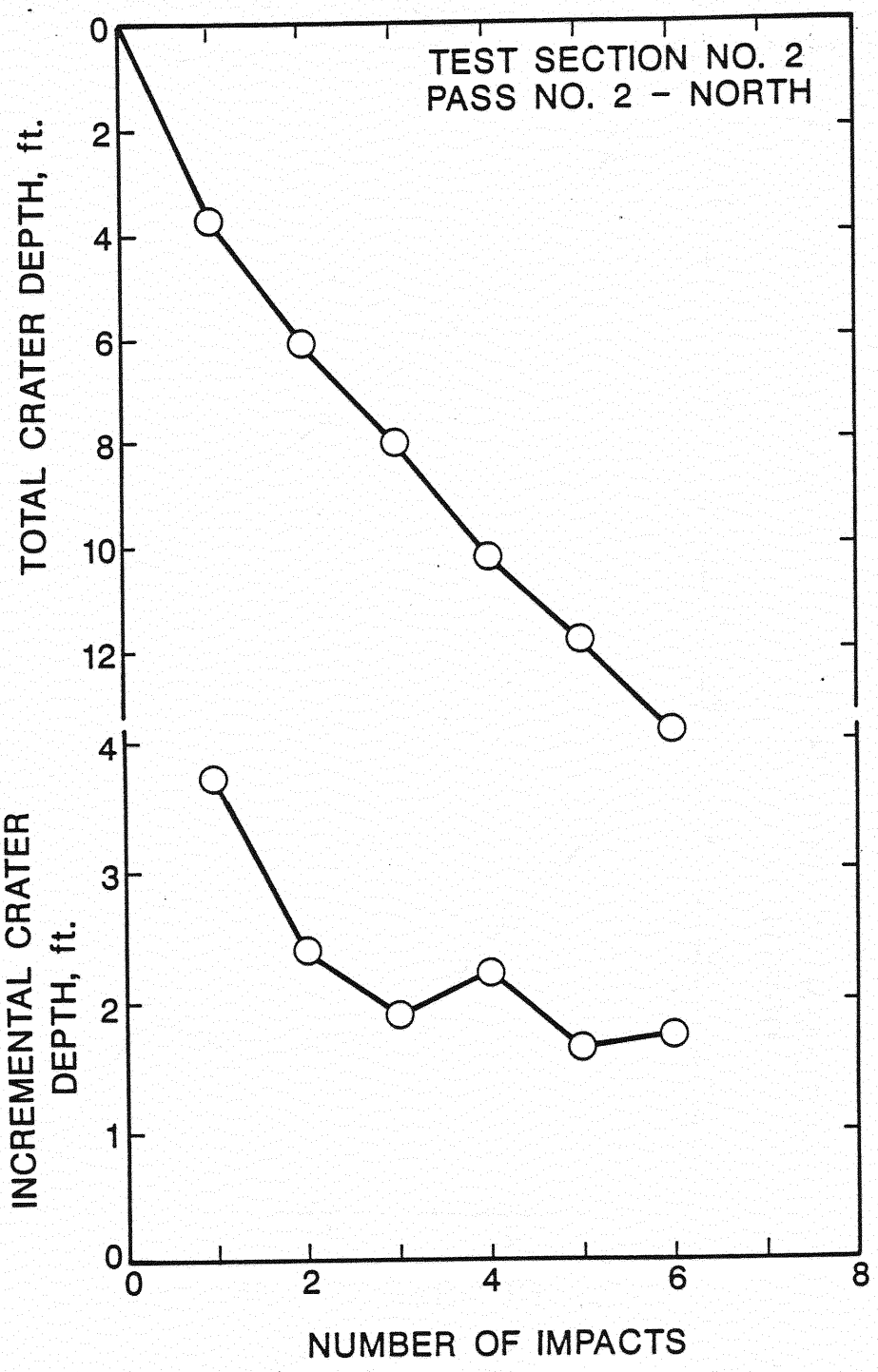

Figure 57. Crater Depth Versus Number of Impacts: Pass No. 2 - North, Test Section No. 2

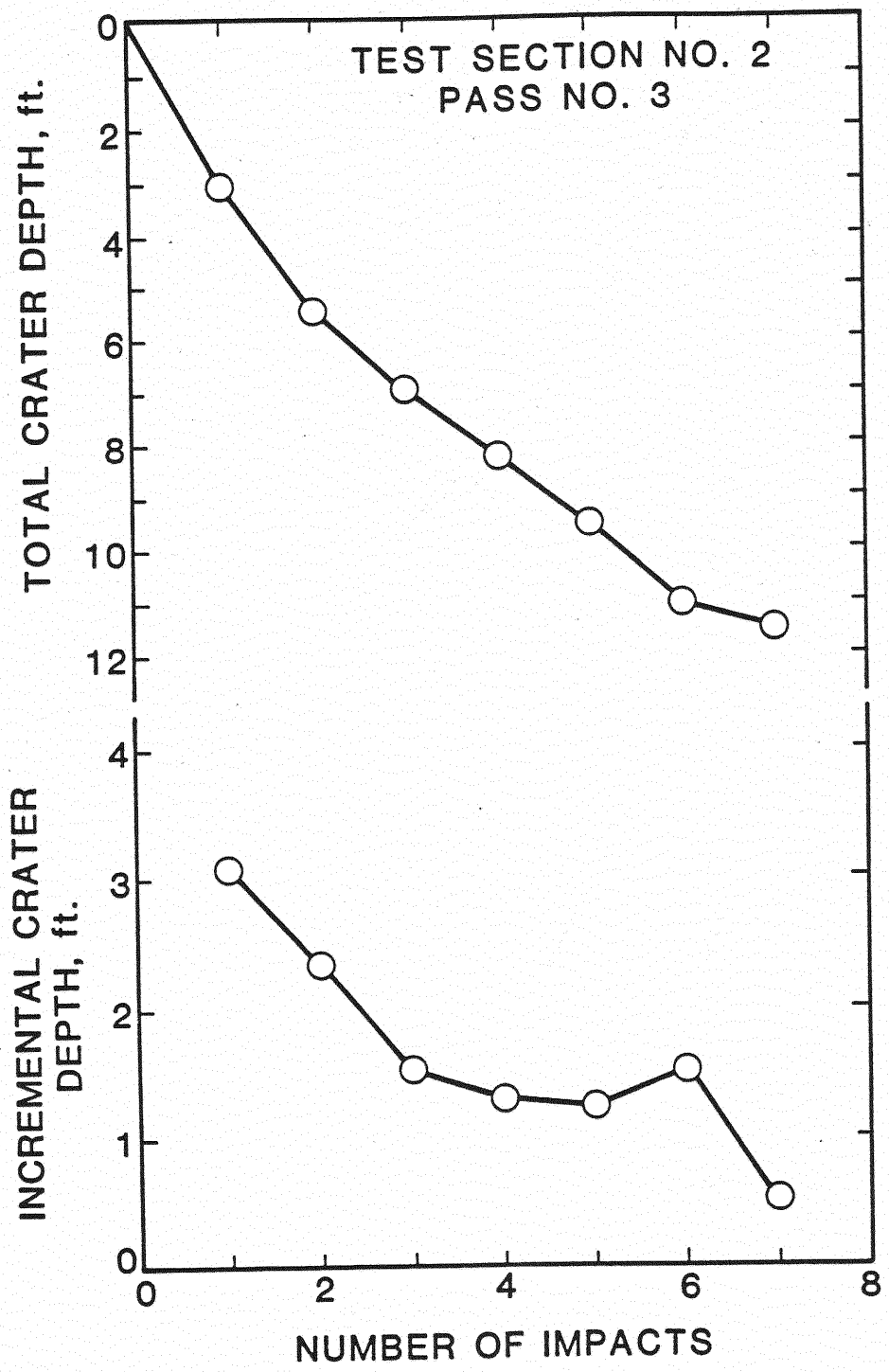

Figure 58. Crater Depth Versus Number of Impacts: Pass No. 3, Test Section No. 2

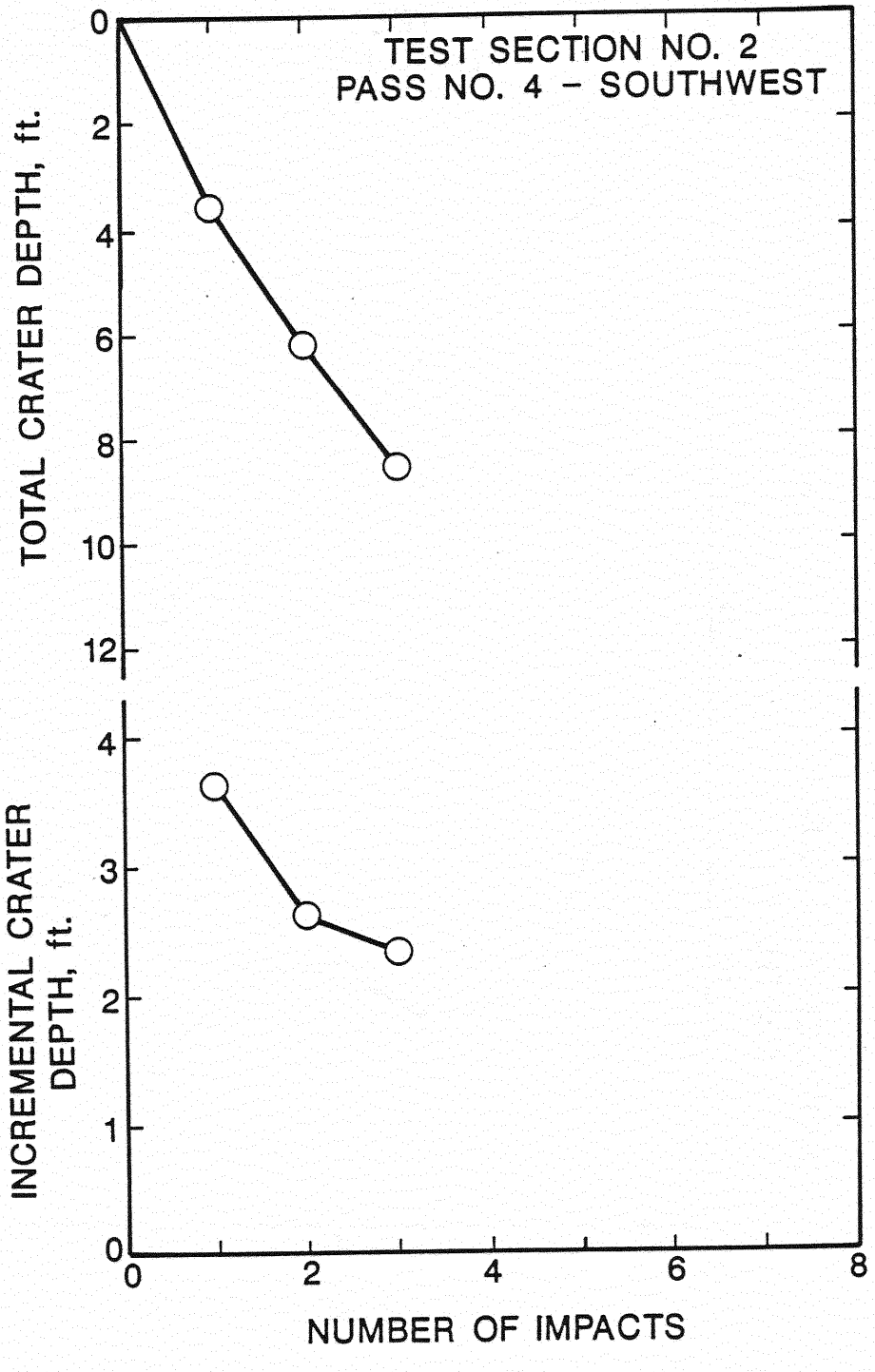

Figure 59. Crater Depth Versus Number of Impacts: Pass No. 4 - Southwest, Test Section No. 2

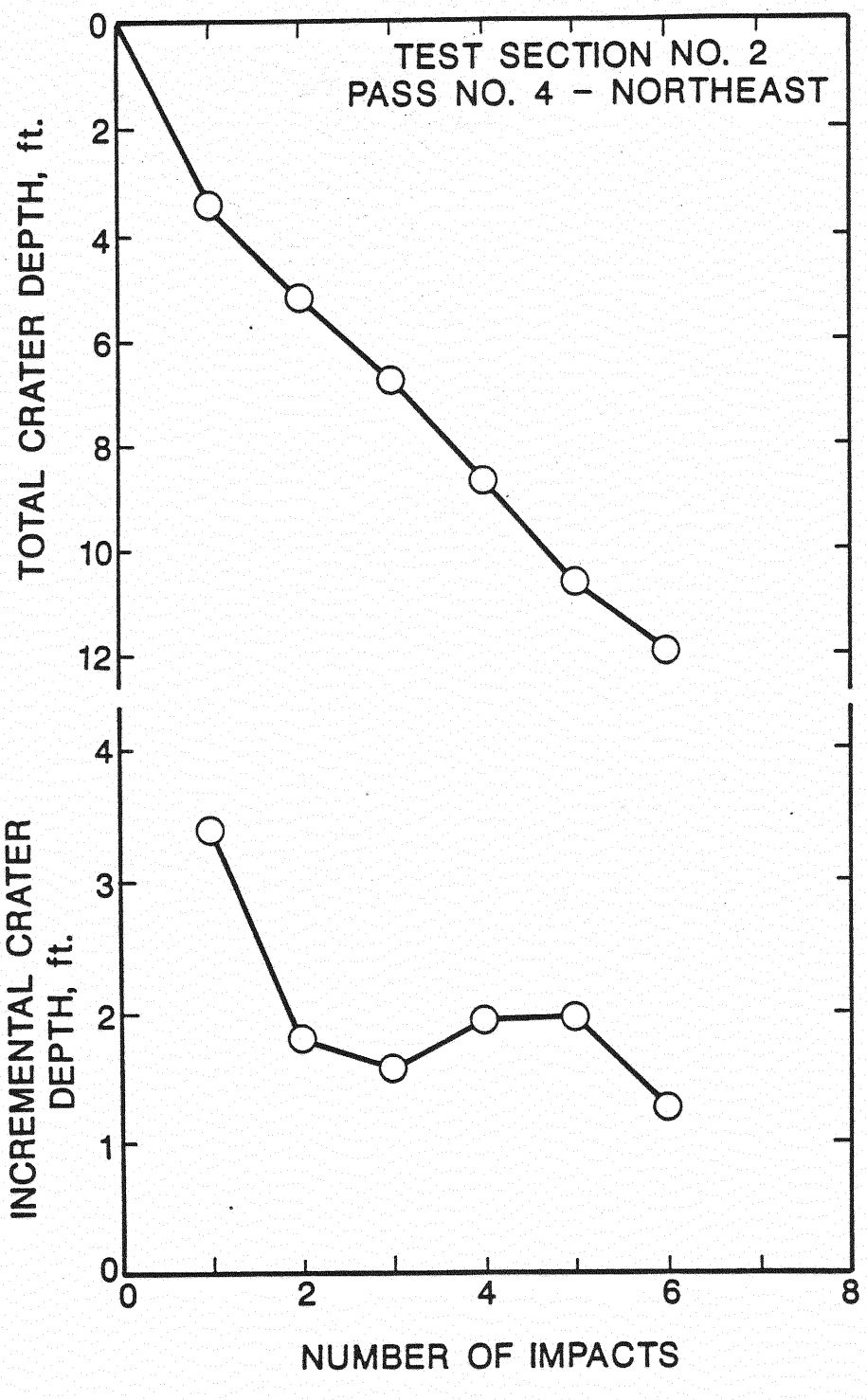

Figure 60. Crater Depth Versus Number of Impacts: Pass No. 4 - Northeast, Test Section No. 2

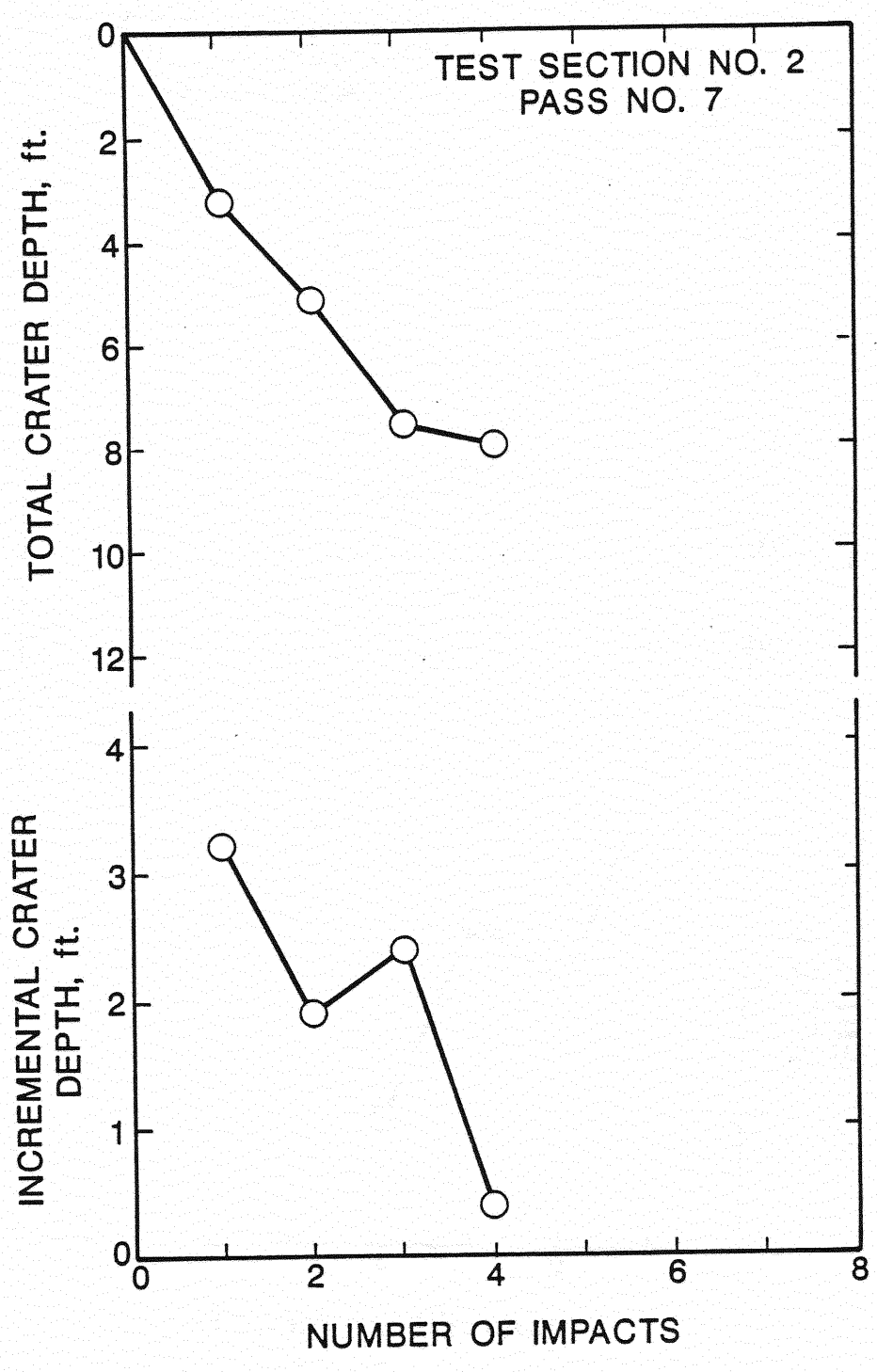

Figure 61. Crater Depth Versus Number of Impacts: Pass No. 7, Test Section No. 2

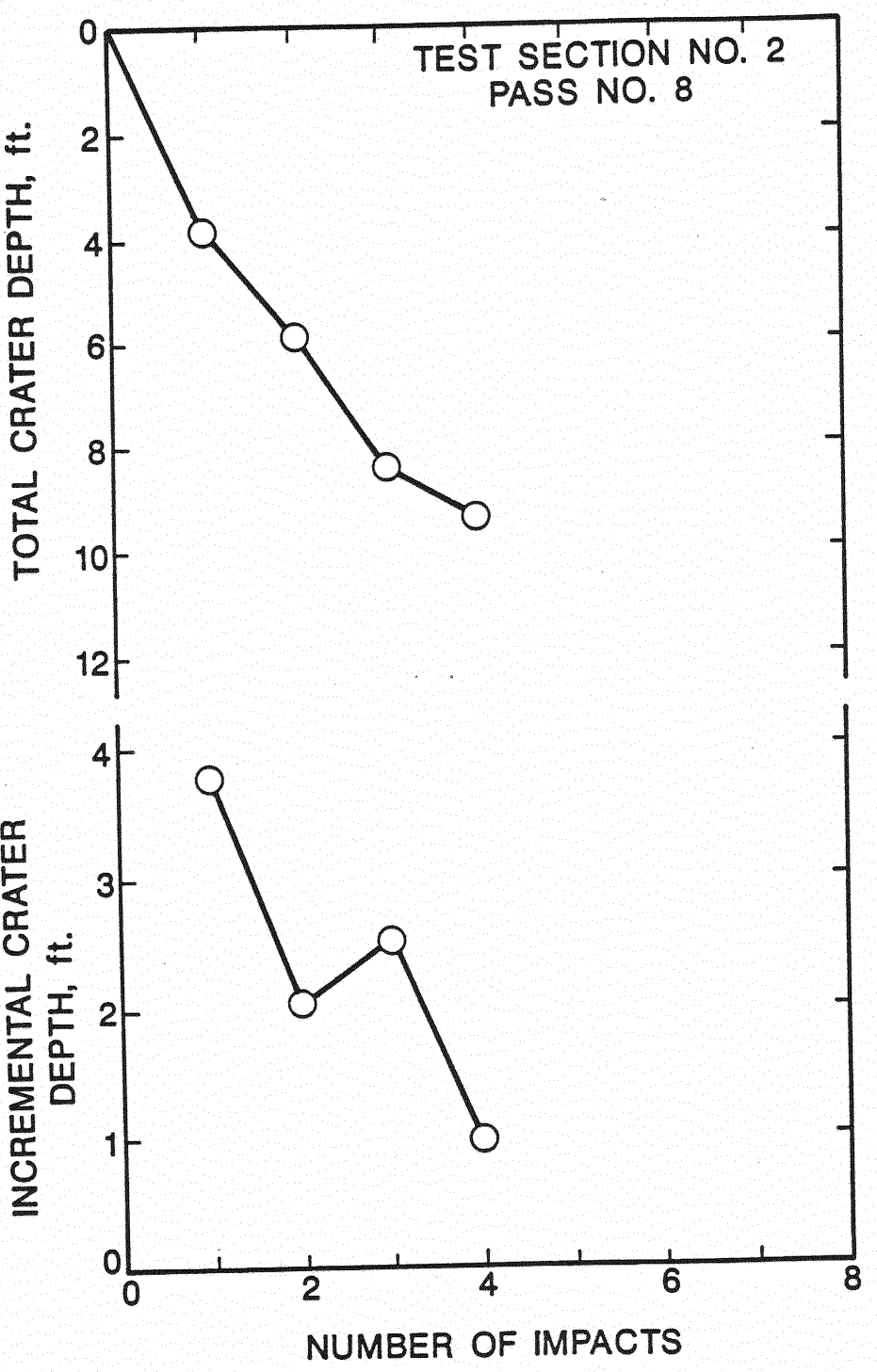

Figure 62. Crater Depth Versus Number of Impacts: Pass No. 8, Test Section No. 2

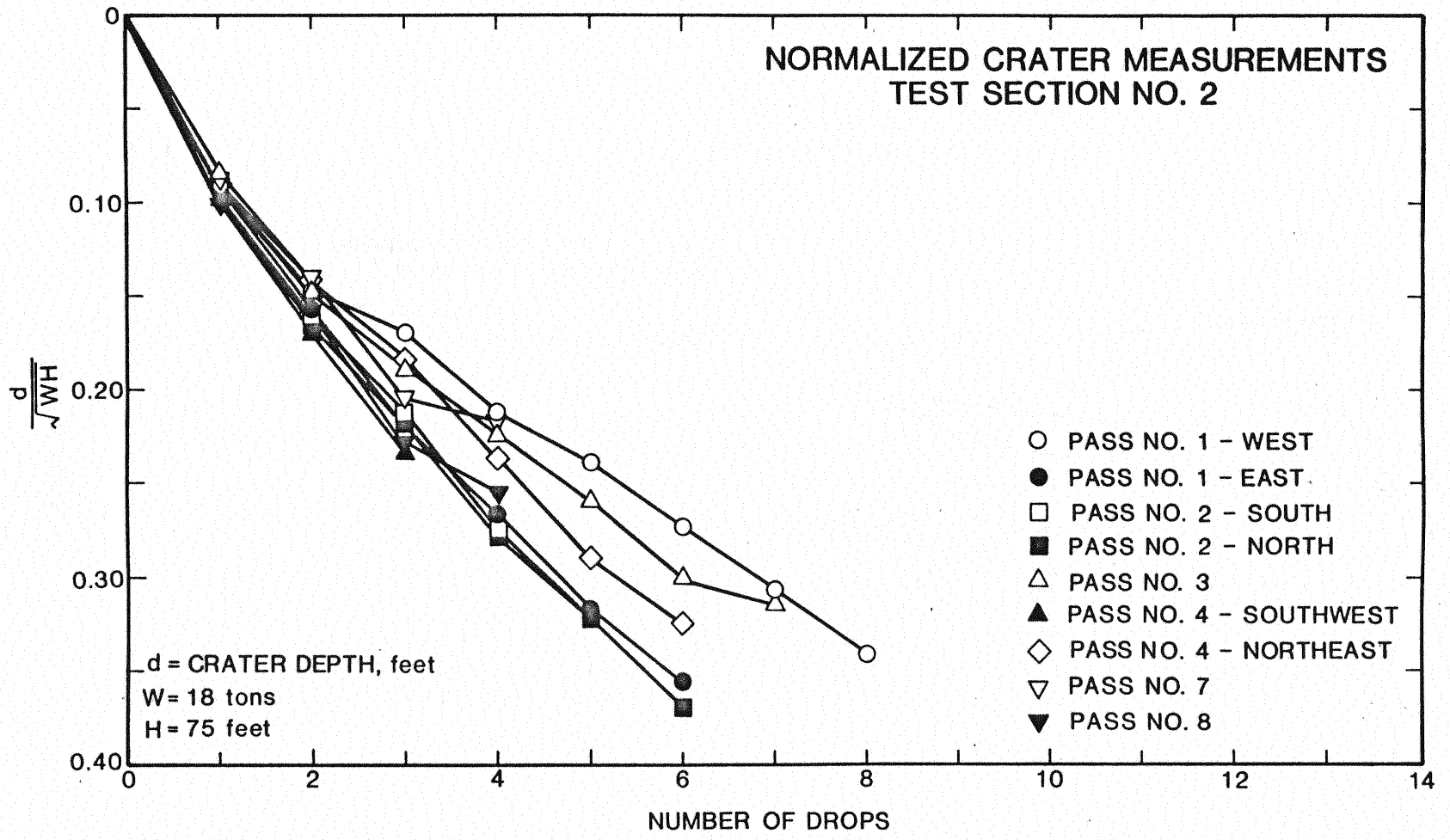

Figure 63. Normalized Crater Measurements, Test Section No. 2

TEST SECTION NO. 2 - BORING NO. 1
(CRL)

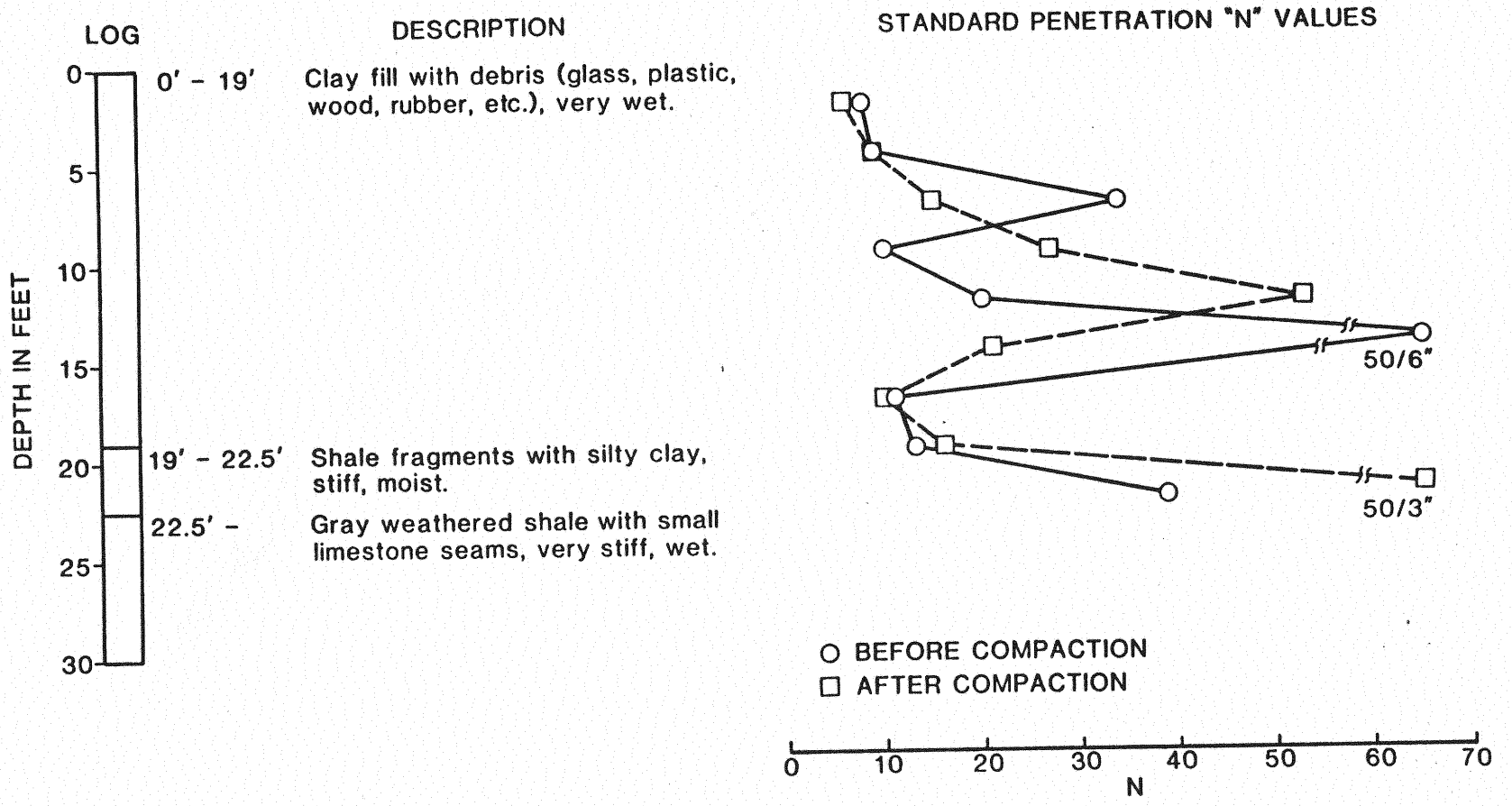

Figure 64. Standard Penetration Test Results, Along CRL, Test Section No. 2

TEST SECTION NO. 2 - BORING NO. 2
(15' SOUTH OF CRL)

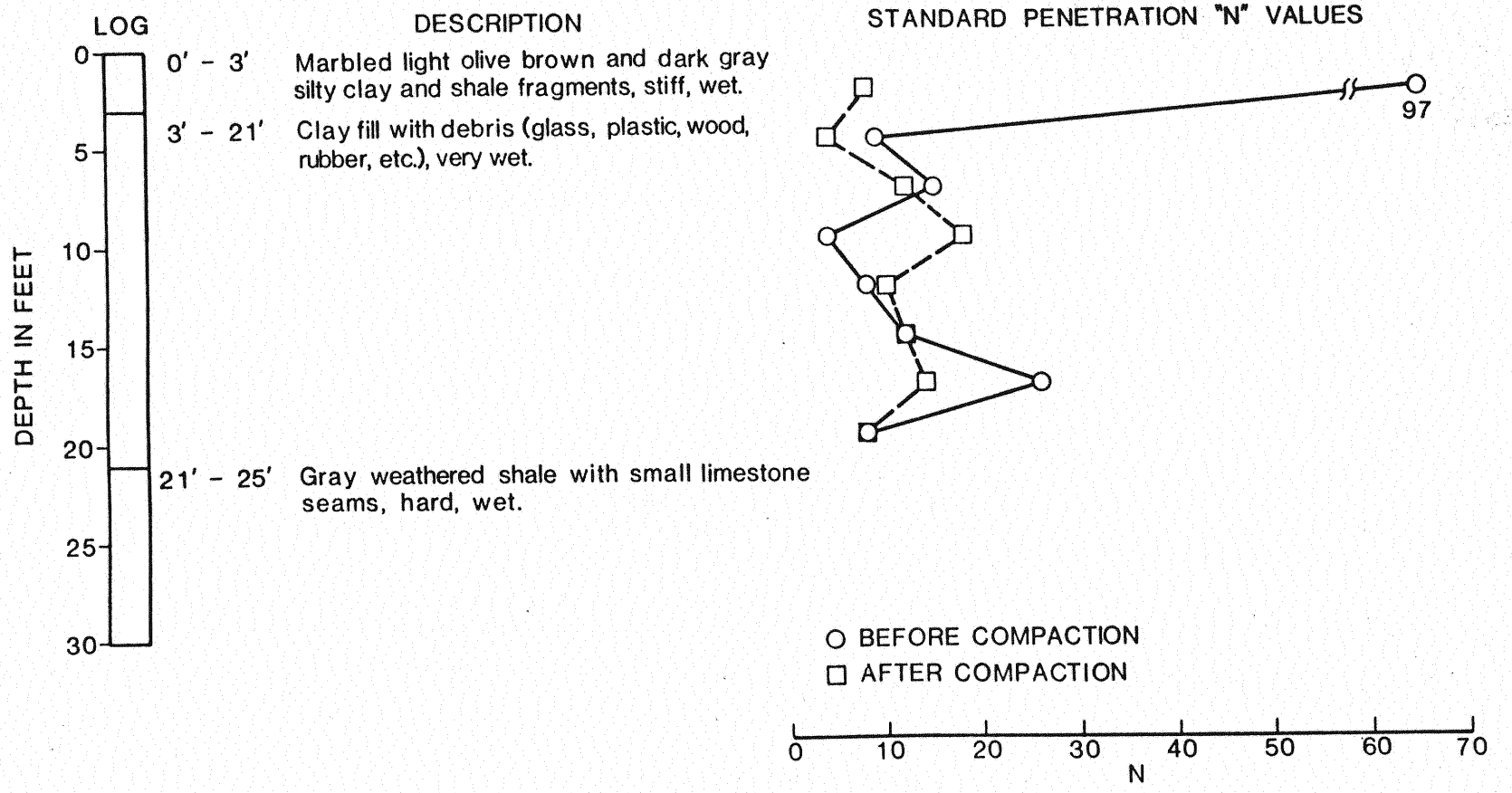

Figure 65. Standard Penetration Test Results, South of CRL, Test Section No. 2

TEST SECTION NO. 2 - BORING NO. 3
(15' NORTH OF CRL)

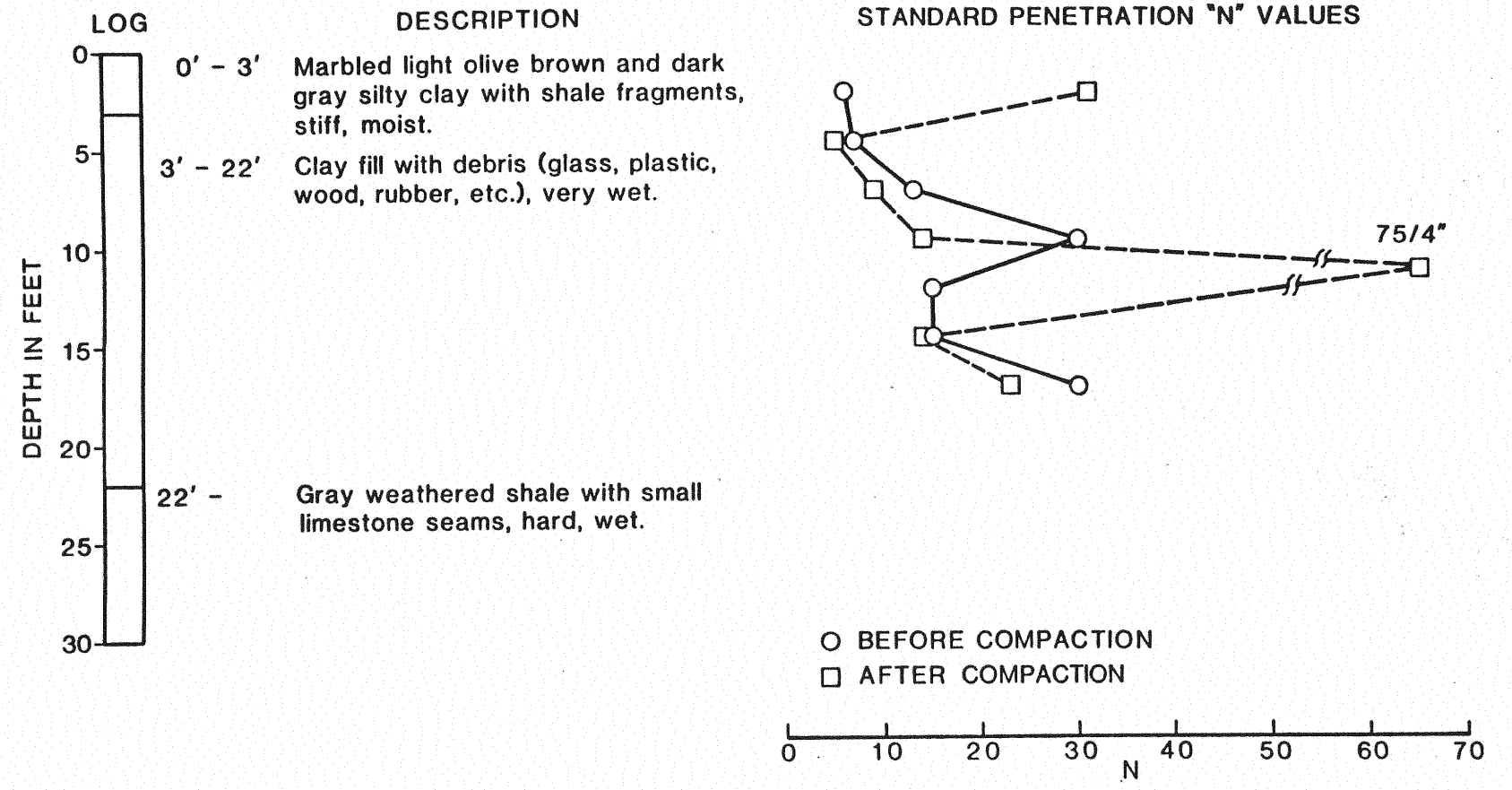

Figure 66. Standard Penetration Test Results, North of CRL, Test Section No. 2

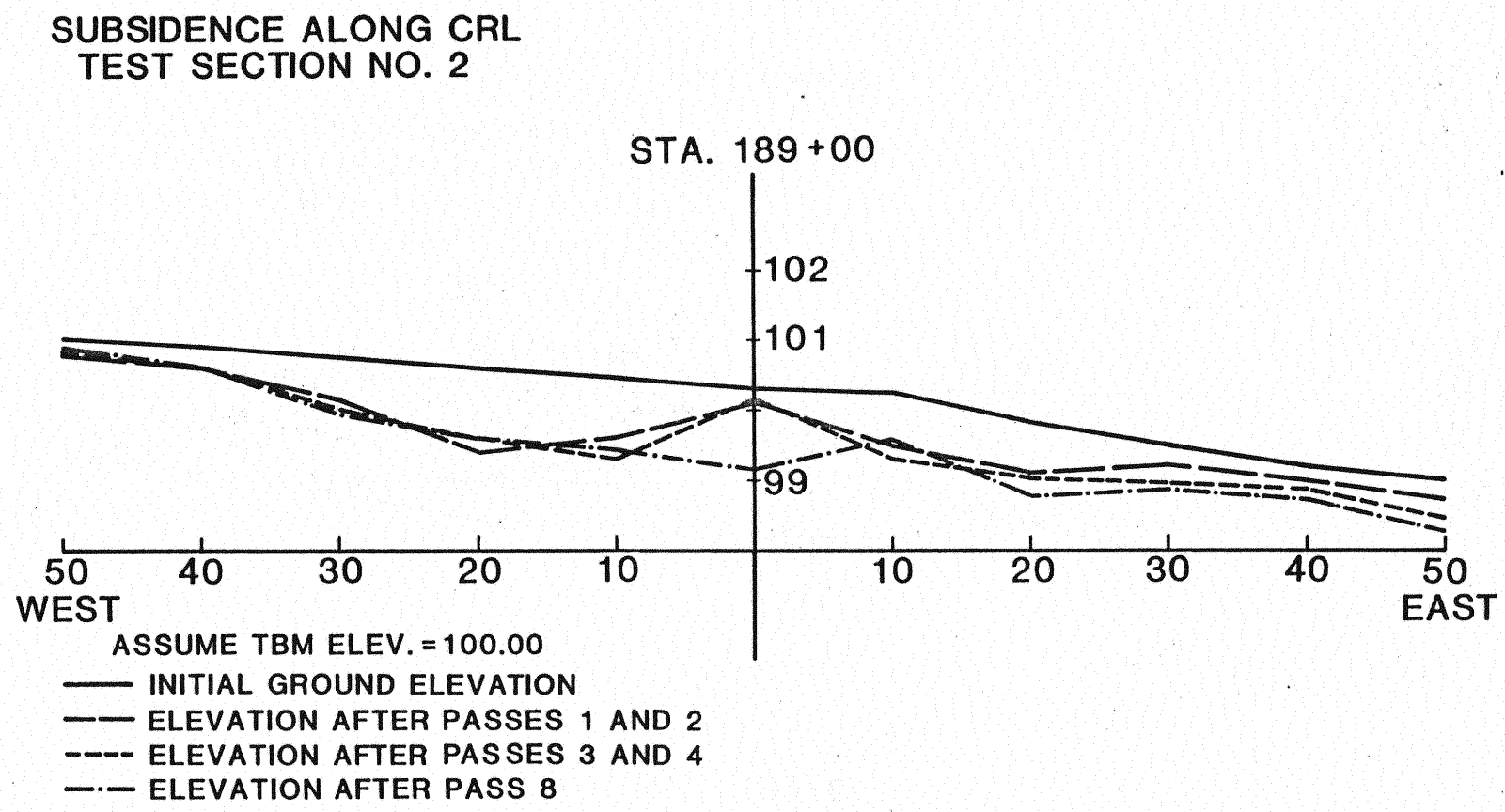

Figure 67. Post-Compaction Subsidence Along CRL, Test Section No. 2

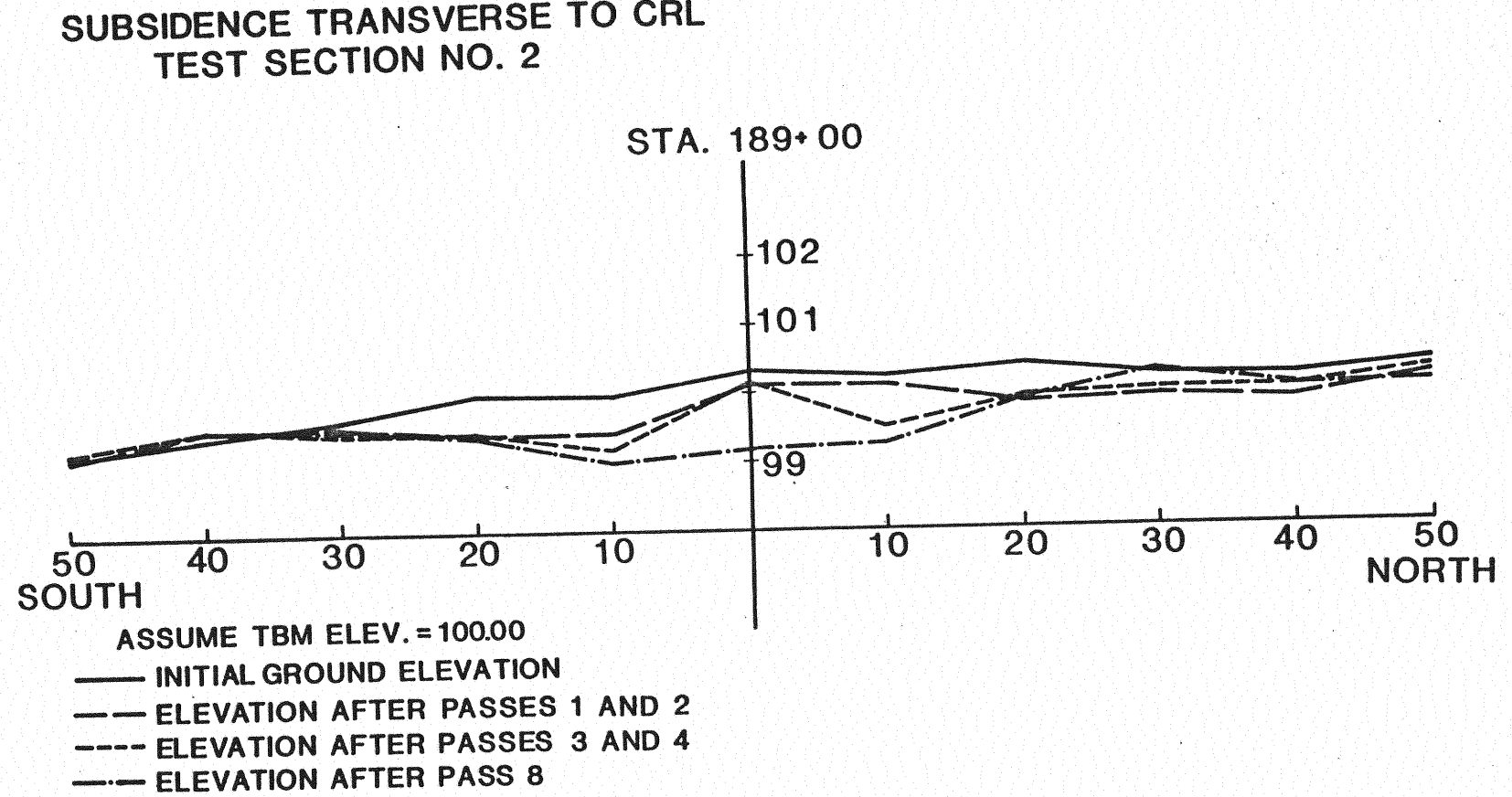

Figure 68. Post-Compaction Subsidence Transverse to CRL, Test Section No. 2

APPENDIX C

RESULTS FROM TEST SECTION NO. 3

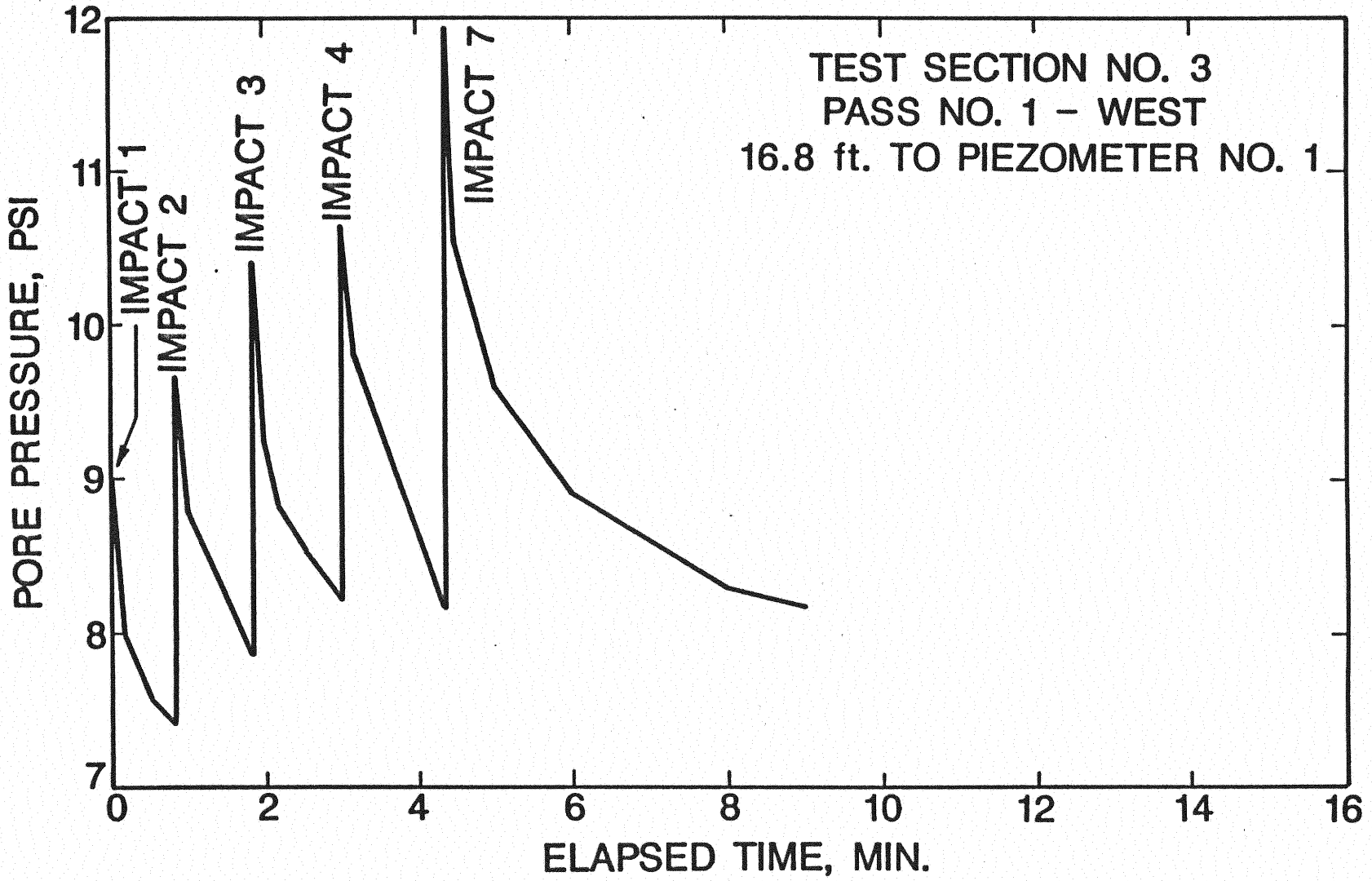

Figure 69. Piezometer No. 1 Data, Pass No. 1 - West, Test Section No. 3

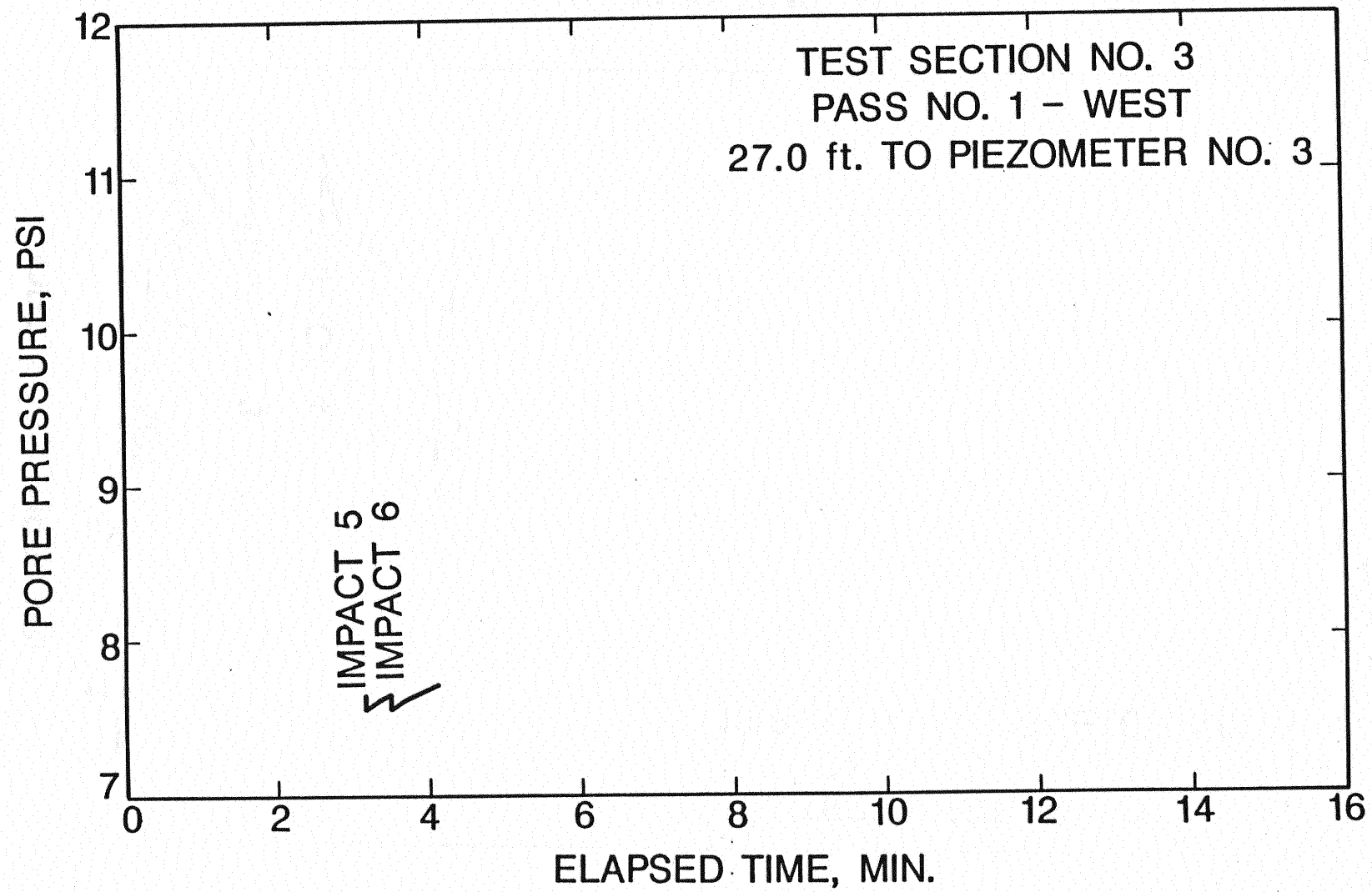

Figure 70. Piezometer No. 3 Data, Pass No. 1 - West, Test Section No. 3

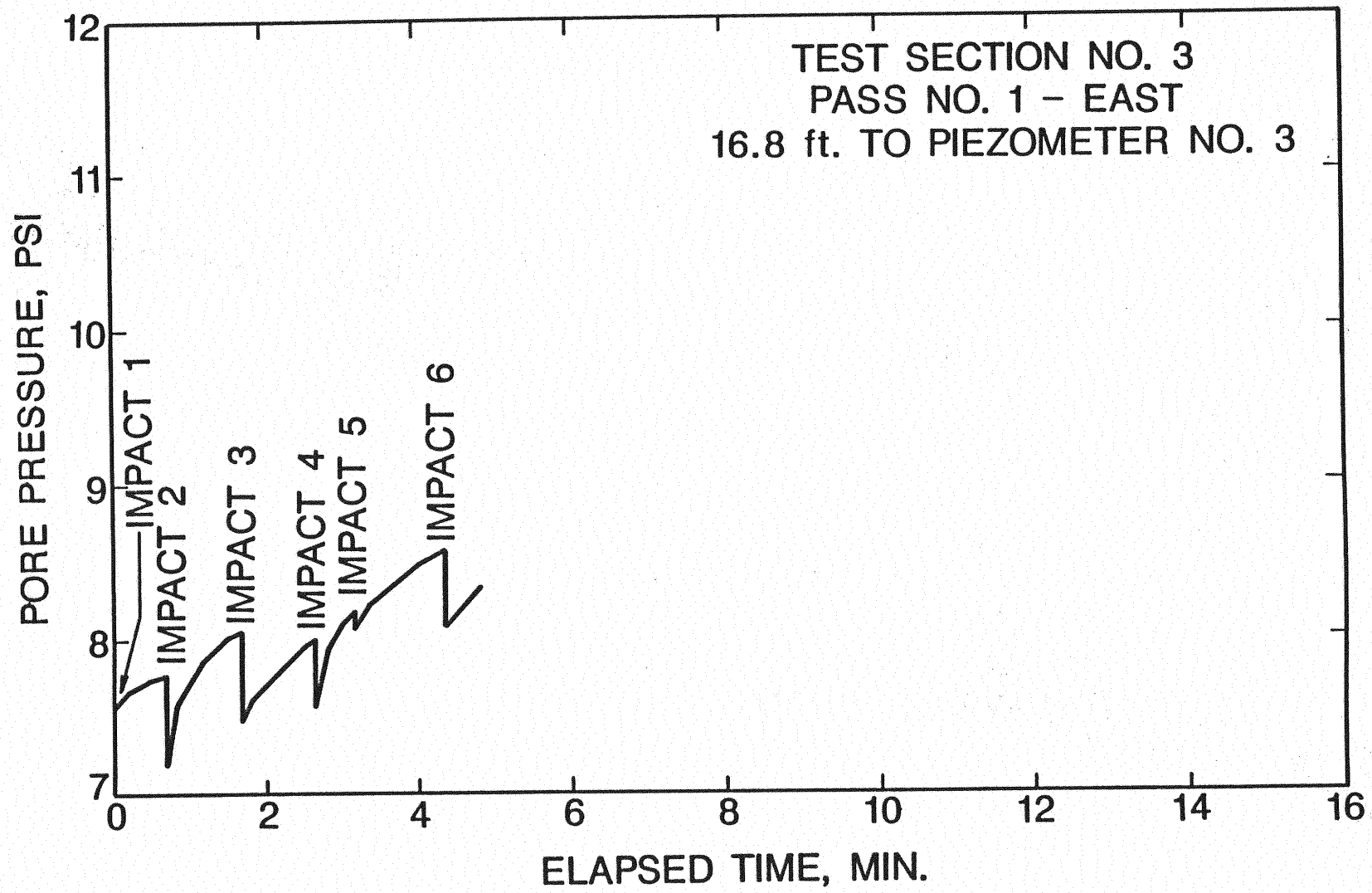

Figure 71. Piezometer No. 3 Data, Pass No. 1 - East, Test Section No. 3

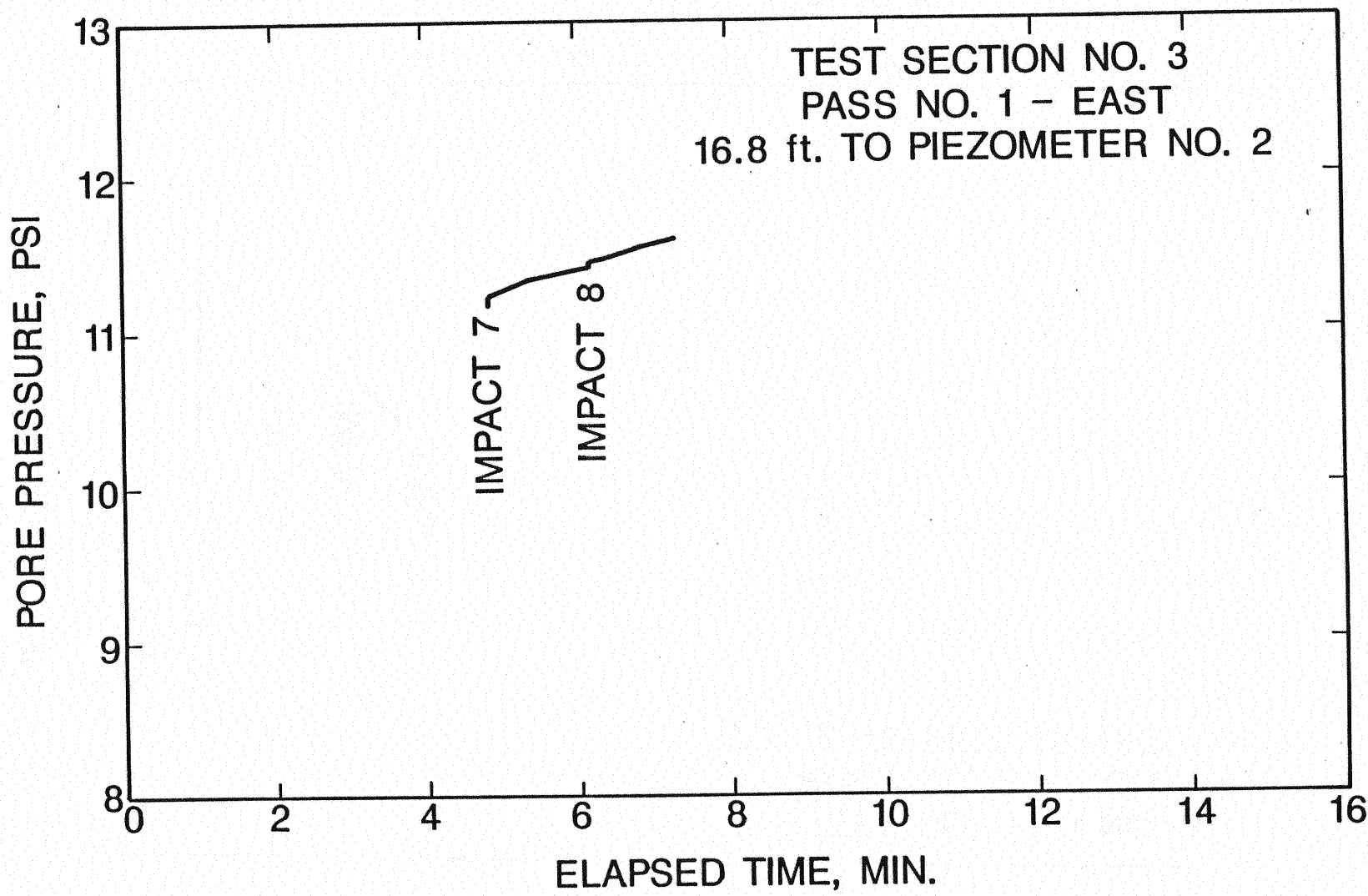

Figure 72. Piezometer No. 2 Data, Pass No. 1 - East, Test Section No. 3

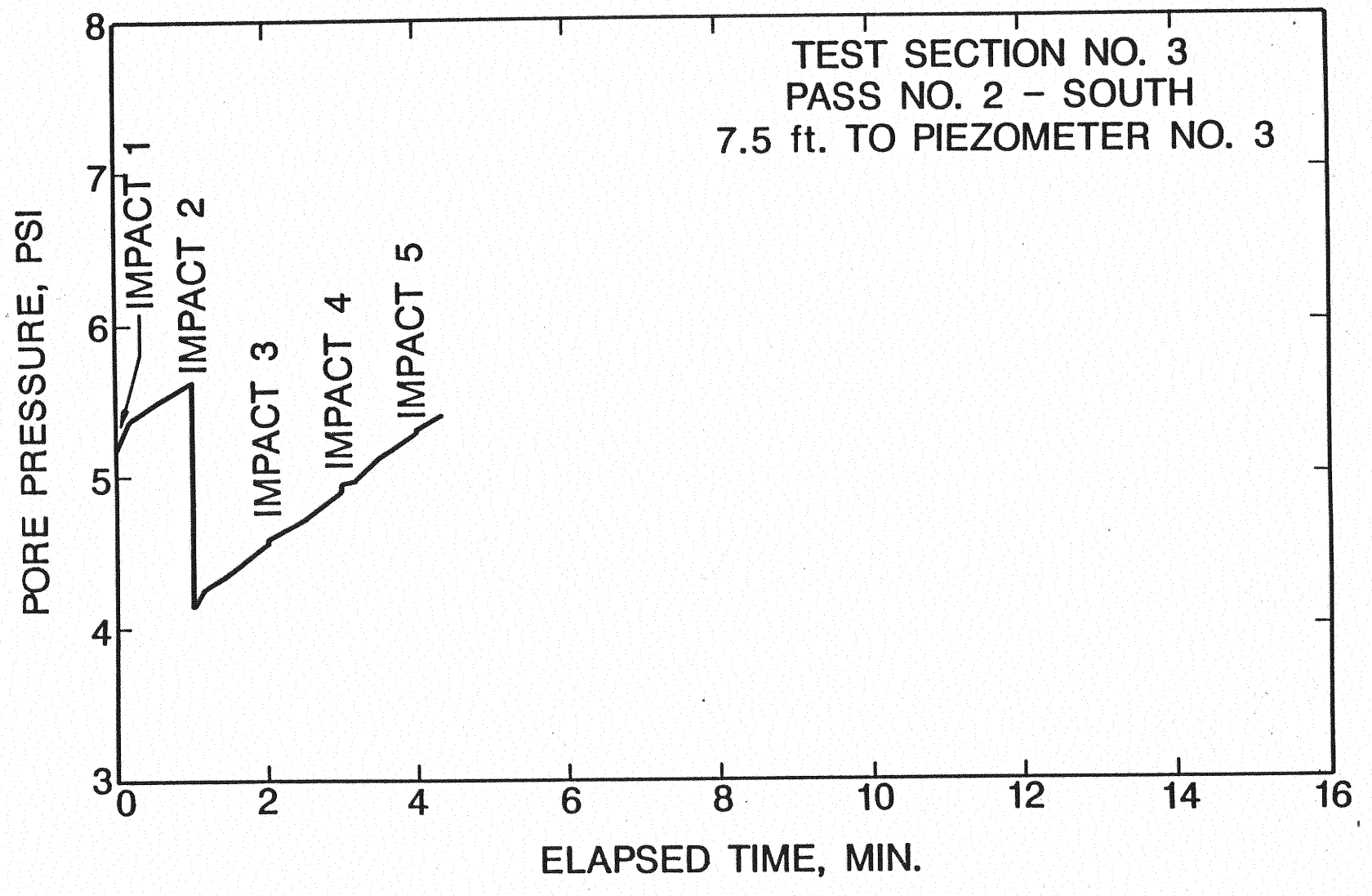

Figure 73. Piezometer No. 3 Data, Pass No. 2 - South, Test Section No. 3

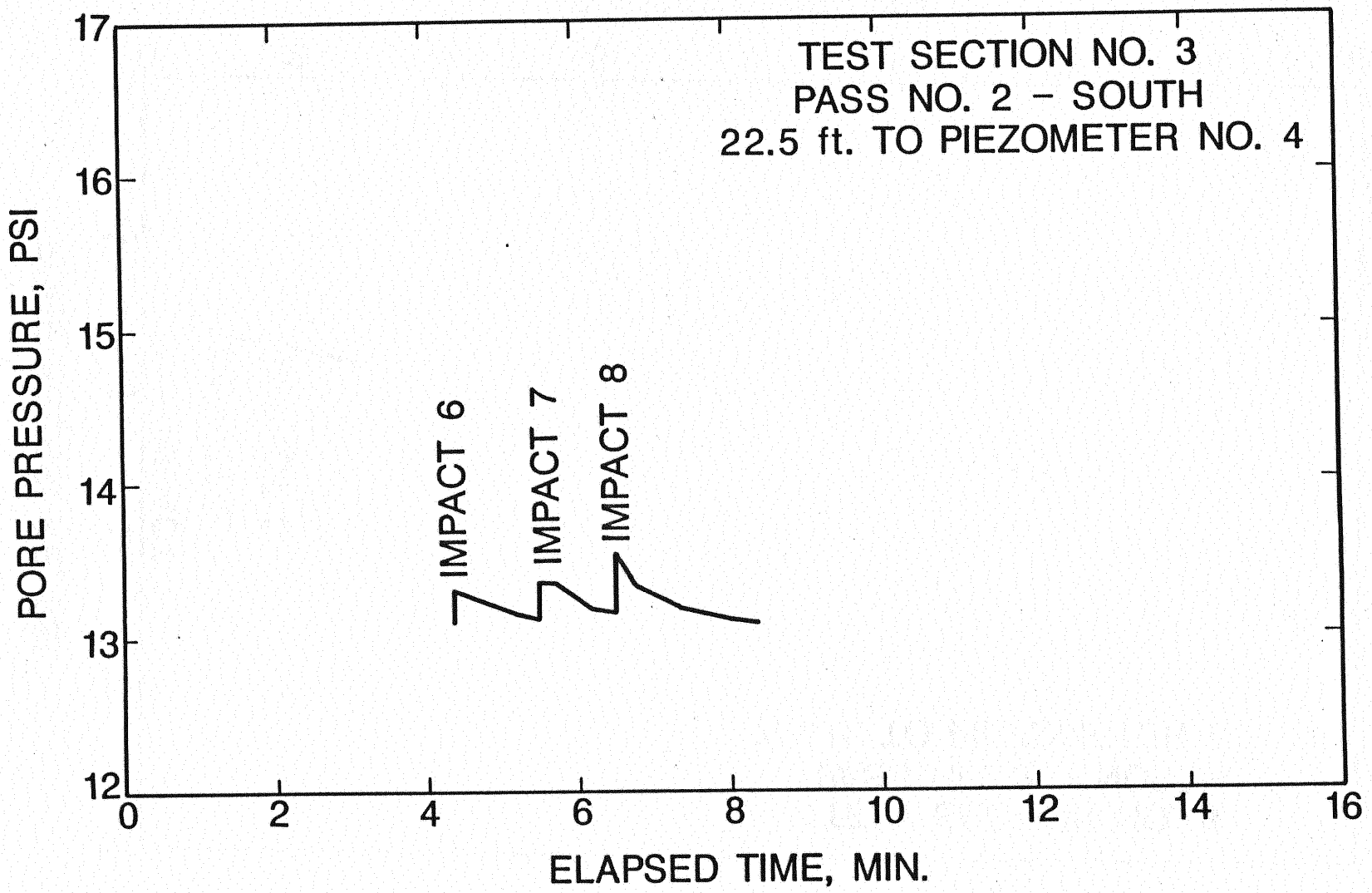

Figure 74. Piezometer No. 4 Data, Pass No. 2 - South, Test Section No. 3

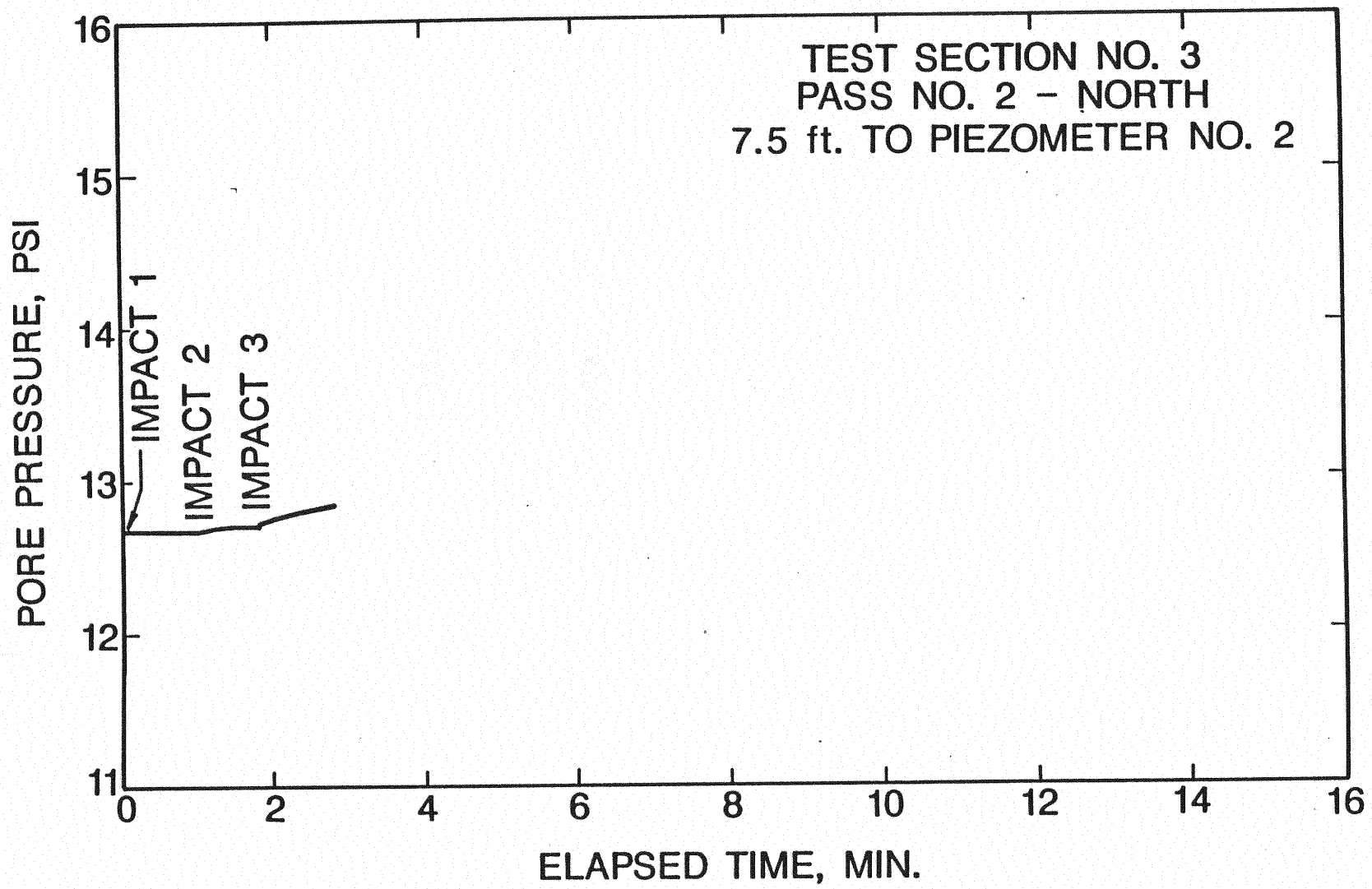

Figure 75. Piezometer No. 2 Data, Pass No. 2 - North, Test Section No. 3

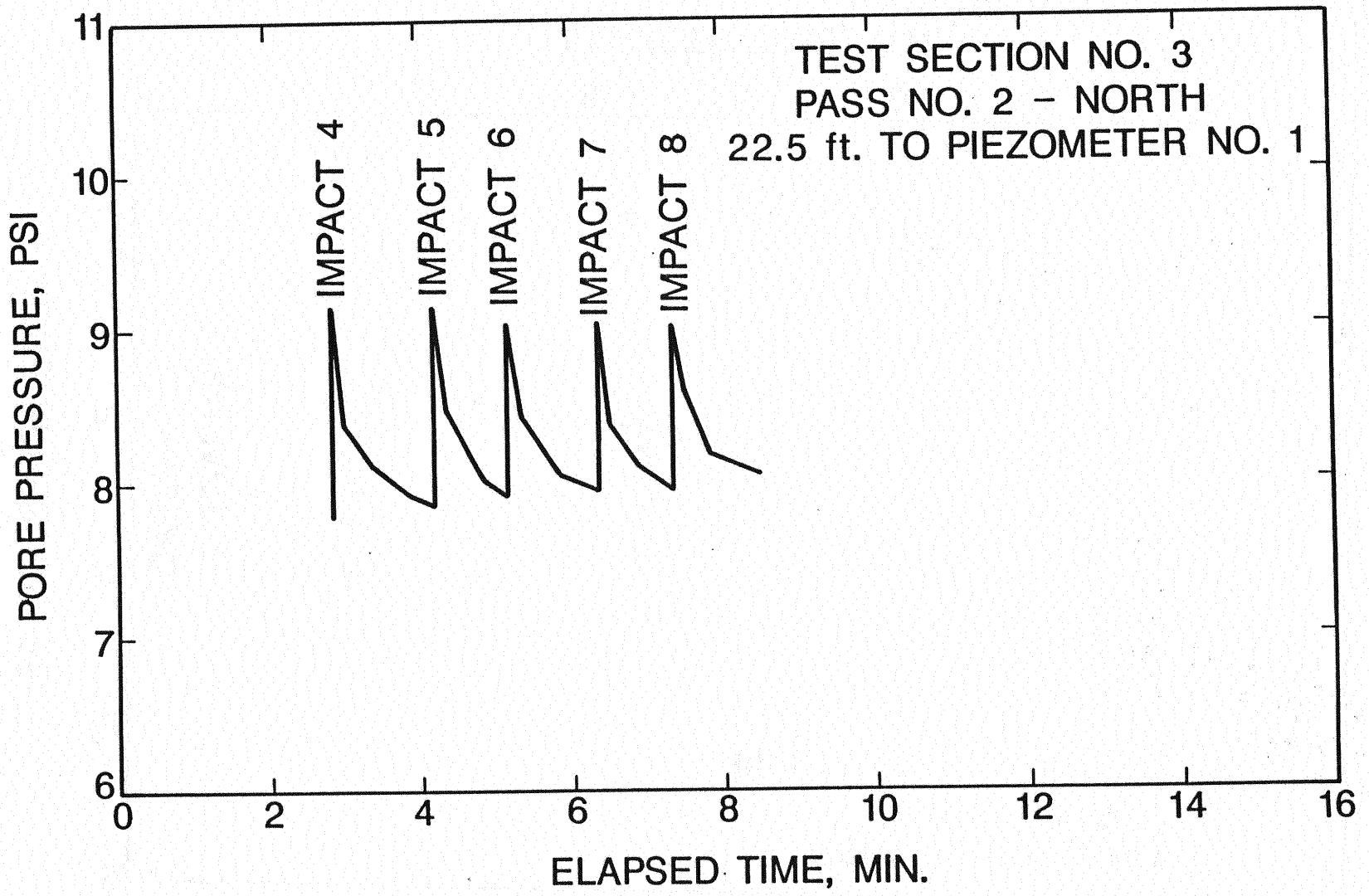

Figure 76. Piezometer No. 1 Data, Pass No. 2 - North, Test Section No. 3

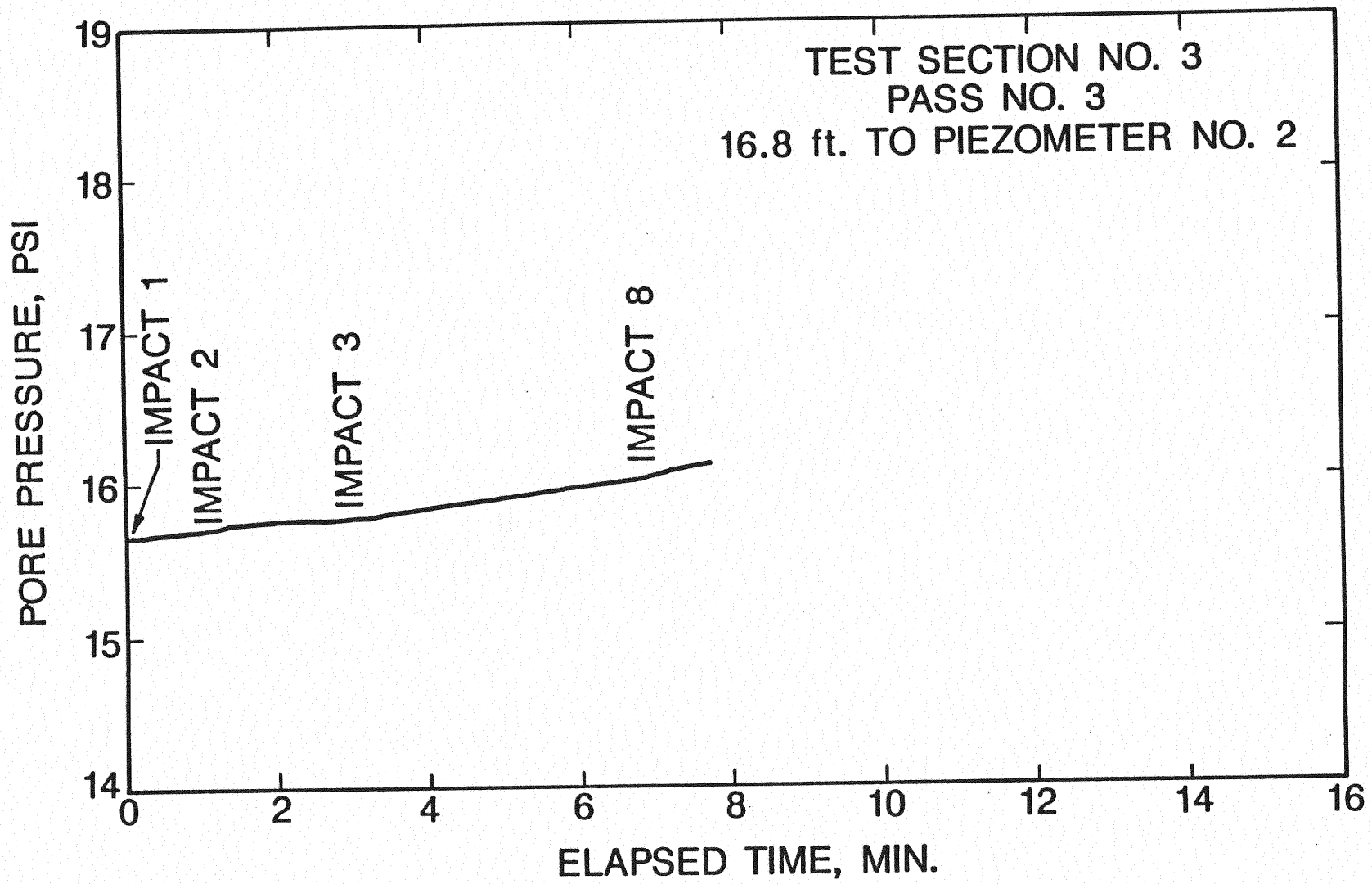

Figure 77. Piezometer No. 2 Data, Pass No. 3, Test Section No. 3

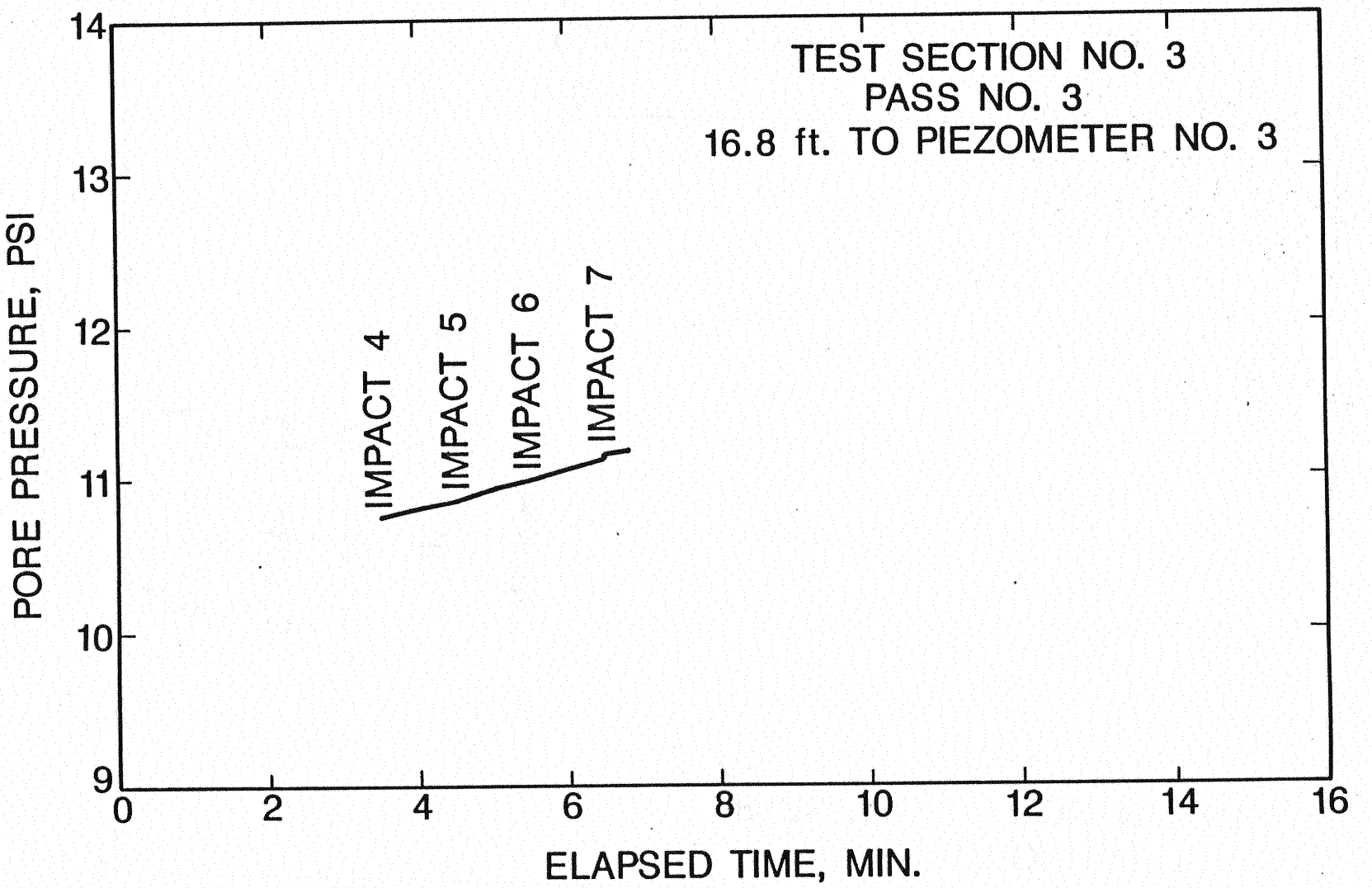

Figure 78. Piezometer No. 3 Data, Pass No. 3, Test Section No. 3

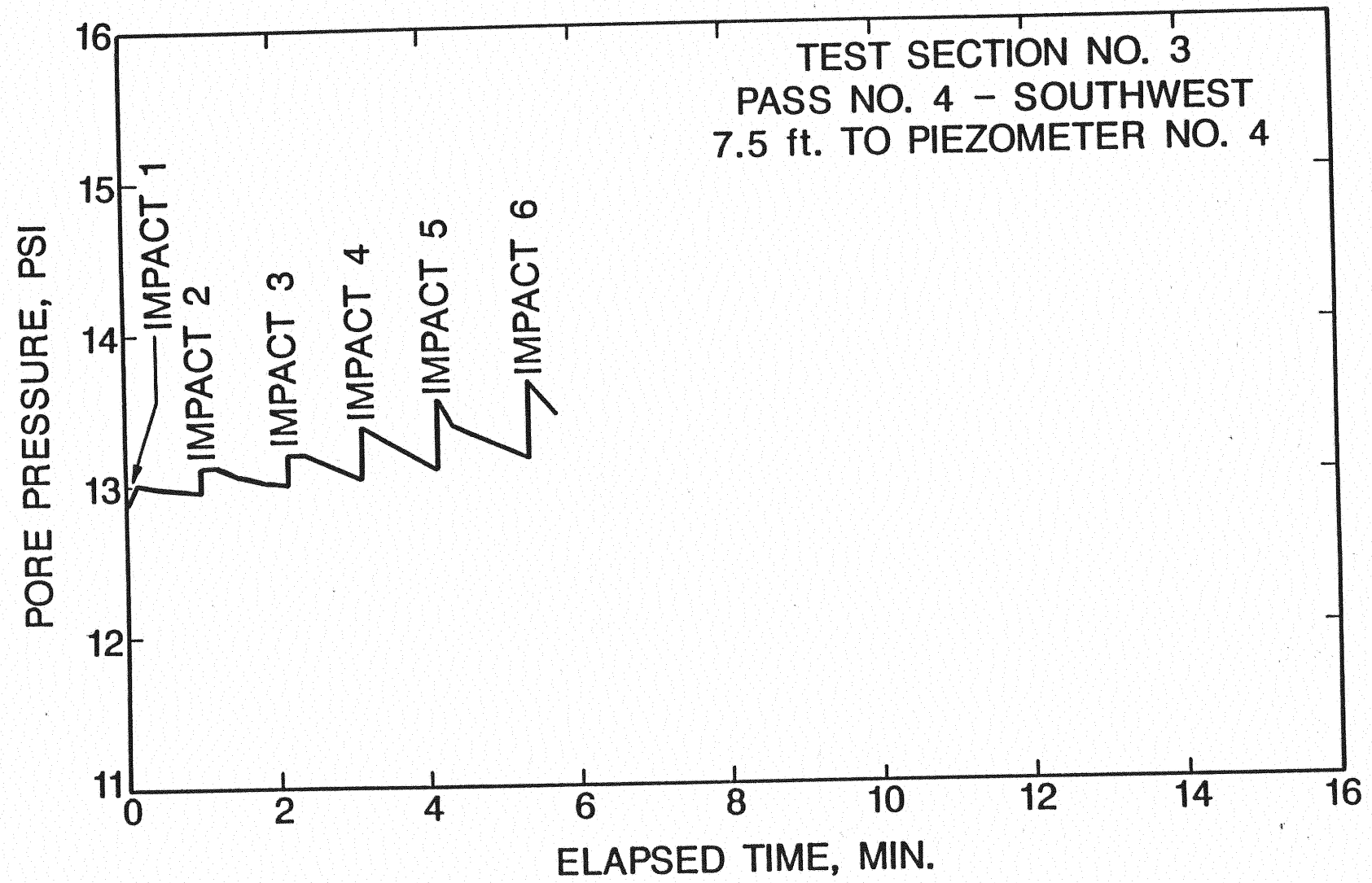

Figure 79. Piezometer No. 4 Data, Pass No. 4 - Southwest, Test Section No. 3

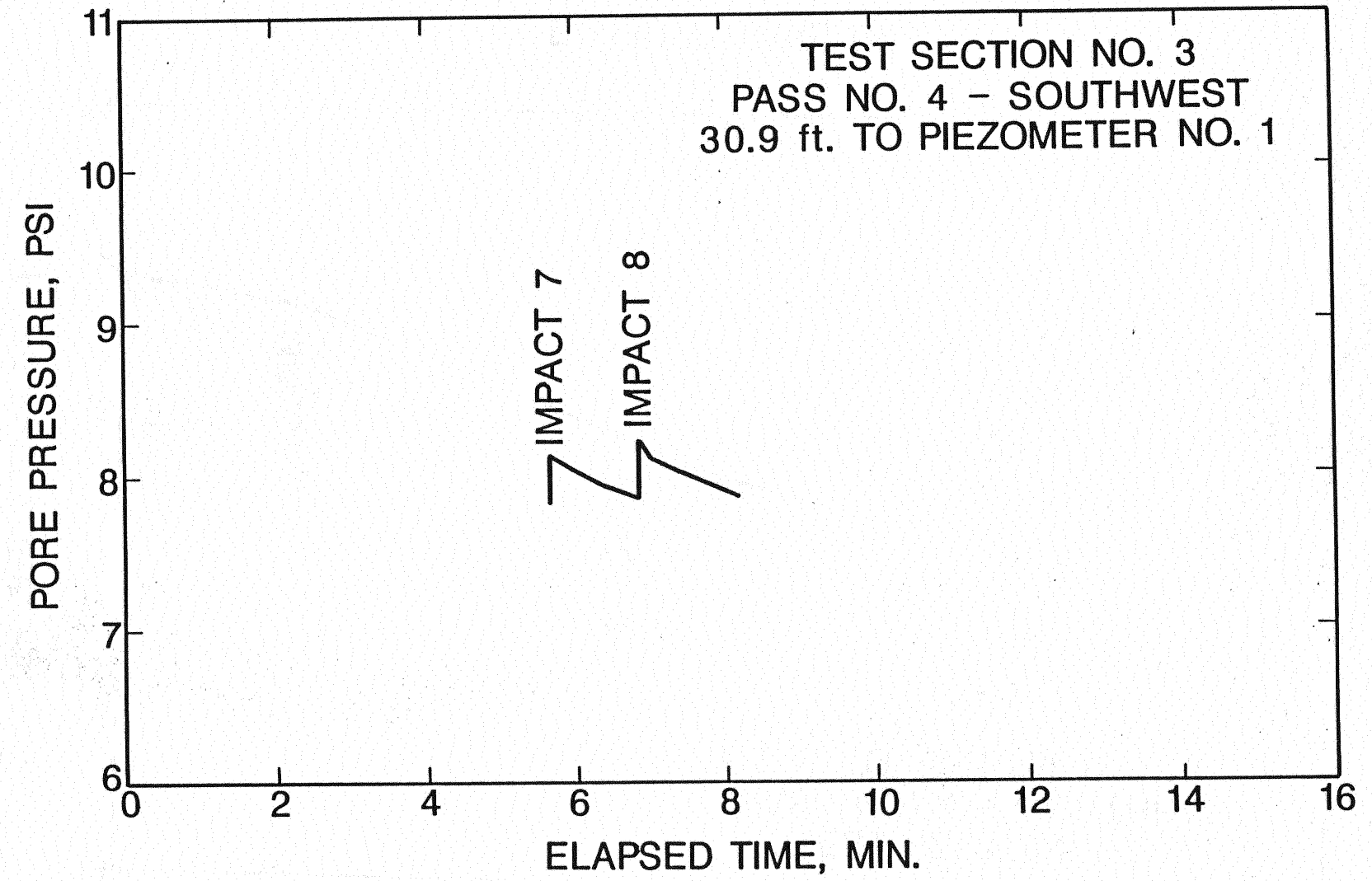

Figure 30. Piezometer No. 1 Data, Pass No. 4 - Southwest, Test Section No. 3

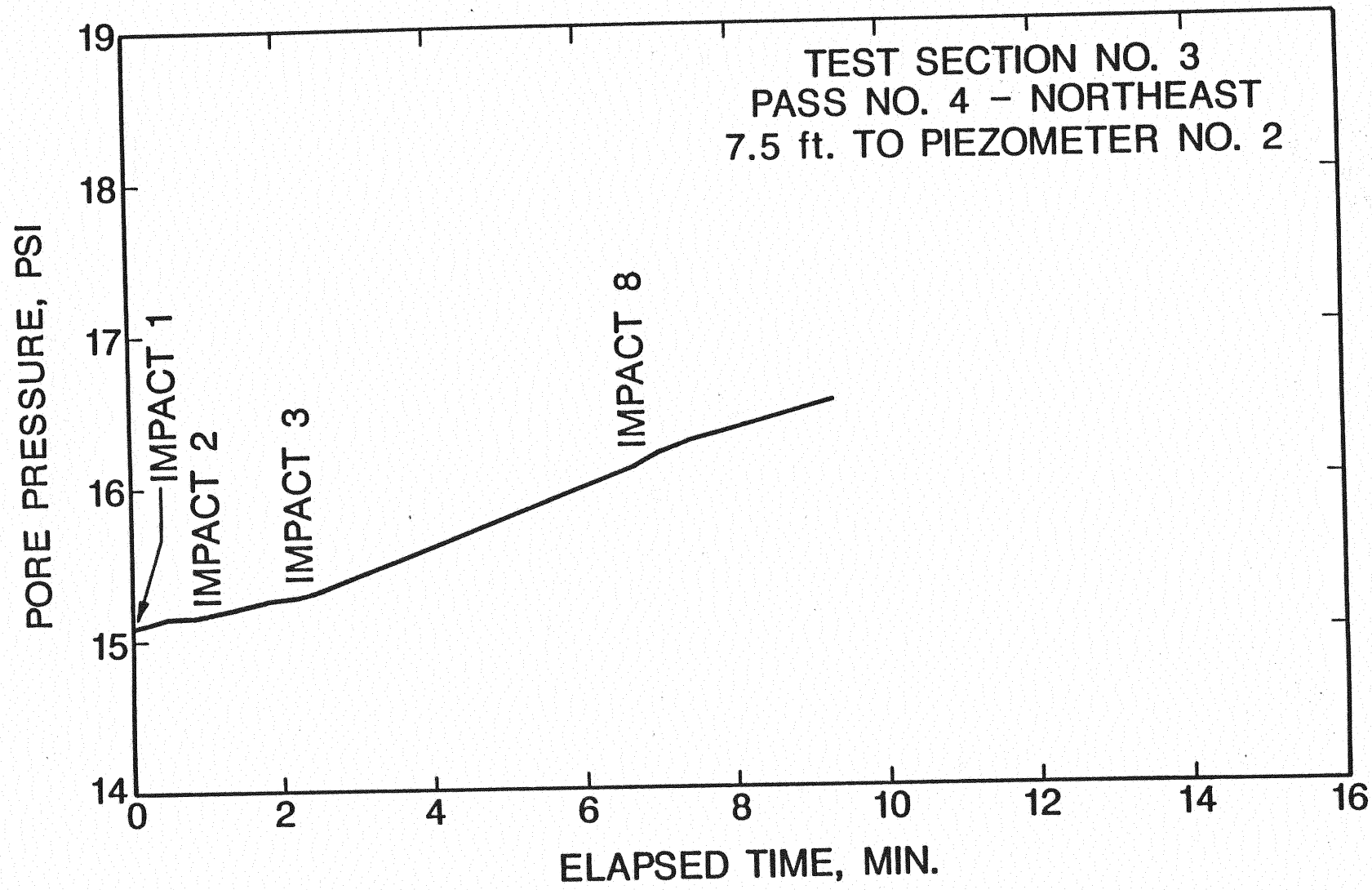

Figure 81. Piezometer No. 2 Data, Pass No. 4 - Northeast, Test Section No. 3

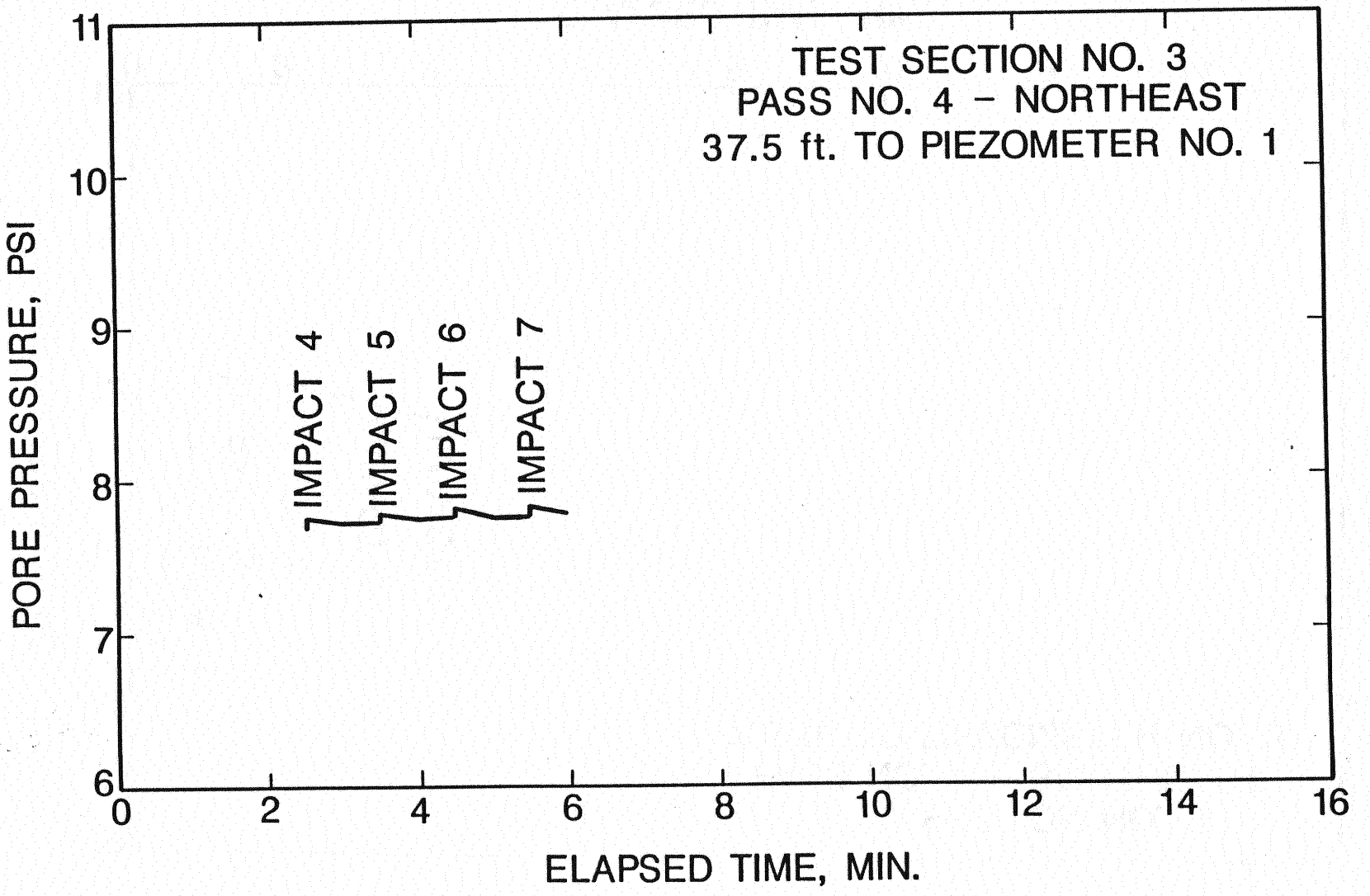

Figure 82. Piezometer No. 1 Data, Pass No. 4 - Northeast, Test Section No. 3

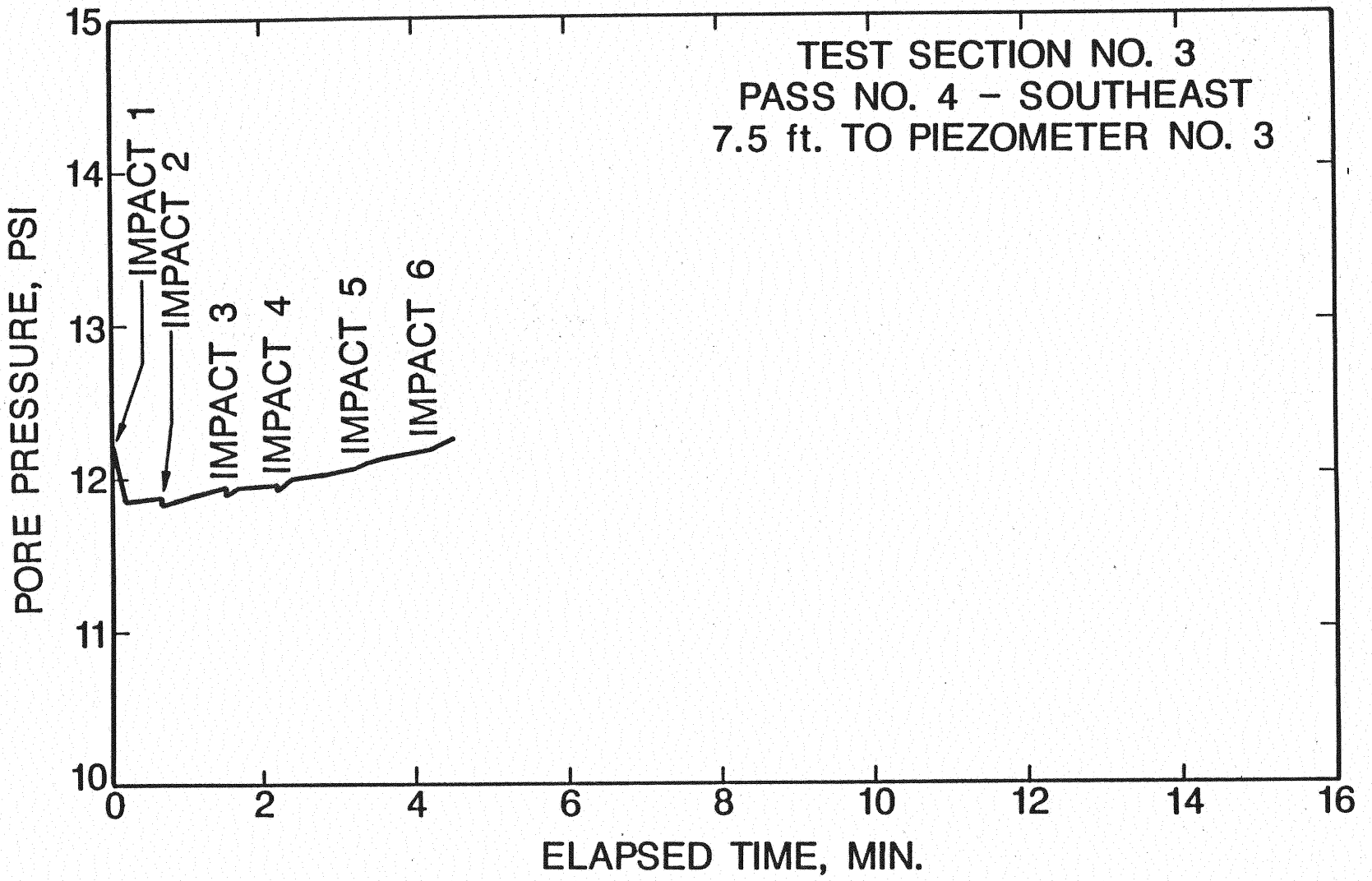

Figure 83. Piezometer No. 3 Data, Pass No. 4 - Southeast, Test Section No. 3

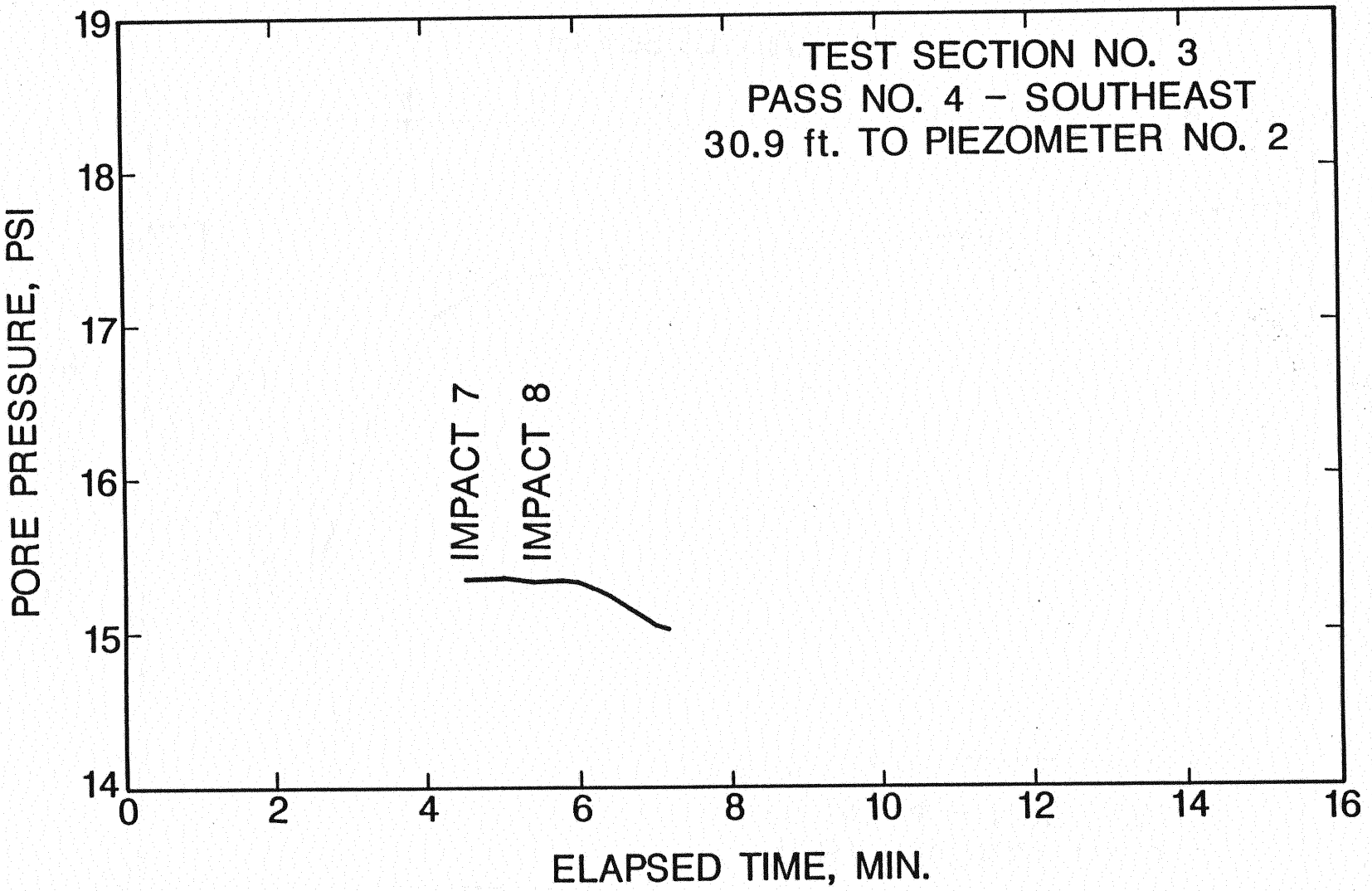

Figure 84. Piezometer No. 2 Data, Pass No. 4 - Southeast, Test Section No. 3

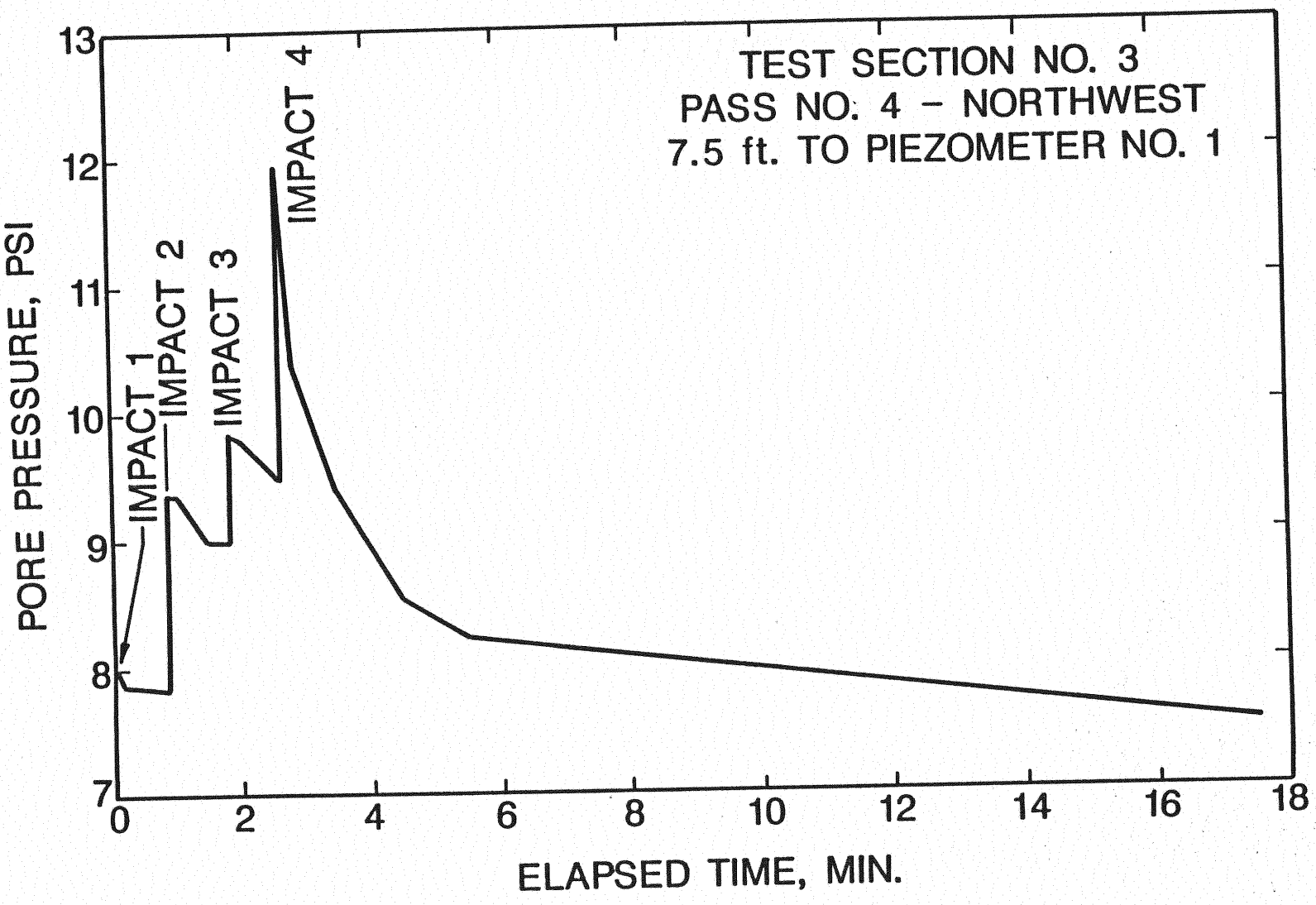

Figure 85. Piezometer No. 1 Data, Pass No. 4 - Northwest, Test Section No. 3

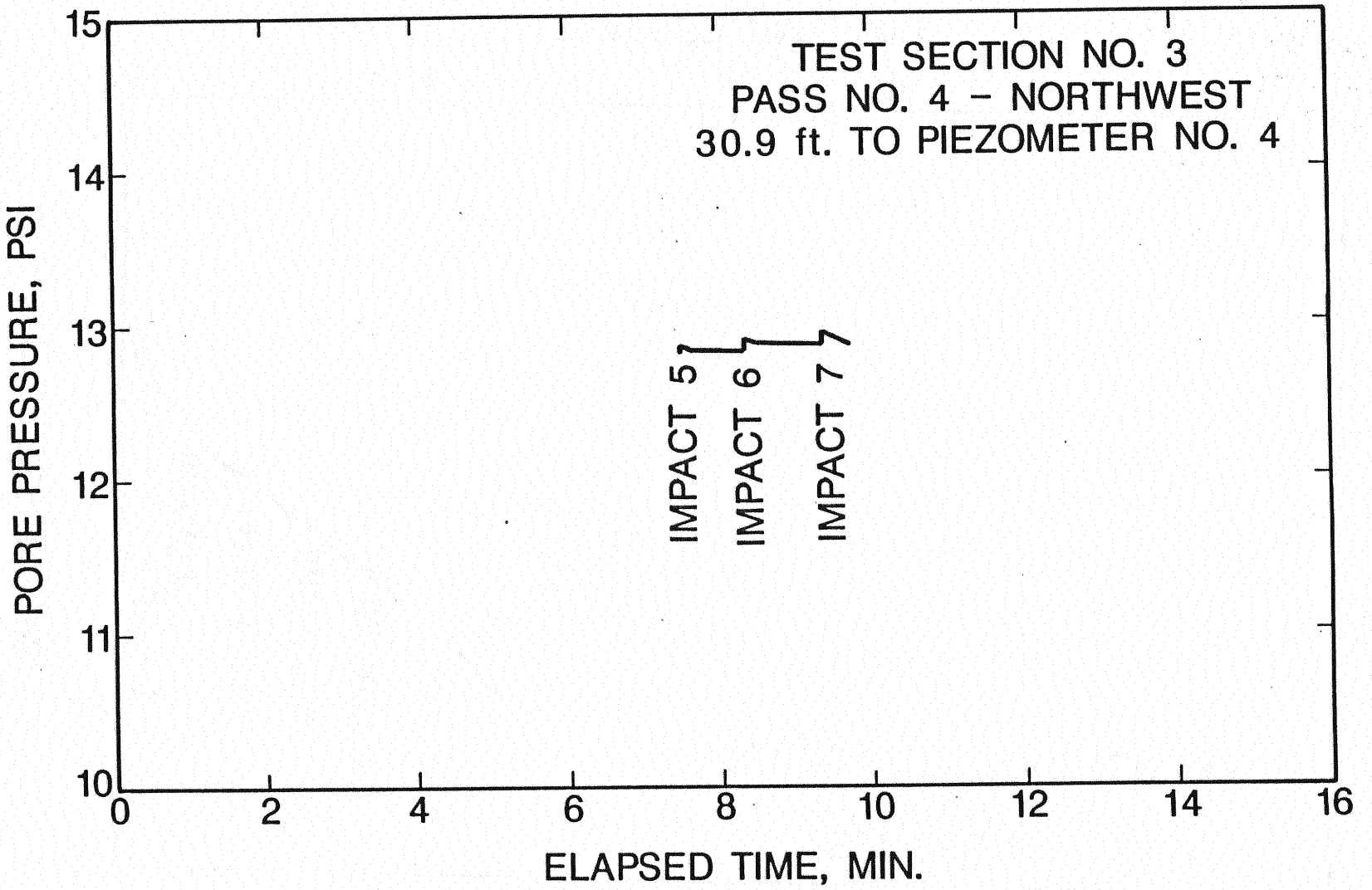

Figure 86. Piezometer No. 4 Data, Pass No. 4 - Northwest, Test Section No. 3

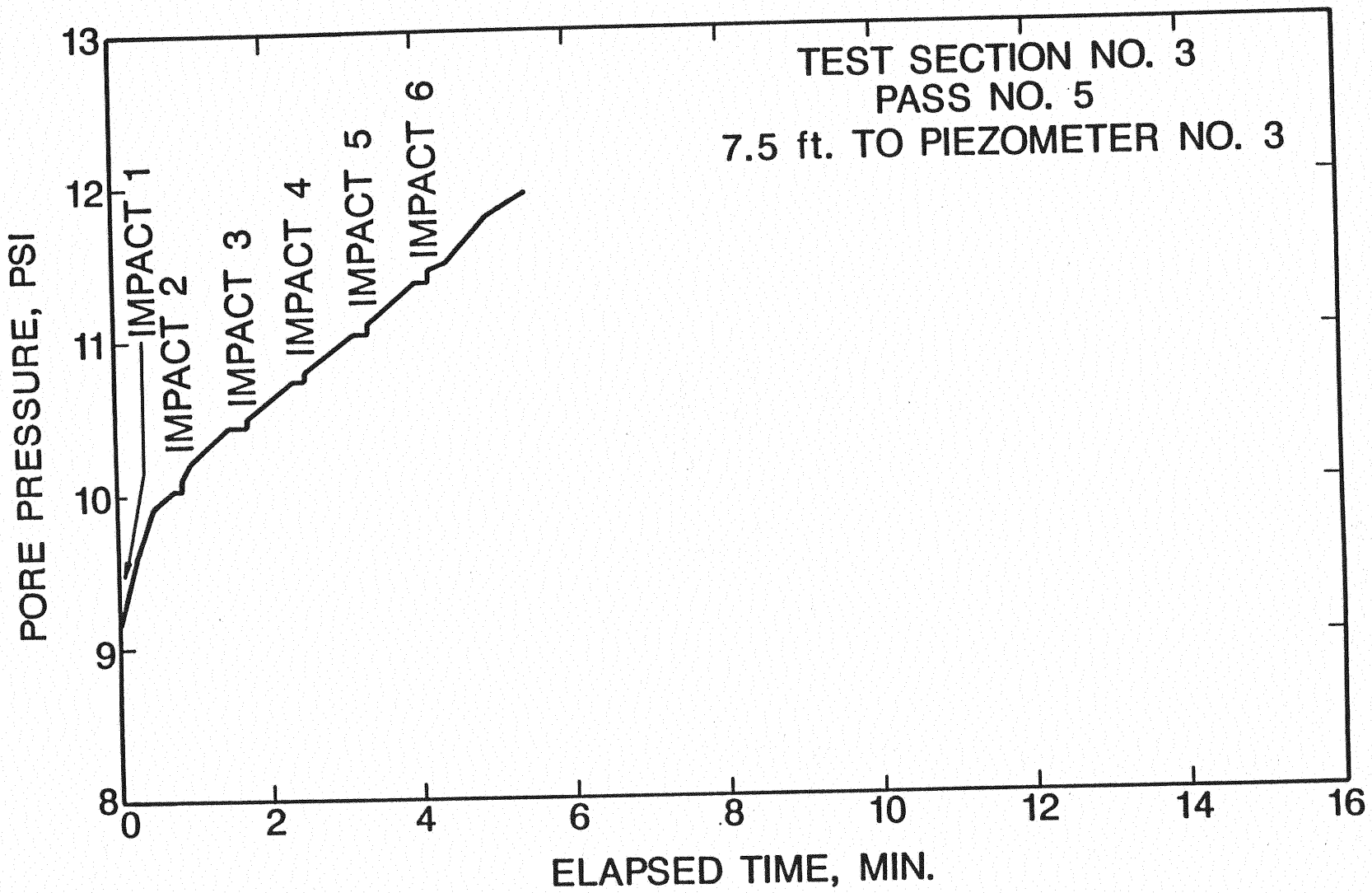

Figure 87. Piezometer No. 3 Data, Pass No. 5, Test Section No. 3

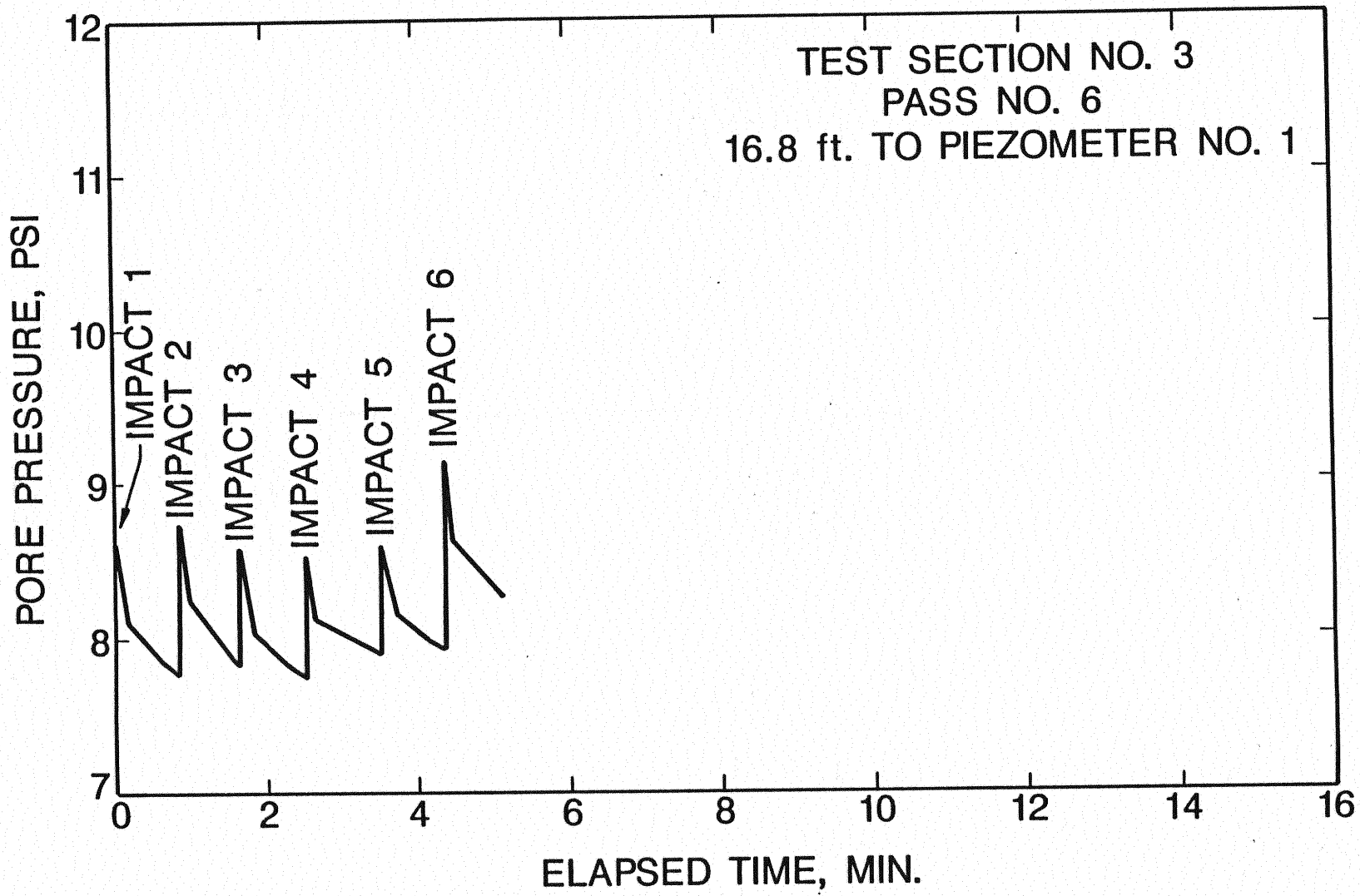

Figure 88. Piezometer No. 1 Data, Pass No. 6, Test Section No. 3

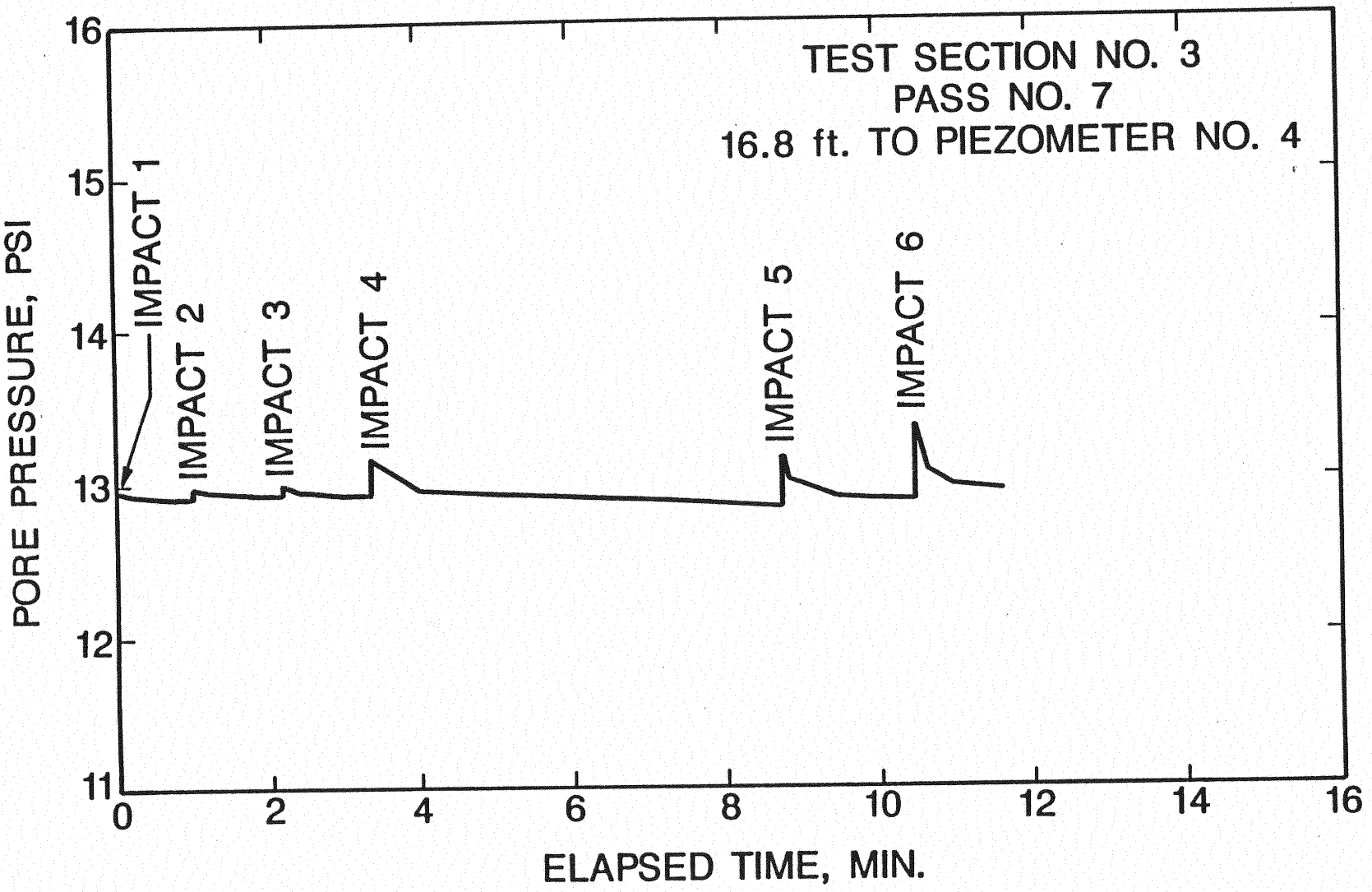

Figure 89. Piezometer No. 4 Data, Pass No. 7, Test Section No. 3

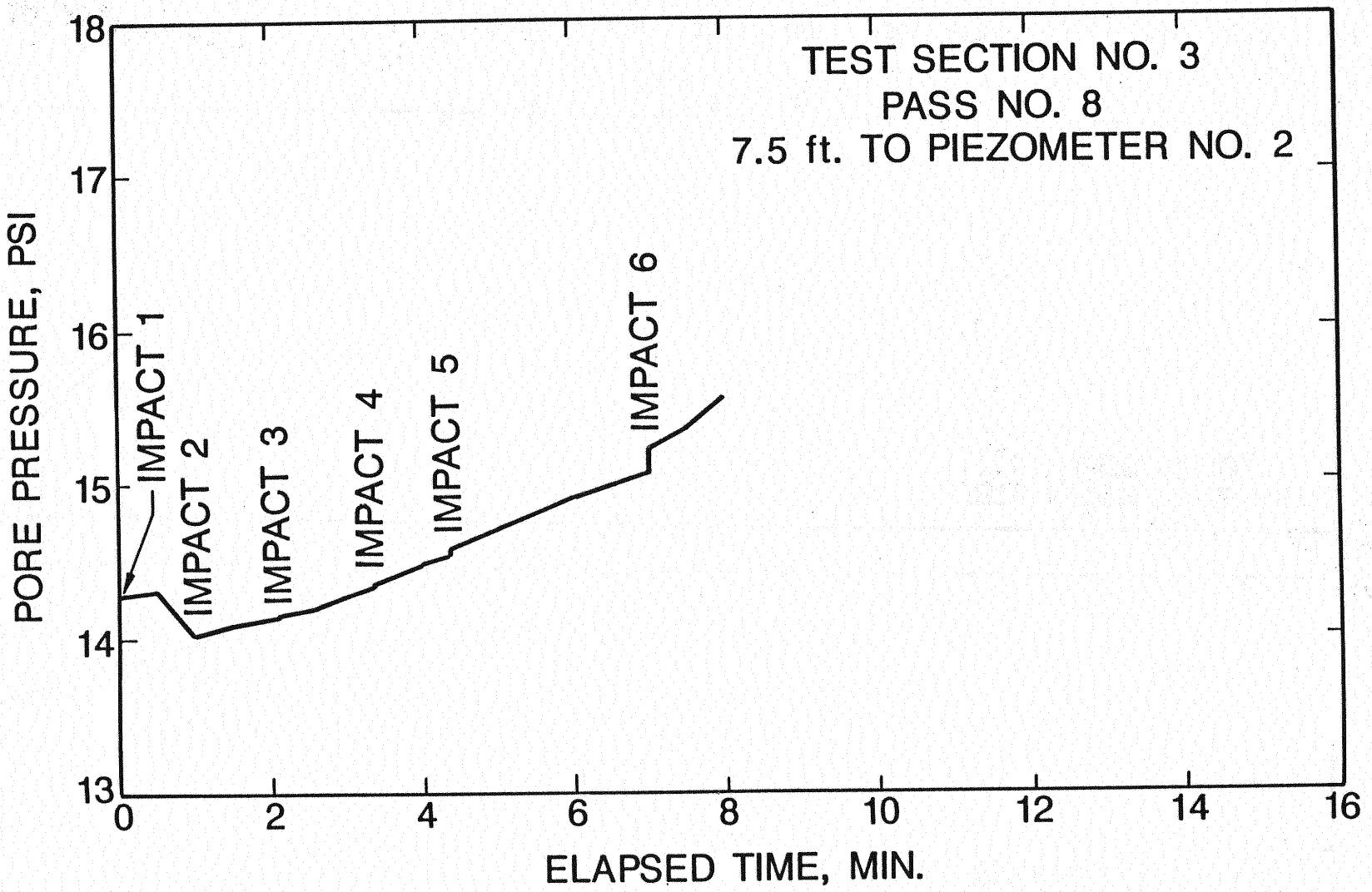

Figure 90. Piezometer No. 2 Data, Pass No. 8, Test Section No. 3

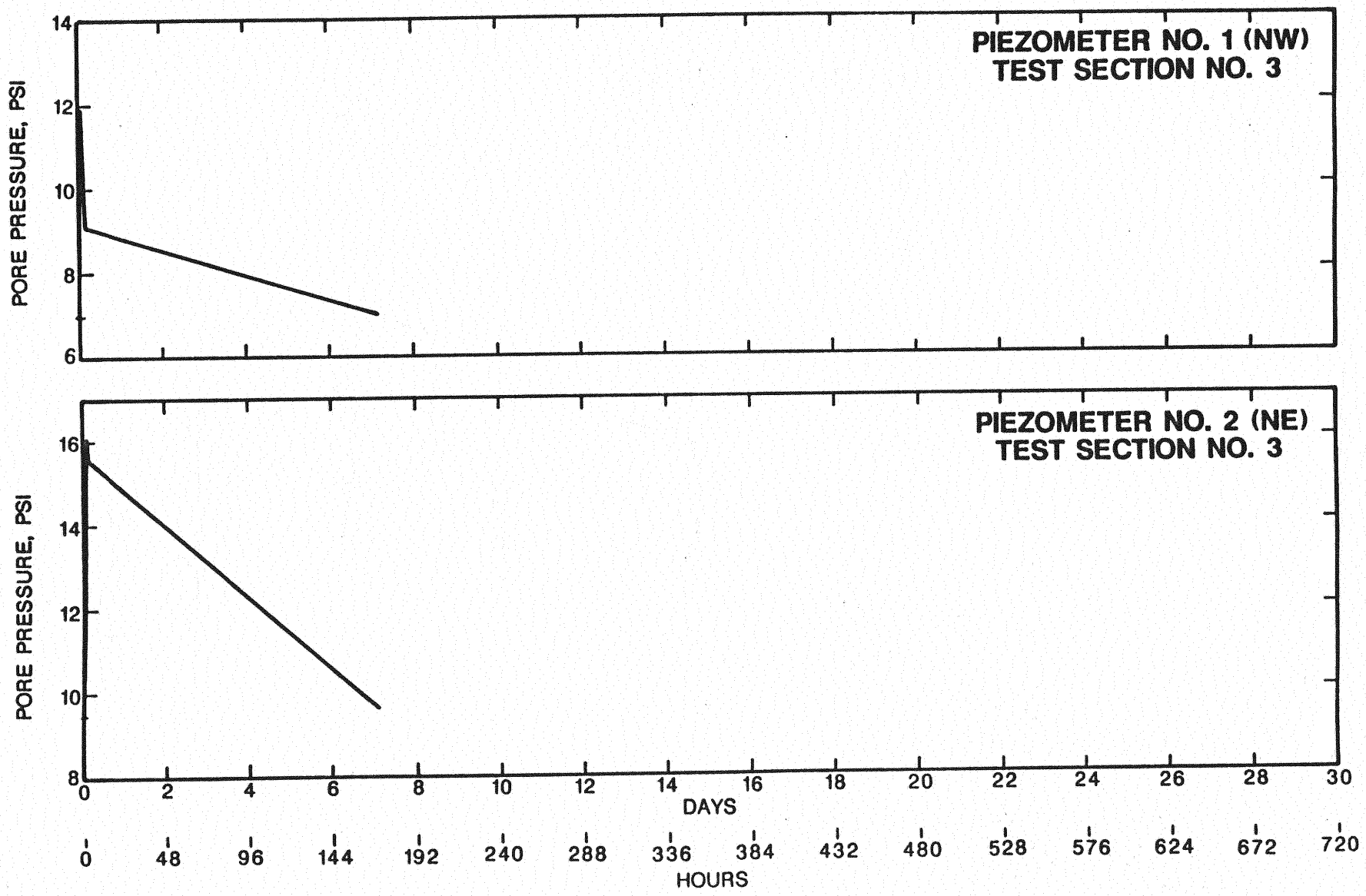

Figure 91. Long-Term Pore Pressure Dissipation (Piezometers 1 and 2), Test Section No. 3

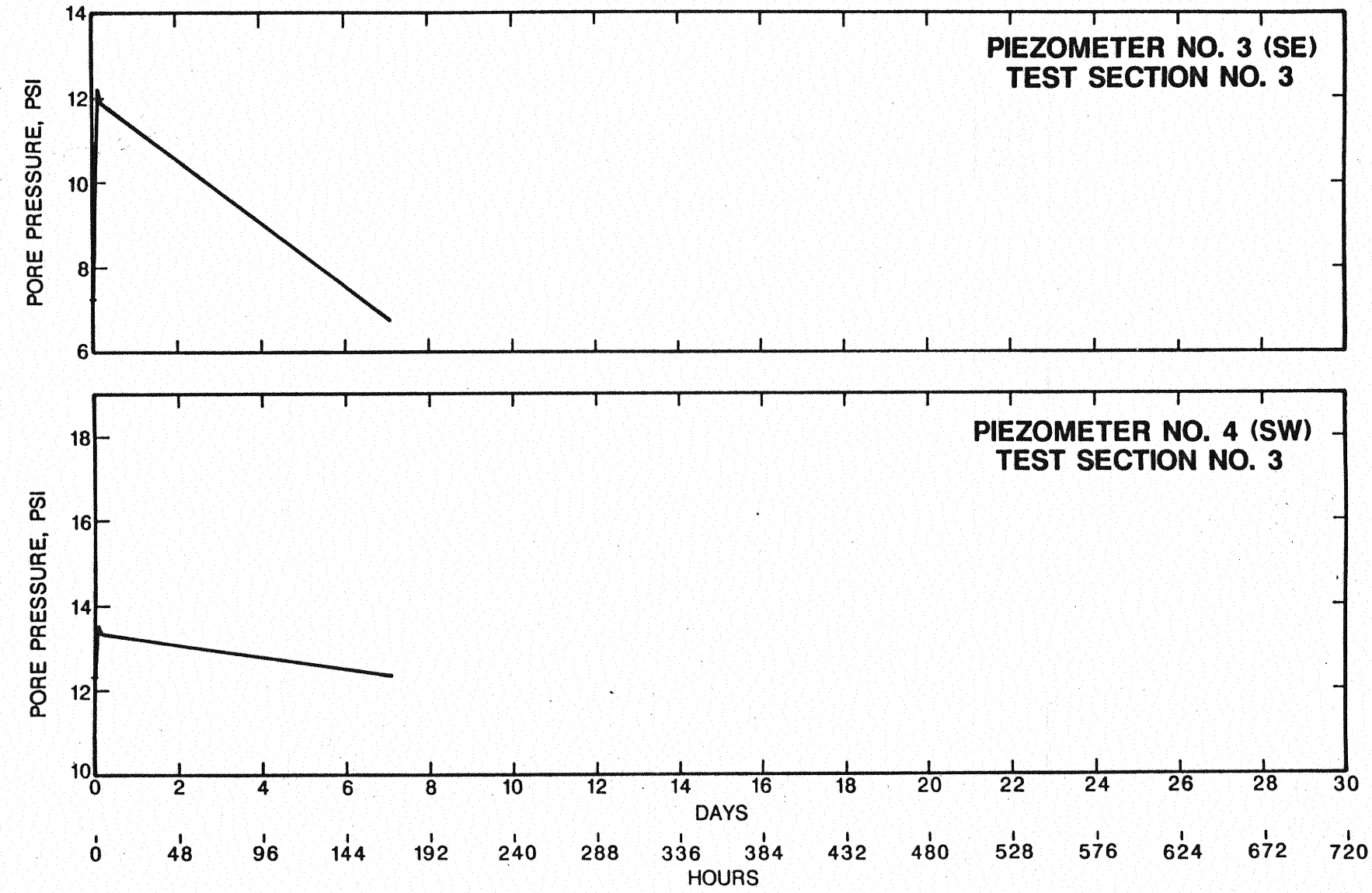

Figure 92. Long-Term Pore Pressure Dissipation (Piezometers 3 and 4), Test Section No. 3

TABLE III

SUMMARY OF CRATER DEPTHS, TEST SECTION NO. 3

Pass No.	Location	Number of Impacts	Crater Depth (Ft)
1	West	7	9.6
1	East	8	8.3
2	North	8	9.2
2	South	8	10.6
3	---	8	10.0
4	Southwest	8	8.8
4	Northeast	8	8.6
4	Southeast	8	10.0*
4	Northwest	8	8.0*
5	---	6	11.5*
6	---	6	9.5*
7	---	6	10.6
8	---	6	9.8

*Depth measured after weight removed from crater.

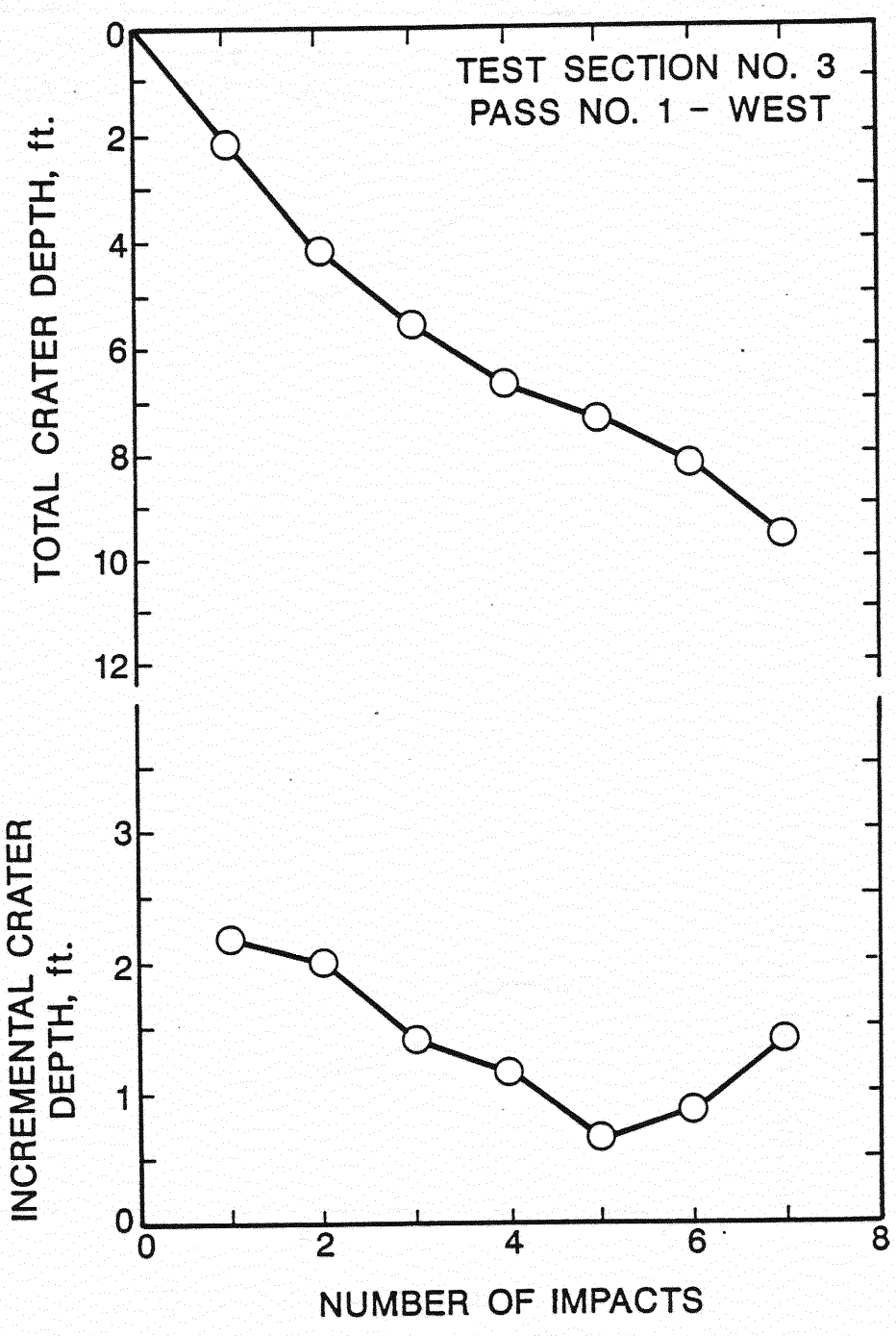

Figure 93. Crater Depth Versus Number of Impacts: Pass No. 1 - West, Test Section No. 3

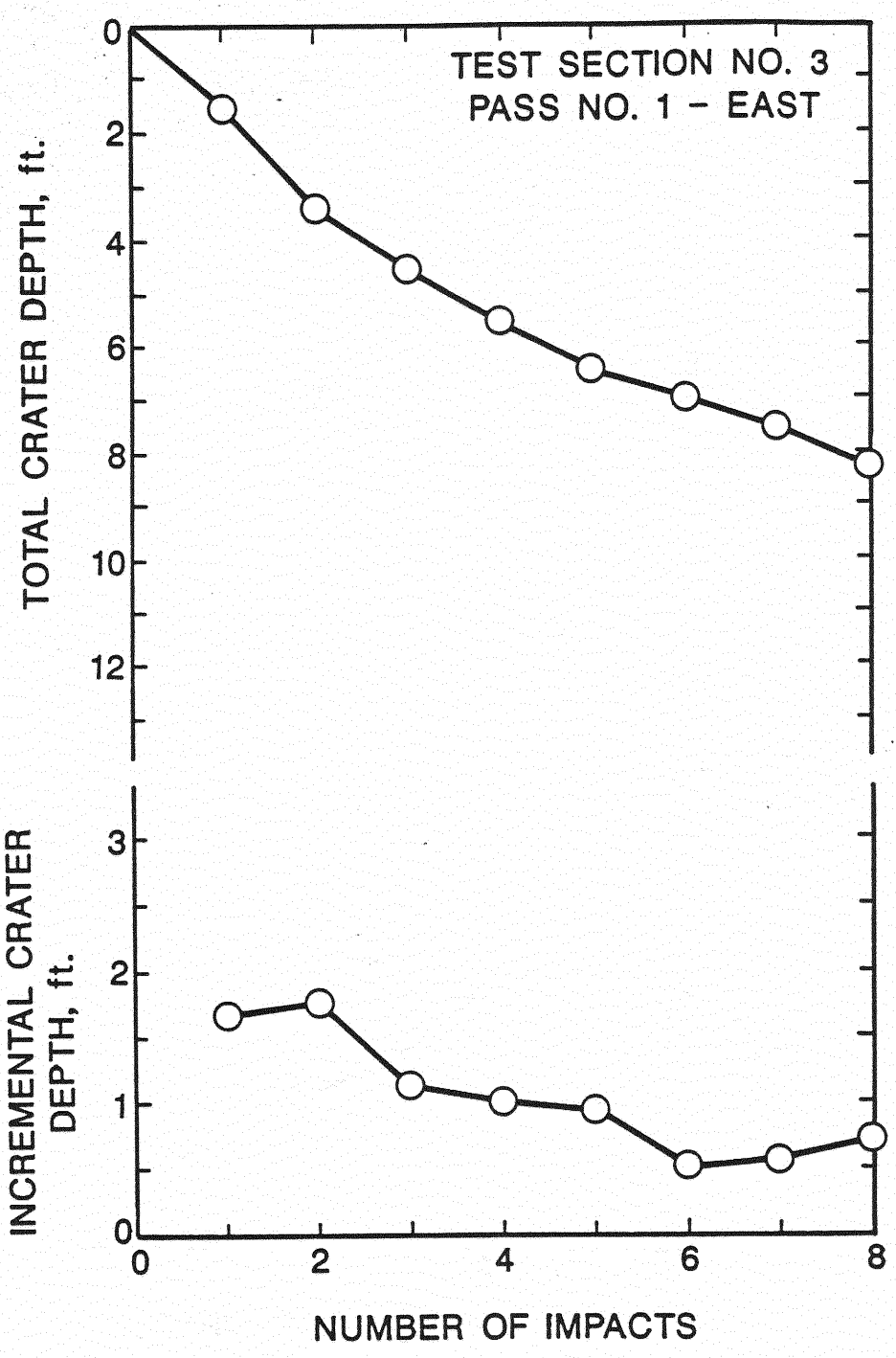

Figure 94. Crater Depth Versus Number of Impacts: Pass No. 1 - East, Test Section No. 3

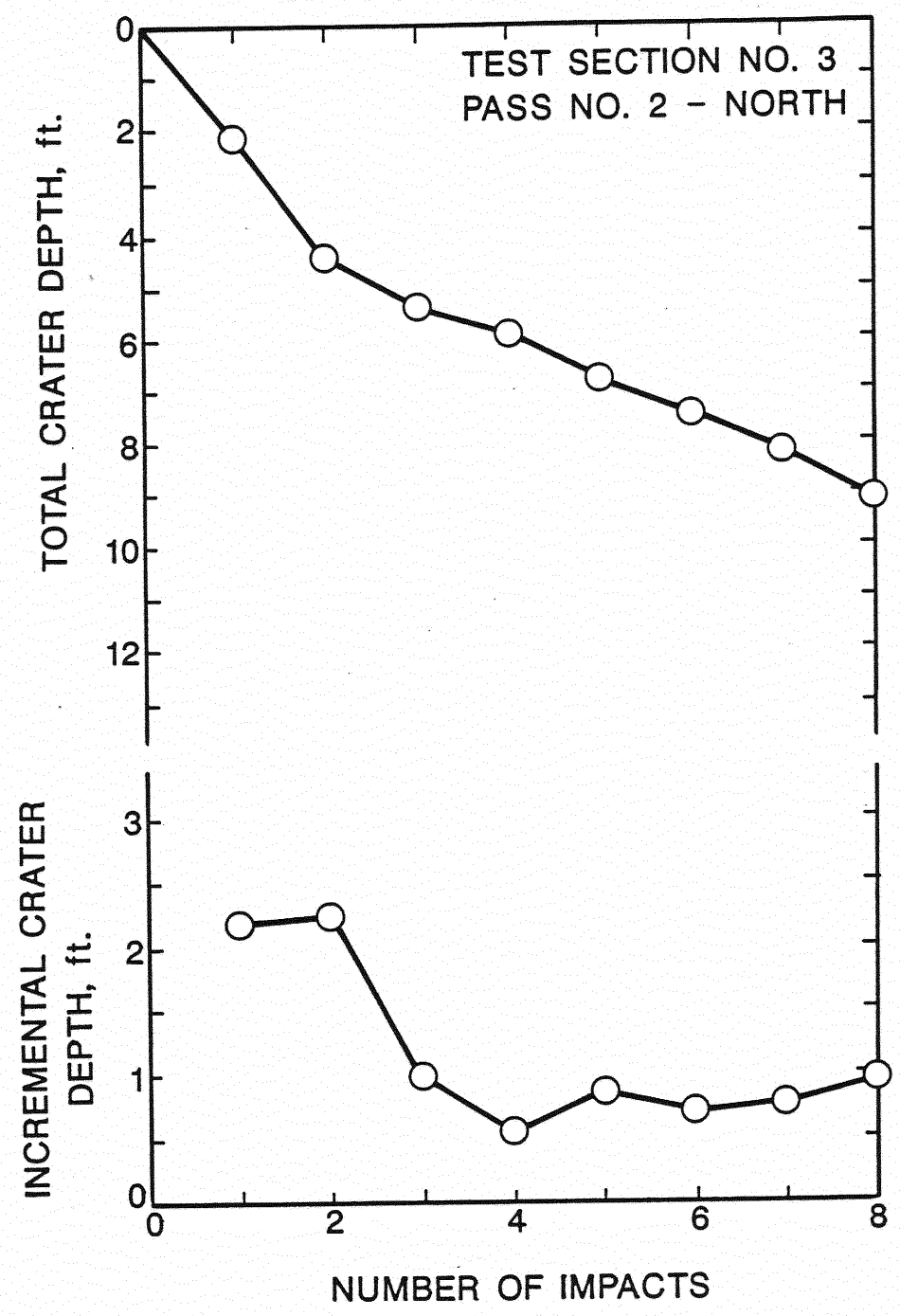

Figure 95. Crater Depth Versus Number of Impacts: Pass No. 2 - North, Test Section No. 3

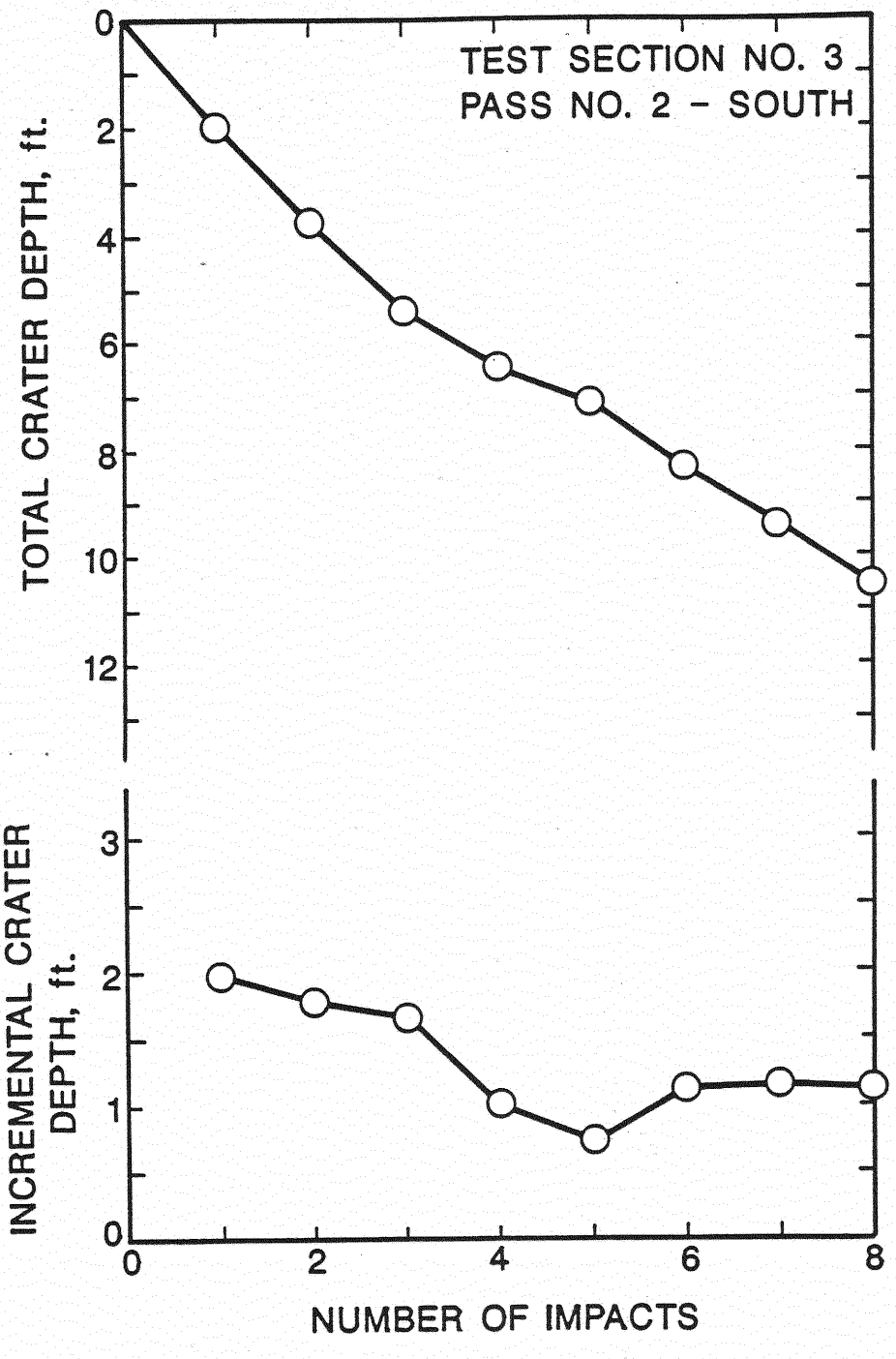

Figure 96. Crater Depth Versus Number of Impacts: Pass No. 2 - South, Test Section No. 3

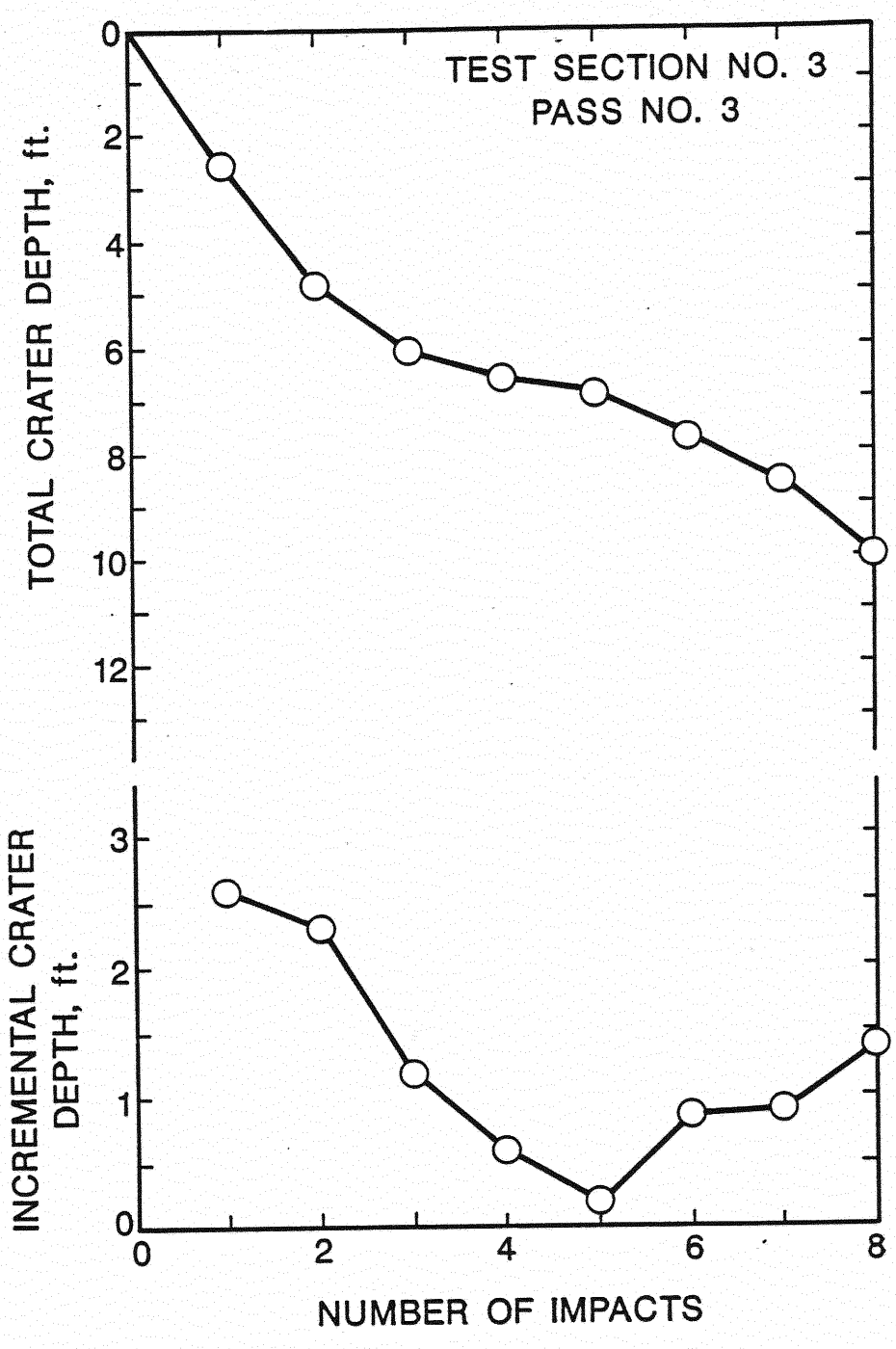

Figure 97. Crater Depth Versus Number of Impacts: Pass No. 3, Test Section No. 3

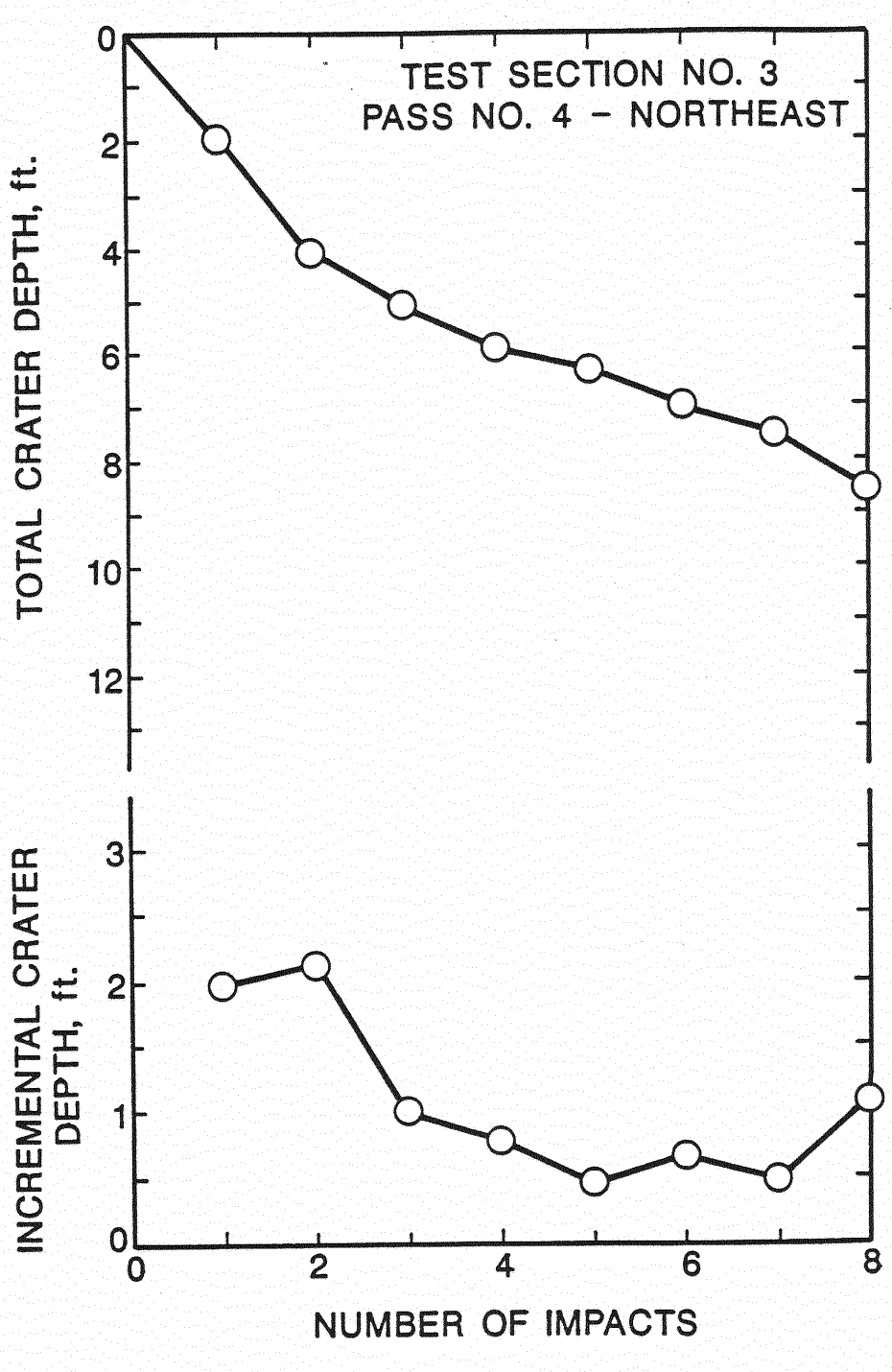

Figure 98. Crater Depth Versus Number of Impacts: Pass No. 4 - Northeast, Test Section No. 3

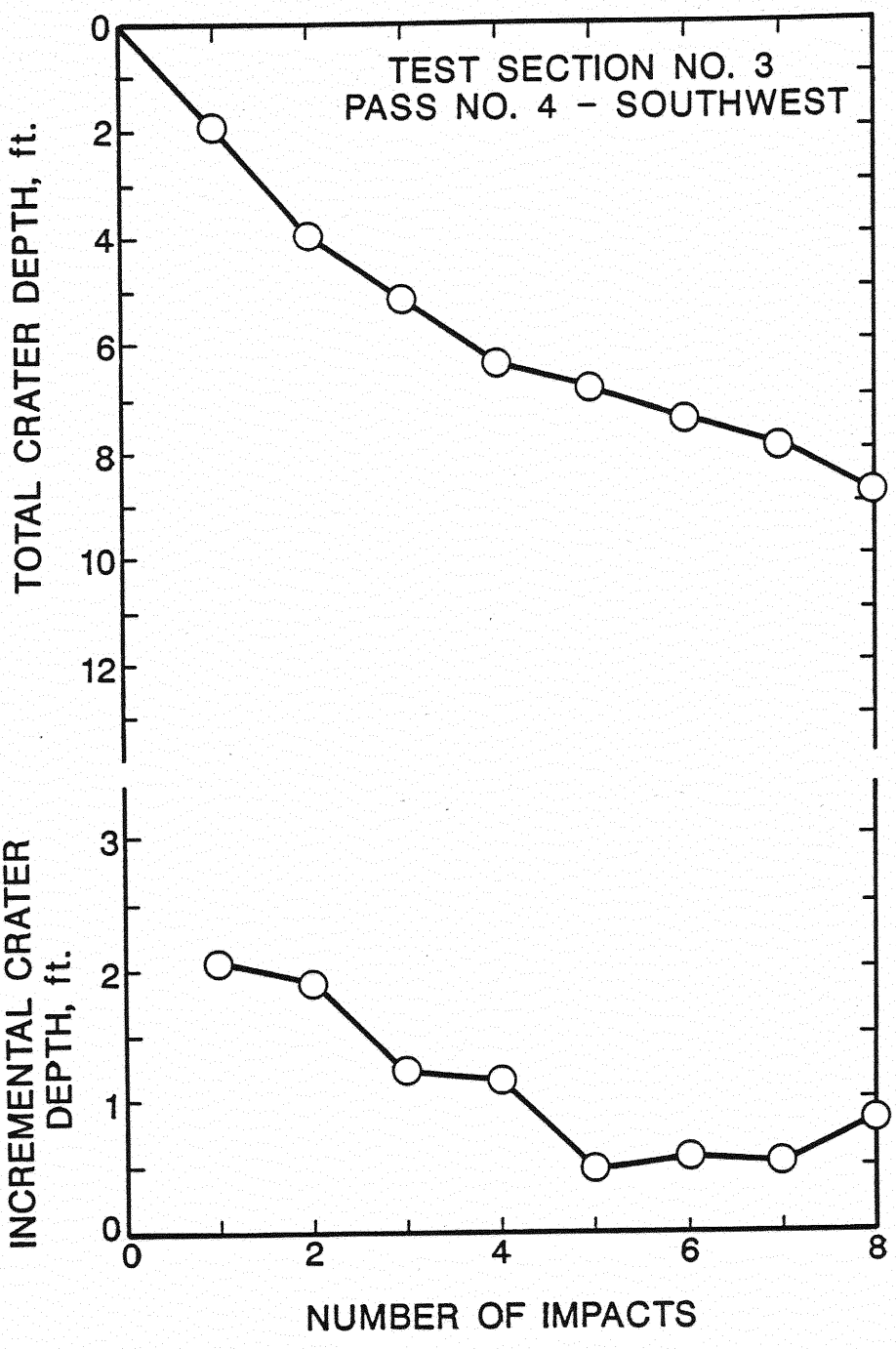

Figure 99. Crater Depth Versus Number of Impacts: Pass No. 4 - Southwest, Test Section No. 3

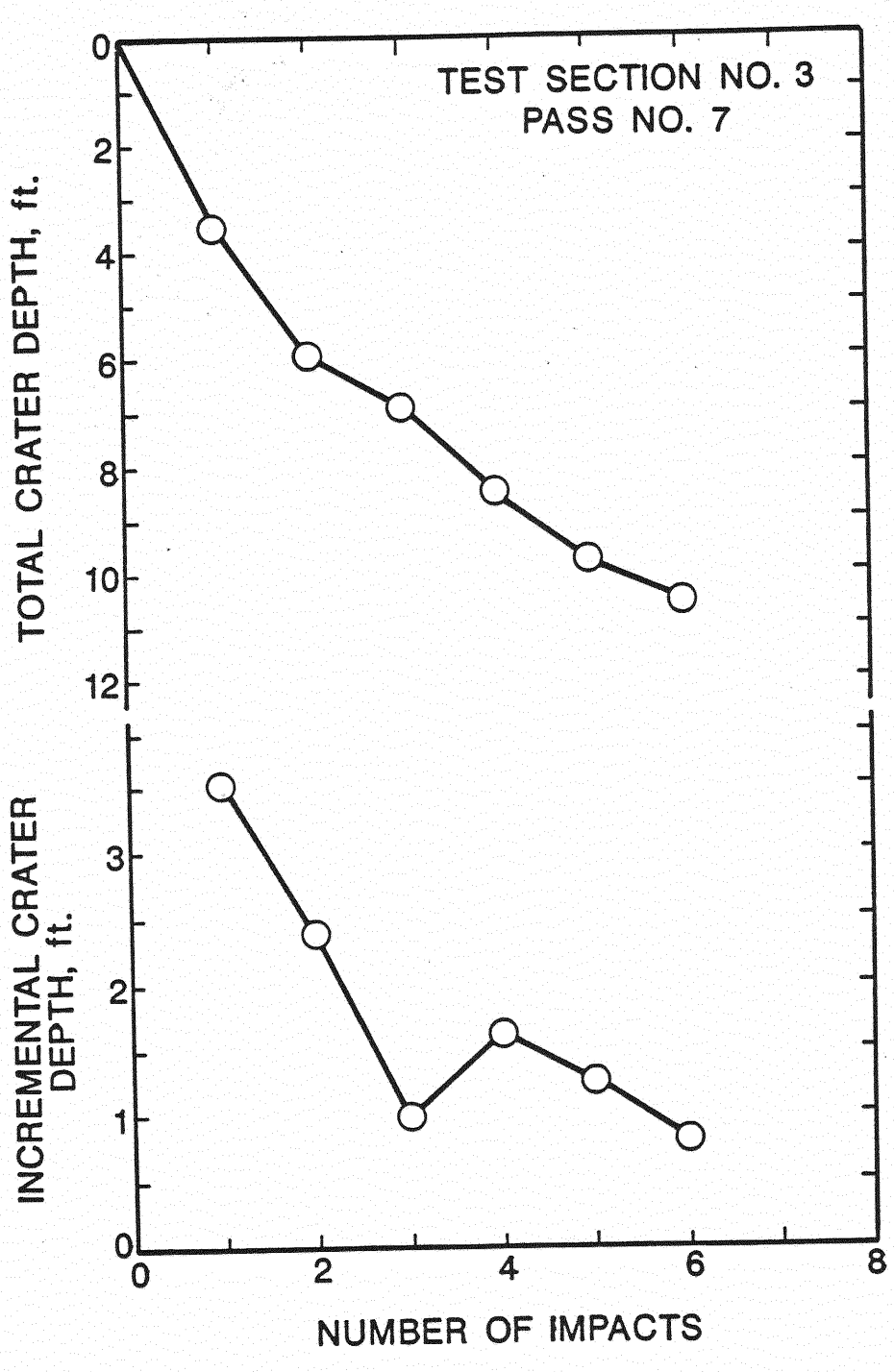

Figure 100. Crater Depth Versus Number of Impacts: Pass No. 7, Test Section No. 3

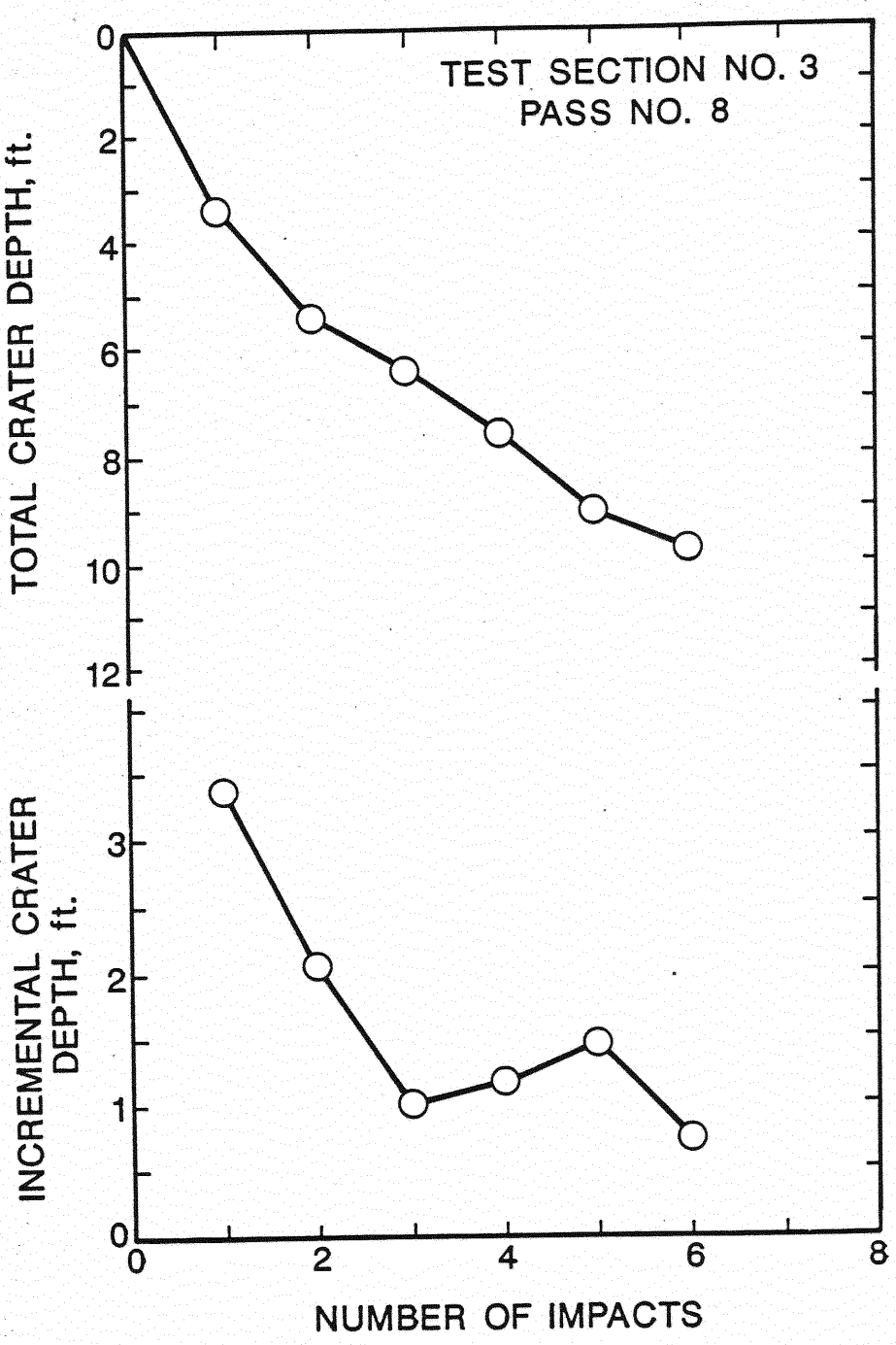

Figure 101. Crater Depth Versus Number of Impacts: Pass No. 8, Test Section No. 3

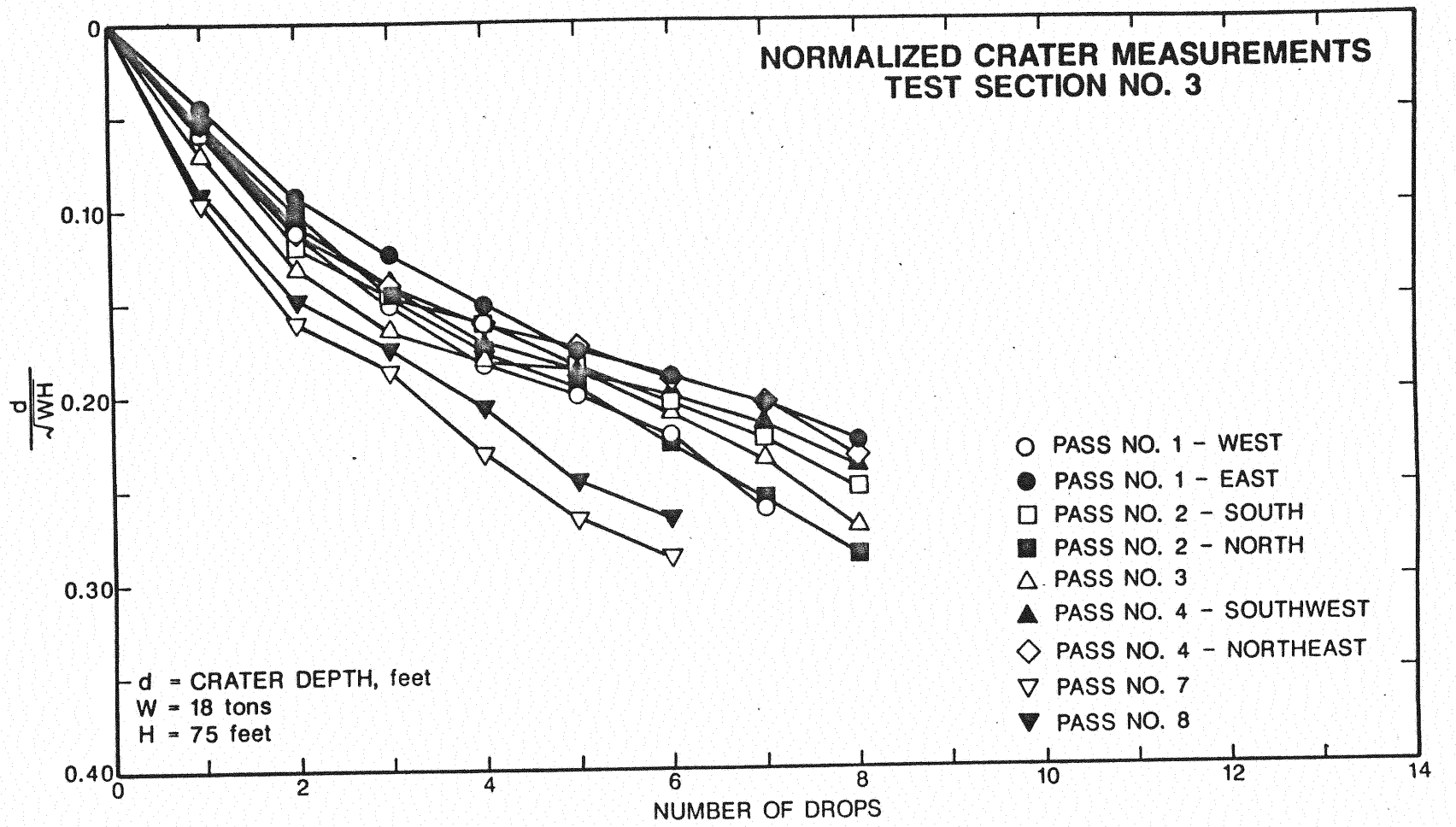

Figure 102. Normalized Crater Measurements, Test Section No. 3

TEST SECTION NO. 3 - BORING NO. 1
(NORTH OF CRL)

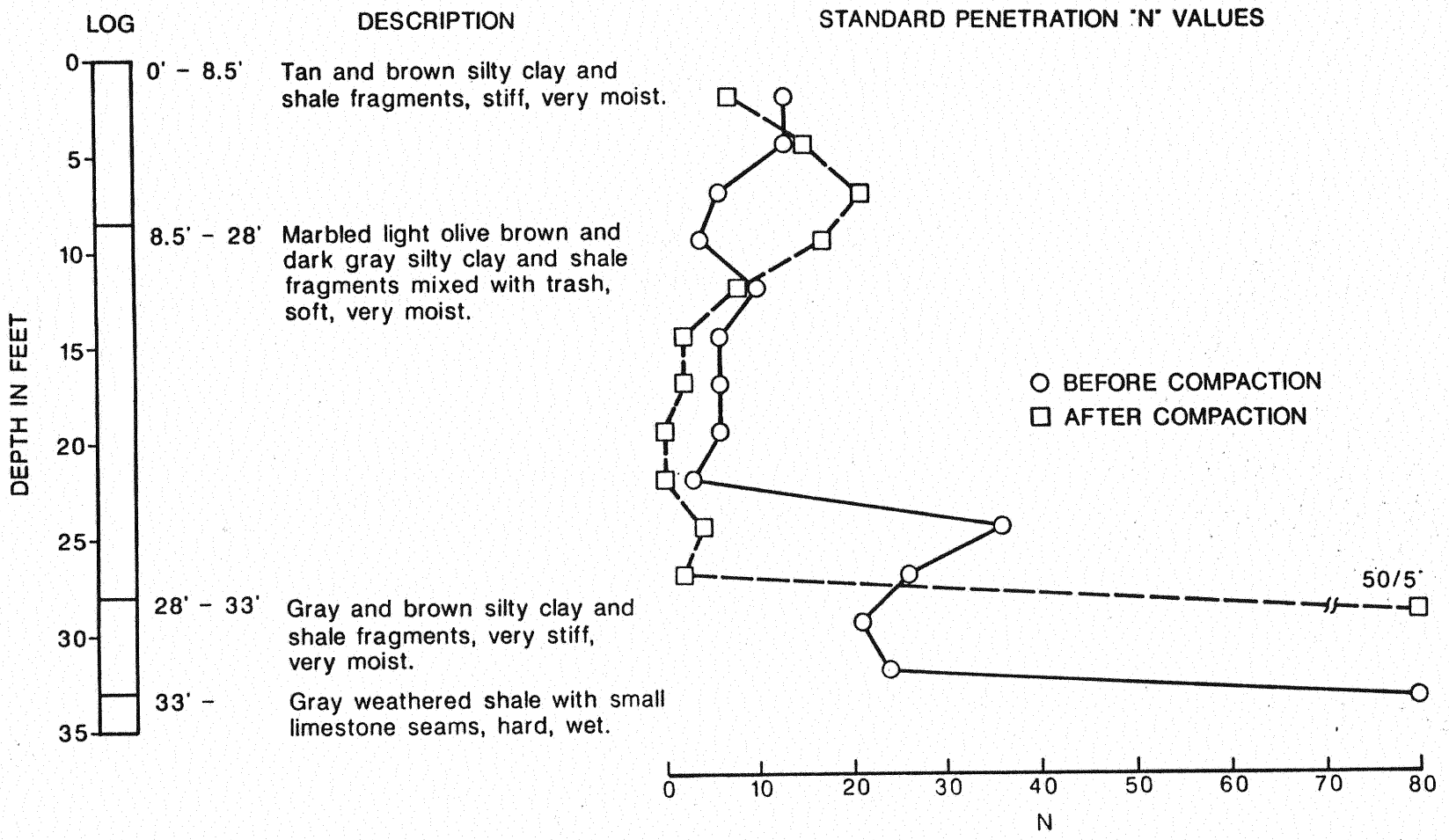

Figure 103. Standard Penetration Test Results, North of CRL, Test Section No. 3

TEST SECTION NO. 3 - BORING NO. 2
(CRL)

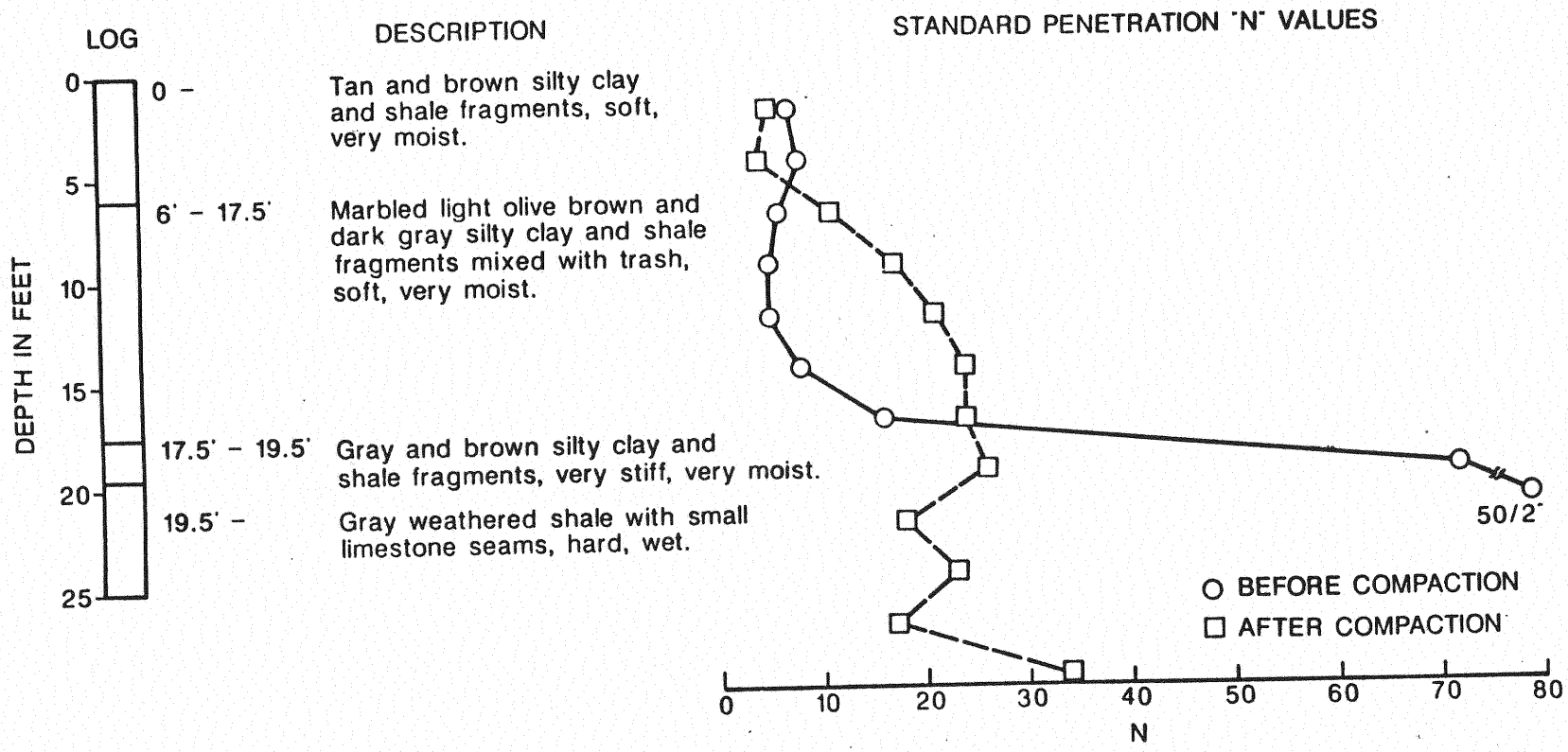

Figure 104. Standard Penetration Test Results, Along CRL, Test Section No. 3

TEST SECTION NO. 3 - BORING NO. 3
(SOUTH OF CRL)

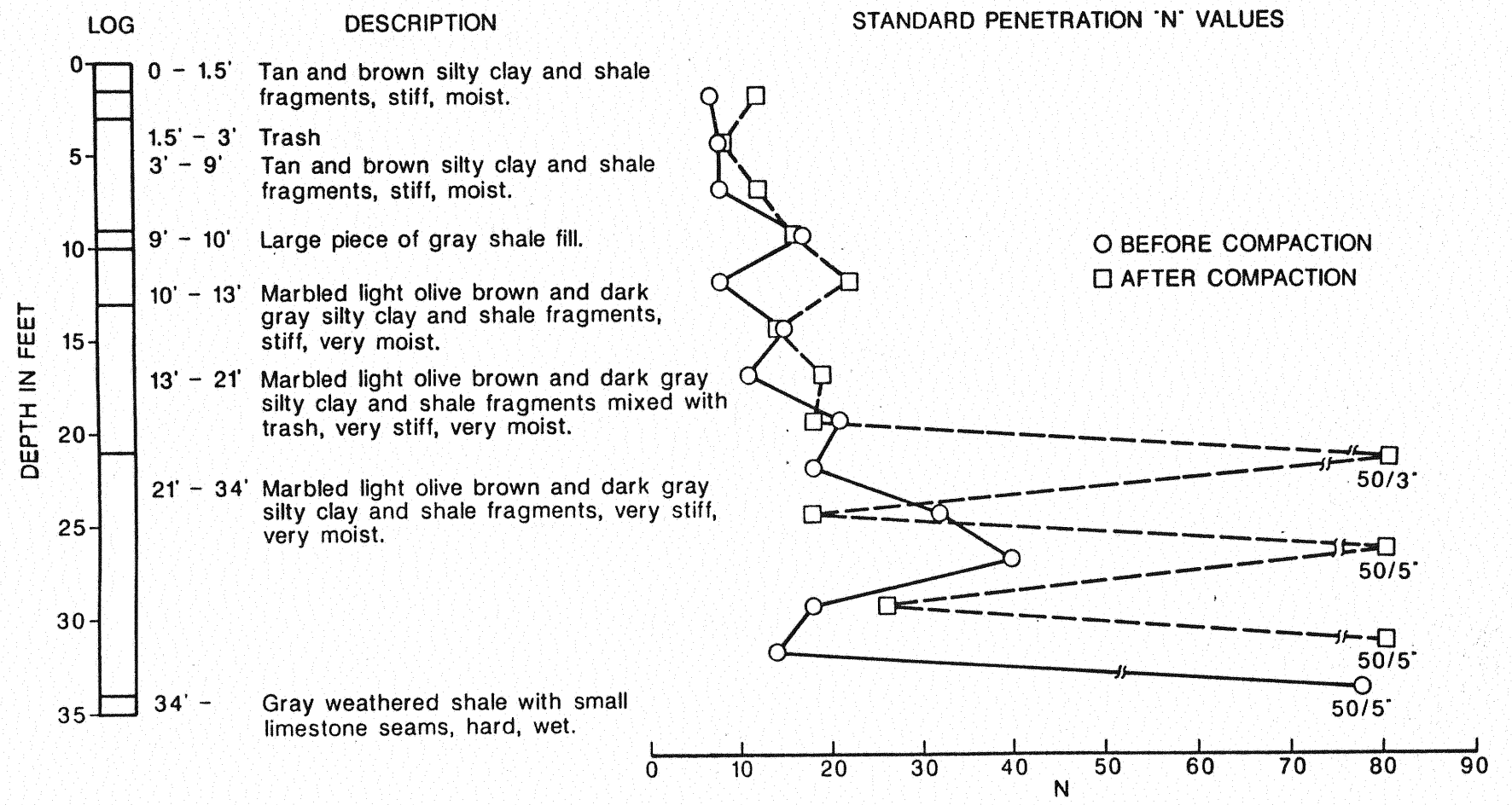

Figure 105. Standard Penetration Test Results, South of CRL, Test Section No. 3

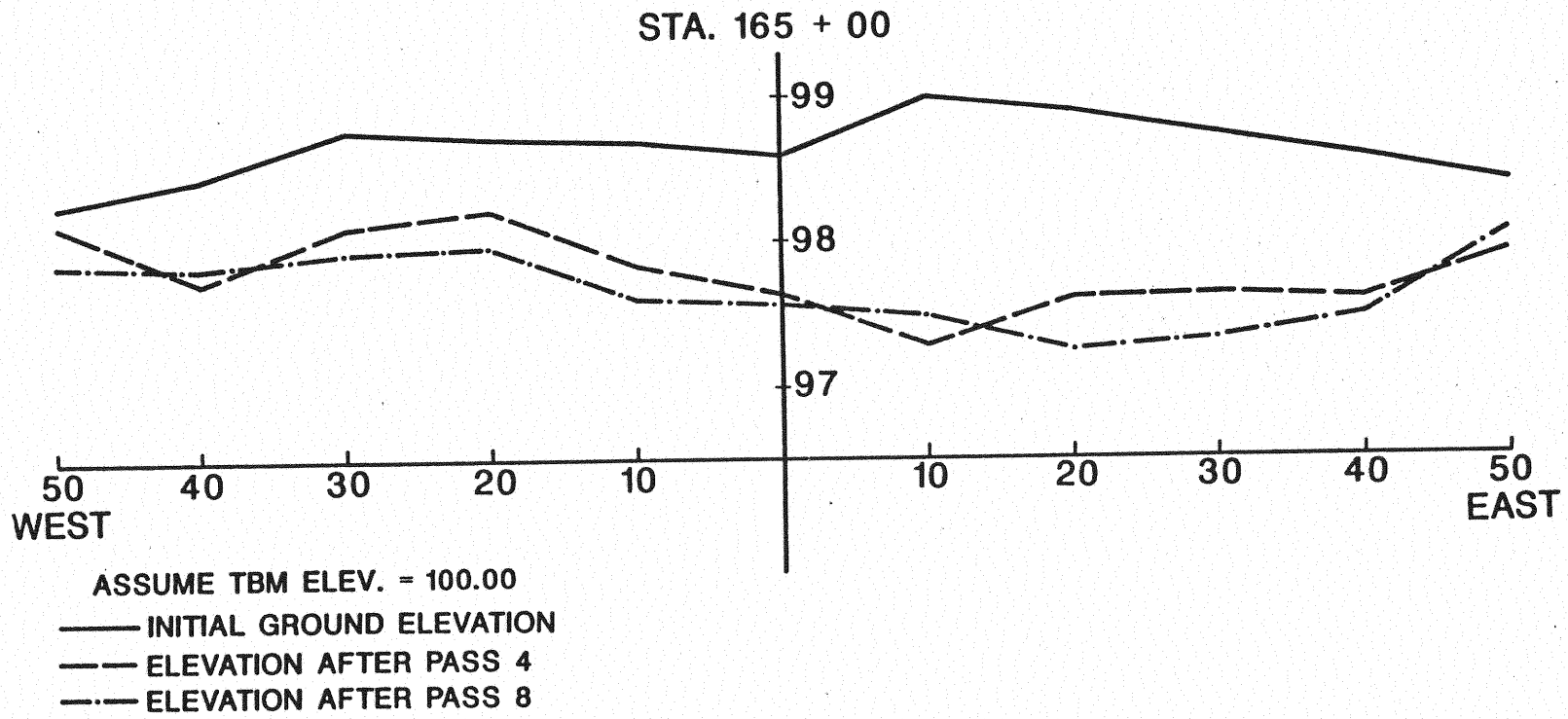

Figure 106. Post-Compaction Subsidence, Along CRL, Test Section No. 3

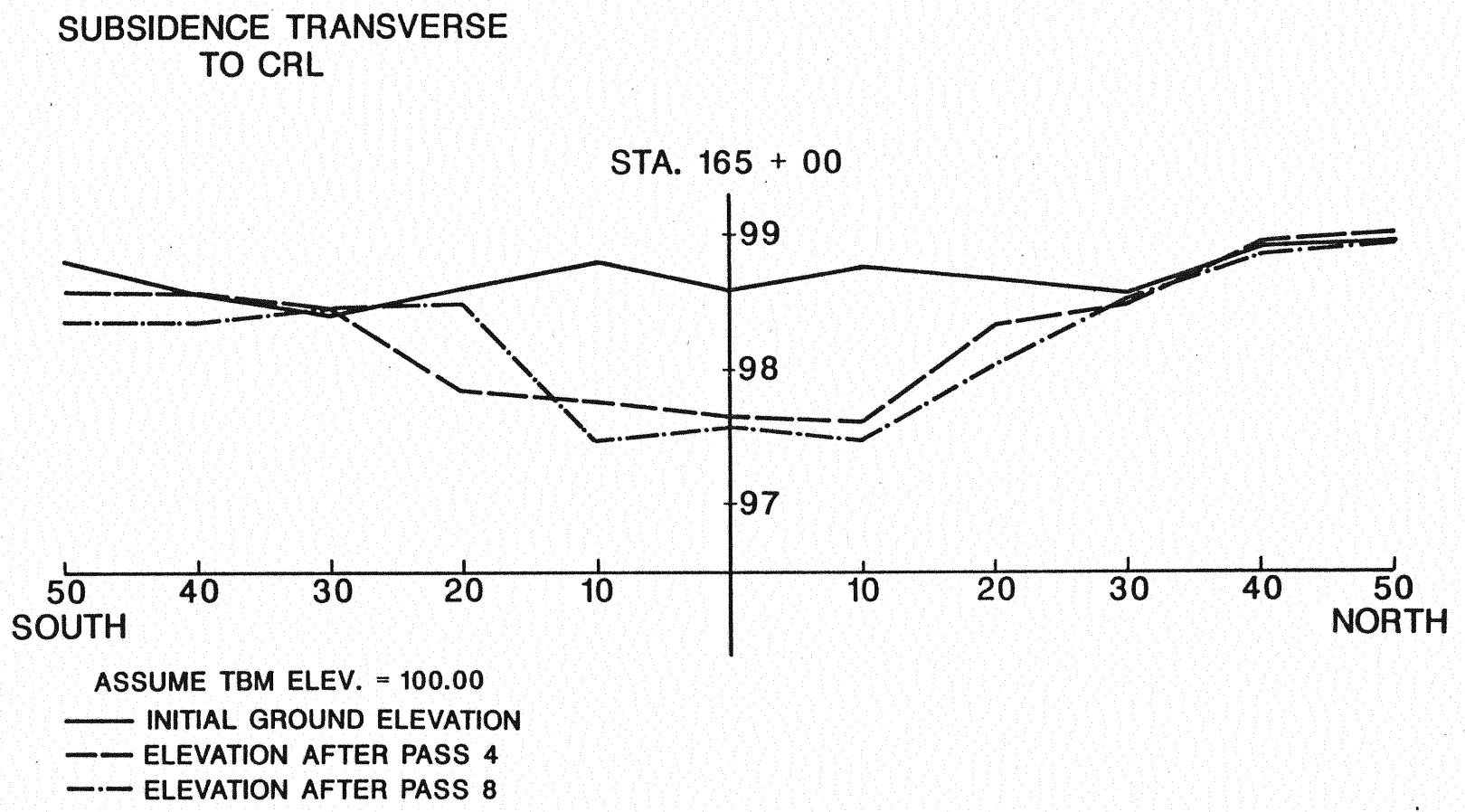

Figure 107. Post-Compaction Subsidence, Transverse to CRL, Test Section No. 3

APPENDIX D

RESULTS OF STONE COLUMN TEST CONSTRUCTION

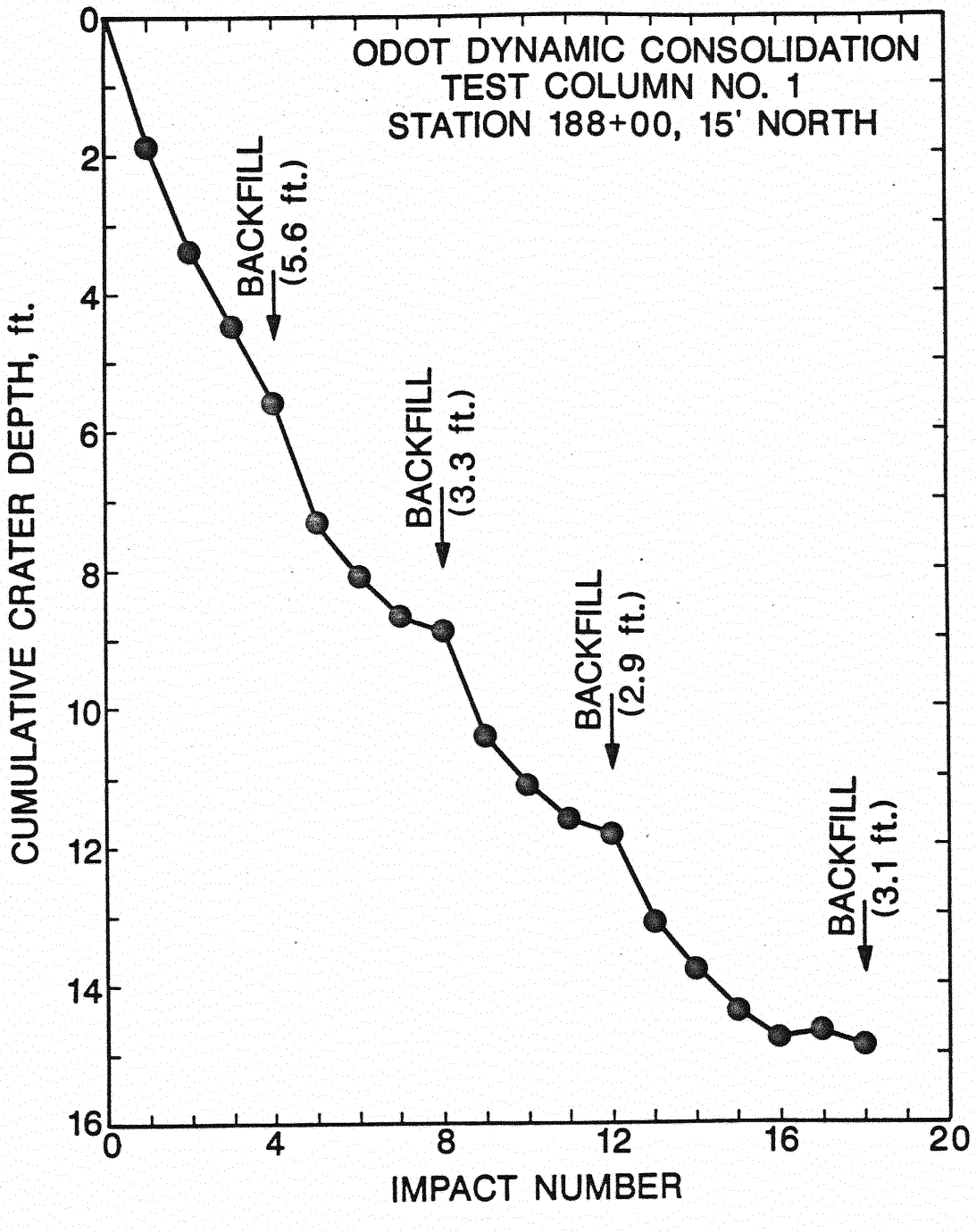

Figure 108. Cumulative Crater Depth Versus Impact, Test Column No. 1

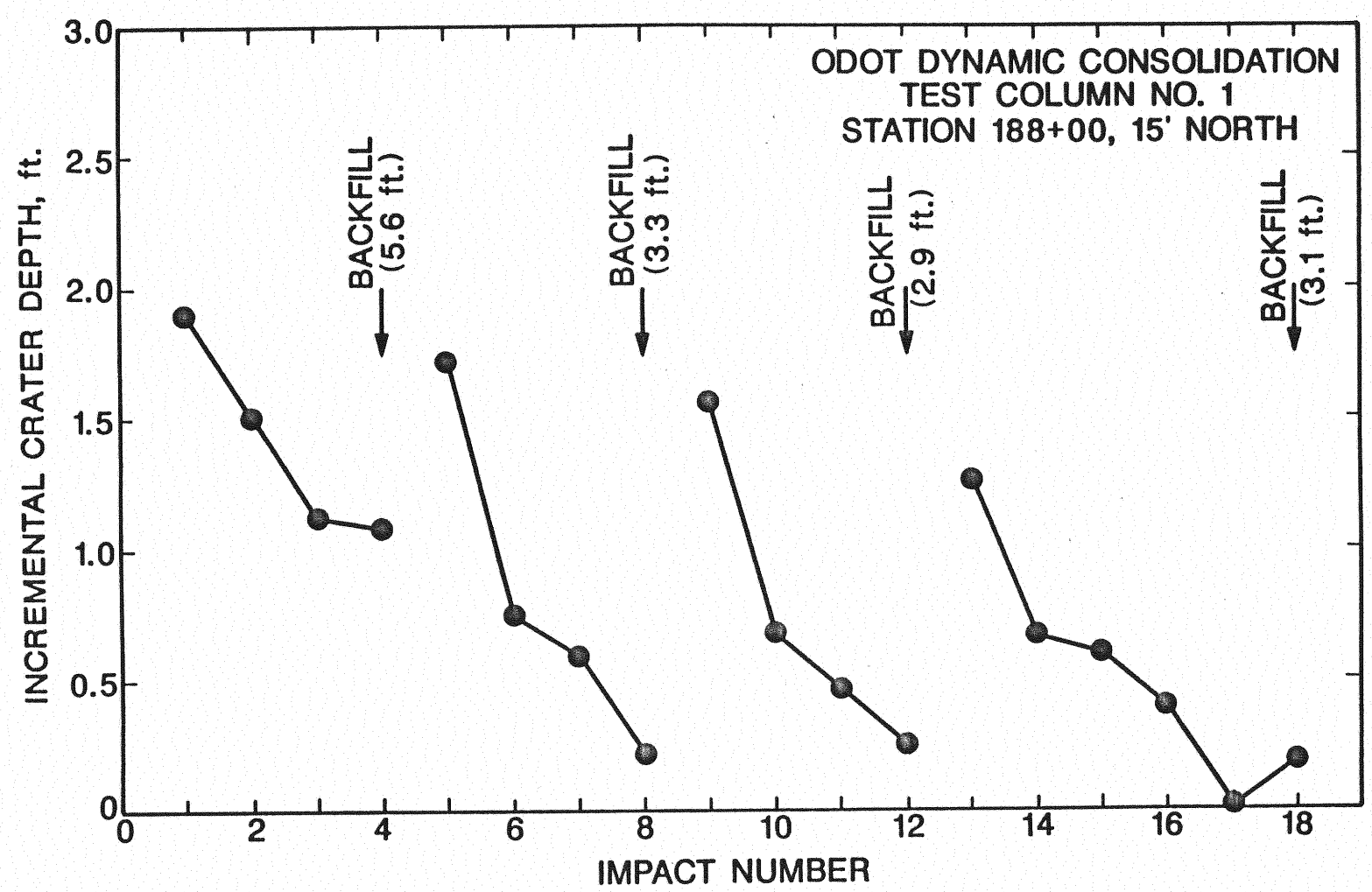

Figure 109. Incremental Crater Depth Versus Impact, Test Column No. 1

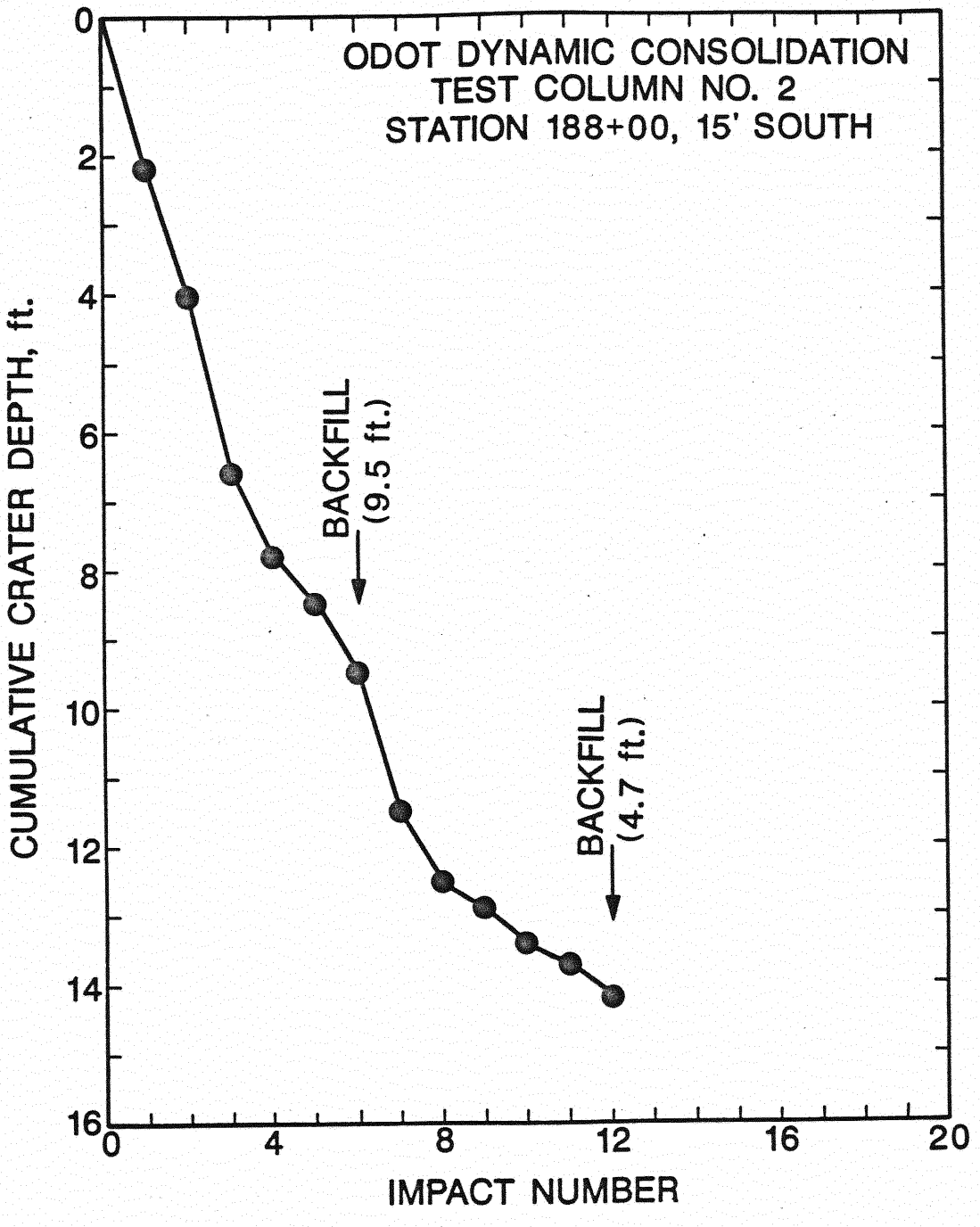

Figure 110. Cumulative Crater Depth Versus Impact, Test Column No. 2

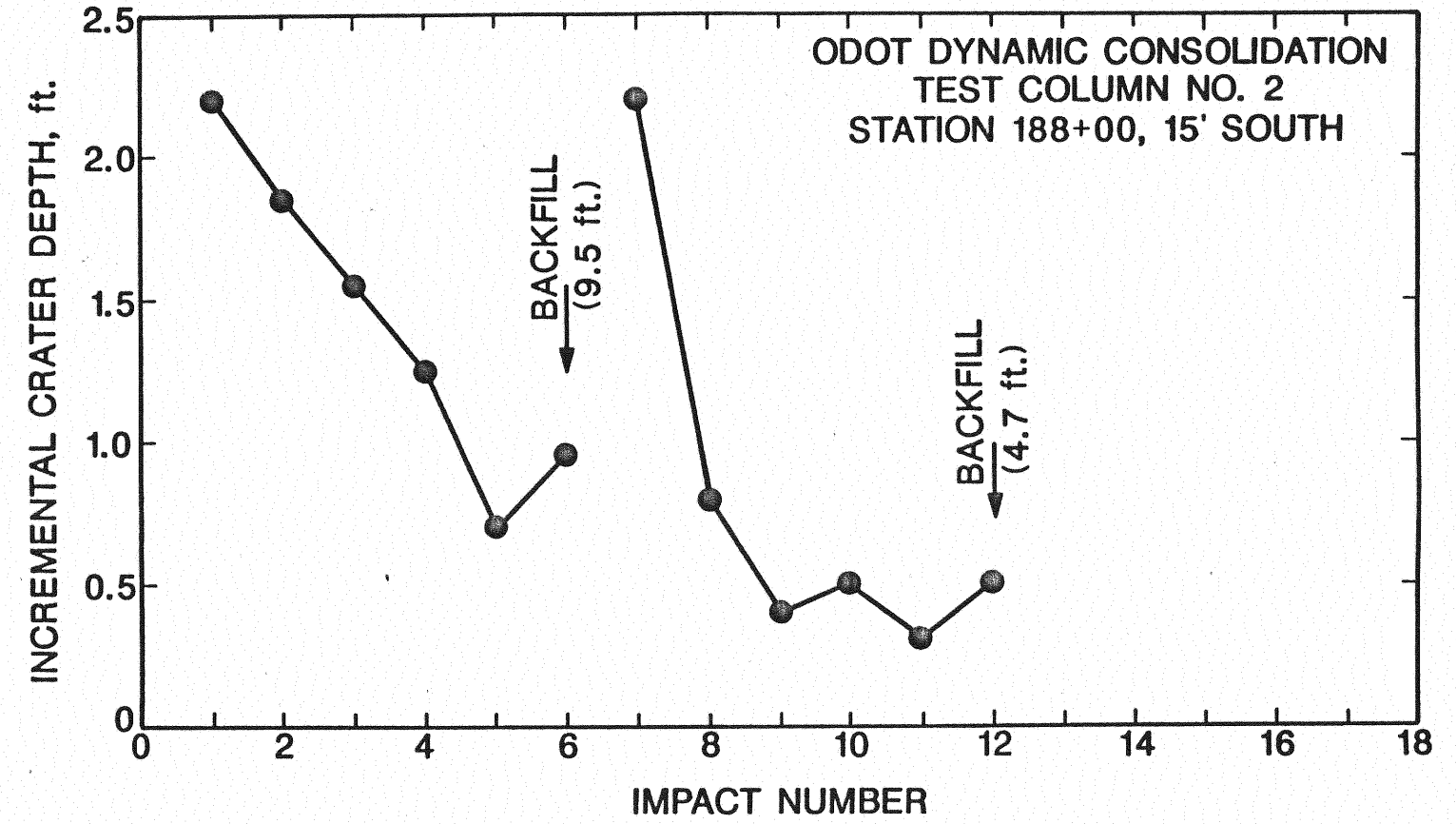

Figure 111. Incremental Crater Depth Versus Impact, Test Column No. 2

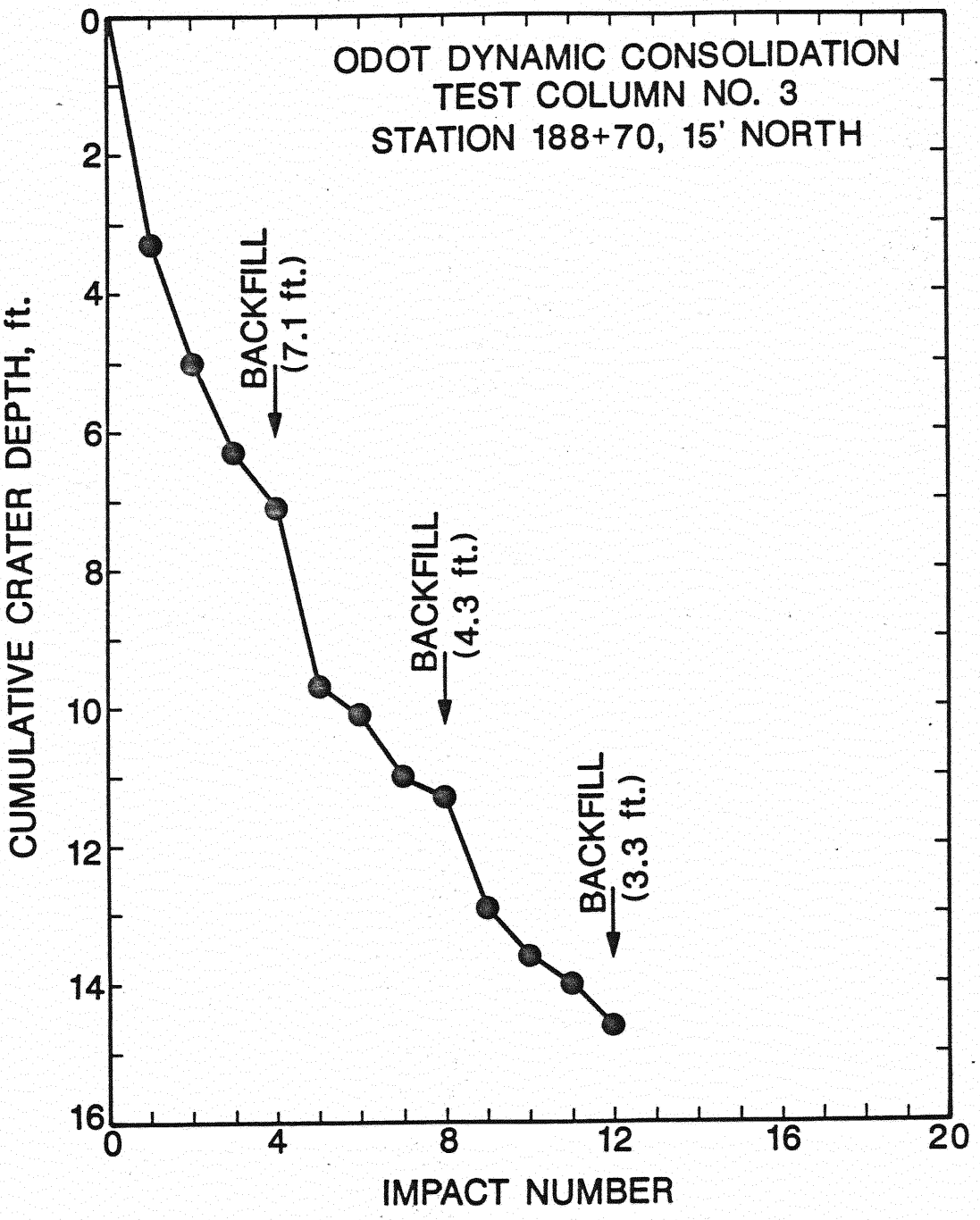

Figure 112. Cumulative Crater Depth Versus Impact, Test Column No. 3

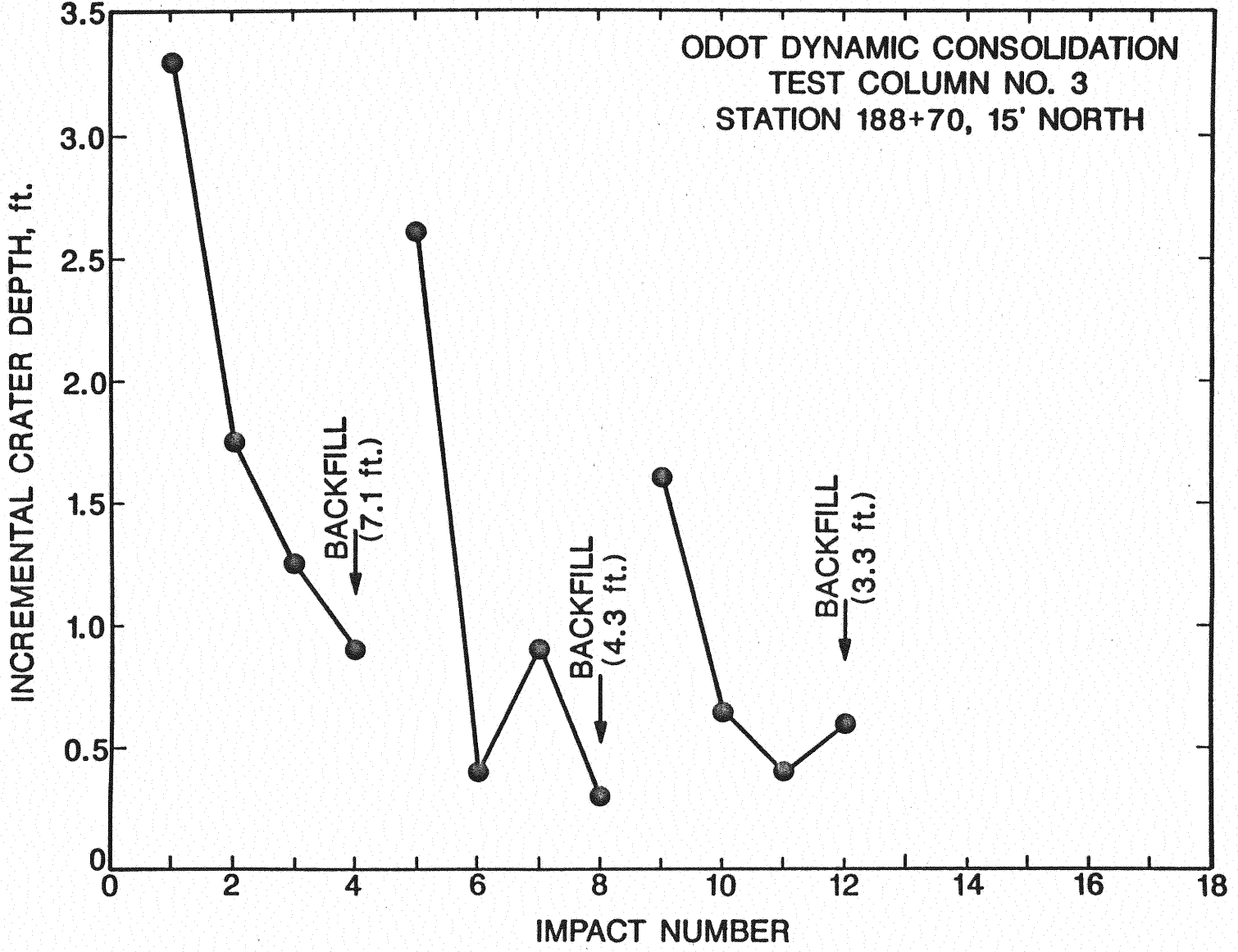

Figure 113. Incremental Crater Depth Versus Impact, Test Column No. 3